IL
NUOVO CIMENTO
ORGANO DELLA SOCIETÀ ITALIANA DI FISICA
SOTTO GLI AUSPICI DEL CONSIGLIO NAZIONALE DELLE RICERCHE
E DEL COMITATO NAZIONALE PER L'ENERGIA NUCLEARE

VOL. XXII, N. 5 *Serie decima* 1° Dicembre 1961

The Effects of the Nuclear Charge Polarization on the Elastic Scattering.

Y. N. KIM

Office of Atomic Energy - Seoul (*)

(ricevuto il 24 Febbraio 1961)

Summary. — The effects of nuclear polarizability on the elastic scattering of low-energy charged particles are discussed. The deviation from the Rutherford scattering due to the dipole polarizabilities is calculated for various cases. The effect of the quadrupole polarization in a strongly deformed nucleus is also examined.

1. – Introduction.

Various aspects of the Coulomb excitation of nuclei by charged ions have long been investigated by many authors. In this paper we deal with the elastic scattering of nuclei by nuclei when the polarizability of either the projectile or the target is considered. The investigation of the possible dynamical effects due to the polarization of a nucleus in an electric field dates as far back as 1927 [1].

Recently the interest in this problem has been renewed [2-4]. It has been suggested that the nuclear polarizability may manifest itself in a deviation

(*) Present address: Department of Physics, University of Washington, Seattle 5, Washington, U.S.A.

[1] W. HARDMEIER: *Phys. Zeit.*, **28**, 181 (1927).

[2] N. F. RAMSEY: *Phys. Rev.*, **83**, 659 (1951).

[3] G. BREIT, M. H. HULL and R. L. GLUCKSTERN: *Phys. Rev.*, **87**, 74 (1952).

[4] K. SAWICKI: *Acta Phys. Pol.*, **13**, 225 (1954).

from the Rutherford scattering if the penetrability of the impinging particles through the Coulomb barrier is negligible. In particular, the loose binding and the resultant large polarizability of the deuteron is such that it has attracted much attention. FRENCH and GOLDBERGER [5] showed that the deuteron structure plays no part in the Coulomb scattering at low energies. However, as was pointed out by MALENKA, KRUSE and RAMSEY [6] this conclusion was reached only because unperturbed wave functions were used, and by introducing perturbed wave functions, they derived an equation which shows that the polarizability of the deuteron is the principal cause of the deviation from the Rutherford scattering. However, to avoid the difficulties of solving this equation, they calculated the deviation classically following Hardmeier's method [1] which is based on the assumption that, for a given impact parameter, the presence of the polarizability term produces a small decrease of the scattering angle. They predicted that 10 MeV deuterons scattered by uranium whould show a deviation of 4.2 % for the differential cross-section in the backward direction.

In this paper we consider only those cases where the incident energies are well below the Coulomb barrier to exclude the specifically nuclear interactions in the collisions of the charged particles. We carried out a quantum-mechanical calculation to find a deviation from the Rutherford scattering due to the dipole polarization of the nucleus. As the first example, we chose the elastic scattering of α-particles by ^{12}C at the center-of-mass energy 1 MeV. The actual calculation was done by using the technique developed by ALDER and WINTHER [7] and BIEDENHARN, MCHALE, and THALER [8]. The angular distribution of the deviation is calculated at 10° intervals. The result shows that the curve of the deviation as a function of the scattering angles is of oscillatory nature.

As the second example, we calculate the scattering of deuterons by uranium at 8 MeV using the W.K.B. method. For the head-on collision the deviation from the Rutherford scattering is 5 %. It may be possible to detect this amount of deviation experimentally. Classical calculation gives 2.1% under the same condition.

We also estimated the magnitude of the effects of the quadrupole polarizations. It is expected that generally the dipole effect is dominant for the closed shell nuclei while the quadrupole effect overshadows the dipole effect in the deformed nuclei. Even in the latter case, however, the quadrupole effect is too small to be experimentally detected at present.

---

(5) J. B. FRENCH and M. L. GOLDBERGER: *Phys. Rev.*, **87**, 899 (1952).
(6) B. J. MALENKA, U. E. KRUSE and N. F. RAMSEY: *Phys. Rev.*, **91**, 1165 (1953).
(7) K. ALDER and A. WINTHER: *Dan. Mat. Fys. Med.*, **29**, no. 18 (1955).
(8) L. C. BIEDENHARN, J. L. MCHALE and R. M. THALER: *Phys. Rev.*, **100**, 376 (1955).

In the latter case, however, the process is mostly non-adiabatic because of the low excitation energy associated with the quadrupole transition. As a result, the quadrupole effect in our problem is greatly diminished.

2. – Deviation from the Rutherford scattering.

For the adiabatic approximation, valid when collision time is large compared to the nuclear period, the polarization effect can be taken into account by introducing an additional potential term in the Schrödinger equation describing the elastic scattering. If we consider only the dipole effect, the scattering is determined by the equation

$$\left(\nabla_R^2 + k^2 - \frac{2m}{\hbar^2}\frac{Z_1 Z_2 e^2}{R}\right)\psi = -\frac{m}{\hbar^2}\alpha Z_1^2 e^2 \frac{1}{R^4}\psi\,, \tag{1}$$

where

$$\alpha = 2e^2 \sum_n{}' \frac{1}{E_n - E_0} \left| \langle 0 | \sum_i^z r_i \cos\theta_i | n \rangle \right|^2, \tag{2}$$

m is the reduced mass of the projectile and of the target with atomic numbers Z_1 and Z_2, respectively. The position vectors $\boldsymbol{R}(R, \Theta, \Phi)$ and $\boldsymbol{r}_i(r_i, \vartheta_i, \varphi_i)$ refer to the projectile and the protons of the target nucleus with respect to the center of mass of the target nucleus.

From eq. (1) we obtain [9],

$$\psi = \psi_c - \frac{m}{\hbar^2}\int K(\boldsymbol{R}, \boldsymbol{R}')\, Z_1^2 e^2 \alpha \frac{1}{R'^4}\psi_c(\boldsymbol{k}_1, \boldsymbol{R}')\, \mathrm{d}\boldsymbol{R}', \tag{3}$$

where

$$K(\boldsymbol{R}, \boldsymbol{R}') \sim \frac{1}{4\pi R}\exp\left[i(kR - \ln 2kR)\right]\psi_c(-\boldsymbol{k}_2, \boldsymbol{R}')\,, \qquad \text{for large } R, \tag{4}$$

and $\psi_c(\boldsymbol{k}, \boldsymbol{R})$ is the solution of

$$\left(\nabla_R^2 + k^2 - \frac{2m}{\hbar^2}\frac{Z_1 Z_2 e^2}{R}\right)\psi = 0\,. \tag{5}$$

In these equations, $\boldsymbol{k}_1$ and $\boldsymbol{k}_2$ are the wave vectors of the Coulomb-distorted plane waves of the incident particle and of the projectile emerging after interaction with the target, respectively.

[9] N. F. Mott and H. S. W. Massey: *The Theory of Atomic Collision* (London, 1942), p. 113.

Perturbation is introduced in $\psi(\boldsymbol{k}_1, \boldsymbol{R}')$, corresponding to the incident particles of momentum $\boldsymbol{k}$, in the second term of the right-hand side of (3). For simplicity, we use for ψ_c only the solution which is regular at the origin. In eq. (4) $-\boldsymbol{k}_2 = -k_1(\boldsymbol{R}/R)$ and, therefore, $\psi_c(-\boldsymbol{k}_2, \boldsymbol{R}')$ has incoming scattered spherical waves. Also $|\boldsymbol{k}_1| = |\boldsymbol{k}_2|$, because we confine our investigation to the elastic scattering only. From eq. (3) we obtain for the scattering amplitude of the wave function ψ

$$f(\theta) = f_{\text{Coul}}(\theta) + f_{\text{pol}}(\theta) \,, \tag{6}$$

where $f_{\text{Coul}}(\theta)$ is the usual Coulomb wave function amplitude and $f_{\text{pol}}(\theta)$ the amplitude due to the polarization of the nucleus;

$$\left\{ \begin{array}{l} f_{\text{Coul}}(\theta) = \dfrac{\eta}{2k \sin^2(\theta/2)} \exp\left[-i\eta \ln\left(\sin^2 \dfrac{\theta}{2}\right) + i\pi + 2i\sigma_0 \right] , \\ \eta = \dfrac{Z_1 Z_2 e^2}{\hbar v} \,, \end{array} \right. \tag{7}$$

and

$$f_{\text{pol}}(\theta) = \frac{m}{\hbar^2} \frac{(Z_1 e)^2}{4\pi} \propto \int \frac{\psi_c(-\boldsymbol{k}_2, \boldsymbol{R})\, \psi_c(\boldsymbol{k}_1, \boldsymbol{R})}{R^4} \, \mathrm{d}\boldsymbol{R} \,. \tag{8}$$

We want to evaluate the deviation δ from the Rutherford scattering

$$\delta = 1 - \frac{\sigma_{\text{pol}}(\theta)}{\sigma_{\text{Coul}}(\theta)} \,, \tag{9}$$

where $\sigma_{\text{Coul}}(\theta)$ is the point charge cross-section and $\sigma_{\text{pol}}(\theta)$ is the part of the cross-section which was caused by the polarization. Neglecting the squared term of $f_{\text{pol}}(\theta)$, we obtain

$$\delta = -\frac{2 \operatorname{Re}\{f_{\text{Coul}}(\theta) f_{\text{pol}}(\theta)\}}{|f_{\text{Coul}}(\theta)|^2} \,. \tag{10}$$

From eq. (8) and eq. (10) we see that the evaluation of δ essentially reduces to the calculation of the integral in eq. (8).

We expand ψ_c in spherical partial waves,

$$\begin{aligned} \psi_c(\boldsymbol{k}_1, \boldsymbol{R}) &= \sum_l \psi_l(\boldsymbol{k}_1, \boldsymbol{R}) = \\ &= \sum_{l,m} [4\pi(2l+1)]^{\frac{1}{2}} \frac{\exp[i(\sigma_l - \sigma_0)]}{k_1 R} F_l(\eta, k_1 R)\, \mathscr{D}^l_{m0}(\tilde{k}_1) i^l Y_{lm}(\Theta\Phi) \,, \end{aligned} \tag{11}$$

where $\mathscr{D}^l_{mn}$ are rotation matrices and $\tilde{k}_1$ is a unit vector in the $\boldsymbol{k}_1$ direction.

F_l are the Coulomb radial wave functions. If we denote the angle between $\boldsymbol{k}_1$ and $\boldsymbol{k}_2$ by θ, we obtain, remembering that $|\boldsymbol{k}_1| = |\boldsymbol{k}_2| = k$, after the integration of the angular part

$$(12) \quad \int \frac{\psi_c(-\boldsymbol{k}_2, \boldsymbol{R})\psi_c(\boldsymbol{k}_1, \boldsymbol{R})}{R^4} \, \mathrm{d}\boldsymbol{R} = \int \frac{\sum_l \psi_l(-\boldsymbol{k}_2, \boldsymbol{R}) \sum_{l'} \psi_{l'}(\boldsymbol{k}_1, \boldsymbol{R})}{R^4} \, \mathrm{d}R =$$

$$= \frac{4\pi^2}{k^2} \sum_l \left[(2l+1) \exp\left[2i(\sigma_l - \sigma_0)\right] \int_0^\infty \frac{F_l^2(\eta, kR)}{R^4} \, \mathrm{d}R \, P_l(\cos\theta) \right].$$

In deriving eq. (12) we used the relation $l = l'$ required for the conservation of parity and total angular momentum. The integral of the type appearing in eq. (12) was tabulated for the case when the denominator is R or R^3 ([10]). We have calculated the integral on the right-hand side of eq. (12) for $0 \leqslant l \leqslant 29$ (Appendix).

We calculated the scattering of α-particles by ^{12}C at the relative energy 1 MeV. Assuming $\alpha = 0.8 \cdot 10^{-39}$ cm^3 for ^{12}C we obtain the angular distribution of the deviation shown in Fig. 1. The oscillatory nature of the deviation curve can be best understood by the uncertainty principle in a similar way as discussed by BOHR ([11]). Although $\eta \gg 1$ assures the validity of the classical approach, the quantum-mechanical differential cross-section due to the polarization does oscillate with changing scattering angle θ around the classical value. In fact, for $\eta \gg 1$ the uncertainty in angle exceeds the angular intervals over which the cross-section undergoes oscillations.

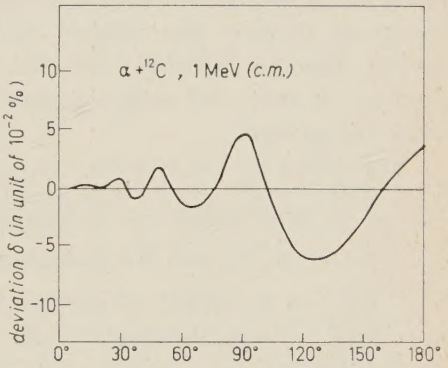

Fig. 1. – Deviation from the Rutherford scattering due to nuclear dipole polarizability. The calculation is made for α-particles elastically scattered by ^{12}C at 1 MeV (c.m.).

A much larger deviation from the Rutherford scattering is expected when the deuterons are scattered by heavy nuclei owing to the large polarizability of the deuterons. We have calculated the deviation when deuteron are scattered by ^{238}U at 8 MeV. We employed the W.K.B. approximation for the radial Coulomb wave functions ([12]). The radial matrix element reduces to

([10]) M. GOLDSTEIN, R. M. THALER and L. C. BIEDENHARN: *Tabulation of the Radial Coulomb Integrals* (m, n, l), Los Alamos Scientific Laboratory Report 2106 (1957).

([11]) N. BOHR: *Dan. Mat. Fys. Medd.*, **18**, no. 8 (1948).

([12]) K. ALDER and A. WINTHER: *Dan. Mat. Fys. Medd.*, **31**, no. 1 (1956).

the following simple form

$$\int_0^\infty \frac{F_l^2(k, r)}{r^4}\,\mathrm{d}r = \frac{k^3}{4\eta^3}\int_{-\infty}^{\infty} \frac{\mathrm{d}\omega}{(\varepsilon\cos\hbar\omega + 1)^3}\,, \tag{13}$$

where

$$\varepsilon = \left\{1 + \frac{l(l+1)}{\eta^2}\right\}^{\frac{1}{2}}.$$

The calculation of eq. (13) is elementary and can be done analytically. Supposing the polarizability of the deuteron to be $0.56 \cdot 10^{-39}$ cm^3 ([13]) the calculation shows deviation of 5.1% for the head-on collision. Classical calculation gives the deviation of 2% under the same condition. For the incident energy of 10 MeV, the classical calculation gives the deviation of about 4% for the head-on collision. At this energy, however, the penetration of the Coulomb barrier and other competing processes such as given below can no more be ignored.

The following cross-sections are estimated:

σ_c = cross-section for the formation of compound nucleus,

σ_s = cross-section for stripping reaction,

σ_e = cross-section for electric break-up during the flight when deuterons are bombarded to uranium. Each cross-section is the average cross-section per unit solid angle. At incident energy 8 MeV, σ_c and σ_s were found to be about 1 mb each, while σ_e is less than 0.1 mb. At 10 MeV, σ_c and σ_s are about 10 mb each, while σ_e is about 0.5 mb. In comparison, the Rutherford cross-section per unit solid angle for the scattering angle 180° is about 150 mb for the incident energy 8 MeV and 100 mb for 10 MeV. Deviations of 5% of these are 7.5 mb and 5 mb respectively.

3. – Quadrupole effects.

Because of the low excitation energies associated with the quadrupole polarization, the quadrupole effect may, under certain circumstances, overshadow the effect of the dipole polarization in the elastic scattering. The comparison of the effects is not so simple, however, because in most cases of quadrupole polarization the adiabatic approach is not justified. In the fol-

([13]) N. F. Ramsey, B. J. Malenka and U. E. Kruse: *Phys. Rev.*, **91**, 1162 (1953); B. W. Downs: *Phys. Rev.*, **98**, 194 (1955).

lowing we first employ the adiabatic approach for both cases and later consider the effects of non-adiabatic process to compare the magnitudes of the two effects.

The potential due to the nuclear polarization can be obtained by a perturbation calculation ([14]),

$$V_{\mathrm{pol}}(R) = 4\pi Z_1^2 e^2 \sum_{l=1}^{\infty} (2l+1)^{-2} R^{-2l-2} \sum_n{}' \frac{B(El, 0 \to n)}{E_0 - E_n}, \tag{14}$$

$B(El)$ is the reduced transition probability defined as follows

$$\begin{aligned} B(El; I_i \to I_f) &= \sum_{M_f m} |\langle I_i M_i | \mathscr{M}(El, m) | I_f M_f \rangle|^2 \\ &= (2I_i + 1)^{-1} |\langle I_i \| \mathscr{M}(El) \| I_f \rangle|^2 , \end{aligned} \tag{15}$$

where

$$\mathscr{M}(El, m) = \sum_k e_k r_k^l Y_{lm}(\theta_k, \varphi_k) , \tag{16}$$

I is the total angular momentum and m the magnetic quantum number. The proper averaging over the initial orientations of the target nucleus and the summing over the final orientatons are included in eq. (14). To find the deviation from the Rutherford scattering, we can proceed in the same way as in the last section. If we denote the contribuitons to the deviation from the dipole and quadrupole polarizations by δ_d and δ_q respectively, we find from eq. (8) and eq. (10), respectively,

$$\frac{\delta_d}{\delta_q} = \frac{\frac{1}{9} \sum_n{}' [B(E1, 0 \to n)/\Delta E_{d,n}] I_4}{\frac{1}{25} \sum_n{}' [B(E2, 0 \to n)/\Delta E_{q,n}] I_6} , \tag{17}$$

where

$$I_n = \int \frac{\psi_c(-\boldsymbol{k}_2, \boldsymbol{R}) \psi_c(\boldsymbol{k}_1, \boldsymbol{R})}{R^n} \, \mathrm{d}\boldsymbol{R} , \tag{18}$$

and $\Delta E_n = E_n - E_0$; the subscripts d and q of ΔE refer to the dipole and quadrupole excitations, respectively. In view of the fact that the adiabatic approximation is not valid for many cases of the quadrupole polarization, we show here a brief discussion of the effects of the quadrupole polarization when the motion is not adiabatic.

([14]) K. Alder, A. Bohr, T. Huus, B. Mottelson and A. Winther: *Rev. Mod. Phys.*, **28**, 432 (1956).

If we denote by f_0 the amplitude of the Coulomb wave function and by f_{pol} the amplitude due to the polarization, then we obtain from eq. (14)

$$f_{\text{pol}}(\text{adiabatic}) \sim \frac{B(E2)\, Z_1^2 e^2}{\Delta E\, a^5 \hbar v}\, f_0 \,, \tag{19}$$

where a is the classical distance of closest approach. In the case of non-adiabatic motion, we take for the potential arising from the quadrupole polarization,

$$V = \frac{Z_1 e}{R^3} \sum_{M_f m} \langle I_i M_i | \mathscr{M}(E2, m) | I_f M_f \rangle \,. \tag{20}$$

Hence we obtain

$$f_{\text{pol}}(\text{non-adiabatic}) \sim B(E2) \left(\frac{Ze}{a^2 \hbar v}\right)^2 f_0 \,. \tag{21}$$

From eqs. (19) and (21)

$$\frac{f_{\text{pol}}(\text{non-adiabatic})}{f_{\text{pol}}\,(\text{adiabatic})} \sim \frac{a\,\Delta E}{\hbar v} = \xi = \frac{(\text{collision time})}{(\text{nuclear period})} \,. \tag{22}$$

Now we compare the effects of the dipole and quadrupole polarization in elastic scattering of α-particles by ^{152}Sm with incident energy just half the Coulomb barrier. The values of $B(E2, 0+ \to 2+)$ can be obtained from the transition probabilities

$$\frac{1}{\text{mean life}} = \frac{8\pi(l+1)}{[l(2l+1)!!]^2 \hbar} \left(\frac{\Delta E}{\hbar c}\right)^{2l+1} B(El, f \to i) \,, \tag{23}$$

where

$$(2l+1)!! = 1 \cdot 3 \cdot 5 \ldots\ldots (2l+1)$$

and

$$B(El, f \to i) = \frac{2i+1}{2f+1}\, B(El, i \to f) \,. \tag{24}$$

The value of $B(El)$ is estimated by assuming the average excitation energy and the sum rule. From eqs. (17) and (22) the deviation due to the quadrupole polarization of ^{152}Sm is estimated to be of the order of only 0.1 %. One may conclude therefore that, even in case of strongly deformed nuclei, it is impossible at present to detect experimentally the effect of quadrupole polarization in elastic scattering.

4. – Comparison of classical and quantum mechanical calculations.

We compare, in this section, the classical and quantum mechanical calculations of the deviation from the Rutherford scattering due to the dipole polarization. The differences are two-fold. First, the deviation as a function of scattering angle shows an oscillatory nature. This is quite contrary to the classical calculation which gives a monotonically increasing deviation as the scattering angle becomes larger.

Secondly, the magnitudes of $\delta_{\text{q.m.}}$ and δ_{cl}, the amounts of deviation calculated quantum mechanically and classically, respectively, are, as will be shown below, different roughly by the order of η which is defined in eq. (7).

In the classical calculation, the potential energy of the projectile in the field of the target nucleus is given by [1]

$$V = \frac{Z_1 Z_2 e^2}{R} - \frac{\alpha Z_1^2 e^2}{2E^4}, \tag{25}$$

where α is the polarizability. This is identical with the potential obtained by the quantum mechanical calculation. We take the deviation proportional to the polarizability. Then from the dimensional analysis we obtain

$$\delta_{\text{cl}} \sim \frac{\alpha Z_1^2 e^2}{R^4 E} = \alpha \cdot \frac{a}{R^4} \cdot \frac{Z_1}{Z_2}, \tag{26}$$

where a is the distance of closest approach in a head-on collision and $E = Z_1 Z_2 e^2 / a$.

For a quantum mechanical calculation we may write

$$\delta_{\text{q.m.}} \sim V'_{\alpha} \frac{a}{\hbar v}, \tag{27}$$

where v is the velocity of the incident particle, and

$$V'_{\alpha} = \frac{\alpha Z_1^2 e^2}{R^4}. \tag{28}$$

We obtain from eqs. (26) through (28)

$$\frac{\delta_{\text{q.m.}}}{\delta_{\text{cl}}} \sim \eta. \tag{29}$$

Eq. (29) may look strange in view of the fact that large η ensures the validity of a classical calculation. This kind of apparent paradoxes is most

clearly understood together with the oscillatory nature of the deviation curve in the light of the discussion by BOHR ([11]) as shown in Section 2. We can see easily from the uncertainty principle that, the larger the value of η is, the larger the uncertainty in the scattering angle. This becomes larger than the angular intervals over which the deviation curve undergoes oscillation. In fact one expects that, in the classical limit, this rapidly oscillating curve would reduce to the monotonically increasing classical curve.

* * *

The author wishes to thank Prof. R. PEIERLS and Prof. A. BOHR. He also wishes to express his gratitude to Prof. N. BOHR for the hospitality at the Universitetets Institut for Teoretisk Fysik, Copenhagen.

APPENDIX

The calculation of the integral appearing on the right-hand side of eq. (12) can be carried out in the following way. For $l \geqslant 2$, the following relation may be used:

$$\text{(A.1)} \qquad \int_0^\infty \frac{F_l^2(\eta, kr)}{r^4}\,\mathrm{d}r = -\frac{kl(l+2)\{(l+1)^2+\eta^2\}}{3\eta(2l+1)(l+1)} \lim_{k_1\to k_2}(0,3;l+1)+$$

$$+\frac{l(l+1)}{3\eta(2l+1)}\left[k(2l+1)+k\eta^2\left\{(l-1)\left(\frac{1}{l^2}+\frac{1}{(l+1)^2}\right)+\frac{3}{(l+1)^2}\right\}\right]\lim_{k_1\to k_2}(0,3;l)-$$

$$-\frac{k(l+1)(l-1)}{3\eta(2l+1)l}(l^2+\eta^2)\lim_{k_1\to k_2}(0,3;l-1)\,,$$

$(0, 3; l)$ etc. are the same as defined in ref. ([8]). Eq. (A.1) does not hold for $l = 0$ and $l = 1$, in which case it is convenient to use the Bessel function expansion of the Coulomb wave function, especially when kr is large while η is not too large.

RIASSUNTO (*)

Si discutono gli effetti della polarizzabilità nucleare sullo scattering elastico delle particelle cariche di bassa energia. Si calcola per vari casi la deviazione dallo scattering di Rutherford dovuta alle polarizzabilità di dipolo. Si esamina anche l'effetto della polarizzazione di quadrupolo in un nucleo fortemente deformato.

(*) *Traduzione a cura della Redazione.*

IL NUOVO CIMENTO Vol. XXII, N. 5 1° Dicembre 1961

Search for a Mass 550 Particle (*) (**).

G. Monnig

Physics Department, Washington University - St. Louis, Mo.

(ricevuto il 15 Maggio 1961)

Summary. — The mass of sea level cosmic ray particles has been determined from simultaneous measurements of range, momentum, and Čerenkov light. No resolved measurements around 550 m_e accompanied 448 stopping μ-mesons. The likelihood of not resolving a bona fide mass 550 particle is estimated to have been not greater than 10%.

1. – Introduction.

This report summarizes a description [1] of an experiment performed at sea level and 50° geomagnetic latitude (St. Louis, Missouri) to search for a particle of mass around 550 m_e in the cosmic radiation.

Alikhanian *et al.* [2], measuring mass of cosmic ray particles at mountain altitude by a range momentum method, found a clearly resolved group of 11 measurements between 440 and 700 m_e in a run containing 255 measurements.

(*) Research supported by the joint program of the Office of Naval Research and the U. S. Atomic Energy Commission.

(**) This article is a condensation of a thesis presented by the author to the Board of Graduate Studies of Washington University in January, 1961 in partial fulfilment of the requirements for the degree of Doctor of Philosophy.

(1) G. Monnig: *Ph. D. Thesis* (Washington University, 1961).

(2) A. I. Alikhanian, N. V. Shostakovich, A. T. Dadaian, V. N. Fedorov and B. N. Deriagin: *Žurn. Éksp. Teor. Fiz.*, **31**, 955 (1956); Trans. *Sov. Phys. JETP*, **4**, 817 (1957).

Allowing for the effect of magnetic field on counting rates, they concluded that mass 550 particles were present with an average abundance relative to μ-mesons stopping in the same range interval of about 0.5%. A number of other experiments in which mass is measured by range and a quantity dependent on energy loss and experiments searching for evidence of production and decay of mass 550 particles have failed to confirm this conclusion, however [3].

In this experiment the range momentum method is used in conjunction with a range-Čerenkov light method of mass measurement. The latter method complements the former in two respects. First, because of the large number of penetrating particles relative to particles stopped by ionization and excitation it is important to guard against the possibility that a small fraction of the more numerous group appears to belong to the latter group. This conceivably could happen if the equipment used to measure range fails, in a small fraction of the events, to register the lower part of the track or, alternatively, if a particle stopped by an interaction with a nucleus is mistaken for a particle stopped by ionization and excitation. It has been estimated [1] that if only 1 in 630 penetrating μ-mesons were, on the average, mistaken for stopping particles this would correspond to an abundance of spurious mass measurements in the region 440 to 700 m_e which is the same as the reported abundance of mass 550 particles. Possibly the resolution between the mass 550 and the light meson groups of measurements could be explained on this basis; however, there does not appear to be any explanation of the observed resolution between the mass 550 and the proton groups.

The simultaneous use of the range-momentum and range-Čerenkov light methods makes it possible to recognize an occasional large range error since it would shift the two mass values in opposite directions from the true mass.

The two methods also complement each other by improving the accuracy of mass measurement in the important region around 550 m_e. The Čerenkov light indicates the velocity of a particle most accurately just above the threshold velocity, and it is possible to choose the index of refraction and thicknesses so that a stopping mass 550 particle would have a velocity just above threshold in the Čerenkov counter. Since the accuracy of mass determination by the range-momentum method is limited by experimental error in measuring curvature and the mass error increases as the mass increases, whereas the error in mass measured by the range-Čerenkov light method decreases as the mass increases, the two methods complement each other nicely.

[3] Among the most recent reports are: N. D. Prasad, M. G. K. Menon and O. P. Sharma: *Nuovo Cimento*, **14**, 1332 (1959); I. B. McDiarmid: *Phys. Rev.*, **146**, 1016 (1959); M. Conversi *et al.*: *Nuovo Cimento*, **12**, 130, 148 (1959); E. Bierman, R. Lea, J. Orear and S. Rosendorff: *Phys. Rev.*, **113**, 710 (1959).

These contain references to earlier work.

2. – Apparatus.

Figs. 1*a* and 1*b* are scale diagrams of the apparatus. Proceeding downward it consists of a Čerenkov cell C viewed by two 5 inch photomultipliers, $C1$ and $C2$, a magnet cloud chamber P and a « range hodoscope » *i.e.* an arrangement of 13 lead plates interspersed with Geiger tubes which permit the plate in which a particle stops to be determined. The interior of the Geiger tubes in tray 1 is 20 g/cm² Pb equivalent below the interior of P, 73 g/cm² below the center of C, and 114 g/cm² below the top of the apparatus; and the corresponding thicknesses for tray 13, which defines the lower boundary of the range hodoscope, are 110, 163, and 204 g/cm² respectively. All thicknesses are given in lead equivalent. The plate above tray 2 is 3.1 g/cm² thick, the plate above tray 13 is 24.5 g/cm² thick and the thicknesses of intermediate trays are such that the interiors of successive trays are at ranges below the interior of P equally spaced on a logarithmic scale. The apparatus was housed in a trailer having negligible roof thickness.

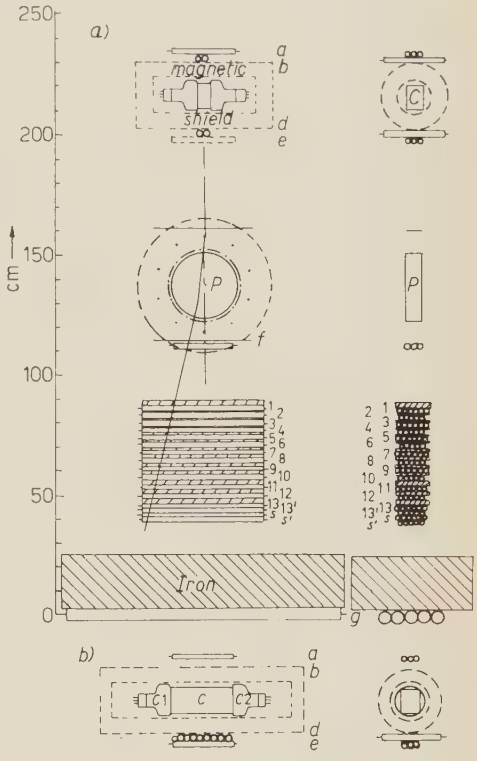

Fig. 1. – *a*) Scale diagram of apparatus using 2 in. Čerenkov counter. *b*) Scale diagram of 10 in. Čerenkov counter and surrounding Geiger tubes.

Other Geiger tubes, as indicated, define the beam and trigger the apparatus. About 10 % of the data was taken using a $(3\times4\times2)$ inch Čerenkov cell and the remainder was taken using a $(3\times4\times10)$ inch cell in order to increase the counting rate. The two were similar in all respects except length. Except for the different arrangements of beam defining Geiger tubes above and below the Čerenkov counter, the other apparatus was not altered and the location of the center of the Čerenkov cell was not changed; consequently only the Čerenkov counter and surrounding Geiger tubes are indicated in Fig. 1*b*. A liquid (Minnesota Mining and Mfg. Co. fluorocarbon FC-75) having an index of refraction of 1.27 was used in the Čerenkov counter. For this value and

the thicknesses used the Čerenkov light emitted by a mass 550 particle stopping in the hodoscopes range interval is less than one half that emitted by a stopping light meson. If water ($n = 1.33$) had been used, this difference in Čerenkov light would exist over a smaller range interval. Thus the basic reason for using a Čerenkov medium having a lower index of refraction than 1.33 is to increase the counting rate.

The magnet cloud chamber P has been described previously ([4]). The wiring of the magnet was changed so that a field of approximately 1 700 gauss was obtained with the same current and temperature conditions employed previously. With this field there is only a small difference (5 %) between the counting rates for light mesons and possible mass 550 particles stopping in the same range interval, and most of the stopping μ-mesons are included in the analysis. This affords a direct check of the errors in measuring mass by the two methods.

The Geiger tubers (1 in. dia. 20 in. long) in the range hodoscope were connected to a system described previously ([4]), in which each tube is connected through an amplifier and coincidence circuit to a univibrator the state of which is indicated by a neon bulb in a position on a board corresponding to the position of the tube in the range hodoscope. A master pulse is fed to the second input of the coincidence circuit and a camera viewing the board is operated by the master pulse, so that «tracks» with granularity corresponding to the Geiger tube diameter are obtained. In order that an event be accepted for analysis, it was required that a prolongation of the track passes through two undischarged Geiger tubes.

The pulses, in coincidence with the master pulse, from photomultipliers $C1$ and $C2$ were individually amplified, lengthened and recorded by Esterline Angus recording milliameters. The gains of the two channels were effectively equalized in the analysis on the basis of recorded pulse heights. The resolutions in the individual tubes were approximately equal, and the two recording channels, after equalization of gains, were weighted equally. The equipment was triggered on penetrating particles (master pulse *abdefg* for the two inch Čerenkov counter and *acfg* for the ten inch Čerenkov counter) for 30 to 45 minutes daily (around six events) in order to secure data for the calibration and checking of the Čerenkov counters and other equipment. Assuming that the particles penetrating tray g (115 g/cm² Pb equivalent below the center of C) are μ-mesons, at least 94 % of the saturation value of Čerenkov light is emitted. Also the sea level μ-meson differential velocity distribution is such that the difference between the Čerenkov light emitted by the majority of penetrating particles and the saturation value is negligible in comparison with the reso-

([4]) B. F. Stearns: *Ph. D. Thesis* (Washington University, 1956); J. De Pagter and R. D. Sard: *Phys. Rev.*, **118**, 1353 (1960).

lution of the photomultipliers. For penetrating particles, the ratio of standard deviation to average pulse height is, respectively, 28 %, 32 %, and 22 % for $C1$, $C2$, and the combination. This is based on 80 events in the 2 inch cell. The corresponding figures for 315 events in the 10 inch cell are, 36 % 35 %, and 20 %. This indicates that the reflective coating (U.S. Stoneware Co. « Tygon » white paint on the inner wall surface) performed well.

The master pulse for stopping particles is *abdef* (S or S') for the two inch Čerenkov cell and *aef* (S or S') for the ten inch cell. Due to the large number of penetrating particles relative to stopping particles it is essential that tubes in successive hodoscope trays be offset horizontally a half diameter otherwise the wall thickness, .015 inch, if assumed to be the width of an insensitive area on the tray, would lead to an expected number of « spurious » stoppings which is appreciable compared to true stoppings.

Elimination of events in which the particle passes through a boundary of the sensitive region of the range hodoscope corresponding to the ends of the Geiger tubes, (thus missing trays S and S') was accomplished by reprojecting the cloud chamber pictures onto a scale diagram of the apparatus, taking into consideration deflection in the fringing field. The Geiger tubes in trays *a*, *b*, *d*, *e*, for the run using the 2 inch cell and trays *a*, *d*, *e*, for the 10 inch cell were also individually hodoscoped. This information, and symmetry of the magnetic field, enabled the trajectory below the cloud chamber to be determined more accurately than could be done solely on the basis of the cloud chamber picture and field distribution.

3. – Analysis.

The error in the range-momentum mass, m_{rp}, is due mainly to curvature error caused by track distortion. The reciprocal momentum, $1/P$, is proportional to track curvature and the standard deviation of the measured values of $1/P$ for events accompanied by more than half the saturation value of Čerenkov light and in which the stopping occurs in a given plate is a direct indication of the error in curvature. These stopping particles are μ-mesons. Range error corresponding to plate thickness contributes negligibly to error in m_{rp} in comparison to the curvature error. Assumed symmetrical errors in $1/P$ lead to asymmetrical errors in m_{rp}. For convenience in combining m_{rp} with the range-Čerenkov light mass, $m_{r\check{c}}$, a symmetrical mass error combination, $m_{rps} \pm \Delta m_{rps}$, is used

$$m_{rps} = m_{rp} + \frac{(+\Delta m_{rp}) - (-\Delta m_{rp})}{2},$$

$$\Delta m_{rps} = \frac{(+\Delta m_{rp}) + (-\Delta m_{rp})}{2},$$

here ($+\Delta m_{rp}$) and ($-\Delta m_{rp}$) denote error in the upward and downward directions respectively.

The error in $m_{r\check{c}}$ is due mainly to error in measuring Čerenkov light. This is assumed to be caused mainly by statistical fluctuation in the number of electrons reaching the first dynode of the photomultipliers. The standard deviation of the Čerenkov pulses recorded for penetrating particles was taken to be the error in a single pulse having saturation height. The error assigned to the Čerenkov pulse recorded for a stopping event is proportional to the square root of its height and, at the saturation value, is equal to 21 % of it. This is the average of the values 22 % and 20 % obtained, as described previously, from penetrating events in the 2 inch and 10 inch cells. As before, range error due to plate thickness contributes negligibly to mass error. The relation between Čerenkov pulse height and mass value for a given range is nearly linear.

The two mass values are averaged, weighting each inversely as the square of its error, to obtain $m_{av} \pm \Delta m_{av}$. Treating the two mass values as independent would cause Δm_{av} to be overestimated if a range error contributes significantly to the individual mass errors. However, m_{rp} and m_{rc} are essentially independent for range error corresponding to hodoscope plate thickness.

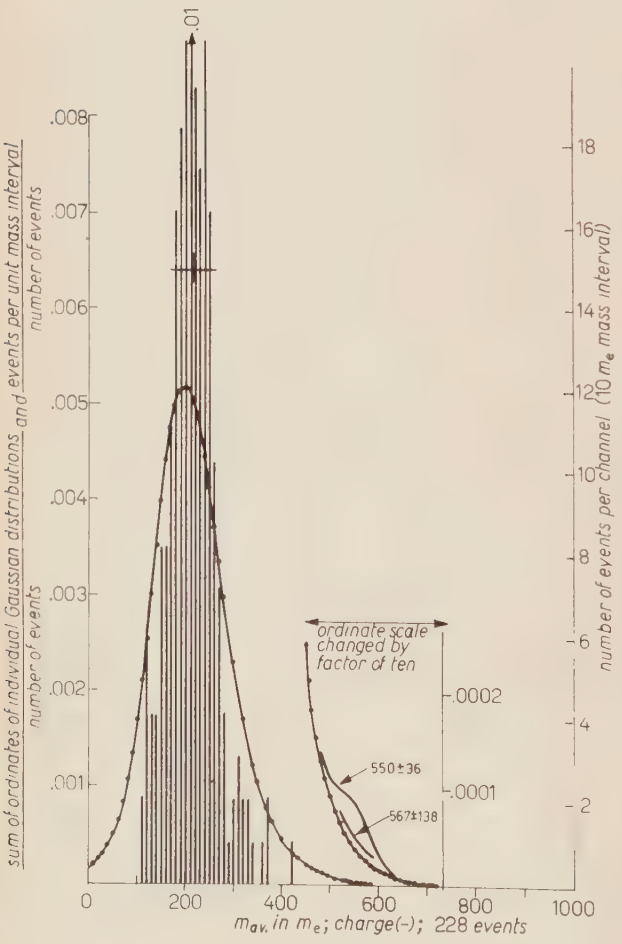

Fig. 2*a*. Distribution of measured masses for negative events. Also shown is the effect that an assumed single mass 550 measurement, as indicated, would produce.

4. – Results.

The error in the weighted average depends on the point of stopping as

Quote sociali e prezzi di abbonamento alle pubblicazioni

● **Quote sociali per l'anno 1962.**

Per l'Italia:		Per l'Estero:	
Soci individuali	L. 9 000	Soci individuali e collettivi . . .	$ 18 (L. 11 250)
» collettivi	» 25 000		
» sostenitori	» 60 000	Soci sostenitori . .	$ 96 (» 60 000)

Ai Soci vengono inviati gratuitamente *Il Nuovo Cimento*, il *Supplemento al Nuovo Cimento* e il *Bollettino della Società Italiana di Fisica*.

● **Abbonamento al *Nuovo Cimento* e al *Supplemento al Nuovo Cimento* per l'anno 1962, per enti e persone *non* Soci della Società Italiana di Fisica.**

Per l'Italia:		Per l'Estero:	
abbonam. ordinario . .	L. 15 000	abbonam. ordinario .	$ 28 (L. 17 500)
» sostenitore .	» 60 000	sostenitore.	$ 96 (» 60 000)

Agli Abbonati viene inviato gratuitamente il *Bollettino della Società Italiana di Fisica*.

EDIZIONE IN CARTA NORMALE E IN CARTA LEGGERA.

Il *Nuovo Cimento* e il *Supplemento* si pubblicano in due edizioni: una in carta normale e una, in ristretto numero di copie, in carta leggera (India bianca). Il prezzo è il medesimo per le due edizioni se spedite per posta normale. Salvo richiesta contraria, si spedisce l'edizione in carta normale.

Coloro che desiderino ricevere l'edizione in carta leggera per posta aerea dovranno assumersi le maggiori spese del trasporto aereo. L'ammontare di dette spese può ricavarsi considerando che l'edizione per il 1962 in carta leggera peserà in totale (*Nuovo Cimento* e *Supplemento* circa (4 ÷ 4,5) kg.

Gli autori sono pregati d'inviare, a fare data dal 1° Gennaio 1962, i propri lavori per la pubblicazione al seguente indirizzo: Direttore del NUOVO CIMENTO. Bologna, Via Irnerio, 46, presso l'Istituto di Fisica dell'Università.

Tutti i pagamenti vanno fatti a NICOLA ZANICHELLI, EDITORE - BOLOGNA (Italia) - (c./c. postale 8/36 - Bologna)

Membership fees and subscription fees to publications

• Membership fees for the year 1962.

For Italy:		For Foreign Countries:	
Individual Members .	Lit. 9 000	Individual and Collective Members.	$ 18 (Lit. 11 250)
Collective » .	» 25 000		
Sponsoring » .	» 60 000	Sponsoring Members.	$ 96 (Lit. 60 000)

To Members *Il Nuovo Cimento*, the *Supplemento al Nuovo Cimento* and the *Bollettino della Società Italiana di Fisica* are sent free of charge.

• Subscription fees to the *Nuovo Cimento* and to the *Supplemento al Nuovo Cimento* for the year 1962 for persons and Institutions *not being* Members of the Italian Physical Society.

For Italy:		For Foreign Countries:	
ordinary subscription .	Lit. 15 000	ordinary subscription	$ 28 (Lit. 17 500)
sponsoring » .	» 60 000	sponsoring »	$ 96 (Lit. 60 000)

To subscribers the *Bollettino della Società Italiana di Fisica* is sent free of charge.

NORMAL PAPER EDITION AND WHITE INDIA PAPER EDITION.

The *Nuovo Cimento* and the *Supplemento* are published in two editions: one on normal paper and the other, in only a limited number of copies, on light paper (white India). The price is the same for both editions when they are shipped by surface mail. Unless instructions to the contrary are given, it is the normal paper edition which will be shipped.

Subscribers who wish to receive the light paper edition by air mail will be charged with the necessary additional postal fees. The amount of these expenses may be gathered from the fact that the white India paper edition (*Nuovo Cimento* and *Supplemento*) will assume for 1962 the total weight of (4 ÷ 4,5) kg.

Authors are kindly requested to send, to begin with Jan. 1st, 1962, their papers submitted for publication to the following address: Direttore del NUOVO CIMENTO, c/o Istituto di Fisica dell'Università, Via Irnerio, 46, Bologna.

All fees have to be paid to NICOLA ZANICHELLI, EDITORE - BOLOGNA (Italy) - Via Irnerio, 34

well as the mass value. In order to avoid the averaging, within channels, of both measured values and errors which is inherent in the conventional histogram presentation, a procedure of adding ordinates of Gaussian distributions associated with individual events was employed. The mode of each individual Gaussian distribution is m_{av} and its standard deviation is Δm_{av}. Ordinates are added over fixed uniformly spaced points on the mass scale. The resulting smooth curves for 228 negative events and 291 positive events for which Čerenkov light was recorded are shown in Figs. 2*a* and 2*b*. For comparison, histograms of the same results are also shown. The ordinate scales are directly comparable and the number of events per channel in the histogram is indicated on the right. The smooth curves are calculated on an IBM 650 Computer and the programming, using the Bell Interpretive System, is given in (1). The description is intended to permit its use by persons familiar only with the input and output operations (5).

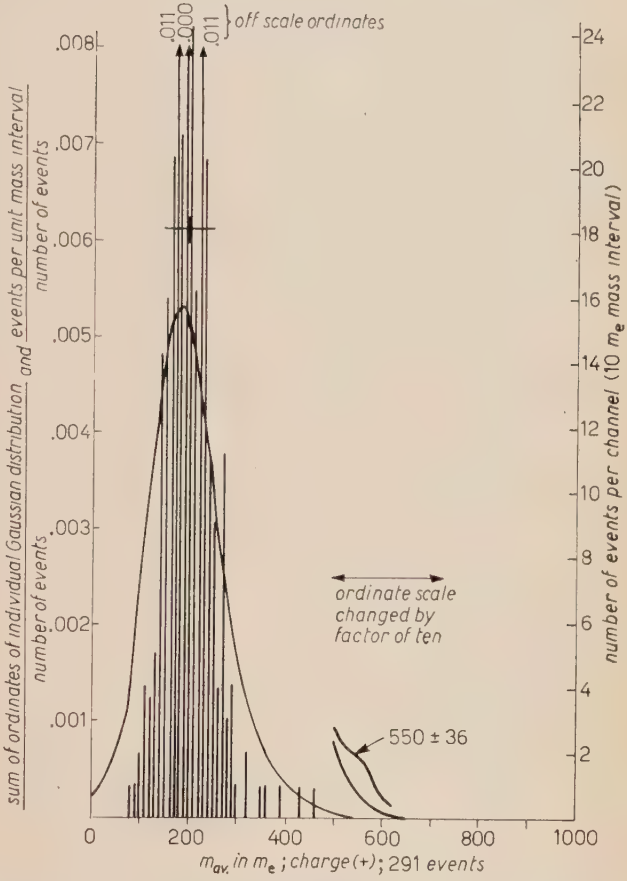

Fig. 2*b*. – Distribution of measured masses for positive events.

5. – Conclusion.

Figs. 2*a* and 2*b*, together representing 519 stoppings, show no evidence of resolved measurements in the mass 550 region. In order to indicate the effect of a single mass 550 particle, an assumed event for which $m_{rp} = m_{re} = 550\ m_e$

(5) *IBM Technical Newletter*, **11** (1956), Section V.

was added to the data and is indicated in Figs. 2. This was done for a stopping *a*) above tray 6 and *b*) above tray 13. The error assigned to the weighted average depends significantly on the point of stopping and trays 6 to 13 represent the region in which a stopping mass 550 particle is expected to give detectable Čerenkov light *i.e.* above one tenth the saturation value. It is seen that, if a single mass 550 measurement had been obtained, it would not have been considered clearly resolved. This illustrates the usefulness of the smooth curve when errors tend to increase with measured value. The steep slope of a histogram at lower values can lead to an erroneous impression of resolution of higher value measurements, in some cases, unless the viewer makes an approximately correct allowance for the error increase. This may be difficult but, of course, is already performed in the calculation of the smooth curve.

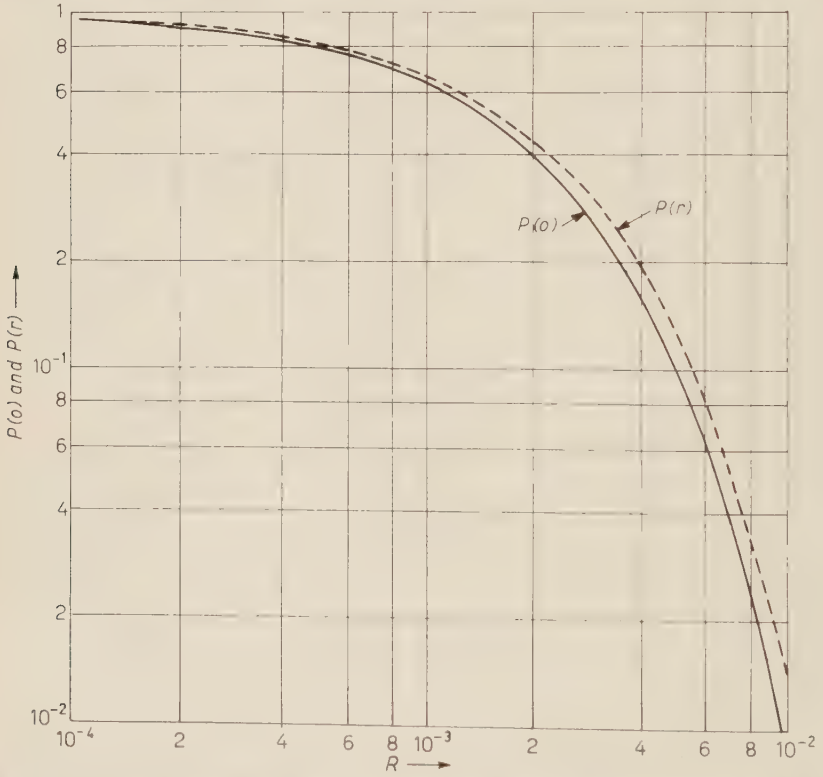

Fig. 3. $P(0)$, the probability that no mass 550 particle accompanies 471 μ-mesons, and $P(r)$, the probability of obtaining no higher mass measurements than those observed *vs.* R, the abundance of mass 550 particles relative to μ-mesons.

The significance of negative information provided by this experiment concerning the existence of mass 550 particles depends on the probability that, if a mass 550 particle had been present, it could have had the appearance of

one of the observed events. Events for which m_{av} is greater than 350 m_e have been investigated individually and the probability that a mass 550 particle, if present, could have led to these measurements has been estimated. There are seven of these high mass events and the probability depends on the point of stopping, but is in all cases less than or equal to 10%. The highest mass value obtained is 464 m_e.

In estimating an upper limit to the abundance of mass 550 particles relative to μ-mesons stopping in the same range interval, only stoppings in the plates below tray 5 are considered, since a mass 550 particle is expected to be accompanied by Čerenkov light only for stoppings in these plates. There are 263 positive and 185 negative events of this type and the sum, 448, is multiplied by the factor 1.05, yielding 471, to account for the fact that more μ-mesons are expected to be eliminated from the analysis than 550 particles due to different deflections in the magnetic field. Thus, in summary, 1) no resolved measurement in the 550 m_e region was obtained in a running time corresponding to 471 stopping μ-mesons and 2) there is an estimated probability of at most 10% that a mass 550 particle, if it had been present, could have had the appearance of one of the events obtained. Assuming that mass 550 particles stop in the range hodoscope with an average abundance, R, relative to stopping μ-mesons; $P(0)$, the probability that no stopping mass 550 particle accompanied 471 stopping μ-mesons, is $\exp[-471R]$, and $P(r)$, the probability of obtaining no higher mass measurements than those observed, is $\exp[(-471 \cdot 0.9)R]$. $P(0)$ and $P(r)$ are plotted *vs.* R in Fig. 3. For the relative abundance reported by ALIKHANIAN *et al.*, 0.5%, there is a 90% probability that a mass 550 particle would have been present and a 88% probability that it would have led to a higher mass measurement than those obtained.

* * *

The writer is indebted to several people for assistance during the work and in particular to Prof. R. D. SARD for his continued interest and many helpful discussions.

RIASSUNTO (*)

Si è misurata la massa delle particelle dei raggi cosmici al livello del mare per mezzo di misure simultanee di range, impulso ed emissione di luce Čerenkov. Non si notò alcun risolvimento intorno a 550 m_e su 448 mesoni μ all'arresto. Si stima che la verosimiglianza che una particella la cui massa potesse fondatamente ritenersi di 550 m_e non sia stata individuata non superi il 10%.

(*) *Traduzione a cura della Redazione.*

The Pion Spectrum in Radiative Hyperon Decay (*).

S. Iwao and J. Leitner

Syracuse University - Syracuse, N. Y.

(ricevuto il 7 Giugno 1961)

Summary. — The calculations of Barshay *et al.* on relative hyperon decay are extended to include the pion momentum spectra. The results show that radiative hyperon decay will appear as an important source of background in the study of hyperon leptonic decay.

1. – Introduction.

The calculation of the rates of hyperon radiative decay

$$(1) \qquad \begin{cases} \Sigma^- \to \pi^- + \mathrm{n} + \gamma \\ \Sigma^+ \to \begin{cases} \pi^+ + \mathrm{n} + \gamma \\ \pi^0 + \mathrm{p} + \gamma \end{cases} \\ \Lambda \to \pi^- + \mathrm{p} + \gamma \end{cases}$$

was first carried out by Barshay and Behrends [1], who were concerned with the possibility of detecting hyperon magnetic moment effects. Specifically, they calculated the total (relative) radiative decay rates along with the nucleon spectra.

We have extended their calculations for a completely different reason. In the search for hyperon *leptonic* decays, the radiative decays are potentially

(*) This work was supported by the Office of Naval Research, the National Science Foundation and Air Force Office of Scientific Research.

(1) S. Barshay and R. F. Behrends: *Phys. Rev.*, **114**, 931 (1959).

a major source of unavoidable background. The detection ([2,3]) of the leptonic decays

$$\Sigma^{\pm} \to \begin{pmatrix} e^{\pm} \\ \mu^{\pm} \end{pmatrix} + n - \begin{pmatrix} \nu \\ \bar{\nu} \end{pmatrix},$$

$$\Lambda \to \begin{pmatrix} e^{-} \\ \mu^{-} \end{pmatrix} + p + \bar{\nu},$$

depends upon the observation of decay product momenta far from the normal 2-body decay value ([4]). Since normal decays are so prevalent, leptonic decays can only be distinguished with assurance if the decay secondary momentum is $\leqslant 100$ MeV/c or thereabout. Since radiative decays with low pion momentum are indistinguishable from muonic decays ([4]), it is necessary to know the relative fraction of all radiative decays which occur below 100 MeV/c or thereabout.

In this report we present 2 results:

A) The pion spectrum for radiative hyperon decay.

B) The relative fraction: number of radiative decays with momenta less than some maximum (q_m), divided by the total (non-radiative) rate of hyperon decay.

We should like to emphasize that the calculation is, to some extent, model-dependent. The radiative decay interaction is described by a phenomenological « $J_\mu A_\mu$ » hamiltonian with an effective coupling constant g. Similarly, the non-radiative decay is described by a « weak » Yukawa interaction with the same g. In this way the *relative* decay rate is independent of g but not of the model in which the calculations are carried out.

Further, no (photon) radiative corrections were included, so that an infrared divergence appears for low photon energies. However, only the high energy part of the γ spectrum contributes to the low energy end of the emitted pion spectrum, so that the results given here are not affected by the divergence.

([2]) J. Leitner, P. Nordin, A. H. Rosenfeld, F. T. Solmitz and R. D. Tripp: *Phys. Rev. Lett.*, **3**, 186 (1959).

([3]) W. E. Humphrey, J. Kirz, A. H. Rosenfeld, J. Leitner and Y. I. Rhee: *Phys. Rev. Lett.*, **6**, 478 (1961).

([4]) Distinction between electronic and muonic modes is made on the basis of ionization—this can be done with about 70% efficiency.

2. – The radiative decay pion spectrum.

We start with the Lagrangian of reference (1), using their notation.

$$L_{Y\to\pi+N+\gamma} = \frac{g}{\mu}\bar{\psi}_2(ia + b\gamma_5)\gamma^\mu\psi_1(\partial_\mu - i\varepsilon_2 A_\mu)\Phi - \sum_i \varepsilon_i\bar{\psi}_i A\psi_i - \\ -\frac{1}{2}\sum_i\frac{\mu_i}{2m_i}\bar{\psi}\,\sigma^{\mu\nu}\psi_i F_{\mu\nu} + ie[(\partial_\mu\varphi^*)\varphi - \varphi^*\partial_\mu\varphi)]A^\mu + \text{h.c.}\,,$$

where: $\varepsilon_i, m_i =$ charge, mass of the i-th baryon,

$i = 1$ is the decaying hyperon,

$i = 2$ is the decay product nucleon,

and $\mu =$ meson mass.

In the standard way, this yields the matrix element M given in eq. (2) of reference (1). The corresponding S matrix is then

$$\langle f|S|i\rangle = (2\pi)^4 M\left(\frac{1}{(2\pi)^{\frac{3}{2}}}\right)^4\left(\frac{1}{\sqrt{2}}\right)^2\sqrt{\frac{m_1}{E_1}}\sqrt{\frac{m_2}{E_2}}\sqrt{\frac{1}{Q}}\sqrt{\frac{1}{K}}\,,$$

where: $E_i, p_i =$ energy, momentum of the i-th baryon,

$Q, p =$ energy, momentum of the pion,

$K, k =$ energy, momentum of the photon.

The transition probability is then

$$P = \frac{1}{2\pi}\int \mathrm{d}^3p_2\,\mathrm{d}^3q\,\mathrm{d}^3k\left|\langle f|S|i\rangle\right|^2\cdot\delta^4(p_1 - p_2 - q - k)\,, \tag{2}$$

where we now carry out the integration over the nucleon energy and the photon variables in order to obtain the π spectrum.

The general result is somewhat complicated. We give below a simplified result which makes use of the following approximations:

a) $|p_2|/E_2 \approx |p_2|/m_2 \ll 1$;

b) in the integration over the angle between the photon and π, terms of the order of $q^2/2m_2$ are neglected compared to m_i, Q, etc., except when they occur in the denominator (where they contribute to the infra-red divergence).

We find, for the pion spectrum

$$\frac{dP}{dq} = \frac{q^2[|a|^2(A_1+B_1)+|b|^2(A_2+B_2)]}{16\pi^3 m_1 m_2 Q}, \tag{3}$$

where

$$A_{1,2} = \frac{1}{4}(1\pm\omega)^2 \frac{m_1}{Q(m_1-Q)(\Delta m - Q - q^2/2m_2)} \cdot$$

$$\cdot\left\{\left|2m_1^2\left(\Delta m - Q - \frac{q^2}{2m_2}\right)(-\omega\pm\omega)+m_1(m_1^2(1\mp\omega)^2-\mu^2)\right|\cdot\right.$$

$$\cdot\left|m_1^2\varepsilon_2^2\left(\frac{1}{\eta+\beta}U+\frac{1}{\eta+\beta}V\right)-2m_1(m_1-Q)\varepsilon_1\varepsilon_2\frac{1}{\eta}V+(m_1-Q)^2\varepsilon_1^2\left(\frac{\eta+\beta}{\eta^2}V-\frac{2\beta}{\eta}\right)\right|$$

$$-(m_1^2(1\mp\omega)^2-\mu^2)\frac{m_2^2}{m_1-Q}\left|m_1^2\varepsilon_2^2\left(\frac{2\beta}{(\eta+\beta)(1-\beta^2)}+\frac{\eta}{(\eta+\beta)^2}U+\frac{\eta}{(\eta+\beta)^2}V\right)-\right.$$

$$-2m_1(m_1-Q)\varepsilon_1\varepsilon_2\left(\frac{1}{\eta+\beta}U+\frac{1}{\eta+\beta}V\right)+(m_1-Q)^2\varepsilon_1^2\frac{1}{\eta}V\Big]-$$

$$-(m_1^2(1\mp\omega)^2-\mu^2)\frac{\mu^2}{Q}\left[m_1^2\varepsilon_2^2\left(\frac{2\eta}{(\eta+\beta)(1-\eta^2)}+\frac{\beta}{(\eta+\beta)^2}V+\frac{\beta}{(\eta+\beta)^2}U\right)-\right.$$

$$\left.\left.-2m_1(m_1-Q)\varepsilon_1\varepsilon_2\frac{2}{1-\eta^2}+(m_1-Q)^2\varepsilon_1^2\left(\frac{2(\eta+\beta)}{\eta(1-\eta^2)}-\frac{\beta}{\eta^2}V\right)\right]\right\},$$

and

$$B_{1,2} = -\left(\mu_1\pm\frac{\mu_2}{\omega}\right)(1\pm\omega)\left(\Delta m - Q - \frac{q^2}{2m_2}\right)\cdot$$

$$\cdot\left\{\frac{m_1\mu^2\varepsilon_2}{Q}\frac{1}{\eta}V-\frac{\mu^2(m_1-Q)\varepsilon_1}{Q}\left(\frac{\eta+\beta}{\eta^2}V-\frac{2\beta}{\eta}\right)\pm\frac{m_1m_2Q\varepsilon_2}{m_1-Q}\left(\frac{\eta+\beta}{\beta^2}U-\frac{2\eta}{\beta}\right)+2m_2Q\varepsilon_1\right\},$$

where

$$\omega \equiv \frac{m_2}{m_1}, \qquad \beta \equiv \frac{q}{m_1-Q}, \qquad \eta \equiv \frac{q}{Q}, \qquad \Delta m = m_1 - m_2,$$

$$U = \ln\left(\frac{1+\beta}{1-\beta}\right), \quad V = \ln\left(\frac{1+\eta}{1-\eta}\right),$$

and μ_1 = magnetic moment of hyperon,

μ_2 = magnetic moment of nucleon.

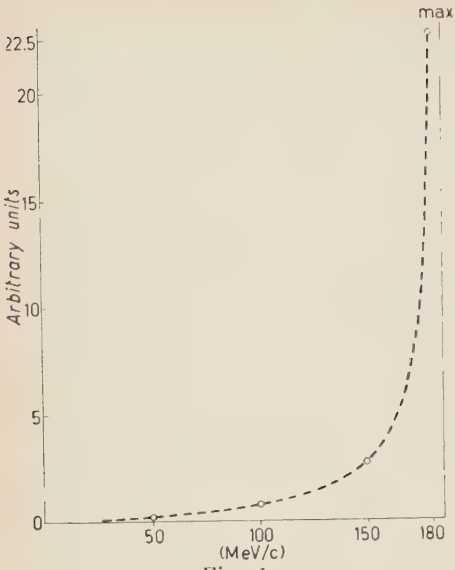

Fig. 1.

In the case of $\Sigma^{\pm} \to \pi^{\pm} + \mathrm{n} + \gamma$ decay ($\varepsilon_2 = 0$) this reduces to the following simple form:

$$(5) \qquad A_{1,2}^{\varepsilon_2 = 0} \simeq \frac{(1+\omega)^2 m_1^2 \Delta m^2 \varepsilon_1^2}{(\Delta m - Q - q^2/2m_2)} \cdot \left[\frac{m_1^2 - m_2^2 + \mu^2}{4 m_1 q} \ln\left(\frac{Q+q}{Q-q}\right) - 1\right] \cdot \begin{cases} (1-\delta^2) \,, \\ 1 \,, \end{cases}$$

where $\delta = \mu/\Delta m$.

$A_{1,2}^{\varepsilon_2 = 0}$ gives the desired spectrum if we neglect the small magnetic moment terms. The function A is plotted as a function of π momentum, (in the Σ rest frame) in Fig. 1.

3. – The integrated radiative decay rate.

The radiative decay rate, integrated up to some maximum pion momentum $q_{\max}$, is obtained directly from (3), (5). The integral cannot be done exactly in closed form. In order to evaluate the integral we use the approximation

$$\ln\left(\frac{1+\eta}{1-\eta}\right) \approx 2\eta\left(1 + \frac{1}{3}\eta^2\right),$$

which is in error by only $\sim 2\,\%$ at $q = 100$ MeV/c. We then obtain

$$(6) \qquad R_{\Sigma \to \pi + \mathrm{N} + \gamma}(0 < q < q_{\max}) = \frac{1}{\pi}\left(\frac{\varepsilon^2}{4\pi}\right)\left(\frac{g^2}{4\pi}\right) \cdot \frac{1}{m_1 m_2 \mu^2}\left[|a|^2(\alpha_1 + \beta_1) + |b|^2(\alpha_2 + \beta_2)\right],$$

where the functions α_i, β_i are

$$(7a) \qquad \alpha_{1,2} = \frac{m_1^5}{2}(1 \pm \omega)^2 \cdot \left\{ 2\omega^2(-\omega \pm \omega) \cdot \left| \frac{4}{3}(\varepsilon_2 - \varepsilon_1)^2 \cdot \left(-\lambda A + (1-\lambda^2)^{\frac{1}{2}} B - C\right) + \right.\right.$$

$$+ \left(-\frac{1}{3}\varepsilon_2^2 + \frac{8}{3}\varepsilon_1\varepsilon_2 - \frac{7}{3}\varepsilon_1^2\right) \cdot \left((1-\lambda^2)^{\frac{1}{2}} B - C - D\right) +$$

$$\left. \left. + \varepsilon_1^2 \left[(1-\lambda^2)^{\frac{1}{2}} B - \left(1 - \frac{\lambda^2}{2}\right) C - \left(1 + \frac{Q}{2m_1}\right) D \right| + \right.$$

$$+\left(\frac{1}{3}\varepsilon_2^2-2\varepsilon_1\varepsilon_2+\frac{1}{3}\varepsilon_1^2\right)\cdot\lambda^2\cdot\left(-\lambda A-\frac{m_1}{Q}D+(1-\lambda^2)^{\frac{1}{2}}B\right)+$$

$$+\left(-\frac{1}{3}\varepsilon_2^2+2\varepsilon_1\varepsilon_2-\frac{1}{3}\varepsilon_1^2\right)\cdot\lambda^2\cdot\left(-\lambda A-\frac{(1+2Q/m_1)}{2(Q^2/m_1^2)}D+\frac{1}{\lambda}E+(1-\lambda^2)^{\frac{1}{2}}B\right)\Bigg|+$$

$$+\left((1\pm\omega)^2-\lambda^2\right)\cdot\frac{4}{3}(\varepsilon_2-\varepsilon_1)^2\cdot\left(-\frac{\mu}{\Delta m}A+\frac{m_1}{\Delta m}\frac{(\Delta m^2-\mu^2)^{\frac{1}{2}}}{(m_1-\Delta m)}G-\frac{(1-\lambda^2)^{\frac{1}{2}}}{\omega}B\right)+$$

$$+\left(-\frac{1}{3}\varepsilon_2^2+\frac{8}{3}\varepsilon_1\varepsilon_2-\frac{7}{3}\varepsilon_1^2\right)\cdot\left(\frac{(\Delta m^2-\mu^2)^{\frac{1}{2}}}{m_1-\Delta m}G+C-\frac{(1-\lambda^2)^{\frac{1}{2}}}{\omega}B\right)+$$

$$+\varepsilon_1^2\cdot\left(\frac{\Delta m}{m_1}\frac{(\Delta m^2-\mu^2)^{\frac{1}{2}}}{m_1-\Delta m}G+(2-\omega)C+D-\frac{(1-\lambda^2)^{\frac{1}{2}}}{\omega}B\right)+$$

$$+\left(\frac{1}{3}\varepsilon_2^2-2\varepsilon_1\varepsilon_2+\frac{1}{3}\varepsilon_1^2\right)\cdot\frac{\mu^2}{\Delta m^2}\cdot\left(-(2-\omega)\lambda A-\frac{\Delta m}{Q}D+\frac{(\Delta m^2-\mu^2)^{\frac{1}{2}}}{m_1-\Delta m}G-\right.$$

$$\left.-\frac{\Delta m^2}{m_1^2}\frac{(1-\lambda^2)^{\frac{1}{2}}}{\omega}\cdot B\right)+\left(-\frac{1}{3}\varepsilon_2^2+2\varepsilon_1\varepsilon_2-\frac{1}{3}\varepsilon_1^2\right)\cdot\frac{\mu^2}{\Delta m^2}\left(-\frac{\mu}{\Delta m}(3-3\omega+\omega^2)A-\right.$$

$$\left.-\frac{2m_1Q+2Q\Delta m+m_1\Delta m}{2Q^2}D+\frac{\Delta m}{\mu}E+\frac{m_1}{\Delta m}\frac{(\Delta m^2-\mu^2)^{\frac{1}{2}}}{m_1-\Delta m}G-\frac{\Delta m^2}{m_1^2}\frac{(1-\lambda^2)^{\frac{1}{2}}}{\omega}B\right)\Bigg|-$$

$$-\left((1\mp\omega)^2-\lambda^2\right)\cdot\left[(\varepsilon_2-\varepsilon_1)^2\cdot\frac{4-\lambda^2}{3}\cdot\left(-\frac{\mu}{\Delta m}\omega^2A+\right.\right.$$

$$\left.+\frac{(\Delta m^2-\mu^2)^{\frac{1}{2}}}{\Delta m}G-\frac{(1-\lambda^2-\omega\lambda^2)(1-\lambda^2)^{\frac{1}{2}}}{1-\lambda^2}B-\frac{2\lambda\omega}{1+\lambda}F\right)+$$

$$+\left(-\frac{2}{3}\varepsilon_2^2+\frac{10}{3}\varepsilon_1\varepsilon_2-\frac{8}{3}\varepsilon_1^2\right)\cdot\left(\frac{(\Delta m^2-\mu^2)^{\frac{1}{2}}}{m_1}G-\frac{(1-\omega-\lambda^2)(1-\lambda^2)^{\frac{1}{2}}}{1-\lambda^2}B-\frac{2\lambda\omega}{1+\lambda}F\right)+$$

$$+\left(\frac{1}{3}\varepsilon_2^2-\frac{2}{3}\varepsilon_1\varepsilon_2+\frac{4}{3}\varepsilon_1^2\right)\cdot\left(\frac{\Delta m(\Delta m^2-\mu^2)^{\frac{1}{2}}}{m}G-\omega^2C+\right.$$

$$\left.+\frac{(-1+2\omega+\lambda^2-\lambda^2\omega)(1-\lambda^2)^{\frac{1}{2}}}{1-\lambda^2}B-\frac{2\lambda\omega}{1+\lambda}F\right)+$$

$$+\frac{2}{3}(\varepsilon_2-\varepsilon_1)^2\cdot\left(-\lambda^3\frac{(m_1^3-3m_1\Delta m^2+2\Delta m^3)}{m_1\Delta m^2}A-\lambda^2\frac{\omega^2}{Q/m_1\cdot\Delta m/m_1}D+\right.$$

$$\left.+\frac{\mu^2}{\Delta m^2}\frac{(\Delta m^2-\mu^2)^{\frac{1}{2}}}{m_1}G-\lambda^2\frac{(2m_1-\Delta m-3m_1\lambda^2+2\Delta m\lambda^2)(1-\lambda^2)^{\frac{1}{2}}}{m_1(1-\lambda^2)}B-\frac{2\lambda^3\omega}{1+\lambda}F\right)-$$

$$-\frac{1}{3}(\varepsilon_2-\varepsilon_1)^2\cdot\left(\lambda^2\frac{(-m_1^3\Delta m^2+2m_1^2\Delta m^3-m_1\Delta m^4+6m_1\Delta m^3Q-4\Delta m^4Q-m_1^3\Delta m Q)}{2\Delta m^3Q^2}D-\right.$$

$$-\lambda^3\frac{m_1^4-4\Delta m^3m_1+3\Delta m^4}{m_1\Delta m^3}A+\omega^2\frac{\mu}{\Delta m}E+\frac{\mu^2}{\Delta m^2}\frac{(\Delta m^2-\mu^2)^{\frac{1}{2}}}{\Delta m}G$$

$$\left.-\lambda^2\frac{(3m_1-2\Delta m-4m_1\lambda^2+3\Delta m\lambda^2)(1-\lambda^2)^{\frac{1}{2}}}{m_1(1-\lambda^2)}B-\frac{2\lambda^3\omega}{1+\lambda}F\right)\Bigg|$$

$$-\left((1\mp\omega)^2-\lambda\right)^2\cdot\left|\frac{1}{3}(\varepsilon_2^2-\varepsilon_1^2)\cdot\left(-\lambda^2\frac{\mu(m_1+\Delta m)}{\Delta m^2}A-\lambda\frac{\mu(m_1-Q)}{\Delta m Q}D+\right.\right.$$

$$+\frac{\mu^2}{\Delta m^2}\frac{(\Delta m^2-\mu^2)^{\frac{1}{2}}}{(m_1-\Delta m)}G-\frac{\lambda^2(1-\lambda^2)^{\frac{1}{2}}}{\omega}B\Big)+\frac{4}{3}(\varepsilon_2^2-\varepsilon_1^2)\cdot$$

$$\cdot\left(-\lambda^2\frac{\mu}{\Delta m}A-\lambda^2\frac{(m_1-2\Delta m)}{\Delta m}\frac{(1-\lambda^2)^{\frac{1}{2}}}{\omega}B-\lambda\frac{\mu}{\Delta m}C-\lambda^2\frac{(\Delta m^2-\mu^2)^{\frac{1}{2}}}{m_1-\Delta m}G\right)+$$

$$+\left(\left(1-\frac{4}{3}\lambda^2\right)\cdot\varepsilon_2^2-2\varepsilon_1\varepsilon_2+\left(1+\frac{4}{3}\lambda^2\right)\varepsilon_1^2\right)\cdot\left(\frac{(\Delta m^2-\mu^2)^{\frac{1}{2}}}{m_1-\Delta m}G+C-\frac{(1-\lambda^2)^{\frac{1}{2}}}{\omega}B\right)+$$

$$+(-\varepsilon_2^2+2\varepsilon_1\varepsilon_2-\varepsilon_1^2)\cdot\left(\frac{\Delta m}{m_1}\frac{(\Delta m^2-\mu^2)^{\frac{1}{2}}}{m_1-\Delta m}G+(2-\omega)C+D-\frac{(1-\lambda^2)^{\frac{1}{2}}}{\omega}B\right)+$$

$$+\left(-\frac{1}{3}\varepsilon_2^2+\frac{1}{3}\varepsilon_1^2\right)\cdot\left(\frac{\lambda^2}{2}\mu^2\frac{(2m_1Q^2-2m_1Q\Delta m-2\Delta m^2Q-m_1\Delta m^2)}{Q^2\Delta m^3}D-\right.$$

$$\left.\left.-\lambda^4\frac{\mu(m_1^2+m_1\Delta m+\Delta m^2)}{\Delta m^3}A+\lambda^2\frac{\mu}{\Delta m}E+\lambda^2\frac{\mu^2}{\Delta m^2}\frac{(\Delta m^2-\mu^2)^{\frac{1}{2}}}{m_1-\Delta m}G-\lambda^4\frac{(1-\lambda^2)^{\frac{1}{2}}}{\omega}B\right)\right]\Bigg\},$$

and

$$(7b)\quad \beta_{1;2}=-m_1^5\cdot\left(\mu_1\pm\frac{\mu_2}{\omega}\right)\cdot(1\pm\omega)\cdot\left[\frac{1}{2}\left\{\varepsilon_2\left(\mp\omega^2\pm\frac{\lambda^2}{2}-\frac{4}{3}\lambda^2\mp\frac{1}{2}\right)+\right.\right.$$

$$\left.+\varepsilon_1\lambda^2\left(\frac{7}{3}-\omega+\frac{\lambda^2}{2\omega}\right)\right\}\cdot\left(\frac{Q}{m_1}D-\lambda^2C\right)+$$

$$+\frac{1}{3}\left\{\varepsilon_2\left(\mp\omega-\frac{2}{3}\frac{\lambda^2}{\omega}\mp\frac{1}{2}\right)+\varepsilon_1\left(\pm\omega\mp\omega^2-\lambda^2+\frac{2}{3}\frac{\lambda^2}{\omega}\mp\frac{3}{4}D^2\right)\right\}\cdot D^3+$$

$$+\frac{1}{4}\left(\mp\frac{\varepsilon_2}{2}\mp\varepsilon_1\omega-\frac{\varepsilon_1\lambda^2}{2\omega}\right)\cdot\left(\frac{Q}{m_1}D^3+\frac{Q}{2m_1}\lambda^2D-\frac{\lambda^4}{2}C\right)+$$

$$+(\varepsilon_2-\varepsilon_1)\cdot\lambda^2\cdot\left(\frac{4}{3}-\frac{4}{3}\omega-\frac{\lambda^2}{2\omega}\right)\cdot(D-\lambda A)+$$

$$+\frac{1}{3}(\varepsilon_2-\varepsilon_1)\cdot\lambda^4\cdot\left\{C-\frac{m_1}{2}D-\left(1-\omega+\frac{\lambda^2}{2\omega}\right)\cdot\left(\frac{E}{\lambda}-\frac{m_1^2}{2Q^2}D\right)\right\}\pm$$

$$\left.\pm\frac{\varepsilon_2}{2}(1+2\omega)\cdot\left((1-\lambda^2)^{\frac{1}{2}}B-C-D\right)\right].$$

With the following notation

$$A=\cos^{-1}\frac{\mu}{Q},$$

$$B=\ln\left|\frac{[(1-\lambda)/(1+\lambda)]^{\frac{1}{2}}+[(Q-\mu)/(Q+\mu)]^{\frac{1}{2}}}{[(1-\lambda)/(1+\lambda)]^{\frac{1}{2}}-[(Q-\mu)/(Q+\mu)]^{\frac{1}{2}}}\right|,$$

$$C = \ln\left(\frac{Q+q}{\mu}\right),$$

$$D = \frac{q}{m_1},$$

$$E = \mathrm{tg}^{-1}\sqrt{\frac{Q-\mu}{Q+\mu}},$$

$$F = \frac{(Q-\mu)/(Q+\mu)]^{\frac{1}{2}}}{[(1-\lambda)/(1+\lambda)] - [(Q-\mu)/(Q+\mu)]},$$

$$G = \ln\left|\frac{[(1-\omega-\lambda)/(1-\omega+\lambda)]^{\frac{1}{2}} + [(Q-\mu)/(Q+\mu)]^{\frac{1}{2}}}{[(1-\omega-\lambda)/(1-\omega+\lambda)]^{\frac{1}{2}} - [(Q-\mu)/(Q+\mu)]^{\frac{1}{2}}}\right|,$$

and $\lambda \equiv \mu/m_1$.

4. – The non-radiative decay rate.

Using the phenomenological Lagrangian,

$$L_{Y\to\pi+N} = \frac{g}{\mu}\bar{\psi}_2(ia + b\gamma_5)\gamma_\mu\psi_1\partial_\mu\varphi,$$

we have calculated, in the standard way, the non-radiative total decay rate, $R_{Y\to N+\pi}$. Details of the calculation are given in Appendix I. We find

$$R_{Y\to\pi+N} = \left(\frac{g^2}{4\pi}\right)\frac{\Delta m^3(1+\omega)^3(1-\delta^2)^{\frac{1}{2}}}{4\mu^2}\left[|a|^2 + |b|^2(1-\delta^2)\right]. \tag{8}$$

5. – The relative radiative decay rate.

The relative radiative decay rate $\mathscr{R}$, obtained from (7) and (8), *i.e.*,

$$\mathscr{R} \equiv \frac{R_{Y\to\pi+N+\gamma}(q<q_{\max})}{R_{Y\to\pi+N}}, \tag{9}$$

is independent of the effective coupling constant g. As a typical example we evaluate $\mathscr{R}$ for Σ^- decay.

It is known from up-down asymmetry measurements [5] that the Σ^- decays through a pure angular momentum state, either s or p. Since either

[5] R. L. Cool, J. W. Cronin, B. Cork and W. A. Wenzel: *Phys. Rev.*, **114**, 912 (1959).

alternative gives approximately the same results, we calculate only the s-wave rate. Setting $b=0$ in (7) and (8), and rewriting α_1, as the product

$$\alpha_1 = \frac{m_1^3}{2}(1+\omega)^2\Delta m^2(1-\delta^2)\,\bar{\alpha}_1\,,$$

where $\bar{\alpha}_1$ is a dimensionless function of the masses and the $q_{\max}$, we get

$$\mathscr{R} \simeq \frac{m_2}{2}\frac{m_2\varepsilon_1^2(1-\delta^2)}{\pi^2\omega^2\Delta m(1+\omega)(1-\eta^2)^{\frac{1}{2}}}\,\bar{\alpha}_1(q_m,\, m_i)\,, \tag{10}$$

or

$$\mathscr{R} \approx 2\cdot 10^{-2}\,\bar{\alpha}(q_m,\, m_i)\,.$$

For the case of Σ^- decay, and with $q_{\max}=100$ MeV/c $\bar{\alpha}_1 \approx 0.02$, neglecting terms of the order of λ^2, $\mathscr{R}\approx 0.04\,\%$.

6. – Conclusions.

The rate of radiative hyperon decays with secondaries below ~ 100 MeV c is small. In particular, for Σ^- decay we find that $\mathscr{R}\approx .04\,\%$. This rate, however, is quite comparable with the observed rate [3] of Σ^- electronic decay [6],

$$R_{\Sigma^-\to e^-+N^0+\bar{\nu}} \simeq \left(0.1^{+.1}_{-.05}\right)\%\,.$$

The uncertainty in the expected radiative rate could easily be a factor of 2 since the calculation is model-dependent.

It seems then that radiative hyperon decay might well be an important source of unavoidable background in a precise measurement of the hyperon leptonic decay rate.

Appendix

Non radiative hyperon decay.

The Lagrangian (4), in the usual way gives rise to an S matrix element

$$\langle f|S|i\rangle = \frac{g}{\mu}\left(\frac{1}{2^{\frac{3}{2}}(2\pi)^{\frac{1}{2}}}\right)\bar{u}(p_2)[-ia\gamma_\mu k_\mu + b\gamma_5\gamma_\mu k_\mu]u(p_1) =$$

$$= \frac{g}{\mu}\left(\frac{1}{2^{\frac{3}{2}}(2\pi)^{\frac{1}{2}}}\right)[ia\,\Delta m\,\bar{u}(p_2)u(p_1) - b(m_1+m_2)\bar{u}(p_2)\gamma_5 u(p_1)]\,,$$

(6) Muonic Σ decay should be even smaller since the available phase space is down by ~ 3.

we get

$$|\langle f|S|i\rangle|^2 = \frac{g^2}{\mu^2}\frac{1}{16\pi}\{a^2\Delta m^2\,\mathrm{Sp}\,[(-i\gamma p_1 + m_1)(-i\gamma p_2 + m_2)] - \\ - b^2 M^2\,\mathrm{Sp}\,[(i\gamma p_1 + m_1)(-i\gamma p_2 + m_2)]\}\,,$$

averaging over spin states,

$$= \left(\frac{1}{2\sigma_\Sigma + 1}\right)\frac{g^2}{\mu^2}\frac{1}{4\pi}\{a^2\Delta m^2[-p_1p_2 + m_1m_2] - b^2M^2[p_1p_2 + m_1m_2]\}\,.$$

In the Σ rest frame, this becomes

$$= \frac{g^2}{2\mu^2}\frac{1}{4\pi}\{a^2\Delta m^2(m_1E_2 + m_1m_2) + b^2M^2(m_1E_2 - m_1m_2)\}\,,$$

which, with $F_2 = (m_1^2 + m_2^2 - \mu^2)/2m_1$, becomes

$$= \frac{g^2}{\mu^2}\frac{1}{16\pi}\Delta m^2M^2\left\{a^2\left(1 - \frac{\mu^2}{M^2}\right) + b^2\left(1 - \frac{\mu^2}{\Delta m^2}\right)\right\} \approx \frac{g^2}{\mu^2}\frac{\Delta m^2M^2}{16\pi}\left|a^2 + b^2\left(1 - \frac{\mu^2}{\Delta m^2}\right)\right|\,.$$

The total transition rate is then

$$R_{\Sigma\to\pi+\mathcal{N}} = \frac{1}{m_1 2\pi}\int \delta^4(p_1 - k - p_2)\,\frac{\mathrm{d}^3k}{K}\,\frac{\mathrm{d}^3p_2}{E_2}\,|\langle f|S|i\rangle|^2 = \\ = \frac{1}{2\pi m_1}\int \delta^3(-k - p_2)\,\delta(m_1 - K - E_2)\,\frac{\mathrm{d}^3k}{K}\,\frac{\mathrm{d}^3p}{E_2}\,|\langle f|S|i\rangle|^2 = \\ = \frac{1}{2\pi m_1}\int \frac{\mathrm{d}^3k}{K}\,\frac{1}{\sqrt{m_2^2 + k^2}}\,\delta\left(m_1 - K - \sqrt{m_2^2 + k^2}\right)\,|\langle f|S|i\rangle|^2 = \\ \equiv \frac{2}{m_1}\int \frac{k^2}{K\sqrt{m_2^2 + k^2}}\,\frac{d(f(k))}{\partial f(k)/\partial k}\,\delta(f(k))\,|\langle f|S|i\rangle|^2 = \\ = \frac{2}{m_1}\,\frac{k^2}{K\sqrt{m_2^2 + k^2}}\cdot\frac{1}{km_1/K\sqrt{(m_2^2 + k^2}}\,|\langle f|S|i\rangle|^2 = \frac{2k}{m_1^2}\,|\langle f|S|i\rangle|^2.$$

In the Σ rest frame $k = p_2 \simeq \Delta m\,M(1 - \delta^2)^{\frac{1}{2}}/2m_1$, hence

$$R_{\Sigma\to\pi+\mathcal{N}} \simeq \left(\frac{g^2}{4\pi}\right)\cdot\frac{(\Delta m)^3(1 + \omega)^3(1 - \delta^2)^{\frac{1}{2}}}{4\mu^2}\,[a^2 + b^2(1 - \delta^2)^{\frac{1}{2}}].$$

RIASSUNTO (*)

Si estendono i calcoli di Barshay *et al.* sul decadimento radiativo degli iperoni in modo da includere gli spettri del momento del pione. I risultati mostrano che il decadimento radiativo degli iperoni apparirà, come un'importante causa di fondo nello studio del decadimento leptonico degli iperoni.

(*) *Traduzione a cura della Redazione.*

Electromagnetic Properties of Superconductors.

V. Ambegaokar (*) and L. P. Kadanoff (**)

Institute for Theoretical Physics, University of Copenhagen - Copenhagen

(ricevuto il 19 Luglio 1961)

Summary. — A method of calculating the response of superconductors to weak electromagnetic fields is formulated. The response is generated from a single-particle Green's function, defined in the presence of an electromagnetic perturbation, that satisfies the conditions imposed by gauge invariance and charge conservation. The response function is thus itself explicitly gauge invariant and charge conserving. The single-particle Green's function is obtained by making Gorkov's factorization of the two-particle Green's function in the presence of the external field. The symmetry properties of the approximation are used to simplify the calculation considerably. This is trivially carried out in the London limit. An economical derivation is thus obtained of Anderson's result that the Bardeen, Cooper and Schrieffer quasi-particle excitations must be supplemented by a collective excitation in order to satisfy the conservation laws.

1. – Introduction.

A reasonable calculation of the electromagnetic properties of a many-particle system must satisfy certain consistency conditions. It should be gauge invariant, which means that the calculated response should be unchanged when the perturbing potentials are re-gauged. In addition, the induced charge and current densities should satisfy a continuity equation. We give here a calculation of the response of superconductors to weak electromagnetic disturbances that explicitly satisfies these conditions, using a method that imposes them from the start (1). The essential idea of the method is that in the pres-

(*) Ford Foundation Fellow.

(**) National Science Foundation Post-doctoral Fellow.

(1) G. Baym and L. P. Kadanoff: *Phys. Rev.* **124**, 287 (1961).

ence of an electromagnetic perturbation one must generalize the original pairing of BARDEEN, COOPER and SCHRIEFFER (2), (between electrons of opposite momentum and spin) and pair electrons that themselves feel the effects of the perturbation. This pairing is most easily introduced in the Green's function formulation of the theory (3). It is achieved by making Gorkov's factorization of the two-particle Green's function in the presence of the external fields. The factorization leads to an approximate determination of the single-particle Green's function. From this Green's function one can generate a linear response function that has the correct invariance properties.

The method turns out to be equivalent to the generalized Hartree-Fock method (4), though it seems better equipped for keeping the formal transformation properties of the approximation exhibited. The part of the response linear in the external fields corresponds to the generalized random phase approximation first used by ANDERSON (5), and we obtain his result, namely, that the superconductor has, in addition to the quasi-particle excitations of BCS, a collective vibration. This collective mode is not excited by a static magnetic field in the transverse gauge, so that the BCS calculation of the Meissner effect is correct in the gauge they use. However, the collective mode can be excited by an electric field, and it plays an important role in the gauge invariance of the theory.

A conceptually very simple interpretation of the result emerges from the mathematics of our treatment. We find that for long wavelength disturbances (wavenumber $\ll$ Fermi wavenumber) the response can be thought of as due to the motion of the BCS quasi-particles alone, under the influence however of certain effective potentials which reflect the modification of the external potentials by the dynamical medium in which the quasi-particles move. In part this modification is just the usual self-consistent field correction to the mean potential energy in the system. In addition, however, there is a correction due to the motion of paired particles in the medium. This correction

(2) J. BARDEEN, L. COOPER and J. R. SCHRIEFFER: *Phys. Rev.*, **108**, 1175 (1957), hereafter referred to as BCS. See also N. N. BOGOLIUBOV, TOLMACHEV and SHIRKOV: *A New Method in the Theory of Superconductivity* (Moscow, 1958); J. G. VALATIN: *Nuovo Cimento*, **7**, 843 (1958).

(3) L. P. GORKOV: *Žurn. Èksp. Teor. Fiz.*, **34**, 735 (1958); translation: *Sov. Phys. JETP*, **7** (34), 505 (1958); P. C. MARTIN and L. P. KADANOFF: to be published; J. SAWICKI: *Ann. Phys.*, **13**, 237 (1961); D. J. THOULESS: *Ann. Phys.*, **10**, 553 (1960).

(4) Y. NAMBU: *Phys. Rev.*, **117**, 648 (1960); J. G. VALATIN: *Phys. Rev.*, **122**, 1012 (1960); N. N. BOGOLIUBOV: *Usp. Fiz. Nauk*, **67**, 549 (1959), translation: *Sov. Phys. Usp.*, **67**, 236 (1959).

(5) P. W. ANDERSON: *Phys. Rev.*, **112**, 1900 (1958). Also G. RICKAYZEN: *Phys. Rev.*, **115**, 795 (1959); N. N. BOGOLIUBOV *et al.*: op. cit.; Y. NAMBU: op. cit.; additional references to the fairly extensive literature on gauge invariance and the BCS theory are given in this last paper.

has the remarkable effect of subtracting from the external scalar potential at a point a quantity proportional to the mean energy per paired particle at that point, and from the external vector potential a quantity proportional to the mean momentum per paired particle. In other words, the quasi-particles effectively measure their zeros of energy and momentum with respect to the background of paired particles. The collective vibration occurs, as in previous work, as a resonance, infinitely sharp in this approximation, in the response of the paired particles to the external disturbance.

In performing the calculation, important use is made of the symmetry properties, mentioned above, of the approximation, and of an additional symmetry which it possesses. This is a symmetry between particles and holes which occurs in the long wavelength limit. As a result of this use of symmetries the method is algebraically quite economical.

2. – Green's functions and conservation laws.

This section is concerned with some formal preliminaries. We define the Green's functions, establish the conditions imposed upon them by the conservation laws, and show how to construct approximations which satisfy these conditions.

Consider a system of particles interacting through a two-body potential in an external electromagnetic field. The Hamiltonian for the system may be written as

$$H(t) = \int \left(\psi^{\dagger}(x) h(x t; \boldsymbol{A}\varphi)\, \psi(x)\right) \mathrm{d}\tau + \tag{2.1}$$

$$+ \frac{1}{2} \int \left(\psi^{\dagger}(x)\left(\psi^{\dagger}(x')\, \psi(x')\right) \psi(x)\right) v(x, x')\, \mathrm{d}\tau\, \mathrm{d}\tau' ,$$

where

$$h(1; \boldsymbol{A}\varphi) = \frac{1}{2m}\left(\boldsymbol{\nabla}_1 - \frac{e}{c}\boldsymbol{A}(1)\right)^2 + e\varphi(1) - \mu . \tag{2.2}$$

Above, $\psi(x)$ is the usual quantized field operator; those brackets whose meaning is not otherwise obvious indicate spin summation; and μ is the chemical potential with respect to which it is convenient to measure single-particle energies. The equation of motion for the Heisenberg representation field operator $\psi(1)$ under the influence of (2.1) is

$$\left(i\frac{\partial}{\partial t_1} - h(1; \boldsymbol{A}\varphi)\right) \psi(1) = v(1\bar{1})\left(\psi^{\dagger}(\bar{1})\, \psi(\bar{1})\right) \psi(1) . \tag{2.3}$$

Here $v(11') = v(x, x')\,\delta(t - t')$ and we have used a « summation convention » that saves writing namely that symbols with a bar over them are to be integrated over all space and time. Let us require that at $t = \pm\infty$ the electromagnetic perturbation is zero. Then the solution of (2.3) has the well-known form [6]

$$\psi(1) = U(-\infty, t)\exp[iH_0 t]\,\psi(x)\exp[-iH_0 t]\,U(t, -\infty)\,, \tag{2.4}$$

where

$$U(t, -\infty) = T\exp\left[-i\int_{-\infty}^{t} V_I(t')\,\mathrm{d}t'\right], \tag{2.5}$$

with

$$H_0 = H(-\infty) \tag{2.6}$$

and

$$V_I(t) = \exp[iH_0 t][H(t) - H_0]\exp[-iH_0 t]\,. \tag{2.7}$$

In (2.5) T is the Wick time ordering symbol. The single-particle Green's function in the presence of the perturbation is defined as

$$G(11', \boldsymbol{A}\varphi) = -iT\langle\langle\psi(1; \boldsymbol{A}\varphi)\,\psi^{\dagger}(1', \boldsymbol{A}\varphi)\rangle\rangle \equiv \tag{2.8}$$

$$\equiv -iT\,\frac{\langle U(\infty, -\infty)\,\psi(1, \boldsymbol{A}\varphi)\,\psi^{\dagger}(1, \boldsymbol{A}\varphi)\rangle}{\langle U(\infty, -\infty)\rangle}\,,$$

where $\langle\ldots\rangle$ indicates an expectation value in the ground state of H_0 since we restrict ourselves for simplicity to zero temperature.

How does the exact Green's function (2.8) behave under a gauge transformation? From the equation of motion (2.3) we see that if the external fields are regauged according to

$$\begin{cases} \boldsymbol{A} \to \boldsymbol{A}' = \boldsymbol{A} - \boldsymbol{\nabla}\Lambda\,, \\ \varphi \to \varphi' = \varphi + \dfrac{1}{c}\dfrac{\partial\Lambda}{\partial t}\,, \end{cases} \tag{2.9}$$

the field operators transform according to

$$\psi(1; \boldsymbol{A}'\varphi') = \exp\left[-\frac{ie}{c}\Lambda(1)\right]\psi(1; \boldsymbol{A}\varphi)\,. \tag{2.10}$$

---

[6] See for example S. Schweber, H. A. Bethe and F. de Hoffmann: *Mesons and Fields*, vol. **1** (New York, 1955).

Similarly one finds

$$\psi^\dagger(1; \boldsymbol{A}'\varphi') = \exp\left[\frac{ie}{c}\Lambda(1)\right]\psi^\dagger(1; \boldsymbol{A}\varphi)\,. \tag{2.10*}$$

Thus the transformation properties of (2.8) are

$$G(11'; \boldsymbol{A}'\varphi') = \exp\left[-\frac{ie}{c}\Lambda(1)\right] G(11'; \boldsymbol{A}\varphi) \exp\left[+\frac{ie}{c}\Lambda(1')\right]. \tag{2.11}$$

A gauge invariant approximation for G must also satisfy (2.11).

Now let us look at the question of charge conservation and what it implies for G. Charge conservation implies that in the presence of arbitrary fields

$$\left\langle \frac{\partial}{\partial t_1}\varrho(1) + \boldsymbol{\nabla}_1\cdot\boldsymbol{J}(1)\right\rangle_{\boldsymbol{A},\varphi} = 0\,, \tag{2.12}$$

where

$$\varrho(1) = e\langle\psi^\dagger(1)\,\psi(1)\rangle\,, \tag{2.13}$$

and

$$\boldsymbol{J}(1) = \frac{e}{2mi}\left[(\psi^\dagger(1)\,\boldsymbol{\nabla}_1\psi(1)) - (\boldsymbol{\nabla}_1\psi^\dagger(1)\cdot\psi(1))\right] - \frac{e}{mc^2}\boldsymbol{A}(1)\varrho(1) \equiv \boldsymbol{j}(1) - \frac{e}{mc^2}\boldsymbol{A}(1)\varrho(1)\,. \tag{2.14}$$

Written in terms of G (2.12) requires that

$$\frac{\partial}{\partial t_1}G(11^+) + (\boldsymbol{\nabla}_1 + \boldsymbol{\nabla}_1')\cdot\frac{(\boldsymbol{\nabla}_1 - \boldsymbol{\nabla}_1')}{2mi}\,G(11')\Big|_{1'=1^+} - \frac{e}{mc}\,\boldsymbol{\nabla}_1\cdot\boldsymbol{A}(1)\,G(11^+) = 0\,. \tag{2.15}$$

$[1^+ \equiv (x, t+0)]$.

Now (2.15) is trivially satisfied for the exact G because (2.12) is satisfied without the expectation value. However, in order to see how to construct approximations for G which satisfy (2.15), let us see how this identity comes about from the equations of motion. From (2.3) we have

$$\left[i\frac{\partial}{\partial t_1} - \frac{1}{2m}\left(\frac{1}{i}\boldsymbol{\nabla}_1 - \frac{e}{c}\boldsymbol{A}(1)\right)^2 - e\varphi(1) + \mu\right] G(11'; \boldsymbol{A}\varphi) = \delta(11') - iv(1\bar{1})\,G(1\bar{1}; 1'\bar{1}^+; \boldsymbol{A}\varphi)\,, \tag{2.16}$$

where $\delta(11')$ term comes from the discontinuity in G for $t = t'$. In (2.16) there

occurs the two-particle Green's function which is defined according to

$$G(12;34;\boldsymbol{A}\varphi) = (-i)^2 T\langle\langle \psi(1)\psi(2)\psi^\dagger(4)\psi^\dagger(3)\rangle\rangle \,. \tag{2.17}$$

From the equation of motion for the adjoint operator $\psi^\dagger(1)$ one also gets

$$\left[-i\frac{\partial}{\partial t_1} - \frac{1}{2m}\left(-\frac{1}{i}\nabla_1' - \frac{e}{c}\boldsymbol{A}(1')\right)^2 - e\varphi(1') + \mu\right] G(11') = \tag{2.18}$$
$$= \delta(11') - iv(\bar{1}1')G(1\bar{1}^-;1'\bar{1}) \,.$$

Subtracting (2.18) from (2.16) and setting $1' = 1^+$ one gets (2.15). In the approximate calculation of G we will make subsequently, an approximation for $G_2(\boldsymbol{A},\varphi)$ will be substituted in (2.16) and (2.18). The approximation will be such that the steps leading from (2.16) and (2.18) to (2.15) go through, and thus the latter will be satisfied.

We have exhibited the conditions imposed on $G(11';\boldsymbol{A}\varphi)$ by gauge invariance and number conservation and hinted that we shall be able to calculate it approximately in such a way that these conditions are satisfied. It remains to show how the gauge invariant and number conserving response of the system to weak external fields is obtained from G. Suppose we expanded the exact G in powers of $\boldsymbol{A}$ and φ. Writing this quantity in the interaction representation, we have trivially

$$G(11';\boldsymbol{A}\varphi) = -i\frac{T\langle S\psi(1)\psi^\dagger(1')\rangle}{\langle S\rangle} \,, \tag{2.19}$$

where the time-dependence of ψ is now determined by H_0 alone and S is given by

$$S \equiv \boldsymbol{U}(\infty,-\infty) = T\exp\left[-i\int_{-\infty}^{\infty} V_I(t)\,\mathrm{d}t'\right]. \tag{2.20}$$

Thus

$$\left.\frac{\delta G(11';\boldsymbol{A}\varphi)}{\delta\varphi(2)}\right|_{\varphi=0} = -i^2[T\langle\psi(1)\psi^\dagger(1')\varrho(2)\rangle - T\langle\psi(1)\psi^\dagger(1')\rangle\langle\varrho(2)\rangle] = \tag{2.21}$$
$$= -e[G(12;1'2'^+) - G(11')G(22^+)] \,,$$

and

$$\left.\frac{\delta G(11';\boldsymbol{A}\varphi)}{\delta\boldsymbol{A}(2)}\right|_{\varphi=0} = \frac{e}{c}\frac{\nabla_2 - \nabla_2'}{2mi}[G(12;1'2') - G(11')G(22')]_{2'=2^+} \,. \tag{2.22}$$

Now because $G(11';\boldsymbol{A}\varphi)$ satisfies (2.15) the right-hand sides of (2.21) and (2.22) also satisfy a continuity equation in the variables 1 and 1'. Similarly we can generate according to (2.21) and (2.22) an *approximate* G_2 in the absence of

fields from the approximate G_1 which satisfies (2.15) when the fields are present. If the approximate G_1 also satisfies the gauge invariance condition (2.11), the linear response of the system, which is related to $G_2(V=0)$ in the straightforward way we review below, will be both gauge invariant and charge conserving.

The causal response of a system to weak electromagnetic fields may be written in the form (first order time-dependent perturbation theory)

$$\text{(2.23)}\qquad \begin{cases} \langle \varrho(1)\rangle_c = -i\left\{\langle[\varrho(1),\varrho(\bar{1})]\,\varphi(\bar{1}) - \frac{1}{c}\,[\varrho(1),\boldsymbol{j}(\bar{1})]\cdot\boldsymbol{A}(\bar{1})\right\}\theta(t_1-\bar{t}_1)\,, \\ \langle \boldsymbol{J}(1)\rangle_c = -i\left\{\langle[\boldsymbol{j}(1),\varrho(\bar{1})]\,\varphi(\bar{1}) - \frac{1}{c}\,[\boldsymbol{j}(1),\boldsymbol{j}(\bar{1})]\cdot\boldsymbol{A}(\bar{1})\right\}\theta(t_1-\bar{t}_1) - \\ \qquad\qquad - \dfrac{ne^2}{mc}\boldsymbol{A}(1)\,, \end{cases}$$

where

$$\text{(2.24)}\qquad \theta(t) = 1\,,\quad t>0\,;\qquad 0\,,\quad t<0\,,$$

and n is the number density of particles in the system. The operators on the right of (2.23) were defined in (2.13)–(2.14) and are in the interaction representation. The expectation values on the right of (2.23) contain products of four field operators and are trivially related to G_2. Substituting the conserving G_2 generated by the variational derivatives (2.21) and (2.22) into (2.23), one finds

$$\text{(2.25)}\qquad \begin{cases} \langle \varrho(1)\rangle_c = 4e\ \mathrm{Im}\left\{\dfrac{\delta G(11^+)}{\delta\varphi(1)}\,\varphi(\bar{1}) + \dfrac{\delta G(11^+)}{\delta\boldsymbol{A}(1)}\cdot\boldsymbol{A}(\bar{1})\right\}\theta(t_1-\bar{t}_1)\,, \\ \langle \boldsymbol{J}(1)\rangle_c = 4e\ \mathrm{Im}\,\dfrac{\boldsymbol{\nabla}_1-\boldsymbol{\nabla}_1'}{2mi}\left\{\dfrac{\delta G(11')}{\delta\varphi(\bar{1})}\,\varphi(\bar{1}) + \dfrac{\delta G(11')}{\delta\boldsymbol{A}(1)}\cdot\boldsymbol{A}(\bar{1})\right\}_{1'=1}\theta(t_1-\bar{t}_1) - \\ \qquad\qquad - \dfrac{ne^2}{mc}\boldsymbol{A}(1)\,. \end{cases}$$

Eq. (2.25) formally solves the problem of generating a consistent approximation for the linear response of a system from an approximate single-particle Green's function that satisfies (2.11) and (2.15). However, the necessity for taking imaginary parts somewhat complicates an actual calculation of (2.25). It is easier to calculate the time ordered response functions defined by

$$\text{(2.26)}\qquad \begin{cases} \langle \varrho(1)\rangle = -2ie\left[\dfrac{\delta G(11^+)}{\delta\varphi(\bar{1})}\,\varphi(\bar{1}) + \dfrac{\delta G(11^+)}{\delta\boldsymbol{A}(1)}\cdot\boldsymbol{A}(\bar{1})\right], \\ \langle \boldsymbol{J}(1)\rangle = -2ie\,\dfrac{\boldsymbol{\nabla}_1-\boldsymbol{\nabla}_1'}{2mi}\left[\dfrac{\delta G(11')}{\delta\varphi(\bar{1})}\,\varphi(\bar{1}) + \dfrac{\delta G(11')}{\delta\boldsymbol{A}(1)}\cdot\boldsymbol{A}(\bar{1})\right]_{1'=1^+} - \dfrac{ne^2}{mc}\boldsymbol{A}(1)\,. \end{cases}$$

An examination of the spectral representations of the exact causal and time ordered response functions shows that these two quantities are related. In particular, one finds that one can obtain the Fourier transform with respect to time of the former from that of the latter by moving all the singularities to just below the real axis of the complex frequency plane. It is therefore convenient to work with (2.26) and to go over to (2.23) at the very end by this device.

The application of these ideas (which are presented in more detail in reference [1]) to the problem of calculating the linear response function of a superconductor will be given in what follows.

3. – Linear response function for superconductors.

In this section we shall construct an approximation for the single-particle Green's function for a superconductor in an electromagnetic field. The approximation is gauge invariant and charge conserving in the sense discussed in the last section. From it we generate a linear response function satisfying the conservation laws.

We shall be using the model Hamiltonian introduced by GORKOV [3]. In the presence of an electromagnetic perturbation this takes the form

$$H = \int \left(\psi^{\dagger}(x)\, h(xt;\, \boldsymbol{A}\varphi)\, \psi(x)\right) \mathrm{d}\tau + \frac{V}{2} \int \left(\psi^{\dagger}(x)\left(\psi^{\dagger}(x)\,\psi(x)\right)\psi(x)\right) \mathrm{d}\tau \,. \tag{3.1}$$

Here $h(1;\, \boldsymbol{A}\varphi)$ is given by (2.2). The attractive interaction ($V<0$) is assumed only to connect states within a shell of width $2\omega_{\mathrm{D}}$ (ω_{D} is the Debye frequency) about the Fermi surface. (Some of the effects of the Coulomb interaction are included in (3.1). The Coulomb interaction will also have important long range effects which will be taken into account in the next section.) The equation of motion of the single-particle Green's function for the Hamiltonian (3.1) is

$$\left[i\,\frac{\partial}{\partial t_1} - h(1;\, \boldsymbol{A}\varphi)\right] G(11';\, \boldsymbol{A}\varphi) = \delta(11') - iVT\,\langle\!\langle \left(\psi^{\dagger}(1)\,\psi(1)\right)\psi(1)\,\psi^{\dagger}(1')\rangle\!\rangle \,. \tag{3.2}$$

The essential feature of the superconducting state is introduced into (3.2) by making a physically motivated factorization of the two-particle Green's function that occurs on the right. One recognizes that the two-particle Green's function $G_2(12;\, 1'2')$ describes the propagation of two electrons in the N-particle medium. For weak fields $\boldsymbol{A}$, φ we expect that these electrons will find it energetically favorable to propagate as a correlated pair [2], and that the N-particle medium itself will contain a large number of pairs. Thus it seems

reasonable that operating on the « ground » (7) state of the N-particle superconductor with two creation operators will lead with a large probability to the « ground » state of the $N-2$-particle superconductor. If in addition we keep the possibility of purely independent propagation, we are led to write

$$G_2(12;1'2') = G(11')G(22') - G(12')G(1'2) - F(12)\bar{F}(2'1)\,. \tag{3.3}$$

Here

$$F(12) = T\langle\langle N\,|\psi(1)\psi(2)\,|N+2\rangle\rangle\,, \qquad \bar{F}(12) = T\langle\langle N+2\,|\psi^\dagger(1)\psi^\dagger(2)\,|N\rangle\rangle\,. \tag{3.4}$$

In the last two equations N and $N-2$ are the states discussed above. (In (3.3)–(3.4) the dependence on the fields $\boldsymbol{A}$, q is, for brevity, not explicitly indicated. Where no statement to the contrary is made, this dependence is also implied in the equations that follow.) The factorization (3.3) was first made by Gorkov ([3]). As we have discussed above, this approximation only takes into account the possibility of independent particle propagation, and bound pair formation and disruption. For the special case of the two particle Green's function that occurs in (3.2), eq. (3.3) leads to

$$-iVT\langle\langle(\psi^\dagger(1)\psi(1))\,\psi(1)\psi^\dagger(1')\rangle\rangle = u_{\mathrm{H}}G(11') + u_{\mathrm{F}}G(11') + iVF(1^+1)\,\bar{F}(11')\,, \tag{3.5}$$

where

$$u_{\mathrm{H}}(1) = -\,2u_{\mathrm{F}}(1) = V\langle\langle(\psi^\dagger(1)\psi(1))\rangle\rangle \tag{3.6}$$

are the Hartree and Hartree-Fock fields. Let us for the moment neglect these fields. (The parts independent of $\boldsymbol{A}$ and q correspond only to a shift in the chemical potential μ. We shall show later how to include the effects linear in the external potentials as well.) Then eq. (3.2) reduces to

$$\left[i\frac{\partial}{\partial t_1} - h(1)\right] G(11') = \delta(11') + iVF(1^+1)\,\bar{F}(11')\,. \tag{3.7}$$

One now needs an equation for $\bar{F}(11')$. This is obtained by making a factorization similar to (3.3) of the expectation value involving four field operators that occurs on the right-hand side of the exact equation of motion for this quantity. Again neglecting for the moment the self-consistent field terms, one gets

$$\left[-i\frac{\partial}{\partial t_1} - h(1)\right] \bar{F}(11') = iV\bar{F}(1^+1)\,G(11')\,. \tag{3.8}$$

(7) By « ground state » we mean the representative state of the system that evolves from the ground state under the influence of the electromagnetic perturbation.

For formal manipulations it is convenient to notice that the operators on the left sides of (3.7) and (3.8) are inverse single-particle Green's functions for the system neglecting the two-body interactions in (3.1). For then the single-particle Green's function $G_0(11')$ satisfies

$$(3.9) \qquad i\frac{\partial}{\partial t_1} - h(1)\Big] G_0(11') = \Big[-i\frac{\partial}{\partial t_1'} - h(1')\Big] G_0(11') = \delta(11') .$$

This may be written (summation convention)

$$(3.10) \qquad G_0^{-1}(1\bar{1})\, G_0(\bar{1}1') = G_0^{-1}(\bar{1}1')\, G_0(1\bar{1}) = \delta(11') ,$$

with

$$(3.11) \qquad G_0^{-1}(11') = \left(i\frac{\partial}{\partial t_1} - h(1)\right)\delta(11') = \left(-i\frac{\partial}{\partial t_1'} - h(1')\right)\delta(11') .$$

Using this shorthand, eqs. (3.7) and (3.8) become

$$(3.12) \qquad G_0^{-1}(1\bar{1})\, G(\bar{1}1') - iV\, F(1^+1)\,\bar{F}(11') = \delta(11') ,$$

$$(3.13) \qquad G_0^{-1}(\bar{1}1)\,\bar{F}(\bar{1}1') - iV\,\bar{F}(1^+1)\, G(11') = 0 .$$

The quantities F, $\bar{F}$ and G are so far matrices in spin space. The spin dependence is trivial and may be removed at once. Since the interaction (3.1) is spin independent G must be proportional to the unit matrix in spin space. Also because of the Fermi statistics F and $\bar{F}$ must be antisymmetric. Following Gorkov we write $F \sim 1'$ where

$$(3.14) \qquad 1' = \begin{pmatrix} 0 & 1 \\ -1 & 0 \end{pmatrix} .$$

It follows that $\bar{F} \sim -1'$ and since $1' \cdot 1' = -1$ the form of (3.12)–(3.13) is unchanged. From now on we understand these equations as containing quantities independent of spin.

The set of eqs. (3.12) and (3.13) may be easily solved . From (3.13)

$$(3.15) \qquad \bar{F}(11) = i\Delta^*(\bar{1})\, G(\bar{1}1')\, G_0(\bar{1}1) .$$

Substituting this in (3.12) we get

$$(3.16) \qquad G^{-1}(11') = G_0^{-1}(11') + \Delta(1)\, G_0(1'1)\, \Delta^*(1') ,$$

where we have introduced the notation

$$(3.17) \qquad V\bar{F}(11) \equiv \Delta^*(1) , \qquad V F(11) = \Delta(1) .$$

Eqs. (3.15) and (3.16) together with an equation for F similar to the former, namely,

$$F(11') = i\,G_0(1\bar{1})\,G(1'\bar{1})\,\Lambda(\bar{1})\,, \tag{3.18}$$

serve to determine an approximate Green's function for the superconductor in the presence of an electromagnetic disturbance. (The original BCS theory is obtained by solving these equations for $\boldsymbol{A} = \varphi = 0$. This is briefly reviewed in Appendix A.)

Let us now check the invariance properties of the approximation. Looking first at the gauge invariance, it is easy to see that $G_0^{-1}(\boldsymbol{A}, \varphi)$ (from now on we explicitly exhibit the field-dependence), and consequently $G_0(\boldsymbol{A}, \varphi)$, transforms according to (2.11). Thus we find

$$\begin{aligned} \exp\left[-\frac{ie}{c}\Lambda(1)\right] G^{-1}(11';\,\boldsymbol{A}\varphi)\exp\left[+\frac{ie}{c}\Lambda(1')\right] &= G_0^{-1}(11';\,\boldsymbol{A}'\varphi') + \\ + \left(\Lambda(1;\,\boldsymbol{A}\varphi)\exp\left[-\frac{2ie}{c}\Lambda(1)\right]\right) G_0(1'1;\,\boldsymbol{A}'\varphi') \left(\Lambda^*(1';\,\boldsymbol{A}\varphi)\exp\left[\frac{2ie}{c}\Lambda(1')\right]\right). \end{aligned} \tag{3.19}$$

Thus G^{-1}, and consequently G, transforms in the correct way if we note that Λ and Λ^* also depend on the gauge according to

$$\begin{cases} \Lambda\,(1;\,\boldsymbol{A}'\varphi') = \exp\left[-\dfrac{2ie}{c}\Lambda(1)\right]\Lambda(1;\,\boldsymbol{A}\varphi)\,, \\ \Lambda^*(1;\,\boldsymbol{A}'\varphi') = \exp\left[\dfrac{2ie}{c}\Lambda(1)\right]\Lambda^*(1;\,\boldsymbol{A}\varphi)\,. \end{cases} \tag{3.20}$$

These transformation properties are exactly those we expect for products of two annihilation operators and two creation operators, respectively.

The charge conservation condition is verified by subtracting the equation of motion for the approximate G from the adjoint equation and setting $1'=1^+$. The proof given for the exact G in eqs. (2.15)–(2.18) goes through.

We have thus obtained a conserving approximation for $G_1(\boldsymbol{A}, \varphi)$ from which to generate the linear response of the system. The most direct way of doing this would be to expand (3.15), (3.16) and (3.18) to terms linear in $\boldsymbol{A}$ and φ [8]. One would then obtain equations similar to those used by MIGDAL [9] for a different purpose. In the long wavelength limit, however, one can avoid some of the algebra involved in this procedure and also gain some insight into the problem by making use of an additional symmetry which the equations pos-

[8] V. AMBEGAOKAR and L. P. KADANOFF: to appear in the lecture notes for the Bergen summer school (1961).

[9] A. B. MIGDAL: *Nucl. Phys.*, **13**, 655 (1959).

sess. This is a symmetry between particles and holes which occurs when the disturbance has a wavenumber, k, which satisfies

$$k < k_F \,, \tag{3.21}$$

where k_F is the Fermi wavenumber. As a consequence, one can show (Appendix B) by examining eqs. (3.15)–(3.16) and (3.18) without any detailed expansions that to terms linear in $\boldsymbol{A}$ and φ the following relation holds

$$\Delta(0)\Delta^*(1; \boldsymbol{A}, \varphi) = \Delta(1; -\boldsymbol{A}, -\varphi)\Delta^*(0) \,. \tag{3.22}$$

Here

$$\Delta(0) = \Delta(1; \ \boldsymbol{A} = 0, \ \varphi = 0) \,,$$

which because of translational invariance and the fact that the single-particle energies are measured with respect to μ, is independent of its space and time argument. $\Delta(0)$ is the gap parameter of the BCS theory (see Appendix A.) We thus see from (3.22) that the linear effect of an electromagnetic perturbation is to change the phase but not the magnitude of the gap parameter. Thus as far as the linear response goes we can write

$$\begin{cases} \Delta \ (1; \boldsymbol{A}\varphi) = \exp\left[\dfrac{2ie}{c} \ W(1; \boldsymbol{A}\varphi)\right]\Delta(0) \,, \\ \Delta^*(1; \boldsymbol{A}\varphi) = \exp\left[-\dfrac{2ie}{c} \ W(1; \boldsymbol{A}\varphi)\right]\Delta^*(0) \,. \end{cases} \tag{3.23}$$

Let us substitute this into the expression for the Green's function (3.16). We get

$$G^{-1}(11'; \boldsymbol{A}\varphi) = G_0^{-1}(11': \boldsymbol{A}\varphi) + \Delta(0) \exp\left[\frac{2ie}{c} \ W(1; \boldsymbol{A}\varphi)\right] \cdot \tag{3.24}$$

$$\cdot G_0(1'1; \boldsymbol{A}\varphi) \exp\left[-\frac{2ie}{c} \ W(1'; \boldsymbol{A}\varphi)\right] \Delta^*(0) \cdot$$

But from the transformation property (2.11) of the G's we see that the phase factors in (3.24) can be removed by a choice of gauge. In particular, we have

$$G^{-1}(11'; \bar{\boldsymbol{A}}\bar{\varphi}) = G_0^{-1}(11'; \bar{\boldsymbol{A}}\bar{\varphi}) + \Delta(0) G(1'1; \bar{\boldsymbol{A}}\bar{\varphi})\Delta^*(0) \,, \tag{3.25}$$

where

$$\bar{\boldsymbol{A}} = \boldsymbol{A} - \nabla W \,, \qquad \bar{\varphi} = \varphi + \frac{1}{c}\frac{\partial W}{\partial t} \,. \tag{3.26}$$

We see from (3.25) that it will be simpler to expand the Green's function in terms of the effective potentials $\bar{\varphi}$, $\bar{A}$ rather than the external potentials φ, A. What is the physical meaning of these effective potentials? Now, $\Delta(1)$ can be interpreted as the wave function for a pair, and we have from (3.23) that

$$-\frac{e}{c}\frac{\partial W}{\partial t}(1)=\frac{1}{2}\frac{\Delta^*(1)i(\partial/\partial t_1)\Delta(1)}{\Delta^*(1)\Delta(1)}\,. \tag{3.27}$$

Thus this quantity can be interpreted as the mean energy per paired particle at the point 1. Similarly one finds for the mean momentum per paired particle

$$\frac{e}{c}\nabla W(1)=\frac{1}{2}\frac{\Delta^*(1)(1/i)\nabla_1\Delta(1)}{\Delta^*(1)\Delta(1)}\,. \tag{3.28}$$

Thus the effective potentials $\bar{\varphi}$, $\bar{\boldsymbol{A}}$ correspond to measuring energies with respect to the mean energy and momenta with respect to the mean momentum of the paired particles.

Let us now expand the Green's function (3.25) to terms linear in $\bar{\varphi}$ and $\bar{A}$. Doing this explicitly for $\bar{\varphi}$ we have

$$-G^{-1}(1\bar{1})\frac{\delta G(11')}{\delta\bar{\varphi}(2)}G(11')=-e\delta(12)\delta(12')+e\Delta(0)G_0(1'2)G_0(21)\Delta^*(0)\,. \tag{3.29}$$

Multiplying on both sides by G and using the defining equations for F and $\bar{F}$. (3.18) and (3.15) respectively, we have

$$-\frac{\delta G(11')}{\delta\bar{\varphi}(2)}\bigg|_{A,\varphi=0}=e[-G(12)G(21')-F(12)\bar{F}(21')]_{A,\varphi=0}\,. \tag{3.30}$$

Similarly, one finds

$$-\frac{\delta G(11')}{\delta\bar{\boldsymbol{A}}(2)}\bigg|_{A,\varphi=0}=-\frac{e}{c}\frac{\nabla_2-\nabla_2'}{2mi}[-G(12')G(21')-F(12)\bar{F}(2'1')]_{\substack{2'=2+\\A,\varphi=0}}\,. \tag{3.31}$$

Now the quantity in the square brackets in (3.30), (3.31) exactly corresponds to a Gorkov factorization (eq. (3.3)) of $G_2(12;1'2')-G(11')G(22')$ in the absence of the electromagnetic fields. If one uses this approximation for $G_2(\boldsymbol{A}=q=0)$ to determine the response functions in (2.23) directly, one obtains the BCS electrodynamics. (We shall see this explicitly in a particular limit below.) Therefore we see that the more consistent picture we have developed is the same as the BCS independent quasi-particle picture except that here the quasi-particles feel the effective fields $\bar{\boldsymbol{A}}$, $\bar{\varphi}$ and not the external fields $\boldsymbol{A}$, φ.

From (3.30), (3.31) one can construct the time-ordered response (2.26). We shall discuss the result explicitly only in the extreme long wavelength or London limit and for very low frequencies, namely for wavenumbers, k, and frequencies, ω, that satisfy

$$k < \Delta(0)/v_{\mathrm{F}}\,, \qquad \omega < 2\Delta(0)\,, \tag{3.32}$$

where v_{F} is the Fermi velocity. In this limit, when Gorkov's expressions for G and F (eqs. (A.9) and (A.10) respectively) are substituted into (3.30), (3.31) the integrations in (2.26) are straightforward and one finds

$$\langle \varrho(1)\rangle = -2e^2 N(0)\,\overline{\varphi}(1) = -2e^2 N(0)\left[\varphi(1) + \frac{1}{c}\frac{\partial W}{\partial t}(1)\right], \tag{3.33}$$

$$\langle \boldsymbol{J}(1)\rangle = -\frac{ne^2}{mc}\,\overline{\boldsymbol{A}}(1) = -\frac{ne^2}{mc}\,[\boldsymbol{A}(1) - \boldsymbol{\nabla} W(1)]\,. \tag{3.34}$$

Here $N(0)$ is the density of states for electrons of one spin at the Fermi surface. (We see here explicitly that replacing $\boldsymbol{A}$ and $\overline{\varphi}$ by $\boldsymbol{A}$ and φ gives a BCS result.) Eqs. (3.33), (3.34) contain the still unknown quantity W. This can be determined from the conservation condition we have built into the approximation, namely,

$$\frac{\partial}{\partial t_1}\langle \varrho(1)\rangle + \boldsymbol{\nabla}_1 \cdot \langle \boldsymbol{J}(1)\rangle = 0\,.$$

Substituting, we find

$$\left(\nabla^2 - \frac{1}{v^2}\frac{\partial^2}{\partial t^2}\right) W = \boldsymbol{\nabla}\cdot\boldsymbol{A} + \frac{c}{v^2}\frac{\partial \varphi}{\partial t}\,, \tag{3.35}$$

where

$$v^2 = \frac{n}{2mN(0)} = v_{\mathrm{F}}^2/3\,. \tag{3.36}$$

We notice from (3.35) that in our approximation the system can perform free sound vibrations with a velocity given by (3.36). This is the collective mode ([4,5]). We shall see in the next section how this mode is modified by the self-consistent fields.

Fourier transforming (3.35) and fixing the behaviour at the singularities to obtain the causal response as discussed in Section 2, we get

$$W(\boldsymbol{k}, \omega) = -i\,\frac{v^2 \boldsymbol{k}\cdot\boldsymbol{A}(\boldsymbol{k}, \omega) - \omega c \varphi(\boldsymbol{k}, \omega)}{(kv - \omega - i\delta)(kv + \omega + i\delta)}\,, \tag{3.37}$$

thus the causal response charge and current densities are

$$\langle \varrho(\boldsymbol{k}, \omega)\rangle = -\frac{ne^2}{mc}\left[\frac{ck^2 q(\boldsymbol{k}, \omega) - \omega(\boldsymbol{k}\cdot\boldsymbol{A}(\boldsymbol{k}, \omega))}{(kv - \omega - i\delta)(kv - \omega + i\delta)}\right], \tag{3.38}$$

and

$$\langle \boldsymbol{J}(\boldsymbol{k}, \omega)\rangle = -\frac{ne^2}{mc}\left[\boldsymbol{A}(\boldsymbol{k}, \omega) - \frac{\boldsymbol{k}(\boldsymbol{k}\cdot\boldsymbol{A}(\boldsymbol{k}, \omega))v^2 - \boldsymbol{k}\omega c q(\boldsymbol{k}, \omega)}{(kv - \omega - i\delta)(kv + \omega + i\delta)}\right]. \tag{3.39}$$

It is easy to verify that (3.38), (3.39) are explicitly gauge invariant. In the limit $\omega = 0$ (static magnetic field) one has from (3.39)

$$\langle J_\mu(\boldsymbol{k})\rangle = -\frac{ne^2}{mc}\left(\delta_{\mu\nu} - \frac{k_\mu k_\nu}{k^2}\right) A_\nu(\boldsymbol{k}) . \tag{3.40}$$

i.e. the gauge invariant London equation.

4. – Inclusion of the self-consistent field.

So far we seem to have entirely omitted the self-consistent field. Actually, most of the work done above still applies when this is included. We have only to note that the self-consistent field can be lumped together with the scalar potential q, so that the quantity that enters the single-particle Hamiltonian $h_1(\boldsymbol{A}q)$ is an effective scalar potential q_{eff} given by

$$q_{\text{eff}}(1) = q(1) + \frac{1}{e^2} v(1\bar{1})\langle \varrho(\bar{1})\rangle . \tag{4.1}$$

where v is a two-body Hamiltonian we want to take into account self-consistently. The new point is that the self-consistent field is itself a functional of the external fields. We shall show how to take this into account. It is clear that the appropriate first thing to do is to expand the response in powers of $\bar{A}$ and $\bar{\varphi}_{\text{eff}}$. We have the result in eqs. (3.33), (3.34) namely

$$\langle \varrho(1)\rangle = -2e^2 N(0)\bar{\varphi}_{\text{eff}}(1) , \tag{4.2}$$

$$\langle \boldsymbol{J}(1)\rangle = -\frac{ne^2}{mc}\bar{A}(1) . \tag{4.3}$$

To get an expansion of (4.2) in terms of $\bar{\varphi}$ we need $\delta\bar{\varphi}_{\text{eff}}\delta/\bar{\varphi}$ and this is obtained from (4.1)

$$\delta\bar{\varphi}_{\text{eff}}(1)/\delta\bar{\varphi}(2) = \delta(12) + \frac{1}{e^2} v(1\bar{1})\,\delta\langle \varrho(\bar{1})\rangle/\delta\bar{\varphi}(2) . \tag{4.4}$$

Putting this back into (4.2) and Fourier analysing we get

$$\langle \varrho(\boldsymbol{k}, \omega)\rangle [1 + 2N(0)v(k)] = -2e^2 N(0)\overline{\varphi}(\boldsymbol{k}, \omega) \tag{4.5}$$

or

$$\langle \varrho(\boldsymbol{k}, \omega)\rangle = -\frac{2e^2 N(0)}{[1 - 2N(0)v(k)]}\overline{\varphi}(\boldsymbol{k}, \omega) .$$

This equation replaces (3.33); (3.34) is unchanged. Two cases are to be distinguished. First the case when we take into account only the attractive interaction that causes the superconductivity (uncharged case). Then $v(k) = V$ for the Hartree field or $v(k) = V/2$ for the Hartree and Hartree-Fock fields. (See eq. (3.6).) The latter approximation is probably better and we shall make it. In any case, no qualitative change in the results (3.38) and (3.39) is obtained. The only change is in the velocity of the sound mode which now becomes

$$v_{\text{s.c.}}^2 = \frac{v_F^2}{3}[1 + N(0)V] . \tag{4.6}$$

A result of this form was first obtained by ANDERSON [5]. He, however, had a factor of 4, which we do not find, multiplying the second term in the bracket. The response changes qualitatively when the long range part of the Coulomb force is taken into account self-consistently. We have

$$v(k) = 4\pi e^2/k^2 \tag{4.7}$$

and in the long wavelength limit this overpowers the 1 in the denominator of (4.5) and the weak attractive self consistent field. Thus the relevant system of equations is now

$$\begin{cases} \langle \varrho(\boldsymbol{k}, \omega)\rangle = -\dfrac{k^2}{4\pi}\overline{\varphi}(\boldsymbol{k}, \omega) = -\dfrac{k^2}{4\pi}\left[\varphi(\boldsymbol{k}, \omega) + \dfrac{i\omega}{c} W(\boldsymbol{k}, \omega)\right], \\ \langle \boldsymbol{J}(\boldsymbol{k}, \omega)\rangle = -\dfrac{ne^2}{mc}\boldsymbol{A}(\boldsymbol{k}, \omega) = -\dfrac{ne^2}{mc}[\boldsymbol{A}(\boldsymbol{k}, \omega) + i\boldsymbol{k} W(\boldsymbol{k}, \omega)] . \end{cases} \tag{4.8}$$

Again one can use the number conservation condition to find W. The equation satisfied by W is now

$$iW[\omega_p^2 - \omega^2] = \omega c\varphi - \omega_p^2 \boldsymbol{k}\cdot\boldsymbol{A}/k^2 , \tag{4.9}$$

where

$$\omega_p^2 = 4\pi ne^2/m \tag{4.10}$$

so that the collective mode has the plasma frequency. Eliminating W from (4.8) we find the explicitly gauge invariant result ([10])

$$\langle \varrho(\boldsymbol{k}, \omega)\rangle = -\frac{\omega_p^2}{4\pi c}\left[\frac{ck^2\varphi(\boldsymbol{k}, \omega) - \omega \boldsymbol{k}\cdot\boldsymbol{A}(\boldsymbol{k}, \omega)}{(\omega_p - \omega - i\delta)(\omega_p + \omega + i\delta)}\right], \tag{4.11}$$

$$\langle \boldsymbol{J}(\boldsymbol{k}, \omega)\rangle = -\frac{ne^2}{mc}\left[\boldsymbol{A}(\boldsymbol{k}, \omega) - \boldsymbol{k}\,\frac{\omega_p^2(\boldsymbol{k}\cdot\boldsymbol{A}(\boldsymbol{k}, \omega) - k^2\omega c\varphi(\boldsymbol{k}, \omega)}{k^2(\omega_p - \omega - i\delta)(\omega_p + \omega + i\delta)}\right]. \tag{4.12}$$

For static magnetic fields $\omega = 0$ we again get the gauge invariant London equation (3.40).

5. – Conclusions.

In the Bardeen, Cooper, Schrieffer picture of the superconducting state, two electrons in a superconductor can either move as independent quasi-particles, or form a bound pair with total momentum zero. This picture leads to an inconsistent electrodynamics. We find, as have several other authors, that only a very slight modification of this physical picture is required in order to construct a consistent electrodynamics. In our picture one still has the same quasi-particles, and these can still move independently. However, the mean momentum of the background of paired particles is no longer constrained to be zero. The motion of the bound pairs has a very simple effect. One can think of it as solely modifying the electromagnetic fields that act on the quasi-particles. In the simplest approximation, these modified or effective fields correspond to measuring the external scalar and vector potentials with respect to the mean energy and momentum of the dynamical background. In the next approximation the effective fields correspond to measuring not the external but the self-consistent fields with respect to the same background. The response of the quasi-particles to the effective fields in our picture is thus the same as that of the quasi-particles to the external fields in the BCS picture. The response of our system to the external fields is of course different. In particular, at certain frequency-wavenumber combinations the effective fields

([10]) In (4.11)-(4.12) only the Coulomb interaction between electrons has been taken into account self-consistently. To treat the magnetic interactions self-consistently one must interpret the vector potential A in these equations as the self-consistent or effective field given by

$$A_{\text{eff}}(1) = A_{\text{ext}}(1) + A_{\text{int}}(1)\,,$$

where $A_{\text{int}}(1)$ satisfies

$$\Box A_{\text{int}}(1) = -4\pi j_{\perp}(1)/c\,.$$

become independent of the external fields. At these frequencies and wavenumbers a resonance occurs in the response of the bound pairs to the external fields. This corresponds to the excitation of Anderson's collective mode.

* * *

We thank Professor NIELS BOHR and the members of this Institute for the hospitality afforded us during the course of this work.

APPENDIX A

A very brief sketch of Gorkov's [3] formulation of the BCS theory is given here for completeness. The basic equations are

$$G^{-1}(11') = G_0^{-1}(11') + \Delta(1) G_0(1'1) \Delta^*(1') , \tag{A.1}$$

and

$$F(11') = i G_0(1\bar{1}) G(1\bar{1}) \Delta(\bar{1}) ,$$

with

$$\Delta(1) \equiv V F(11) . \tag{A.2}$$

These equations are identical to (3.15)-(3.17) except that here there is no electromagnetic perturbation. As a consequence $\Delta(1)$ and $\Delta^*(1)$ are independent of their argument, and there is no loss of generality in setting them equal. Fourier transforming (A.1) we get

$$G^{-1}(p) = G_0^{-1}(p) + \Delta^2 G_0(-p) , \tag{A.3}$$

where

$$G_0^{-1}(p) = \int \mathrm{d}^3x \, \mathrm{d}t \, G^{-1}(x, t) \exp\left[-i(\boldsymbol{p}\cdot\boldsymbol{x} - p_0 t)\right] . \tag{A.4}$$

Now

$$G_0^{-1}(11') = \left(i \frac{\partial}{\partial t_1} + \frac{\nabla_1^2}{2m} + \mu \right) \delta(11') , \tag{A.5}$$

so that

$$G_0^{-1}(p) = p_0 - \varepsilon_p , \qquad \varepsilon_p \equiv \frac{p^2}{2m} - \mu . \tag{A.6}$$

Thus

$$G^{-1}(p) = \frac{p_0^2 - E_p^2}{p_0 + \varepsilon_p} , \qquad |\varepsilon_p| < \omega_D , \tag{A.7}$$

where

$$E_p^2 = \varepsilon_p^2 + \Delta^2 . \tag{A.8}$$

(Outside the region $|\varepsilon_p| < \omega_D$, $F(p)$ is zero and we have $G(p) = G_0(p)$). The differential eqs. (3.12) and (3.13) do not determine the behaviour of $G(p)$ at its singularities. This comes from the boundary conditions in time which supplement these equations. At absolute zero one finds in the usual way

$$G(p) = \frac{p_0 + \varepsilon_p}{p_0^2 - (E_p - i\delta)^2} , \tag{A.9}$$

where δ is a small positive quantity. The temperature of the system enters only at this point. The differential eqs. (3.12) and (3.13) also apply at finite temperatures which would be described by taking the expectation values occurring in G and F in a thermal ensemble. The boundary conditions in time are then, however, different ([11]) and (A.9) is modified.

To complete the Gorkov formulation of the BCS theory one needs an equation to determine the energy-gap parameter. This is obtained from (A.2). We have

$$F(p) = i\Delta G(p) G_0(-p) = \frac{-i\Delta}{(p_0 - E_p + i\delta)(p_0 + E_p - i\delta)} , \tag{A.10}$$

and thus

$$\Delta = V \int \frac{\mathrm{d}^4 p}{(2\pi)^4} F(p) = -i\Delta V \int \frac{\mathrm{d}^4 p}{(2\pi)^4} \frac{1}{(p_0 - E_p + i\delta)(p_0 + E_p - i\delta)} . \tag{A.11}$$

Doing the p_0-integration and remembering to cut off the interaction in momentum space leads to the BCS gap equation

$$1 = -\frac{V}{2(2\pi)^3} \int_{-\omega_D}^{\omega_D} \frac{N(\varepsilon)\, \mathrm{d}\varepsilon}{\sqrt{\varepsilon^2 + \Delta^2}} \tag{A.12}$$

with the solution in the weak coupling limit

$$\Delta = 2\omega_D \exp\left[-\frac{1}{N(0)|V|}\right] . \tag{A.13}$$

([11]) L. D. LANDAU: *Žurn. Eksp. Teor. Fiz.*, **34**, 262 (1958), translation: *Sov. Phys. JETP*, 7 (34), 182 (1958); P. C. MARTIN and J. SCHWINGER: *Phys. Rev.*, **115**, 1342 (1959).

APPENDIX B

In this appendix, we exhibit the hole-particle symmetry of the Green's functions which was used in deriving eq. (3.22). This symmetry is most naturally discussed in terms of the momentum-space Green's functions defined by

$$\text{(B.1)}\qquad \begin{cases} G^{-1}(11') = \int \dfrac{\mathrm{d}p\,\mathrm{d}k}{(2\pi)^8} \exp\left[i\left(p+\dfrac{k}{2}\right)\cdot 1 - i\left(p-\dfrac{k}{2}\right)\cdot 1'\right]\cdot G^{-1}(p;k)\,, \\ \Delta(1) \quad = \int \dfrac{\mathrm{d}k}{(2\pi)^4} \exp\left[ik\cdot 1\right]\Delta(k)\,, \\ \Delta^*(1) \quad = \int \dfrac{\mathrm{d}k}{(2\pi)^4} \exp\left[-ik\cdot 1\right]\Delta^*(k)\,. \end{cases}$$

The basic equations of the Green's function approximation, (3.15)-(3.18), may be rewritten in momentum-space as

$$\text{(B.2)}\qquad G^{-1}(p;k) = G_0^{-1}(p;k) + \int \frac{\mathrm{d}q\,\mathrm{d}q'}{(2\pi)^8}\,\Delta(q)\,G_0\left(-p+\frac{q+q'}{2};\,k-q+q'\right)\Delta^*(q'),$$

$$\text{(B.3)}\qquad \Delta(k) = iV\int \frac{\mathrm{d}p\,\mathrm{d}q\,\mathrm{d}k'}{(2\pi)^{12}}\,G\left(p+\frac{k+k'}{4};\,q+\frac{k-k'}{4}\right)\cdot$$
$$\cdot G_0\left(-p+\frac{k+k'}{4};\,-q+\frac{k-k'}{2}\right)\Delta(k')\,,$$

$$\text{(B.4)}\qquad \Delta^*(k) = iV\int \frac{\mathrm{d}p\,\mathrm{d}q\,\mathrm{d}k'}{(2\pi)^{12}}\,G\left(p+\frac{k+k'}{4};\,-q-\frac{k-k'}{2}\right)\cdot$$
$$\cdot G_0\left(-p+\frac{k+k'}{4};\,q-\frac{k-k'}{2}\right)\Delta^*(k')\,.$$

Instead of working with the variables $\boldsymbol{p}$ we shall use

$$\text{(B.5)}\qquad \varepsilon = p^2/2m - \mu\,, \qquad \boldsymbol{\Omega} = \boldsymbol{p}/|\boldsymbol{p}|\,.$$

In terms of these variables, we can represent the transformation which takes particles into holes and holes into particles as

$$\text{(B.6)}\qquad \begin{cases} G_0(\varepsilon,\boldsymbol{\Omega},p_0;k) \to G_0(\varepsilon,\boldsymbol{\Omega},p_0;k)' = -\,G_0(-\varepsilon,\boldsymbol{\Omega},-p_0;k)\,, \\ G(\varepsilon,\boldsymbol{\Omega},p_0;k) \to G(\varepsilon,\boldsymbol{\Omega},p_0;k)' = -\,G(-\varepsilon,\boldsymbol{\Omega},-p_0;k)\,, \\ \Delta(k) \to \Delta(k)' = \Delta^*(-k)\,, \\ \Delta^*(k) \to \Delta^*(k)' = \Delta\ (-k)\,. \end{cases}$$

In the limit as the wavenumber of the disturbance is much less than k_F, eqs. (B.2), (B.3) and (B.4) remain invariant under the transformation (B.6). To see this, consider, for example, eq. (B.2). In terms of the variables ε and $\boldsymbol{\Omega}$, (B.2) may be written as

$$G^{-1}(\varepsilon, \boldsymbol{\Omega}, p_0; k) = G_0^{-1}(\varepsilon, \boldsymbol{\Omega}, p_0; k) + \tag{B.7}$$
$$+\int \frac{\mathrm{d}q\,\mathrm{d}q'}{(2\pi)^8}\, \Lambda(q) G_0\left(\varepsilon - v_F \boldsymbol{\Omega}\cdot\frac{\boldsymbol{q}+\boldsymbol{q}'}{2}, -\boldsymbol{\Omega}, -p_0 + \frac{q_0+q_0'}{2}; k-q+q'\right)\Lambda^*(q')$$

In writing eq. (B.2) in the form (B.7) we have neglected terms of order $(\boldsymbol{q}+\boldsymbol{q}')^2/m$ in comparison with $\varepsilon - v_F\boldsymbol{\Omega}\cdot(\boldsymbol{q}+\boldsymbol{q}')$. This approximation is valid so long as the wavenumber of the disturbance is small in comparison with the Fermi wavenumber $k_F = mv_F$. Furthermore, we have used the fact that the disturbance only involves particles near the edge of the Fermi sea to replace $(p/m)\boldsymbol{\Omega}\cdot(\boldsymbol{q}+\boldsymbol{q}')$ by $v_F\boldsymbol{\Omega}\cdot(\boldsymbol{q}+\boldsymbol{q}')$.

With these two approximations, eq. (B.7) is invariant under the transformation (B.6). If we change ε to $-\varepsilon$, p_0 to $-p_0$, (B.7) becomes

$$G^{-1}(\varepsilon, \boldsymbol{\Omega}, p_0; k)' = -G_0^{-1}(-\varepsilon, \boldsymbol{\Omega}, -p_0; k) - \tag{B.8}$$
$$-\int \frac{\mathrm{d}q\,\mathrm{d}q'}{(2\pi)^8}\, \Lambda^*(-q)' G_0\left(-\varepsilon - v_F\boldsymbol{\Omega}\cdot\frac{\boldsymbol{q}+\boldsymbol{q}'}{2}, -\boldsymbol{\Omega}, p_0 - \frac{q_0+q_0'}{2}; k-q-q'\right)\Lambda(-q')' -$$
$$= G_0^{-1}(\varepsilon, \boldsymbol{\Omega}, p_0; k)' + \int \frac{\mathrm{d}q\,\mathrm{d}q'}{(2\pi)^8}\, \Lambda^*(q')' \cdot$$
$$\cdot G_0\left(\varepsilon - v_F\boldsymbol{\Omega}\cdot\frac{\boldsymbol{q}+\boldsymbol{q}'}{2}, -\boldsymbol{\Omega}, -p_0 + \frac{q_0+q_0'}{2}; k-q+q'\right)'\Lambda(q)'.$$

Notice that eq. (B.8) is of the same form as (B.7) except that all the unprimed Green's functions in (B.7) have been replaced by the transformed Green's functions.

Exactly the same argument indicates that eqs. (B.3) and (B.4) are also satisfied by the transformed Green's function. Therefore the primed functions are related to one another in exactly the same way as the original set of Green's functions.

However,

$$G_0^{-1}(\varepsilon, \boldsymbol{\Omega}, p_0; k) = p_0 - \varepsilon - e\varphi(k) + \frac{|p|}{m}\,\boldsymbol{\Omega}\cdot\frac{e}{c}\boldsymbol{A}(k) - \frac{A^2(k)e^2}{2mc^2}\,.$$

Since we are interested in the linear response to the disturbance, we can drop the A^2 term in G_0^{-1}. We again replace $|p|/m$ by v_F. Then,

$$G_0^{-1}(\varepsilon, \boldsymbol{\Omega}, p_0; k; \boldsymbol{A}, \varphi) = p_0 - \varepsilon - e\varphi(k) + v_F\boldsymbol{\Omega}\cdot\frac{e}{c}\boldsymbol{A}(k)\,. \tag{B.9}$$

Notice that

$$G_0^{-1}(\boldsymbol{A}, \varphi)' = G_0^{-1}(-\boldsymbol{A}, -\varphi)\,. \tag{B.10}$$

Since G', Δ' and $\Delta^{*\prime}$ are related to G_0' in exactly the same way as G, Δ, and Δ^* are related to G_0, it follows that $G(\boldsymbol{A}, \varphi)'$, $\Delta(\boldsymbol{A}, \varphi)'$, and $\Delta^*(\boldsymbol{A}, \varphi)'$ obey exactly the same equations as $G(-\boldsymbol{A}, -\varphi)$, $\Delta(-\boldsymbol{A}, -\varphi)$ and $\Delta^*(-\boldsymbol{A}, -\varphi)$. These quantities must be identical except for the ambiguity in phase which appears in our initial solution.

This ambiguity does not appear in $\Delta(k; \boldsymbol{A}, \varphi)/\Delta(\boldsymbol{A} = 0, \varphi = 0)$. Therefore, we may conclude that

$$\frac{\Delta(k; \boldsymbol{A}, \varphi)'}{\Delta(0)'} = \frac{\Delta(k; -\boldsymbol{A}, -\varphi)}{\Delta(0)}, \tag{B.11}$$

so that

$$\Delta(0)\Delta^*(-k; \boldsymbol{A}, \varphi) = \Delta(k; -\boldsymbol{A}, -\varphi)\Delta^*(0). \tag{B.12}$$

Eq. (3.22) follows directly from (B.12).

RIASSUNTO (*)

Si espone un metodo per calcolare la risposta dei superconduttori ai deboli campi elettromagnetici. La risposta è generata da una funzione di Green per singola particella, definita in presenza di una perturbazione elettromagnetica, che soddisfa le condizioni imposte dall'invarianza di gauge e dalla conservazione della carica. La funzione di risposta deve anch'essa soddisfare esplicitamente all'invarianza di gauge e alla conservazione della carica. La funzione di Green per singola particella viene ottenuta applicando una fattorizzazione di Gorkov alla funzione di Green per due particelle in presenza di un campo esterno. Le proprietà di simmetria dell'approssimazione vengono usate per semplificare notevolmente i calcoli. Questi vengono semplicemente eseguiti nell'approssimazione di London. Si ottiene così una derivazione semplificata del risultato di Anderson che le eccitazioni delle quasi-particelle di Bardeen, Cooper e Schrieffer deve essere affiancata da una eccitazione collettiva per soddisfare alle leggi di conservazione.

(*) *Traduzione a cura della Redazione.*

The Stark Shift of the Hyperfine Structure of an Atom with a $^2S_{\frac{1}{2}}$ Ground State (*).

L. W. Anderson

Department of Physics, University of Wisconsin - Madison, Wis.

(ricevuto l'11 Agosto 1961)

Summary. — The energy levels of an atom in a $^2S_{\frac{1}{2}}$ ground state are examined in the presence of an electric field. It is found that the hyperfine structure of the ground state is Stark shifted. This Stark shift is estimated in a crude fashion. This estimate is in reasonable agreement with the experimental result in the case of ^{133}Cs where the Stark shift of the hyperfine structure has been measured. The g factor of the ground state is not influenced by an electric field.

When an atom is placed in a uniform electric field the energy levels of the atom are shifted from their zero field values. In general the shift of the hyperfine separation of an atom will be very small. However, since the hyperfine structure of the ground state of an atom can often be studied with high precision, the Stark shift of the hyperfine structure can be measured in some atoms.

Haun and Zacharias (1) measured the Stark effect on the ^{133}Cs hyperfine structure by the atomic beam magnetic resonance method. They found that the shift of the $(F=4,\ M=0) \leftrightarrow (F=3,\ M=0)$ transition frequency was given by $\Delta(E) = -2.29 \cdot 10^{-6}(1 \pm 0.03)E^2$ Hz where E is the electric field in V/cm. Haun and Zacharias made a very crude estimate of the Stark shift of the hyperfine structure of ^{133}Cs. The calculation presented here is much more accurate than that given by Haun and Zacharias. Schwartz (1) has calculated the Stark shift of the hyperfine structure of atomic hydrogen ac-

(*) This research was supported by a grant from the Research Corporation.

(1) R. D. Haun and J. R. Zacharias: *Phys. Rev.*, **107**, 107 (1957).

curately. The calculation presented here is in close agreement with his value for hydrogen. Schwartz's calculation for hydrogen is not applicable to the alkali metals.

In order to estimate the Stark shift of the hyperfine structure of an atom, whose ground state is ${}^2S_{\frac{1}{2}}$, let the atom be placed in a uniform electric field E along the Z axis and let ez represent the electric moment of the atom. The hyperfine structure of an atom with an S-state is given by FERMI [2] as

$$\Delta W = W_{F=I+\frac{1}{2}} - W_{I-F=\frac{1}{2}} = \left(\frac{8\pi}{3}\right)\binom{2I+1}{I}\mu_0\mu\psi^2(0)\,,$$

where I is the nuclear spin, μ_0 is the Bohr magneton, μ is the nuclear moment and $\psi^2(0)$ is the square of the wave function for the valence electron at the origin. A calculation of $\psi^2(0)$ to second order in a uniform electric field will give the expansion of the electron cloud in the field and hence the decrease in the hyperfine structure of the ground state. In this calculation of ψ there is no need to consider the electronic or nuclear spins as these will give rise to only small effects.

Suppose the ground state of the atom is denoted by $\psi_{n,l=0}$ where n is the radial quantum number of the valence electron and l is the orbital angular momentum. The wave function of the ground state of the atom in a electric field is

$$\psi = \psi_{n,l=0} + eE\sum_{n'}\frac{\psi_{n',l'=1}(n',l'=1\,|\,z\,|\,n,l=0)}{W^0_{n,l=0}-W^0_{n',l'=1}} -$$

$$-\frac{1}{2}e^2E^2\sum_{n'}\frac{\psi_{n',l=0}\,|(n,l=0\,|\,z\,|\,n',l'=1)|^2}{(W^0_{n,l=0}-W^0_{n',l'=1})^2} +$$

$$+e^2E^2\sum_{\substack{n',n''\\ l''=0,2}}^{n'',l''\neq n,l=0}\frac{\psi_{n'',l''}(n'',l''\,|\,z\,|\,n',l'=1)(n',l'=1\,|\,z\,|\,n,l=0)}{(W^0_{n,l=0}-W^0_{n',l'=1})(W^0_{n,l=0}-W^0_{n'',l''=1})}\,,$$

since the only non vanishing matrix elements of the operator z are those for which l changes by one unit. The term containing $\psi_{n',l'=1}$ will be dropped from the sum since $\psi_{n',l'=1}(0)=0$.

Suppose that the energy denominators are assumed to be the same for each term in a sum so that they can be factored out of the sum. Using this approximation and the completeness of the wave functions one finds that

$$\psi(0) \simeq \psi_{n,l=0}(0)\left\{1 - e^2E^2(n,l=0\,|\,z^2\,|\,n,l=0)\cdot\right.$$

$$\left.\cdot\left[\frac{1}{2(W^0_{n,l=0}-\overline{W}^0_{n',l'=1})^2} + \frac{1}{(W^0_{n,l=0}-\overline{W}^0_{n',l'=1})(W^0_{n,l=0}-\overline{\overline{W}}^0_{n'',l''=0,2})}\right]\right\}\,,$$

([2]) E. FERMI: *Zeits. f. Phys.*, **60**, 320 (1930).

where the value $(W^0_{n,l=0} - \overline{W}^0_{n',l'=1})^{-2}$ is the average value assumed for each energy denominator in the second order term involving $\psi_{n,l=0}$ and

$$(W^0_{n,l=0} - \overline{W}^0_{n',l'=1})^{-1}(W^0_{n,l=0} - \overline{W}^0_{n'',l''=0,2})^{-1}$$

is the value assumed for each energy denominator in the second order term involving $\psi_{n'',l''}$.

Now it can be noted that the polarizability α of an atom in an S-state is given by the relationship

$$\frac{1}{2}\alpha E^2 = e^2E^2 \sum_n \frac{|(n', l'=1\,|\,z\,|\,n, l=0)|^2}{(W^0_{n',l'=1} - W^0_{n,l=0})}.$$

If the same approximation as before is used then

$$\frac{1}{2}\alpha E^2 \simeq \frac{e^2E^2(n,\ l=0\,|\,z^2\,|\,n,\ l=0)}{(\overline{W}^0_{n',l'=1} - W^0_{n,l=0})}.$$

If it is assumed that the $\overline{W}^0_{n',l'=1}$ which appears in the expression for the polarizability, is the same as that, which appears in $\psi(0)$, then

$$\psi(0) \simeq \psi_{n,l=0}(0)\left\{1 - \frac{1}{2}\alpha E^2\left[\frac{1}{2(\overline{W}^0_{n',l'=1} - W^0_{n,l=0})} + \frac{1}{(\overline{W}^0_{n'',l''=0,2} - W^0_{n,l=0})}\right]\right\}.$$

Thus the Stark shift of the hyperfine structure divided by the zero field hyperfine splitting is given by

$$\frac{\Delta(E)}{\Delta W} = -\alpha E^2\left\{\frac{1}{2(\overline{W}^0_{n',l'=1} - W^0_{n,l=0})} + \frac{1}{(\overline{W}^0_{n'',l''=0,2} - W^0_{n,l=0})}\right\},$$

where ΔW is the hyperfine splitting.

The selection of the values of $\overline{W}^0_{n',l'=1}$ and $\overline{W}^0_{n'',l''=0,2}$ is the only remaining problem in evaluating the Stark shifts. For the case of atomic hydrogen the value of $\overline{W}^0_{n',l'=1}$, which yields the correct value of α, is that corresponding to the $n=3$ state. If it is assumed that the $n=3$ state is used to obtain both $\overline{W}^0_{n',l'=1}$ and $\overline{W}^0_{n'',l''=0,2}$ then the Stark shift of the hyperfine structure of atomic hydrogen is

$$\frac{\Delta(E)}{\Delta W} = -\frac{486}{32}\left(\frac{a_0^4}{e^2}\right)E^2 = -15.2\left(\frac{a_0^4}{e^2}\right)E^2,$$

where a_0 is the Bohr radius and where use has been made of the fact that $\alpha = (9/2)a_0^3$. This is in good agreement with the calculation by a different

method of the Stark shift of the hyperfine structure of atomic hydrogen by SCHWARTZ (see HAUN and ZACHARIAS [1]).

For the alkali metals, values of $\overline{W}^0_{n',l'=2}$ and $\overline{W}^0_{n'',l''=0,2}$, which seem reasonable, are respectively the energy associated with the lowest lying P state and the lower of the lowest lying S-states or lowest lying D-states. These were selected since the lowest P-state has the same radial quantum number as the ground state and the matrix element $(n, l=1\,|\,z\,|\,n, l=0)$ would be expected to be quite large.

The values of $\Delta(E)/\Delta W$, found in this manner, are given in Table I. It can be seen that the value estimated for ^{133}Cs agrees fairly well with the experimental value. The value calculated for atomic hydrogen is close to the

TABLE I. – *The calculated values of* $\Delta(E)/\Delta W$.

Atom	$W^0_{n',l'=1} - W^0_{n,l=0}$ (eV)	$W^0_{n'',l''=0,2} - W^0_{n,l=0}$ (eV)	α (cm^3)	$\Delta(E)/\Delta W$
Cs	$W_{6,1} - W_{6,0} = 1.48$	$W_{5,2} - W_{6,0} = 1.88$	42	$-(2.3\cdot10^{-16})E^2$
Rb	$W_{5,1} - W_{5,0} = 1.60$	$W_{4,2} - W_{5,0} = 2.44$	31	$-(1.4\cdot10^{-16})E^2$
K	$W_{4,1} - W_{4,0} = 1.55$	$W_{5,0} - W_{4,0} = 2.17$	29	$-(1.4\cdot10^{-16})E^2$
Na	$W_{3,1} - W_{3,0} = 2.12$	$W_{4,0} - W_{3,0} = 3.21$	20	$-(6.9\cdot10^{-17})E^2$
Li	$W_{2,1} - W_{2,0} = 1.84$	$W_{3,0} - W_{2,0} = 3.35$	14	$-(5.1\cdot10^{-17})E^2$
H	$W_{3,1} - W_{1,0} = 12.1$	$W_{3,0} - W_{1,0} = 12.1$	0.67	$-(5.2\cdot10^{-19})E^2$

The values of the atomis energy levels were taken from BACHER and GOUDSMIT [3]. The values of α were taken from SCHEFFERS and STARK [4] and CHAMBERLAIN and ZORN [5]. The measured value of $\Delta(E)/\Delta W$ for ^{133}Cs is $\Delta(E)/\Delta W = 2.5\cdot10^{-16}E^2$ [HAUN and ZACHARIAS [1]]. The value of $\Delta(E)/\Delta W$ for H calculated by SCHWARTZ is $\Delta(E)/\Delta W = -(5.1\cdot10^{-19})E^2$ [HAUN and ZACHARIAS [1]].

value calculated in a different manner by SCHWARTZ. The calculations for the remaining alkali metals would be expected to be about as accurate as the estimate for ^{133} Cs.

If one has both a magnetic field H and an electric field E applied along the z axis then the interaction Hamiltonian for an atom whose ground state

[3] R. F. BACHER and S. GOUDSMIT: *Atomic Energy States* (New York, 1932).

[4] H. SCHEFFERS and J. STARK: *Phys. Zeits.*, **35**, 625 (1934).

[5] G. E. CHAMBERLAIN and J. C. ZORN: *Bull. Am. Phys. Soc.*, **5**, 242 (1960).

[6] F. J. ADRIAN: *Journ. Chem. Phys.*, **32**, 972 (1960). Although no direct reference is made to this paper, many of the ideas on shifts in h.f.s. were first obtained in it.

is $^2S_{\frac{1}{2}}$ is

$$\mathscr{H}_{\text{int}} = \frac{\Delta W}{(I+\frac{1}{2})}\, I\cdot J - \mu_0 H(L_z + 2S_z) - g_I\mu_0 H I_z + ezE\,,$$

where L is the electronic orbital angular momentum, S is the electronic spin angular momentum, I is nuclear spin, J is the total electronic angular momentum ($J=L+S$), μ_0 is the Bohr magneton, and g_I is the nuclear g factor. Of course $L_z + 2S_z$ can be replaced by $g_J J_z$ when a matrix element which is diagonal in J is evaluated. In this expression g_J is the Lande g factor for the state used in evaluating the diagonal matrix element. If one evaluates this Hamiltonian by perturbation theory in a low field representation where the eigen functions are $\psi_{n,l,S=\frac{1}{2},J,F,m_F}$ then the resulting energies are

$$\begin{aligned}
W_{F,m_F} = {} & \frac{\Delta W}{I+\frac{1}{2}}\frac{1}{2}\left[F(F+1) - I(I+1) - \frac{1}{2}\left(\frac{1}{2}+1\right)\right] - \\
& - g_I\mu_0 H m_F - \frac{(g_J-g_I)\mu_0 H}{2}\,\frac{[F(F+1)+\frac{1}{2}(\frac{1}{2}+1)-I(I+1)]}{F(F+1)}\,m_F - \\
& + e^2E^2 \sum_{n',F'} \frac{|(n',l'=1,F'|z|n,l=0,F)|^2}{W^0_{n,l=0,F} - W^0_{n',l'=1,F'}} \pm \frac{(g_J-g_I)^2\mu_0^2H^2}{\Delta W}\left\{\left(I+\frac{3}{2}\right)^2 - m_F^2\right\}\cdot \\
& \cdot\left\{\frac{[(I+\frac{1}{2})^2-(I-\frac{1}{2})][(I+\frac{3}{2})^2-(I+\frac{1}{2})^2]}{4(I+\frac{1}{2})^2[4(I+\frac{1}{2})^2-1]}\right\} + \\
& + e^2E^2(g_J-g_I)\mu_0 H_0 \sum_{n',F'} \frac{|(n',l'=1,F'|z|n,l=0,F)|^2}{(W^0_{n,l=0,F} - W^0_{n',l'=1,F'})^2}\cdot \\
& \cdot\frac{[F(F+1)+\frac{1}{2}(\frac{1}{2}+1)-I(I+1)]}{F(F+1)}\,m_F - \mu_0 H_0 e^2E^2\cdot \\
& \cdot \sum_{\substack{n',F',J' \\ n'',F'',J''}} \frac{1}{(W^0_{n,l=0} - W^0_{n',l'=1})^2}\cdot(n,l=0,J=\tfrac{1}{2},F,m|z|n',l'=1,J',F',m)\cdot \\
& \cdot(n',l'=1,J',F',m|(L_z+2S_z-g_I I_z)|n',l'=1,J'',F'',m)\cdot \\
& \cdot(n',l'=1,J'',F'',m|z|n,l=0,J=\tfrac{1}{2},m) + \text{third order terms in } H + \ldots\,,
\end{aligned}$$

where $F=I+J$, where g_J is the Lande g factor for the ground state, and where the $\pm$ sign in the fifth term is chosen so that the two hyperfine levels repel each other.

As is discussed in the Appendix the term

$$e^2E^2 \sum_{n',F',J'} \frac{|(n',l'=1,J',F'|z|n,l=0,J=\frac{1}{2},F)|^2}{(W^0_{n,l=0,F} - W^0_{n',l'=1,F'})^2}\,,$$

gives a shift of an F level, which is independent of m_F. The difference of the

shifts of the two levels $F=I-\frac{1}{2}$ and $F=I-\frac{1}{2}$ gives the Stark shift of the hyperfine structure, which has already been estimated.

The terms involving H and E^2 could be interpreted as giving a Stark shift of the electronic g factor of the state if it were not for the fact that the two terms involving H and E^2 are equal in magnitude and opposite in sign. Thus to a high degree of accuracy the electronic g factor of the ${}^2S_{\frac{1}{2}}$ ground state of the atom is unchanged by the application of an electric field, even though the electric field mixes states having g factors different from the g factor of the unperturbed ground state into the electronic configuration.

The remaining terms are those, which would occur for an atom in a magnetic field H.

Thus when an atom, whose ground state is ${}^2S_{\frac{1}{2}}$, is studied in an electric field E and in a magnetic field H the energy levels of the ground state can be found by using the Hamiltonian

$$H=\frac{\Delta W'}{(I+\frac{1}{2})}\,I\cdot J-g_J\mu_0 HJ_z-g_I\mu_0 HI_z\,,$$

where the hyperfine constant $\Delta W'$ is a function of E. An approximate value for $\Delta W'$ is

$$\Delta W'\simeq\Delta W\left\{1-\alpha E^2\left[\frac{1}{2(\overline{W}^0_{n',l'=1}-\overline{W}^0_{n,l=0})}+\frac{1}{(\overline{W}^0_{n'',l''=0,2}-\overline{W}^0_{n,l=0})}\right]\right\}.$$

As was previously noted this is in reasonable agreement with the experimental results on $\Delta W'$ for ^{133}Cs. The shifts $\Delta W'$ for the other alkali metals and hydrogen can probably be measured with known techniques.

Appendix

Another method of estimating the Stark shift of the hyperfine structure of an atom in a ${}^2S_{\frac{1}{2}}$ ground state is as outlined by Haun and Zacharias [1]. Suppose the atom is placed in a uniform electric field E and suppose that ez is the electric dipole moment of the atom. Because the atom has no permanent dipole moment there is no first order shift of the energy levels. In second order the shift of a given F level is

$$\Delta_F(E)=e^2E^2\sum_{n',F'}\frac{|(n',l'=1,F'|z|n,l=0,F)|^2}{(\overline{W}^0_{n,l=0,F}-\overline{W}^0_{n',l'=1,F'})}\,.$$

The Stark shift of the hyperfine structure is then given by

$$\Delta(E)=\Delta_{F=I+\frac{1}{2}}-\Delta_{F=I-\frac{1}{2}}\,.$$

In this calculation the wave functions $\psi_{n,l\ 0,\ F\ l+\frac{1}{2}}$ and $\psi_{n,l\ 0,\ F-l-\frac{1}{2}}$ cannot be considered to be the same, but must be known to first order in the hyperfine interaction (*i.e.* to an accuracy $\Delta W/(W^0_{n,l=0} - W^0_{n',l'\ 1})$). The energy denominators must, also, be taken into account since $W^0_{n,l\ 0,\ F=l+\frac{1}{2}} - W^0_{n,l=0,\ F\ l-\frac{1}{2}} = \Delta W$. When both these effects are considered, and when approximations similar to those used previously are introduced, the result obtained for $\Delta(E)/\Delta W$ is the same as was obtained by estimating $\psi^2(0)$.

The fact that these two methods yield the same results is to be expected. The Hamiltonian, which must be used to calculate the hyperfine splitting of a state, is

$$H = -2\mu_0 \left| -\frac{8\pi}{3} S\cdot\mu\,\delta(r) + \frac{1}{r^3}(s\cdot\mu)(\mu\cdot r) - \frac{1}{r^3}(L\cdot\mu) \right|,$$

where r is the radius vector and where the other symbols are the same as before. The first term in this Hamiltonian yields the expression, derived by Fermi, for a spherically symmetric state. This contact interaction is much larger than the contributions, which the P and D states will make when they act on the remaining terms in the Hamiltonian. Hence the value of ΔW estimated from $\psi^2(0)$ must be a fairly good approximation.

It should be noted that the Stark shift of the hyperfine structure is independent of m. This is valid only for states for which $J = \frac{1}{2}$. The result that the terms involving E^2H vanish is correct only for S state atoms.

Naturally the Stark shift of the hyperfine structure obtained by using zero-th order wave functions and the same energy denominator for both hyperfine levels in third order perturbation theory is the same as is obtained in second order if one uses wave function correct to first order in the hyperfine interaction and includes the hyperfine separation in the energy denominators.

RIASSUNTO (*)

Si esaminano i livelli di energia di un atomo nello stato fondamentale $^2S_{\frac{1}{2}}$ in presenza di un campo elettrico. Si trova che la struttura iperfina dello stato fondamentale subisce uno spostamento di Stark. Si valuta in maniera grossolana questo spostamento. Questa valutazione è in buon accordo con i risultati sperimentali nel caso del ^{133}Cs, in cui lo spostamento di Stark della struttura iperfina è stato misurato. Il fattore g dello stato fondamentale non è influenzato dal campo elettrico.

(*) *Traduzione a cura della Redazione.*

Remarks on the Derivation of the Lorentz Trasformation.

E. M. Dewan

Electromagnetic Radiation Laboratory, Electronics Research Directorate, Air Force Cambridge Research Laboratories, Office of Aerospace Research, United States Air Force - Bedford, Mass.

(ricevuto il 22 Agosto 1961)

Summary. — An attempt is made to replace the principle of relativity in the derivation of the Lorentz transformation by an alternative postulate concerning the behavior of clocks. It will be shown by means of thought experiments that this postulate is not quite sufficient to obtain the Lorentz transformations and that an additional postulate concerning the absence of length contraction of a rod in the direction normal to its motion (proved indirectly via the Ives-Stilwell experiment) is needed to complete the derivation.

1. – Introduction.

A comparison [1] has been made between the derivation of the Lorentz transformation by means of the principle of relativity and the derivation by means of three crucial experiments (*). In the present paper the Lorentz transformation are derived (**) by means of thought experiments and an attempt

(*) Both derivations made use of the fact that the speed of light does not depend upon the speed of the source. One derivation considers this as a postulate and the other derivation considers it as an experimental fact. It should be noted that some authors, Tolman for example, consider it to be part of the principle of relativity.

(**) Other interesting derivations of the Lorentz transformation will be found in references [2] to [25].

[1] H. P. Robertson: *Rev. Mod. Phys.*, **21**, 379 (1949).
[2] P. Frank and H. Rothe: *Ann. d. Phys.*, **34**, 825 (1911).
[3] E. V. Huntington: *Phil. Mag.*, **23**, 494 (1912).
[4] L. A. Pars: *Phil. Mag.*, **42**, 249 (1921).

is made to replace the principle of relativity by the postulate that the rate of a clock is independent of its orientation; however, although the resulting transformations (*) admit the equation $ds^2 = 0$, they give the following relation between ds and ds', $(ds')^2 = \lambda(ds)^2$, where λ is not necessarily equal to unity but can depend on the relative velocity of the two inertial frames.

It is thus necessary to add an assumption to the one mentioned above. This latter assumption can take the following forms: the transformations form a group (a direct consequence of the principle of relativity); there is an absence of contraction of measuring rods orientated perpendicular to the relative velocity; or finally, the time dilates by a certain function of velocity as shown by the experiments of Ives and Stilwell.

2. – Derivation of the Lorentz transformations.

2·1. *Postulates and conventions.*

Postulate I. – *The velocity of light is independent of the velocity of its source.* This postulate is based on the fact that two extraterrestrial phenomena

(5) C. Caratheodory: *Berlin Sitz.*, **5**, 12 (1924).
(6) V. V. Narliker: *Proc. Camb. Phil. Soc.*, **28**, 460 (1932).
(7) G. J. Whitrow: *Quart. Journ. Math.*, **4**, 161 (1933).
(8) L. R. Gomes: *Lincei Rend.*, **21**, 433 (1935).
(9) N. R. Sen: *Ind. Journ. Phys.*, **10**, 341 (1936).
(10) F. Severi: *Proc. Phys. Math. Soc. Japan*, **18**, 257 (1936).
(11) E. Esclangon: *Compt. Rend.*, **202**, 708 (1936); *Bull. Astron.*, **10**, 1 (1937).
(12) J. Meures: *Zeits. f. Phys.*, **102**, 611 (1936).
(13) V. Lalan: *Compt. Rend.*, **203**, 1491 (1936); *Bull. Soc. Math. France*, **65**, 83 (1937).
(14) G. Temple: *Quart. Journ. Math.*, **9**, 283 (1938).
(15) H. E. Ives: *Proc. Amer. Phil. Soc.*, **95**, 125 (1951); *Phil. Mag.*, **36**, 392 (1945).
(16) H. P. Robertson: *Rev. Mod. Phys.*, **21**, 378 (1949).
(17) A. Metz: *Journ. Phys. Rad.*, **13**, 224 (1952).
(18) W. H. McCrae: *Proc. Roy. Irish Acad.*, **45**, 23 (1938).
(19) K. D. Stiegler: *Compt. Rend.*, **234**, 1250 (1952); *Nuovo Cimento*, **8**, 922 (1958).
(20) A. W. Ingleton: *Nature*, **171**, 618 (1953).
(21) Y. Mimura and T. Iwatsuki: *Journ. Sci. Hiroshima U.*, A **1**, 111 (1931).
(22) E. Leroy: *Compt. Rend.*, **202**, 794 (1936).
(23) B. C. Mukherjee: *Ind. Journ. Phys.*, **10**, 237 (1937).
(24) U. Ueno: *Studies in Logic; the Axiomatic Method* (Amsterdam, 1959), p. 322.
(25) W. Panofsky and M. Phillips: *Classical Electricity and Magnetism* (New York, 1955).

(*) $ds^2 \equiv (dx)^2 + (dy)^2 + (dz)^2 - c^2(dt)^2$, $(ds')^2 \equiv (dx')^2 + (dy')^2 + (dz')^2 - c^2(dt')^2$, where c = the velocity of light.

contradict any form of « emission theory » (*). All the usual derivation which rely on the principle of relativity incorporate this postulate.

POSTULATE II. – *The rate of a clock in an inertial frame does not depend upon the clock's orientation in space.*

This postulate was proven by the Michelson-Morley experiment for a « mirror clock » (that is, one that involves a light pulse bouncing between two mirrors, each round trip constituting one « tick » of the clock). By definition, all clocks behave consistently; hence Postulate II must hold for any type of clock regardless of its construction or its mode of operation (**).

Finally, we shall assume a certain famous *convention* for synchronizing clocks separated by spatial distances. This convention is discussed at length elsewhere ([26-30]). One way of stating it is: « Distant clocks shall be synchronized by using light signals in such a way that the "one way" velocity of light is the same as the "round trip" velocity. »

2·2. *The length contraction effect.* – In the following derivation of the Lorentz transformations we consider two identically constructed mirror clocks, one at rest in inertial frame S and the other at rest in a different inertial frame S' which moves with velocity v with respect to S. Let us view the comparison of these two clocks from the *point of view of an observer at rest in* S and see how the velocity of the S' clock affects its operation and structure.

As mentioned previously, the Michelson-Morley experiment implies that the rate of a mirror clock in any inertial frame does not depend upon its orientation (Postulate II). With this in mind, we now consider the *path length of a light pulse* for one period of the mirror clock located in the S' frame and calculate it for two orientations: perpendicular and parallel to the velocity. There will of course be no loss in generality if we consider only one perpendicular direction.

(*) DESITTER showed that eclipsing binary stars do not give any observable evidence of a certain eccentricity that would be present if the velocity of light were to depend additively upon the source; MILLER showed that there were none of the complications of the interference pattern due to the sun's rotations when the Michelson-Morley experiment was performed with sunlight.

(**) Gravitational forces are ruled out of this discussion since only inertial systems will be considered.

([26]) A. EINSTEIN: *On the electrodynamics of moving bodies* (1905), reprinted in A. EINSTEIN, H. A. LORENTZ, H. MINKOWSKI and H. WEYL: *The Principle of Relativity* (London, 1923).

([27]) A. EDDINGTON: *The Mathematical Theory of Relativity* (London, 1923), p. 18.

([28]) A. GRÜNBAUM: *Am. Journ. Phys.*, **23**, 450 (1958).

([29]) H. REINCHENBACH: *Space and Time* (1958), Section **19**.

([30]) G. BUILDER: *Austr. Journ. Phys.*, **11**, 459 (1958).

2·2.1. Mirror clock perpendicular to the velocity. – Let l_S be the length of the clock in S and $l_{S'}$, be the length of the identical clock in S' as measured in S when it is in the perpendicular position. Let $\tau_{S'}$ be the period of this clock as measured from the S frame (Fig. 1). From Fig. 1 we see that the path length for half the period $\tau_{S'}$

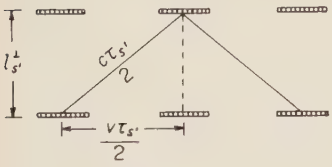

Fig. 1.

$$\left(\frac{c\tau_{S'}}{2}\right)^2 = \left(\frac{v\tau_{S'}}{2}\right)^2 + (l^{\perp}_{S'})^2 .$$

Hence, the path length for a complete period is

$$L = c\tau_{S'} = \frac{2l^{\perp}_{S'}}{\sqrt{1-\beta^2}} , \tag{1}$$

where $\beta = v/c$.

It is implicitly assumed here that the movement of the mirrors does not affect the velocity of the light pulse (Postulate I.)

2·2.2. Mirror clock parallel to the velocity. – Let $l^{\parallel}_{S'}$ be the length as measured in S of the S' clock when it is oriented in a direction parallel to its velocity. Also let Δt_1 be the time for the light pulse to move from mirror (1) to mirror (2) (see Fig. 2) as the apparatus moves a distance $v\,\Delta t_1$ to the right, and let Δt_2 be the time for the return trip. We have from Fig. 2 and using Postulate I

$$c\,\Delta t_1 = l^{\parallel}_{S'} + v\,\Delta t_1 ;$$

$$c\,\Delta t_2 = l^{\parallel}_{S'} - v\,\Delta t_2 .$$

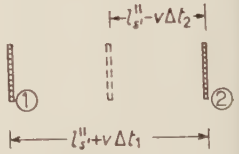

Fig. 2.

Hence,

$$\Delta t_1 = l^{\parallel}_{S'}/(c - v) , \qquad \Delta t_2 = l^{\parallel}_{S'}/(c + v) ;$$

and since

$$\tau_{S'} = \Delta t_1 + \Delta t_2 ,$$

the path length $L_{\parallel}$ is given by

$$c\tau_{S'} = \frac{2l^{\parallel}_{S'}}{1-\beta^2} = L_{\parallel} , \tag{2}$$

Postulate II entails

$$L_{\parallel} = L_{\perp} ,$$

which in turn implies that the S' clock must contract in such a way that the relation

$$l^{\parallel}_{S'} = \sqrt{1-\beta^2}\, l^{\perp}_{S'} , \tag{3}$$

prevails. Thus we may conclude that Postulates I and II imply

$$l^{\parallel}_{S'} = (1-\beta^2)^{n/2}\, l_S f(\beta) \tag{4}$$

and

$$l^{\perp}_{S'} = (1-\beta)^{(n-1)/2}\, l_S f(\beta) , \tag{5}$$

where n is an arbitrary integer and $f(\beta)$ is a function (*) that does not go to zero for $0<\beta<1$, is not pathologic, and $f(0)=1$.

2·3. *The time dilation effect and the Kennedy-Thorndike experiment.* – We now investigate the implications of the fact that all clocks must, by definition, behave consistently. As we shall see, the Kennedy-Thorndike experiment can be considered to be a partial check on the physical realizability of such a definition. For further discussion of this consistency see the works of Sciama, Dirac, and Dicke, where the possibility of « time-dependent » laws of nature is discussed ([31-36]). If a relative change in the rates of clocks using differing forces for their operation actually did become manifest, then one *could not* assume the time invariance of physical laws and it is rather evident that this could have a tremendous effect on our concept of physical time.

In the Kennedy-Thorndike experiment an interferometer with two unequal arms was used. Let the rest lengths of these two arms be l_0 and kl_0, where k is a positive number such that $0 \leqslant k \leqslant 1$.

We now consider the various path lengths of the light beams in the arms

(*) Note that the case where $f(\beta)=1$ is the one discussed by Ives in *Journ. Opt. Soc. Am.*, **27**, 263 (1937).

([31]) D. W. Sciama: *Mont. Not. Roy. Ast. Soc.*, **113**, 34 (1953).

([32]) R. H. Dicke: *Am. Scient.*, **47**, 25 (1959).

([33]) P. A. M. Dirac: *Proc. Roy. Soc.*, A **165**, 199 (1938).

([34]) P. Jordan: *Schwerkraft und Weltall* (Berlin, 1952).

([35]) R. H. Dicke: *Science*, **129**, 621 (1959).

([36]) R. H. Dicke: *Rev. Mod. Phys.*, **29**, 355 (1957).

for the perpendicular and parallel orientations of the interferometer, assuming again that it has a velocity v with respect to S.

2·3.1. Long arm parallel to the velocity. – From eq. (1) and (2), the path lengths in the short and long arms are respectively

$$L_{\perp} = \frac{2kl_{S'}^{\perp}}{\sqrt{1-\beta^2}},$$

and

$$L_{\parallel} = \frac{2l_{S'}^{\parallel}}{(1-\beta^2)},$$

where $l_{S'}$, and $l_{S'}$ are, as before, moving lengths measured with an apparatus at rest in S (Fig. 3). Using eq. (3) we obtain for the path difference in the two arms

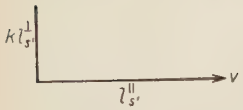

Fig. 3.

$$\delta_{\parallel} = L_{\perp} - L_{\parallel} = \frac{2l_{S'}^{\perp}(k-1)}{\sqrt{1-\beta^2}}. \tag{6}$$

2·3.2. Long arm perpendicular to the velocity. – Here (see Fig. 4),

$$\delta_{\perp} = L_{\perp} - L_{\parallel} = \frac{2kl_{S'}^{\perp}}{(1-\beta^2)} - \frac{2l_{S}^{\parallel}}{\sqrt{1-\beta^2}};$$

and, using eq. (3),

$$\delta = \frac{2l_{S}^{\perp}(k-1)}{\sqrt{1-\beta^2}}.$$

Hence

$$\delta_{\parallel} = \delta_{\perp} \equiv \delta.$$

From this result we see that a rotation of this interferometer would not give a fringe shift; however, in contrast to the case with the Michelson-Morley interferometer where $k = 1$, the path difference *depends on velocity*. One would thus expect a fringe shift to occur after some time, owing to the change in the velocity of the earth as it moves through space. The result of this experiment, however, was that no such shift was observed.

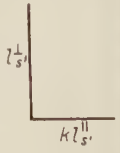

Fig. 4.

To explain this null result we consider the path difference δ as being filled with a constant number m of wave crests for all velocities. The period $\tau_{S'}$ of the light source in S' is given by

$$\tau_{S'} = \delta/cm.$$

Using eq. (5) and (6) we have

$$\tau_{S'} = \frac{2l_S(k-1)(1-\beta^2)^{(n-1)/2} f(\beta)}{cm\sqrt{1-\beta^2}} .$$

Let the period of an identical light source at rest in S be τ_s. Setting $\beta = 0$ in the above equation, we get

$$\tau_s = \frac{2l_s(k-1)}{cm} .$$

Hence [37],

$$\tau_S = \tau_s(1-\beta^2)^{(n-2)/2} f(\beta) . \tag{7}$$

In other words, the null result implies that the period of the light source is, *with the exception of the case where* $n=2$ *and* $f(\beta)=1$, altered in a way that depends on its velocity (*). One gets the usual time dilation effects when $n = f(\beta) = 1$.

It is easy to calculate from eq. (2) and (4) that the relation (7) also holds for the period of a mirror clock, and it is this fact that makes the Kennedy-Thorndike experiment a partial confirmation of the consistency of clock behavior. In this case it is a consistency of the behavior of a mirror clock and a clock consisting of atoms radiating at a certain characteristic frequency (the light source). As we shall presently see, the effects of velocity on clocks and measuring rods (eq. (7) and (4) and (5) respectively) imply that the *round trip* velocity of light is independent of the velocity of the inertial frame used (**). This result *does not depend on the value of* n *or* $f(\beta)$. In order to show this, let us first review the meanings of some of the symbols used up to this point. In eq. (4) and (5) l_S is the length of a rod at rest in S, and $l_{S'}^{\parallel}$ and $l_{S'}^{\perp}$ are the lengths of a rod with rest length l_S but which is moving with velocity v

(*) The reader might amuse himself by investigating what this case means physically.

(**) This is immediately apparent when one realizes that the round-trip light velocity enters into the time-keeping mechanism itself; for, all clocks must be consistent with a mirror clock and this statement is obviously true for the latter. Hence, since c « controls » the rates of clocks, all inertially moving clocks measure it as having the same value. For example: if the velocity of S' relative to S were very great, the S' clock would tick very slowly, and therefore, even though a round trip of a light pulse in a light-velocity measuring experiment in S' would take a long time as seen by S, the (round trip) velocity of this pulse *as measured in* S', would still be c because of length contraction and time dilation.

(37) H. E. Ives: *Journ. Opt. Soc. Am.*, **27**, 177 (1937).

with respect to S. Notice that $l^{\parallel}_{S'}$ and $l^{\perp}_{S'}$ are measured in the units of S (that is by means of apparatus at rest in S), and that they are the lengths of the rod when it is orientated parallel and perpendicular to its velocity respectively. The τ_S and $\tau_{S'}$ in eq. (7) correspond to the periods of identical mirror clocks, τ_S corresponding to the one at rest with respect to S and $\tau_{S'}$ corresponding to the one moving with velocity v with respect to S, and *measured in terms of the units of* S. If τ_S is defined as unity,

$$\tau_{S'} = f(\beta)(1 - \beta^2)^{(n-2)/2} .$$

Now let $t_{S'} \equiv$ the number of cycles registered on the dial of an S' clock; $t_S \equiv$ the number of cycles registered on the dial of an S clock. From eq. (7) for the *units* of time we obtain

$$t_S = t_{S'}(1 - \beta^2)^{(n-2)/2} f(\beta) , \tag{8}$$

for the relation between the dial reading of two clocks assumed to be synchronized at $t = 0$, the moment they coincide.

Also let $y \equiv$ the number of divisions of length between the origin and a certain point along an axis of S perpendicular to the relative velocity; $y' \equiv$ the number of divisions of length between the origin and a certain point along a perpendicular axis of S' parallel and equal in length to y as measured in S; that is, y and y' represent the perpendicular distance from the origin of S and S' to the *same point*, then from eq. (5), which refers to units of length perpendicular to v, we obtain

$$y' = y \frac{(1 - \beta^2)^{(1-n)/2}}{f(\beta)} . \tag{9}$$

Finally, let $l_x \equiv$ the number of divisions of length between the origin of S and a certain point along an axis of S that is parallel to the relative velocity; $l_{x'} \equiv$ the number of divisions of length between the origin of S' and the *same* point along an axis of S' that is parallel to the relative velocity and *at the time when the two origins coincide*. Then, analogously to the above, we obtain from eq. (4).

$$l_{x'} = \frac{l_x(1 - \beta^2)^{-n/2}}{f(\beta)} . \tag{10}$$

Notice that $n = f(\beta) = 1$ gives the usual « time dilation », « length contraction », abd the lack of any change in length in the y direction. Later we shall consider some of the reasons why one must set $n = 1 = f(\beta)$.

We can now show that the speed of light is the same in S and S' regardless of the value of n and $f(\beta)$.

Let $t_{s'}$ be the time in S' (that is, the time registered on a clock dial in S') for a round trip of a light pulse and let $2y'$ be the total distance of this round trip (see Fig. 5). Defining c' to be the velocity of light measured by this method in S', we have $c' \equiv 2y'/t_{s'}$. Let us consider this measurement from the point of view of an observer at rest with respect to S. Not only would he use eq. (8) and (9) to obtain

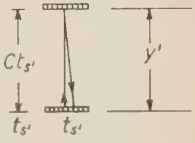

Fig. 5.

$$c' = \frac{2y}{t_s\sqrt{1-\beta^2}}, \tag{11}$$

but he would also have to take into account the effect of the motion of the mirrors on the length of the light path (see Fig. 6). From the figure we obtain

$$\left(\frac{ct_s}{2}\right)^2 = y^2 + \left(\frac{vt_s}{2}\right)^2. \tag{12}$$

Solving eq. (11) for y and inserting into (12) we obtain

$$(c')^2 - (c)^2$$

for all n and $f(\beta)$.

2·4. *Synchronization of distant clocks.* – We now utilize the convention mentioned in Section **2**·1 and consider two identical clocks A and B in the inertial frame S' separated by a distance along the direction of the relative velocity. To synchronize them one first sets their dials to be equal and then « starts » them when they are reached by a light pulse originating from an isotropic light source located at a point midway between them. The light pulse leaving the midway point reaches the two clocks « simultaneously » by definition, provided we take the point of view that S' is at rest. It should be emphasized that since A and B are constructed identically, their *rates* are equal by definition and the above procedure only adjusts the relative « *phase* » of the clocks. It is important to keep these two aspects of clock agreement separate, for there seems to be a tendency among certain students (and even writers) to fuse them together. This tendency exists simply because we have only the *one word* « synchronism » for clock agreement.

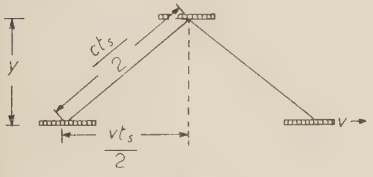

Fig. 6.

Consider the situation now from the point of view that takes S' as being at rest. Clocks A and B would no longer be synchronized because the motion of S' would cause the light to reach A before it reached B. We now calculate this discrepancy seen by S (Fig. 7). Let t_1 be the time the pulse arrives at A, and t_2 the time it arrives at B as measured in S. Let $t=0$ correspond to the emission time at light source. The problem is to find t_2-t_1 and from this the difference between the dial readings of clocks A and B.

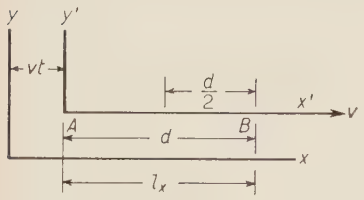

Fig. 7.

Let d be the distance between A and B as measured in S (see Fig. 7). Then

$$t_2 = \frac{d/2}{c-v}, \qquad t_1 = \frac{d/2}{c+v};$$

$$t_2 - t_1 = \frac{dv}{c^2 - v^2} = \frac{dv/c^2}{(1 - v^2/c^2)}.$$

However, the time elapsed between t_2 and t_1 *as registered on the dials of clocks at rest* in S' is dilated (*), that is, during the time between the arrival of the pulse at A and B, the A clock (the one reached first), ticks (as measured in S) at a « dilated rate ». Hence from eq. (8),

$$\frac{1}{f(\beta)}(t_2 - t_1)(1-\beta^2)^{(2-n)/2} = t_2' - t_1'.$$

Thus, the difference between the dial readings of A and B is given by

$$t_2' - t_1' = \frac{vd}{c^2}\frac{(1-\beta^2)^{(n-2)/2}}{f(\beta)}. \tag{13}$$

2·5. *The Lorentz transformations.* – Eq. (8) and (13) lead to the transformation for time as follows. Let t_A' be the dial reading of the clock A that is located $x = vt$. The from (8),

$$t_A' = (1-\beta^2)^{(2-n)/2} t \frac{1}{f(\beta)},$$

where t is the time in S. If we let t_B' be the dial reading of clock B located at $x = vt + d$ (see Fig. 7), and if we take into account the fact that it *lags* behind

(*) (or contracted, depending on the value of n and $f(\beta)$).

clock A by the amount given in eq. (13), then we obtain

$$t'_B = t\,\frac{(1-\beta^2)^{(2-n)/2}}{f(\beta)} - \frac{dv}{c^2}\,\frac{(1-\beta^2)^{-n/2}}{f(\beta)} = \left(t - \frac{vx}{c^2}\right)\frac{(1-\beta^2)^{-n/2}}{f(\beta)}\,.$$

Thus, in general, a clock in a moving system S' located at a point with a co-ordinate x in S reads

$$t' = \left(t - \frac{vx}{c^2}\right)\frac{(1-\beta^2)^{-n/2}}{f(\beta)}\,. \tag{14}$$

Eq. (10) leads to the transformation for x as follows. Since $l_{x'} = x'$,

$$x'(1-\beta^2)^{n/2} f(\beta) = l_x\,.$$

But from Fig. 9 we see that $l_x = x - vt$. Therefore

$$x' = \frac{x - vt}{f(\beta)(1-\beta^2)^{n/2}}\,. \tag{15}$$

Eq. (9) gives the transformation for a co-ordinate perpendicular to the velocity

$$y' = \frac{y(1-\beta^2)^{(1-n)/2}}{f(\beta)}\,. \tag{9}$$

Eq. (14), (15), and (9) can be solved for the inverse transformations, which are

$$x = (x' + vt')(1-\beta^2)^{(n-2)/2} f(\beta)\,; \tag{16}$$

$$t = \left(t' + \frac{vx'}{c^2}\right)(1-\beta^2)^{(n-2)/2} f(\beta)\,; \tag{17}$$

$$y = y'(1-\beta^2)^{(n-1)/2} f(\beta)\,. \tag{18}$$

Notice that $\beta = v/c$ and v refer to the velocity of S' relative to S as measured operationally by means of *instruments at rest in* S. There is no reference in these equations to the velocity of S with respect to S' as measured with instruments at rest in S'.

Next, if one computes the « interval » and then uses the above transformations, one obtains

$$(\mathrm{d}x)^2 + (\mathrm{d}y)^2 - c^2(\mathrm{d}t)^2 = \lambda[(\mathrm{d}x')^2 + (\mathrm{d}y')^2 - c^2(\mathrm{d}t')^2]\,, \tag{19}$$

where (*)

$$\lambda \equiv (1 - \beta^2)^{n-1} f^2(\beta) .$$

For $n = 1 = f(\beta)$, eq. (14), (18), and (9) go over into the Lorentz transformations and λ becomes equal (**) to 1. Eq. (19) is another expression of the fact that c is invariant for arbitrary n and $f(\beta)$.

We now turn to the experimental determination of the value of n and $f(\beta)$.

A) In order to measure $f(\beta)$ and n, Ives and Stilwell [38] measured the time dilation effect and found the correct relation to be

$$\tau_S - \tau_{S'} / \sqrt{1 - \beta^2} .$$

thus showing experimentally that $n = 1$ and that $f(\beta) = 1$. This was accomplished by measuring the so-called « transverse Doppler shift » of the radiation of fast moving « canal rays ». Their experiment showed that in addition to the usual Doppler shift there would be the above second-order shift toward a lower frequency when the light sources were examined in a direction perpendicular to their motion. Because it was impossible, for practical reasons, to measure the Doppler shift precisely enough in a direction perpendicular to the rays, they resorted to measuring the frequency shifts in the forward and backward directions, and from this calculated the necessary data.

B) A more recent experimental check of this result was made by Schiffer [39] in one of his red-shift measurements which used the Mössbauer effect. He was able to measure the transverse Doppler shift from a source of radiation in a magnetically suspended high speed rotor.

(*) The above procedure has implicitly built into it the fact that the transformations will be linear. If we were to consider transformations to accelerated frames, we would again obtain (19) except that λ would be more arbitrary and the transformations would consist of the four-dimensional conformal group which includes non-linear transformations. Bateman and Cunningham showed that the Maxwell equations were invariant under these more general transformations. For more information about this see E. T. Whittaker: *History of the Theories of Aether and Electricity.*

(**) See the interesting discussions by Jeffreys [*Austral. Journ. Phys.*, **11**, 583 (1958)] and Builder [*Austral. Journ. Phys.*, **12**, 300 (1959)] on the clock paradox. Jeffreys must have been unaware that the experiment we describe fixes n and $f(\beta)$ uniquely. The resulting questions and answers raised are nevertheless stimulating.

(38) H. E. Ives and H. R. Stilwell: *Journ. Opt. Soc. Am.*, **28**, 215 (1938); **31**, 369 (1941).

(39) H. J. Hay, J. P. Schiffer, T. E. Cranshaw and P. A. Egelstaff: *Phys. Rev. Lett.*, **4**, 165 (1960).

C) POUND ([40]) measured the transverse Doppler shift due to *thermal motions* in a source of radiation during his gravitational red-shift measurements. The great accuracy of his experiment took him by surprise at first in that this effect originally appeared in his data as an error (soon caught).

3. – Relative velocity and λ.

Let $v_{S'S} \equiv$ the velocity of S' relative to S, measured by means of instruments at rest in S. The actual measurement of this velocity is performed as follows (Fig. 8). The observer in S measures the speed of a fixed point in S' (the arrow extends from this point in the figure) along his x axis by means of clocks a and b. He computes the velocity by dividing the difference in the readings of clocks at a and b by the distance between them. Notice that

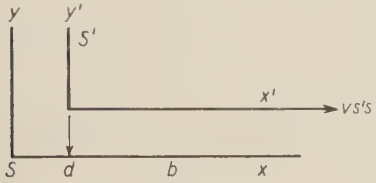

Fig. 8.

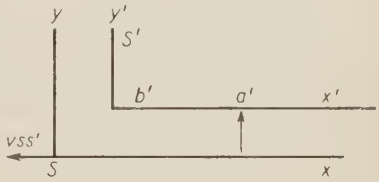

Fig. 9.

$v_{S'S}$ is calculated by means of a *proper length* and a time that is not proper since « proper time » involves only a *single* clock. Also let $-v_{SS'}$ be the velocity of S with respect to S', measured by means of instruments at rest in S'. This measurement is performed in the same way as above except that now the clocks are at rest in S', etc. (see Fig. 9). Operationally speaking, $v_{SS'}$ and $v_{S'S}$ are entirely different quantities and we shall now show (*) that for any n and $f(\beta)$,

$$v_{SS'} = -v_{S'S} . \tag{20}$$

Defining: Δt_p = a proper time interval in S,
$\Delta t_{\tilde{p}}$ = « non-proper » time interval in S, that is, one that involves two clocks instead of one,
Δx_p = a proper distance along the x direction (a rest distance),
$\Delta x_{\tilde{p}}$ = a « non-proper » distance along the x direction; that is, one that is *moving* with respect to S but measured by means of instruments at rest in S.

([40]) R. V. POUND and G. A. REBKA: *Phys. Rev. Lett.*, **4**, 337 (1960).

(*) If the postulate of relativity were invoked, not only would $f(\beta) = n = 1$ but eq. (20) would follow directly from the postulate.

and letting $\Delta t'_{\mu}$, $\Delta t'_{\tilde{\nu}}$, $\Delta x'_{\mu}$, $\Delta x'_{\tilde{\nu}}$ be the analogous quantities in S', we then have, using $x' = t' = 0$ in eq. (16) and (17), and $x = t = 0$ in eq. (15) and (14), respectively,

$$v_{S'S} \equiv \frac{\Delta x_{\tilde{\nu}}}{\Delta t_{\tilde{\nu}}} = \frac{\Delta x'_{\tilde{\nu}}(1-\beta^2)^{(n-2)/2} f(\beta)}{\Delta t'_{\nu}(1-\beta^2)^{(n-2)/2} f(\beta)} = \frac{\Delta x'_{\tilde{\nu}}}{\Delta t'_{\nu}} = v_{(S'S)S'} , \tag{21}$$

$$v_{SS'} \equiv -\frac{\Delta x'_{\nu}}{\Delta t'_{\tilde{\nu}}} = -\frac{\Delta x_{\tilde{\nu}}(1-\beta^2)^{-n/2} f(\beta)}{\Delta t_{\nu}(1-\beta^2)^{-n/2} f(\beta)} = -\frac{\Delta x_{\tilde{\nu}}}{\Delta t_{\nu}} = v_{(SS')S} . \tag{22}$$

The quantities $v_{(S'S)S'}$ and $v_{(SS')S}$ are the « speedometer » velocities of S' relative to S in S' units, and of S relative to S' in S units. Now, as can be seen from eq. (21) and (22),

$$v_{S'S} = -v_{SS'} , \tag{23}$$

if

$$v_{S'S} = -v_{(SS')S} , \tag{24}$$

or if

$$v_{SS'} = -v_{(S'S)S'} . \tag{25}$$

But both eq. (24) and (25) must be true, for if they were not, the concept of velocity would be inconsistent (notice that the measuring instruments are at rest with respect to the same frame for both sides of these equations). Thus we see eq. (23) must be true (*).

It is important to notice that eq. (23) is *independent of* n; thus, the relative velocity does not depend on λ even though

$$\lambda \left|1-\left(\frac{v_{S'S}}{c^2}\right)^2\right|^{n-1} f^2\left(\frac{v_{S'S}}{c}\right) .$$

With regard to this Fock ([41]) says: « ... the relative velocity of the motion is

(*) Another *gedanken experiment* approach ([25]) to the Lorentz transformations, similar in some respects to the one presented here assumes the principle of relativity to obtain $v_{S'S} = -v_{SS'}$ and then uses the latter to derive eq. (13) with $n = f(\beta) = 1$ for the relation for the relative « phases » of clocks in a moving system. This tells us that Einstein's synchronization convention is in some sense responsible for one's ability to set

$$v_{S'S} = -v_{SS'} .$$

([41]) V. Fock: *The Theory of Space, Time and Gravitation* (translated by N. Kemmer) (London, 1959), p. 17.

not at all connected with the scale factor λ and, therefore, ... this factor cannot depend on the relative velocity. Then one has only to assume that for vanishing relative velocity, length and time measurements in both systems are performed in the same way, in terms of the same units, and one finds $\lambda = 1$. Subject to such very natural requirements, λ will be equal to 1 for *any* inertial frame, whatever its velocity. »

FOCK also says in a footnote to the above: « It is usually said, following EINSTEIN, that the scale factor can "evidently" depend on nothing but the relative velocity, and it is subsequently proved that, in fact, it does not have any such dependence but is equal to 1. »

But we see that $v_{s's} = v_{ss'}$ and

$$\lambda = \left[1 - \left(\frac{v_{s's}}{c}\right)^2\right]^{n-1} f^2\left(\frac{v_{s's}}{c}\right) = \left[1 - \left(\frac{v_{ss'}}{c}\right)\right]^{2n-1} f^2\left(\frac{v_{ss'}}{c}\right),$$

that is, λ is the same function of $v_{ss'}$ as it is of $v_{s's}$. *The mere lack of dependence of relative velocity on λ does not necessarily imply the converse.* Thus we must conclude that the only ways to show $n = f(\beta) = 1$, (or $\lambda = 1$) are by experiment, by the postulate of the principle of relativity, or by a postulate that $y = y'$, that is, there is no contraction of length perpendicular to the velocity, etc. If Fock's statement were correct, then one could derive the Lorentz transformation without the principle of relativity (or the postulate that the transformations must form a group). Indeed, in relativistic kinematics, it would be possible to completely replace the principle of relativity by the postulate that the rate of a clock is independent of its orientation.

* * *

I am indebted to Dr. MARK BERAN for the countless stimulating and helpful discussions we have had on the subject of special relativity. Many of the insights in this paper evolved from these conversations. I also wish to acknowledge helpful conversation with Dr. FREDERIC MORGENTHALER.

RIASSUNTO (*)

Nel derivare la trasformazione di Lorentz si tenta di sostituire il principio di relatività con un postulato sostitutivo concernente il comportamento degli orologi. A mezzo di esperimenti ideali si dimostra che questo postulato non è sufficiente per ottenere la trasformazione di Lorentz e che per completare la derivazione è necessario un postulato addizionale concernente l'assenza della contrazione della lunghezza di una sbarretta nella direzione normale al suo moto (provata in maniera indiretta tramite l'esperimento di Ives-Stilwell).

(*) *Traduzione a cura della Redazione.*

IL NUOVO CIMENTO Vol. XXII, N. 5 1° Dicembre 1961

Statistical Theory of Multiple Meson Production with Angular Momentum Conservation.

F. Cerulus

CERN - Geneva
Institut Interuniversitaire des Sciences Nucléaires - Belgique

(ricevuto il 23 Agosto 1961)

Summary. — The conventional statistical theory (with energy-momentum but without angular momentum conservation) is shown to give the same results (multiplicities and spectra) as one can obtain from a model which assumes the existence of an intermediate « hot spot » in the collision of two high-energy particles, if the « hot-spot » formation is statistically independent of its decay into many particles. The model is suggested by the formulae used in statistical theory, which in effect put the probability to produce n particles proportional to the probability to find n particles together in a volume Ω. Angular momentum conservation (together with energy and momentum conservation) can be satisfied by considering only states of n particles with prescribed values of total J, energy and momentum. By using the formalism of the density matrix and an explicit expression for the projection operators on states of given angular momentum one arrives at a modified form of the phase-space integral, which is simply related to the probability to produce n particles. The theory with angular momentum but without momentum conservation, as given by Koba, is shown to be a special case easily derivable from the present formalism. The « classical » theory of angular momentum conservation by Ericson is shown to be a limiting case of wide applicability, however. The conventional theory is strictly speaking valid only if all end particles are in s-states. The formulae have been derived for a spherical Gaussian shape for Ω. Contracted shapes can in principle be allowed for. A Monte-Carlo program is proposed to evaluate this phase-space integral. The method will allow to compute spectra of the longitudinal and the transverse momenta of the final particles. The effect on multiplicity of J-conservation is evaluated. Compared to the conventional theory multiplicity is increased by 10% in p-$\bar{\text{p}}$ annihilation and decreased by 10% in 6 GeV p-p collisions.

PART I

THEORY OF ANGULAR MOMENTUM CONSERVATION IN STATISTICAL MODELS OF MESON PRODUCTION

1. – The hypotheses of the statistical theory.

In the conventional statistical theories of meson production one takes as starting point the following formula for the probability W_n to produce n particles with masses m_1, m_2, ..., m_n in a high-energy collision with given total energy E, in the centre-of-mass system (c.m.s.)

$$\left\{ \begin{array}{l} W_n = C f_{n,T,\ldots} \Omega^{n-1} \varrho_n(E;0) , \\ \varrho_n(E;0) = \int \mathrm{d}\boldsymbol{p}_1 \ldots \int \mathrm{d}\boldsymbol{p}_n \delta\Big(E - \sum_{i=1}^{n} \sqrt{m_i^2 + p_i^2}\Big) \delta\Big(\sum_{i=1}^{n} \boldsymbol{p}_i\Big) , \end{array} \right. \tag{1.1}$$

where $f_{n,T,\ldots}$ is a numerical coefficient depending on the spins and isospins of the particles, on their number and on the total isospin and Ω is a three-dimensional volume. C is a normalizing factor, such that $\sum_n W_n = 1$, where the sum is over all numbers and kinds of particles that can be produced in such a collision, without violating any of the strong-interaction conservation laws.

This formula can be derived from S-matrix theory, with suitable hypotheses as to the behaviour of the S-matrix elements as a function of total energy, isospin, etc. [1,2] (*).

We shall try in the present work to look at it also from a more intuitive point of view, and ask what physical assumptions are made in stating such a formula.

To arrive at a physical interpretation, let us assume that we have described the n particles in the end-states by a superposition of plane waves,

$$\Psi_f(\boldsymbol{p}_1, \ldots; \boldsymbol{x}_1, \ldots) = \exp\Big[i \sum_{i=1}^{n} (\boldsymbol{p}_i, \boldsymbol{x}_i)\Big] .$$

(1) R. HAGEDORN: *Nuovo Cimento*, **15**, 434 (1960).

(2) R. HAGEDORN: *Fortschr. d. Phys.*, **9**, 1 (1961).

(*) This formula, in its simplest form due to Fermi, has been derived and treated by many authors; see the above references for detailed references to previous literature.

We could then write formula (1.1) in the following form (omitting the factor f_{n,T_n})

$$W_n = C\Omega^{n-1}\int \mathrm{d}\boldsymbol{p}_1 \ldots \int \mathrm{d}\boldsymbol{p}_n \exp\Big[-i\sum_{i=1}^{n}(\boldsymbol{p}_i, \boldsymbol{x}_i)\Big]\cdot \tag{1.2}$$

$$\cdot\,\delta\Big(E - \sum_{1}^{n}\sqrt{m_i^2 + \boldsymbol{p}_i^2}\Big)\,\delta\Big(\sum_{1}^{n}\boldsymbol{p}_i\Big)\exp i\Big[\sum_{i=1}^{n}(\boldsymbol{p}_i, \boldsymbol{x}_i)\Big]$$

$$= C\int_{\Omega}\mathrm{d}\boldsymbol{x}_1 \ldots \int_{\Omega}\mathrm{d}\boldsymbol{x}_n \int \mathrm{d}\boldsymbol{p}_1 \ldots \int \mathrm{d}\boldsymbol{p}_n \cdot \tag{1.2'}$$

$$\cdot\,|\Psi_f(\boldsymbol{p}_1, \ldots; \boldsymbol{x}_1, \ldots)|^2\,\delta\Big(E - \sum_{i=1}^{n}\sqrt{m_i^2 + p_i^2}\Big)\,\delta\Big(\sum_{i=1}^{n}\boldsymbol{p}_i\Big)\,\delta\Big(\sum_{i=1}^{n}\boldsymbol{x}_i\Big).$$

The last δ-function has been introduced essentially for dimensional reasons, and means that the average co-ordinate has been taken as 0; because the total momentum is zero a constraint of this type is necessary. If we interpret $|\Psi_f(\boldsymbol{p}_1, \ldots; \boldsymbol{x}_1, \ldots)|^2$ (which is strictly speaking equal to $|\exp[i(\boldsymbol{p}, \boldsymbol{x})]|^2 \equiv 1$), as the density of particles in the region of phase-space around $\boldsymbol{p}_1 \ldots$; $\boldsymbol{x}_1 \ldots$ the formula means that the probability to produce n particles is proportional to the probability to find n particles in a region of phase-space which corresponds to a volume Ω (for each particle) in configuration space times the volume of a complicated hypersurface (defined by the δ-functions) in momentum space. Because $|\Psi_f|^2 = 1$ the phase-space density is constant, and all states in the above defined region are equally probable. Another way of saying the same thing is: W_n is proportional to the sum of the probabilities to find the n particles—which are in a state described by $\boldsymbol{p}_1, \ldots, \boldsymbol{p}_n$—in the volume Ω, where the sum is over all states with the given total energy E and total momentum zero, and all states in the sum have equal probability. Ω plays the role of an adjustable parameter.

How can one understand this result? Let us start, as in the derivation [1] of (1.1) from S-matrix theory by stating that

$$W_n = \sum_f |\langle f|S|i\rangle|^2, \tag{1.3}$$

where S is the S-matrix, $|i\rangle$ the initial state (two colliding particles) and $|f\rangle$ an n-particle state. The sum is over all n-particle final states.

Because we believe that time-invariance holds in strong interactions and because S is unitary we have

$$|\langle f|S|i\rangle|^2 = |\langle i_T|S|f_T\rangle|^2.$$

On the r.h.s. we have the value of the matrix element squared between an n-particle initial state and a two-particle final state, *i.e.* the probability of the

inverse reaction. We could hence also write

$$W_n = \sum_f |\langle i_T | S | f_T \rangle|^2 ,$$

and by comparing with (1.2′) we see that the sum of the probabilities to go from any n-particle state to a two-particle state is effectively put equal to the probability to find the n initial particles in a volume Ω; the *sum* of the squared matrix element, can be expressed—extracting the δ-functions for energy-momentum conservation—by the *average* of a reduced squared matrix element S'

$$W_n = |\langle i_T | S' | f_T \rangle|^2 \sum_f \delta\Big(E - \sum_i \sqrt{p_i^2 + m_i^2}\Big)\, \delta\Big(\sum_i \boldsymbol{p}_i\Big) . \tag{1.4}$$

The statistical hypothesis means then that *on the average* the reduced matrix element squared is equal to the probability to find the n initial particles (in the reverse reaction) in the volume Ω.

We see therefore that one has not made any detailed hypothesis on the S-matrix element between the given two-particle state and a particular n-particle state; the statistical theory as condensed in (1.1) makes only a statement about the average behaviour of the S-matrix elements.

One can now make a model which leads also to (1.2′) and shows therefore the same average behaviour of the transition probabilities as was assumed for the S-matrix: if one assumes that in the collision a « hot spot » is formed, which can afterwards decay in any of the allowed n-particle states, and that the probability of formation of the hot spot is independent of the probability of decay. One sees that this assumption is closely akin to the compound nucleus idea in nuclear physics.

Denoting the probability for hot-spot formation by $W_{2\to c}$ and for its decay by $W_{c\to n}$ the model means

$$W_n = W_{2\to c} W_{c\to n}$$

and for the reverse reaction

$$W_n = W_{n\to c} W_{c\to 2} .$$

If now in addition one makes the further physical assumption that $W_{n\to c} = C_n \cdot$ $\cdot$(probability to find the particle in Ω) [*i.e.*, probability in the reverse reaction to form a hot spot is proportional to the probability to find all particles together in a volume Ω] then we get

$$W_n = C_n W_{c\to 2}\, \Omega^{n-1} \varrho_n(E; 0) . \tag{1.5}$$

Here Ω has got evidently a very precise meaning: its linear extension has to be of the order of magnitude of the range of the strong interactions. This formula will only be identical with (1.1) if we assume furthermore that the proportionality constant C_n is in fact independent of n, *i.e.* that hot-spot formation depends only on all the particles being in Ω, whatever is their number (or their momenta for that matter).

One sees also that it is necessary to make the hot-spot model to arrive at (1.1): according to (1.1) W_n depends only on the probability for the n particles to be in Ω, which is physically only the first phase of the (reverse) process. The total probability W_n is only independent of the second phase (2 particles coming out of Ω) if the two phases are statistically independent.

We emphasize again that for the validity of (1.1) this model need not be true, in all its details. The true S-matrix should only on *the average* give the same results as this model. However, the contents of what one calls usually statistical theory are not exhausted by formula (1.1), which can only predict multiplicities, but no spectra or angular distribution. In order to get information about spectra, one usually takes the formula

$$W_n(p)\,\mathrm{d}p_n = C f_{n,T\ldots}\,\Omega^{n-1}\varrho_{n-1}\left(E - \sqrt{p_n^2 + m_n^2},\, p_n\right) 4\pi p_n^2\,\mathrm{d}p_n\,, \tag{1.6}$$

$$\varrho_{n-1}(E - \sqrt{p_n^2 + m_n^2},\, p_n) = \int \mathrm{d}\boldsymbol{p}_1 \ldots \int \mathrm{d}\boldsymbol{p}_{n-1} \int \mathrm{d}\boldsymbol{e}_n\, \delta\Big(E - \sum_{i=1}^{n} \sqrt{p_i^2 + m_i^2}\Big)\,\delta\Big(\sum_{i=1}^{n} \boldsymbol{p}_i\Big)\,, \tag{1.6'}$$

where $\boldsymbol{e}_n$ is the unit vector along $\boldsymbol{p}_n$. One gets (1.6) in effect from (1.6') by omitting the integration over the magnitude of p_n, and takes $W_n(p_n)\,\mathrm{d}p_n$ to be the probability that p_n shall fall between p_n and $p_n + \mathrm{d}p_n$. One can now make the same kind of reasoning as before, by taking for the allowed n-particle states only those with given total energy-momentum *and* with the n-th particle momentum equal p_n:

$$|\langle f | S' | i \rangle|^2 = S'(p_n)\,, \tag{1.7}$$

and in order to get (1.6) one must put this proportional to the average of the probabilities that n particles with total energy E in their c.m.s., the last particle having momentum p_n, will find themselves together in Ω, when the density in the allowed part of phase-space is uniform. One sees immediately that (1.6) demands that $S'(p_n)$ be in fact independent of p_n, (and equal to a constant of the form Ω^{n-1}), and here we take in effect the « hot-spot » model more seriously. One should point out that on the other hand the spectrum of particles within a given multiplicity n is independent of the assumption C_n—constant.

Formally, it is possible to go on in this vein, to leave, *e.g.* also the angles $\boldsymbol{e}_n$ out of the integration in (1.1) and derive a new formula where the S-matrix element squared averaged over a still smaller number of variables is put equal

to the corresponding average from the hot-spot model; this yields an isotropic distribution, as in the integrand of (1.6) no direction $\boldsymbol{e}_n$ is privileged:

$$(1.8) \qquad W_n(\boldsymbol{p}_n) = C f_{n,T\dots n} \Omega^{n-1} \int \mathrm{d}\boldsymbol{p}_1 \dots \int \mathrm{d}\boldsymbol{p}_{n-1} \delta\Big(E - \sum_{i=1}^{n} \sqrt{p_i^2 + m_i^2}\Big)\, \delta\Big(\sum_{i=1}^{n} \boldsymbol{p}_i\Big) .$$

At this point we have to introduce explicitly angular momentum conservation. Formula (1.1) is not in contradiction with this conservation law, because the S-matrix element will take care of it by its dependence on the $\boldsymbol{p}_i$ (magnitude and direction); after averaging no explicit trace of this remains, except perhaps in the magnitude of Ω. The same cannot be said of (1.6) and *a fortiori* of (1.8), where the assumed independence of the reduced matrix element squared from p_n or $\boldsymbol{p}_n$ may be in contradiction with angular momentum conservation. This contradiction may be avoided by restricting the allowed n-particle states to those having given total energy E, momentum $\boldsymbol{P}_{\mathrm{tot}}$, angular momentum squared $j(j+1)$ and z component of angular momentum m (as we operate in the c.m.s. where $\boldsymbol{P}_{\mathrm{tot}} = 0$ these four quantum numbers can be specified simultaneously). E, $P = 0$, j and m are of course the same as in the initial state, and the states left out by restricting the averaging to those with fixed j and m would have contributed zero to the integral. Averaging then $|\langle i_T | S | f_T \rangle|^2$ over these more restricted final states (specified by E, $P = 0$, j, m and p_n) one shall get a different function $S''(p_n)$, because the region of integration is different. Taking this function independent of p_n is an assumption which involves no contradiction with angular momentum conservation. The hot-spot model which should yield the same average is obtained restricting here also the allowed initial states $|f_T\rangle$ for the reverse reaction to n-particle states having well-defined values, E, $P = 0$, j, m, and taking consequently the probability $W_{n\to c}$ for hot-spot formation proportional to the probability to find the n particles—with the quantum specified above—in the volume Ω. Taking the spectrum and the angular distribution from this hot-spot model will certainly give a better approximation to $W_n(p_n)$ or $W_n(\boldsymbol{p}_n)$ than formulae (1.6) or (1.6′); but there is of course no *a priori* reason that it will yield the whole story, *i.e.* that $S''(p_n)$ is really independent of p_n.

Specifying n-particle states with the quantum numbers given above, and finding an expression for this last probability is not a trivial problem; the next section is devoted to it.

2. – The density matrix.

In this section we shall answer the following question: « what is the probability W_n, that n particles are found inside a volume Ω, assuming that the n particles have well-defined total energy, total angular momentum and that their total momentum is zero? ».

Having stated that the n-particle system has sharp values of H, J^2, J_3 and has $P=0$ is of course not sufficient to define the state of the system. We have seen on the other hand that the statistical theory of meson-production considers every state as equally probable, provided no conservation laws are violated. This then leads in a natural way to the description of the n-particle system by a density matrix. A density matrix can be written quite generally as

$$\varrho = \sum_{\substack{\alpha, E \\ j, j_3}} |\alpha, E, j, j_3, \boldsymbol{P}=0\rangle p_{\alpha, E, j, j_3} \langle \alpha, E, j, j_3, \boldsymbol{P}=0| . \tag{2.1}$$

We have already taken advantage in writing this that we shall only be interested in states with $\boldsymbol{P}=0$. The α stand for all the quantum numbers necessary to define the state completely in addition to E, j, j_3 and $\boldsymbol{P}=0$. Stating that only states with fixed E, j, j_3 (say E', j', j_3') are allowed means putting the weights $p_{\alpha, E, j, j_3}=0$ if E, j, j_3 have values different from E', j', j_3'. Stating that all allowed states have equal probability means putting

$$p_{\alpha, E', j', j_3'} = \text{constant}$$

independent of α (say C_n; it might in principle still depend on n). One could at this stage allow for final-state interaction by a suitable choice of the system of observables α, and by making $p_{E, \alpha', j', j_3'}$, dependent on α. We shall, however, stick here to the simple assumption

$$p_{\alpha, E, j, j_3} = C_n \, \delta(E-E') \, \delta(j-j') \, \delta(j_3-j_3') , \tag{2.2}$$

where C_n is a proportionality constant. This means that we assume for the density matrix in effect the simple form

$$\varrho = C_n \mathscr{P}_E \mathscr{P}_j \mathscr{P}_m \mathscr{P}_0 , \tag{2.3}$$

where $\mathscr{P}_E$, $\mathscr{P}_j$, $\mathscr{P}_m$ are projection operators on n-particle states having respectively total energy $= E$, total angular momentum $= \hbar j(j+1)$, total angular momentum third component m, and $\mathscr{P}_0$ is the projection operator on total momentum $=0$ states.

This density matrix allows us to state the probability to find a given observable A in a range of values $a_0 \ldots a_n$; as is well-known this is

$$\operatorname{Tr} \varrho \mathscr{P}_a ,$$

where $\mathscr{P}_a$ is the projection operator on the subspace of eigenstates of A having eigenvalues in the range $a_0 \ldots a_n$.

Our question now is to find the probability that the observable $\boldsymbol{x}_i$ (= position of i-th particle) will have an eigenvalue ξ_i inside Ω. The corresponding projection operator is simply

$$\int_{\Omega} \mathrm{d}\xi_i \, \delta(\boldsymbol{x}_i - \xi_i) \, ,$$

and the probability that the n particles are inside Ω is given by

$$W_{n,\Omega} = \int_{\Omega} \mathrm{d}\xi_1 \ldots \int_{\Omega} \mathrm{d}\xi_n \, \mathrm{Tr}\, \varrho \, \delta(\boldsymbol{x}_1 - \xi_1) \ldots \delta(\boldsymbol{x}_n - \xi_n) \, . \tag{2.4}$$

In order to work this out we have to introduce at this stage a complete system of states of n particles. For this we shall take products of plane waves; it will turn out that with this choice the mathematics are still manageable; other choices (*e.g.* spherical waves) are of course allowed in principle, but would make it hard in practice to retain rigorously momentum conservation in the formalism

$$|\boldsymbol{p}_1, \ldots, \boldsymbol{p}_n\rangle = \exp\left[i \sum_{i=1}^{n} (\boldsymbol{p}_i, \boldsymbol{x}_i)\right] .$$

With this choice we have

$$\mathrm{Tr}\, \varrho \, \delta(\boldsymbol{x}_1 - \xi_1) \ldots \delta(\boldsymbol{x}_n - \xi_n) = \int \mathrm{d}\boldsymbol{p}_1 \ldots \int \mathrm{d}\boldsymbol{p}_n \, \langle \boldsymbol{p}_1 \ldots \boldsymbol{p}_n | \varrho \prod_{i=1}^{n} \delta(\boldsymbol{x}_i - \xi_i) \, | \boldsymbol{p}_1 \ldots \boldsymbol{p}_n \rangle =$$

$$= \int \mathrm{d}\boldsymbol{p}_1 \ldots \mathrm{d}\boldsymbol{p}_n \int \mathrm{d}\boldsymbol{x}_1 \ldots \int \mathrm{d}\boldsymbol{x}_n \exp\left[-i \sum_{i=1}^{n} (\boldsymbol{p}_i, \boldsymbol{x}_i)\right] \varrho \prod_{1}^{n} \delta(\boldsymbol{x}_i - \xi_i) \exp\left[i \sum_{i=1}^{n} (\boldsymbol{p}_i, \boldsymbol{x}_i)\right] ,$$

and consequently

$$W_{n,\Omega} = \int \mathrm{d}\boldsymbol{p}_1 \ldots \int \mathrm{d}\boldsymbol{p}_n \int_{\Omega} \mathrm{d}\xi_1 \ldots \int_{\Omega} \mathrm{d}\xi_n \exp\left[-i \sum_{i=1}^{n} (\boldsymbol{p}_i, \xi_i)\right] \varrho \exp\left[i \sum_{i=1}^{n} (\boldsymbol{p}_i, \xi_i)\right] . \tag{2.5}$$

(Strictly speaking, one should first compute the bra $\langle \boldsymbol{p}_1 \ldots \boldsymbol{p}_n | \varrho$ and carry out the $\boldsymbol{x}_i$ integration afterwards; it will be clear that this does not alter the result.)

3. – The projection operators for momentum and energy.

The whole point of the present method lies in the use of a suitable form of the angular momentum projection operator. Because the operators H, $\boldsymbol{P}$, J^2, J_3—of which our states are pure eigenstates—can be considered as infini-

tesimal generators of continuous groups, we are led to the following problem of group theory.

To find the projection operator on a given irreducible representation of a compact group (space-time translation group for H, $\boldsymbol{P}$; rotation group for J^2 and J_3). This problem can be solved quite generally for all finite and compact groups, and the answer is ([3,4])

$$\mathscr{P}_\Gamma = \frac{d^\Gamma}{h} \int g(A)\,\mathrm{d}A\,\chi^{\Gamma *}(A) A\,, \tag{3.1}$$

where A: an operator, element of the group,

Γ: a representation of the group

$\mathscr{P}_\Gamma$: the projection operator on Γ,

d^Γ: the dimension of the representation,

$\chi^\Gamma(A)$: the character of the element A in the representation Γ,

$g(A)\,\mathrm{d}A$: the « volume element » in the integration of the space of the group elements,

$h = \int g(A)\,\mathrm{d}A =$ the « volume » of the group (for a finite group: $h =$ number of elements of the group).

We recall the orthogonality property of the characters:

$$\int g(A)\chi^{\Gamma' *}(A)\chi^\Gamma(A)\,\mathrm{d}A = h\delta_{\Gamma\Gamma'}$$

In order to make this clear we apply this formalism to a well-known case and we propose to derive the projection operator on one-particle states with momentum p' along the x-axis. We have then to build the projection operator $\mathscr{P}_{p'}$ on this representation of the group of all linear translations along the x-axis. The elements of the group are the operators of linear displacement:

$$A(a) = \exp\left[a\,\frac{\mathrm{d}}{\mathrm{d}x}\right],$$

because evidently $f(x+a) = \exp[a(\mathrm{d}/\mathrm{d}x)]\,f(x)$. This group is Abelian, all representations are one-dimensional functions of a and consequently the characters equal the representative functions

$$\chi^{(p)}(a) = \exp[ipa]$$

(3) E. Wigner: *Gruppentheorie* ... (Braunschweig, 1931).

(4) V. Heine: *Group Theory in Quantum Mechanics* (London, 1960).

whose orthogonality relations are

$$\int_{-\infty}^{+\infty} \mathrm{d}a\, \chi^{(p')*}(a)\chi^{(p)}(a) = \int_{-\infty}^{+\infty} \exp\left[i(p-p')a\right] \mathrm{d}a = 2\pi\delta(p-p') .$$

Consequently

$$\mathscr{P}_p = \frac{1}{2\pi} \int_{-\infty}^{+\infty} \mathrm{d}a \exp\left[-ipa\right] \exp\left[a \frac{\mathrm{d}}{\mathrm{d}x}\right] . \tag{3.2}$$

Let us apply this to a function with known Fourier transform

$$f(x) = \int_{-\infty}^{+\infty} \mathrm{d}k \exp\left[ikx\right] \varphi(k) , \tag{3.3}$$

$$\mathscr{P}_p f(x) = \frac{1}{2\pi} \int_{-\infty}^{+\infty} \mathrm{d}a \int_{-\infty}^{+\infty} \mathrm{d}k \varphi(k) \exp\left[-ipa\right] \exp\left[a \frac{\mathrm{d}}{\mathrm{d}x}\right] \exp\left[ikx\right] = \tag{3.4}$$

$$= \frac{1}{2\pi} \int_{-\infty}^{+\infty} \mathrm{d}a \int_{-\infty}^{+\infty} \mathrm{d}k \varphi(k) \exp\left[-i(p-k)a\right] \exp\left[ikx\right] =$$

$$= \int_{-\infty}^{+\infty} \mathrm{d}k \varphi(k) \exp\left[ikx\right] \delta(p-k) =$$

$$= \varphi(p) \exp\left[ipx\right] . \tag{3.5}$$

This gives the well-known result; comparing (3.4) with the definition of $f(x)$, we see also that one could put, when $\mathscr{P}_p$ is applied to an eigenfunction of momentum p_x (*i.e.* a representation of the translation group along the x-axis),

$$\mathscr{P}_p \exp\left[ikx\right] = \delta(p-k) \exp\left[ikx\right] . \tag{3.6}$$

We can now apply this immediately to our problem and write

$$\exp\left[-i \sum_{i=1}^{n} (\boldsymbol{p}_i, \boldsymbol{\xi}_i)\right] \mathscr{P}_E \mathscr{P}_0 = \exp\left[-i \sum_{i=1}^{n} (\boldsymbol{p}_i, \boldsymbol{\xi}_i)\right] \delta\Big(E - \sum_{i=1}^{n} \sqrt{p_i^2 + m_i^2}\Big)\, \delta\Big(\sum_{i=1}^{n} \boldsymbol{p}_i\Big) . \tag{3.7}$$

in order to get this result one should remember that for independent particles $H = \sum_{i=1}^{n} H_i$ (H_i = energy operator on i-th particle) and the time variation of

the plane waves is $\exp\left[-i\sum_i \varepsilon i t\right]$. A similar argument on time translations gives then the δ-function for the energy.

4. – The projection operators for angular momentum.

Were it not for the operators $\mathscr{P}_j \mathscr{P}_m$ this would lead at once to the result obtained by the traditional theory, without angular momentum conservation

$$W_{n_\bullet\Omega} \sim \Omega^n \int \mathrm{d}\boldsymbol{p}_1 \ldots \int \mathrm{d}\boldsymbol{p}_n \, \delta\Big(E - \sum_i \sqrt{p_i^2 + m_i^2}\Big)\, \delta\Big(\sum_i \boldsymbol{p}_i\Big)\,. \tag{4.1}$$

In order to have an explicit form of $\mathscr{P}_j$ we have to choose first suitable parameters to describe rotations. We shall use in the following two equivalent sets:

a) rotation axis, *i.e.* a unit vector $\boldsymbol{n}$; rotation angle ω, where $0 \leqslant \omega \leqslant \pi$

b) Euler angles: α, β, γ.

For each of those the factors that enter the integrand of the projection operator $\mathscr{P}_j$ are as follows (Table I) ([3,5,6]).

TABLE I.

	$\boldsymbol{n}, \omega$	α, β, γ
d^Γ	$2j+1$	$2j+1$
h	$2\pi^2$	$8\pi^2$
$g(A)$	$\sin^2 \omega/2$	$\sin \beta$
$\chi^\Gamma(A)$	$\sin (j+\frac{1}{2})\omega / \sin \omega/2$	$\sum_{m=-j}^{+j} D^{(j)}_{m,m}(\alpha, \beta, \gamma)$
A	$R(\boldsymbol{n}, \omega) = \exp[i\omega(\boldsymbol{n}, \boldsymbol{J})]$	$R(\alpha, \beta, \gamma) = \exp[-i\alpha J_z] \exp[-i\beta J_y] \exp[-i\gamma J_z]$
	$\boldsymbol{J} = \sum_{i=1}^{n} \boldsymbol{j}_i$	$(\boldsymbol{j}_i = -i\boldsymbol{r}_i \times \boldsymbol{\nabla}_i)$

([5]) A. EDMONDS: *Angular Momentum in Quantum Mechanics* (Princeton, 1957).
([6]) M. ROSE: *Elementary Theory of Angular Momentum* (New York, 1957).

We shall first construct the $\mathscr{P}_j$ operator with the $(\boldsymbol{n}, \omega)$ parameters, which gives the simpler form. Substituting in (3.1) we get (*)

$$(4.2)\qquad \exp\Big[-i\sum_{i=1}^{n}(\boldsymbol{p}_i, \boldsymbol{r}_i)\Big]\mathscr{P}_j \exp\Big[i\sum_{i=1}^{n}(\boldsymbol{p}_i, \boldsymbol{r}_i)\Big] =$$

$$= \frac{2j+1}{2\pi^2}\int \mathrm{d}\boldsymbol{n}\int_0^{\pi}\mathrm{d}\omega \sin^2\frac{\omega}{2}\,\frac{\sin(j+\frac{1}{2})\omega}{\sin\omega/2}\exp\Big[-i\sum_{i=1}^{n}(\boldsymbol{p}_i, \boldsymbol{r}_i)\Big]\cdot$$

$$\cdot\exp\Big[\omega(\boldsymbol{n}, \sum_i \boldsymbol{r}_i\times\boldsymbol{\nabla}_i)\Big]\exp\Big[i\sum_{i=1}^{n}(\boldsymbol{p}_i, \boldsymbol{r}_i)\Big]\,.$$

Our next problem is then to express the effect of a finite rotation of the coordinate system on a plane wave, *i.e.* to compute

$$(4.3)\qquad \exp\Big[\omega(\boldsymbol{n}, \sum_{i=1}^{n}\boldsymbol{r}_i\times\boldsymbol{\nabla}_i)\Big]\exp\Big[i\sum_{i=1}^{n}(\boldsymbol{p}_i, \boldsymbol{r}_i)\Big] =$$

$$= \prod_{i=1}^{n}\exp\Big[\omega(\boldsymbol{n}, \boldsymbol{r}_i\times_i)\Big]\exp\Big[i(\boldsymbol{p}\boldsymbol{\nabla}_i, \boldsymbol{r}_i)\Big]\,.$$

One can compute this by expanding the rotation operator in an exponential series

$$(4.4)\qquad \exp[\omega(\boldsymbol{n}, \boldsymbol{r}\times\boldsymbol{\nabla})] = \sum_{\nu=0}^{\infty}\frac{\omega^\nu}{\nu!}(\boldsymbol{n}, \boldsymbol{r}\times\boldsymbol{\nabla})^\nu\,.$$

To evaluate

$$(\boldsymbol{n}, \boldsymbol{r}\times\boldsymbol{\nabla})^\nu \exp[i(\boldsymbol{p}, \boldsymbol{r})]$$

is not trivial because of the non-vanishing commutators $[\boldsymbol{r}, \boldsymbol{\nabla}]$. The algebra involved is not complicated, however, and the result is

$$(4.5)\qquad \exp[\omega(\boldsymbol{n}, \boldsymbol{r}\times\boldsymbol{\nabla})]\exp[i(\boldsymbol{p}, \boldsymbol{r})] =$$

$$= \exp[i(\boldsymbol{p}, \boldsymbol{r})]\exp[i(\boldsymbol{r}, \boldsymbol{p}\times\boldsymbol{n})\sin\omega - i(\boldsymbol{r}, (\boldsymbol{p}\times\boldsymbol{n})\times\boldsymbol{n})(\cos\omega - 1)],$$

$$(4.6)\qquad = \exp[i(\boldsymbol{r}', \boldsymbol{p})] = \exp[i(\boldsymbol{r}, \boldsymbol{p}')]\,,$$

(*) In this form we consider only orbital angular momenta; one could in principle introduce spinor plane waves for the nucleons, and make R also act on these spinors. This seems at the moment an unnecessary complication, as the bulk of the (high) angular momenta is certainly due to orbital motion of the fast product particles.

where

$$\boldsymbol{r}' = \boldsymbol{r} - (\boldsymbol{r}\times\boldsymbol{n})\,\sin\omega - [(\boldsymbol{r}\times\boldsymbol{n})\times\boldsymbol{n}]\,(\cos\omega - 1)\,, \tag{4.6a}$$

$$\boldsymbol{p}' = \boldsymbol{p} + (\boldsymbol{p}\times\boldsymbol{n})\sin\omega - [(\boldsymbol{p}\times\boldsymbol{n})\times\boldsymbol{n}](\cos\omega - 1)\,. \tag{4.6b}$$

This result is quite natural: $\boldsymbol{r}'$ is the vector $\boldsymbol{r}$ turned over an angle ω around n. One can alternatively consider the operation of rotation as affecting the field, with a stationary frame and this leads then to a rotation of the momentum vectors over an angle $|\omega|$ in the opposite direction. $\boldsymbol{p}'$ is nothing but the original vector $\boldsymbol{p}$ turned over an angle $-\omega$ around $\boldsymbol{n}$, (4.6*a*) and (4.6*b*) express indeed the result of performing a rotation $(n, \pm\omega)$ on a vector [7]; the new vector is a sum of three mutually orthogonal vectors. One sees also that the *difference* between the turned vector and the original vector is orthogonal to the axis of rotation, and its length is

$$\begin{Bmatrix} |\boldsymbol{r}' - \boldsymbol{r}| \\ |\boldsymbol{p}' - \boldsymbol{p}| \end{Bmatrix} = \begin{Bmatrix} r \\ p \end{Bmatrix} |\sin\theta|\,[\sin^2\omega + (\cos\omega - 1)^2]^{\frac{1}{2}} = 2\begin{Bmatrix} r \\ p \end{Bmatrix} |\sin\theta|\sin\frac{\omega}{2}\,. \tag{4.7}$$

The matrix element of the projection operator for total angular momentum $j(j+1)$ between plane waves reads now

$$\exp\Big[-i\sum_{i}(\boldsymbol{p}_i, \boldsymbol{r}_i)\Big]\mathscr{P}_j \exp\Big[i\sum_{i}(\boldsymbol{p}_i, \boldsymbol{r}_i)\Big] = \tag{4.8}$$

$$= \frac{2j+1}{2\pi^2}\int \mathrm{d}\boldsymbol{n}\int_0^{\pi}\mathrm{d}\omega\,\sin\frac{\omega}{2}\,\sin(j+\tfrac{1}{2})\omega\,\exp\Big[i\sum_{i=1}^{n}(\boldsymbol{K}_i, \boldsymbol{r}_i)\Big]\,,$$

where

$$\boldsymbol{K}_i = \sin\omega(\boldsymbol{p}_i\times\boldsymbol{n}) - (\cos\omega - 1)[(\boldsymbol{p}_i\times\boldsymbol{n})\times\boldsymbol{n}]$$

is the difference between the turned vector $\boldsymbol{p}_i'$ and the original vector $\boldsymbol{p}_i$ (see Fig. 1).

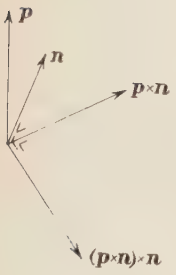

Fig. 1. – The vector $\boldsymbol{p}$, the rotation axis $\boldsymbol{n}$ and the triad of orthogonal vectors $\boldsymbol{n}$, $\boldsymbol{p}\times\boldsymbol{n}$, $(\boldsymbol{p}\times\boldsymbol{n})\times\boldsymbol{n}$ to which the turned vector is referred in formula (4.6*b*).

[7] J. L. Synge: *Classical Dynamics*, in *Handb. d. Phys.*, vol. **3**/1 (Berlin, 1960).

5. – The projection operator for magnetic quantum numbers.

Here we are concerned with states having a well-defined value of J_z, the z-component of the total angular momentum. The operator J is the infinitesimal generator of rotations around the z-axis; one convinces oneself easily that in case of this Abelian group the projection operator is

$$\mathscr{P}_m = \frac{1}{2\pi}\int_0^{2\pi} \mathrm{d}\varphi \, \exp\left[-im\varphi\right] \exp\left[i\varphi J_z\right] . \tag{5.1}$$

The interesting thing, however, for high-energy collisions is the operator

$$\mathscr{P}_j \mathscr{P}_m \qquad \text{with } m = 0.$$

If the z-axis is taken along the collision line the total angular momentum must be orthogonal to the z-axis, and hence only states with $J_z = 0$ can contribute to the final state. So we have to compute

$$\exp\Big[-i\sum_i (\boldsymbol{p}_i, \boldsymbol{r}_i)\Big] \mathscr{P}_j \mathscr{P}_{m=0} \exp\Big[i\sum_i (\boldsymbol{p}_i, \boldsymbol{r}_i)\Big] . \tag{5.2}$$

One can do this by applying in succession the explicit forms (5.1) and (4.8) or else making use of the fact that $\mathscr{P}_j \mathscr{P}_{m=0}$ is a projection operator on a particular line of the $2j+1$ dimensional irreducible representation of the rotation group. The general form of such an operator is [3,4]

$$\frac{d^\Gamma}{h}\int g(A)\, \mathrm{d}(A)\, \mathscr{D}^\Gamma_{m,m}(A)\, \mathrm{d}A , \tag{5.3}$$

where $\mathscr{D}^\Gamma_{m,m}$ is the diagonal element on the particular line m of the representative matrix. Formula (3.1) is a special case of this theorem, because

$$\chi^\Gamma = \sum_m \mathscr{D}^\Gamma_{m,m} .$$

Applied to the problem at hand this gives

$$\mathscr{P}_j \mathscr{P}_{m=0} = \frac{2j+1}{2\pi^2}\int \mathrm{d}\boldsymbol{n} \int_0^\pi \mathrm{d}\omega \, \sin^2\frac{\omega}{2}\, \mathscr{D}^{(j)}_{0,0}(\boldsymbol{n}, \omega) \exp\Big[\omega\Big(\boldsymbol{n}, \sum_i \boldsymbol{r}_i \times \nabla_i\Big)\Big] . \tag{5.4}$$

We see that the only difference with the operator P_j consists in the substitution of $\mathscr{D}^{(j)}_{0,0}(\boldsymbol{n}, \omega)$ for $\chi^{(j)}(\omega)$. The matrix element $\mathscr{D}^{(j)}_{0,0}$ has a particularly simple expression when the rotation is expressed with Euler angles

$$\mathscr{D}^{(j)}_{0,0}(\alpha, \beta, \gamma) = \mathscr{D}^{(j)}_{0,0}(0, \beta, 0) = P_j(\cos\beta) , \tag{5.5}$$

($P_j(\cos\beta)$ = Legendre polynomial of order j). As a function of $\boldsymbol{n}, \omega$ it is obtained by expressing β as a function of $\boldsymbol{n}$ and ω. We notice that

$$\cos\beta = \mathscr{D}^{(1)}_{0,0}(\boldsymbol{n}, \omega) = (\boldsymbol{e}_3, R(\boldsymbol{n}, \omega)\boldsymbol{e}_3) , \tag{5.6}$$

i.e. the unit vector along the z-axis, $\boldsymbol{e}_3$, turned over ω around $\boldsymbol{n}$, and projected on the z-axis.

By using (4.6*a*) one finds

$$\cos\beta = \cos^2\theta + \sin^2\theta\cos\omega ,$$

where θ is the angle between n and the z-axis.
Consequently

$$\mathscr{D}^{(j)}_{0,0}(\boldsymbol{n}, \omega) = P_j(\cos^2\theta + \sin^2\theta\cos\omega) = \tag{5.7}$$

$$= (P_j(\cos\theta))^2 + 2\sum_{m=1}^{j}\frac{(j-m)!}{(j+m)!}(P(\cos\theta))^2\cos m\omega .$$

We see that the parameters $(\boldsymbol{n}, \omega)$ give simple results in the formula for $\mathscr{P}$ only; for expressing $\mathscr{P}_j\mathscr{P}_{m=0}$ it is easier to use the Euler angles.

6. – Statistical theory with J but without P conservation (Koba's theory).

In Section 2 it was pointed out that the formalism of the density matrix leaves one in principle free to choose any complete set of n-particle wave functions. The explicit form of $\mathrm{Tr}\,\varrho\mathscr{P}_n$ will of course depend on the chosen system.

In connection with the theory developed by KOBA ([8,9]) it is interesting to calculate the form of $\mathscr{P}_j\mathscr{P}_m$ using spherical harmonics instead of plane

([8]) Z. KOBA: *Statistical theory of multiple particle production with angular momentum conservation*, preprint Warsaw, October 1960; to be published in *Acta Phys. Polon.*

([9]) Z. KOBA: *The angular momentum weight factor in the statistical theory of multiple production* - I, II, preprints February and April 1961; to be published in *Bulletin of the Polish Academy of Sciences.*

waves. A complete system of wave functions of a free scalar particle is then

$$|klm\rangle \equiv j_l(kr)\,Y_l^m(\theta,\varphi)\,,$$

($j_l(kr)$ = the l-th spherical Bessel function) and a diagonal matrix element of $\mathscr{P}_j\mathscr{P}_m$ is therefore

$$(6.1)\qquad \frac{2j+1}{8\pi^2}\int_0^\infty r_1^2\,\mathrm{d}r_1 \ldots \int_0^\infty r_n^2\,\mathrm{d}r_n\,|\,j_{l_1}(k_1r_1)\ldots j_{l_n}(k_nr_n)\,|^2\cdot$$
$$\cdot\int_0^\pi \sin\theta_1\,\mathrm{d}\theta_1\int_0^{2\pi}\mathrm{d}q_1\ldots\int_0^\pi \sin\theta_n\,\mathrm{d}\theta_n\int_0^{2\pi}\mathrm{d}q_n\int_0^{2\pi}\mathrm{d}\alpha\int_0^\pi\mathrm{d}\beta\int_0^{2\pi}\mathrm{d}\gamma\,\sin\beta\cdot$$
$$\cdot\mathscr{D}^{(j)*}_{m,m}(\alpha,\beta,\gamma)\,Y^{m_1*}_{l_1}(\theta_1\varphi_1)\ldots Y^{m_n*}_{l_n}(\theta_n\varphi_n)R_{(\alpha\beta\gamma)}\,Y^{m_1}_{l_1}(\theta_1\varphi_1)\ldots Y^{m_n}_{l_n}(\theta_n\varphi_n)\,.$$

Because the Y_l^m are orthonormal and belong to a well-defined irreducible representation of the rotation group

$$(6.2)\qquad \int_0^{2\pi}\mathrm{d}\varphi\int_0^\pi \sin\theta\,\mathrm{d}\theta\,Y_l^{m*}R_{(\alpha\beta\gamma)}\,Y_l^m = \mathscr{D}^{(l)}_{m,m}(\alpha\beta\gamma)$$

and the last two lines of formula (6.1) reduce to

$$(6.3)\qquad \int_0^{2\pi}\mathrm{d}\alpha\int_0^\pi\mathrm{d}\beta\int_0^{2\pi}\mathrm{d}\gamma\,\sin\beta\,\mathscr{D}^{(j)*}_{m,m}(\alpha\beta\gamma)\,\mathscr{D}^{(l_1)}_{m_1,m_1}(\alpha\beta\gamma)\ldots\mathscr{D}^{(l_n)}_{m_n,m_n}(\alpha\beta\gamma)\,.$$

If one chooses to *neglect momentum conservation* and consequently takes as density matrix

$$(6.4)\qquad \varrho' = C_n'\,\mathscr{P}_E\,\mathscr{P}_j\,\mathscr{P}_m$$

and compute in this case

$$(6.5)\qquad \mathrm{Tr}\,\varrho'\,\delta(\boldsymbol{x}_1-\boldsymbol{\xi}_1)\ldots\delta(\boldsymbol{x}_n-\boldsymbol{\xi}_n)$$

the trace would involve summing over all m_i (as well as l_i and integrals over k_i). Taking the expression (6.2) and summing over all m_i gives a certain coefficient $Z_m^{(j)}(l_1\ldots l_n)$

$$(6.6)\qquad Z_m^{(j)}(l_1\ldots l_n) = \int_0^{2\pi}\mathrm{d}\alpha\int_0^\pi\mathrm{d}\beta\int_0^{2\pi}\mathrm{d}\gamma\,\sin\beta\,\mathscr{D}^{(j)*}_{m,m}\sum_{m_1=-l_1}^{+l_1}\ldots\sum_{m_n=-l_n}^{+l_n}\mathscr{D}^{(l_1)}_{m_1,m_1}\ldots\mathscr{D}^{(l_n)}_{m_n,m_n}\,.$$

which can in principle be computed, as the $\mathscr{C}^{(l)}_{m\,m}(\alpha\beta\gamma)$ are well-known. This coefficient contains implicitly all the selection rules due to the addition of the the angular momenta $l_1, \ldots, l_n$ to a resultant j, with $m_1+m_2+\ldots+m_n=m$. If *e.g.* $l_1+\ldots+l_n<j$ or $l_n>j+l_1+\ldots+l_{n-1}$ so that the triangular conditions cannot be satisfied, then $Z^{(j)}_m(l_1 \ldots l_n)$ is automatically zero. This method has been used in two previous articles for computing « phase-space integrals » in isospin space, either by recursion using Clebsch-Gordon coefficients [10] or in closed form [11].

The phase space integral for a spherical Ω with radius R looks then as follows (up to a constant coefficient)

$$(6.7)\qquad \int_0^R \mathrm{d}r_1 \ldots \int_0^R \mathrm{d}r_n \int_0^\infty \mathrm{d}k_1 \ldots \int_0^\infty \mathrm{d}k_n \sum_{l_1=0}^{\infty} \ldots \sum_{l_n=0}^{\infty} Z^{(j)}_m(l_1 \ldots l_n) \prod_{i=1}^{n} k_i^2 r_i^2 \; j_{l_i}(k_i r_i)^{\,2} \cdot \cdot \delta\Big(E - \sum_i \sqrt{k_i^2 + m_i^2}\Big) .$$

Formula (6.7) is essentially Koba's formulation of angular momentum conservation in the statistical theory.

7. – Phase-space integral with angular momentum conservation.

The probability to find n particles in volume Ω, with specified E, $P=0$, j, and $m=0$ is then

$$(7.1)\qquad W_{n,\Omega}(E; j; m=0) = = C_n \int \ldots \int \mathrm{d}\boldsymbol{p}_1 \ldots \mathrm{d}\boldsymbol{p}_n \delta\Big(E - \sum_{i=1}^{n} \sqrt{p_i^2 + m_i^2}\Big) \delta\Big(\sum_i \boldsymbol{p}_i\Big) G_j(\boldsymbol{p}_1 \ldots \boldsymbol{p}_n) ,$$

where

$$(7.2)\qquad G_j = \frac{2j+1}{2\pi^2} \int \mathrm{d}\boldsymbol{n} \int_0^\pi \mathrm{d}\omega \sin^2 \frac{\omega}{2} \mathscr{D}^{(j)}_{0,0}(\boldsymbol{n}, \omega) \int_\Omega \mathrm{d}\boldsymbol{r}_1 \ldots \int_\Omega \mathrm{d}\boldsymbol{r}_n \exp\Big[i \sum_{i=0}^{n} (\boldsymbol{r}_i, \boldsymbol{K}_i)\Big] ,$$

or alternatively

$$(7.3)\qquad = \frac{2j+1}{8\pi^2} \int_0^{2\pi} \mathrm{d}\alpha \int_0^\pi \mathrm{d}\beta \int_0^{2\pi} \mathrm{d}\gamma \sin\beta P_j(\cos\beta) \int_\Omega \mathrm{d}\boldsymbol{r}_1 \ldots \int_\Omega \mathrm{d}\boldsymbol{r}_n \exp\Big[i \sum_{i=1}^{n} (\boldsymbol{r}_i, \boldsymbol{K}_i)\Big] .$$

[10] F. CERULUS: *Suppl. Nuovo Cimento*, **15**, 402 (1960).
[11] F. CERULUS: *Nuovo Cimento*, **19**, 528 (1961).

and $\boldsymbol{K}$ is each time the difference between the turned vector $\boldsymbol{p}'$ and the original $\boldsymbol{p}$ (4.6).

The further development depends now on the assumption made about the interaction volume Ω. We shall here take a spherical shape, and replace the sharp cut-off by a Gaussian cut-off. We replace then

$$\int_{\Omega} \mathrm{d}\boldsymbol{r} \exp\left[i(\boldsymbol{K}, \boldsymbol{r})\right] \quad \text{by} \quad \int \mathrm{d}\boldsymbol{r} \exp\left|-\frac{r^2}{4a^2} + i(\boldsymbol{r}, \boldsymbol{K})\right| . \tag{7.4}$$

This form of cut-off is made for computational convenience. The mean square radius of the volume with this cut-off is

$$\langle r^2 \rangle = 6a^2 ,$$

i.e. we could take as radius

$$R = \sqrt{6}a = 2.45a . \tag{7.5}$$

The integral (7.4) is the Fourier transform of the form factor of Ω. For a spherical Gaussian we get

$$\int_{\Omega} \mathrm{d}\boldsymbol{r} \exp\left[i(\boldsymbol{K}, \boldsymbol{r}) \to 8\pi^{\frac{3}{2}} a^3 \exp\left[-a^2K^2\right] = \left(\frac{2\pi}{3}\right)^{\frac{3}{2}} R^3 \exp\left[-\frac{R^2K^2}{6}\right], \tag{7.6}$$

and

$$\int_{\Omega} \mathrm{d}\boldsymbol{r}_1 \ldots \int_{\Omega} \mathrm{d}\boldsymbol{r}_n \exp\left[i \sum_i (\boldsymbol{r}_i, \boldsymbol{K}_i)\right] = \left(\sqrt{\frac{2\pi}{3}} R\right)^{3n} \exp\left[-a^2\left(\sum_{i=1}^{n} K_i^2\right)\right] . \tag{7.7}$$

This expression depends only on the length of the vector $\boldsymbol{K}_i$. This length was already given for the parameters of rotation $\boldsymbol{n}$, ω (4.7).

For the Euler angles it is easily computed as follows:

$$\boldsymbol{K} = \boldsymbol{p}' - \boldsymbol{p} = \mathscr{D}^{(1)}(\alpha\beta\gamma)\boldsymbol{p} - \boldsymbol{p} ,$$

where $\mathscr{D}^{(1)}$ is the transformation matrix of a vector under a rotation $(\alpha\beta\gamma)$. Consequently

$$K^2 = (\mathscr{D}^{(1)}\boldsymbol{p})^2 + \boldsymbol{p}^2 - 2(\boldsymbol{p}, \mathscr{D}^{(1)}\boldsymbol{p}) = 2\left(p^2 - (\boldsymbol{p}, \mathscr{D}^{(1)}\boldsymbol{p})\right) . \tag{7.8}$$

Using the known formulae for the matrix $\mathscr{D}^{(1)}_{m,m'}(\alpha\beta\gamma)$ [5] one finds

$$(\boldsymbol{p}, \mathscr{D}^{(1)}\boldsymbol{p}) = p_z^2 \cos\beta + \boldsymbol{p}_\perp^2 \frac{1 + \cos\beta}{2} \cos(\alpha\beta\gamma) , \tag{7.9}$$

where p_z and $\boldsymbol{p}$ are the components of $\boldsymbol{p}$ along the z-axis and perpendicular to the z-axis.

We are now led to the following expression for the probability to find n particles in a spherical Gaussian volume Ω

$$W_{n,\Omega}(E, j, 0) = C_n(2j+1)\left(\frac{1}{2}\sqrt{\frac{2\pi}{3}}\right)^n \left(\frac{4\pi}{3}R^3\right)^n \cdot \int \mathrm{d}\boldsymbol{p}_1 \ldots \int \mathrm{d}\boldsymbol{p}_n \delta\Big(E - \sum_{i=1}^{n} \sqrt{p_i^2 + m_i^2}\Big)\, \delta\Big(\sum_i \boldsymbol{p}_i\Big)\, \mathscr{F}_j \,. \tag{7.10}$$

The change, with respect to the statistical theory without J-conservation is

a) a factor $2j+1$,

b) a factor $(\frac{1}{2}\sqrt{2\pi/3})$,

(this amounts in effect only to an unimportant change of the interaction volume, due to the introduction of a Gaussian cut-off);

c) a weight function $\mathscr{F}_j(p_1 \ldots p_n)$ in the integrand.

By analogy with the usual statistical theory we shall henceforth call « phase-space integral » the expression

$$\varrho^*_{m_1 \ldots m_n}(E, \boldsymbol{P} = 0, j, m = 0) \int \mathrm{d}\boldsymbol{p}_1 \ldots \int \mathrm{d}\boldsymbol{p}_n \delta\Big(E - \sum_i \sqrt{p_i^2 + m_i^2}\Big)\, \delta\Big(\sum_i \boldsymbol{p}_i\Big)\, \mathscr{F} \,. \tag{7.11}$$

also to be denoted for short by $\varrho^*_n(E, j, 0)$.

The weight function $\mathscr{F}_j$ is expressed as a triple integral over the parameters of the rotation

$$\mathscr{F}_j(\boldsymbol{p}_1 \ldots \boldsymbol{p}_n) = \frac{1}{8\pi^2} \exp\left[-a^2Q^2\right] \int_0^{2\pi} \mathrm{d}\alpha \int_0^{\pi} \mathrm{d}\beta \int_0^{2\pi} \mathrm{d}\gamma \sin\beta\, P_j(\cos\beta) \cdot \exp\left[2a^2Z^2 \cos\beta\right] \exp\left[a^2T^2(1+\cos\beta)\cos(\alpha+\gamma)\right], \tag{7.12}$$

where

$$Q^2 \equiv \sum_{i=1}^{n} \boldsymbol{p}_i^2 = Z^2 + T^2 \,,$$

$$Z^2 \equiv \sum_{i=1}^{n} p_{zi}^2 \,,$$

$$T^2 \equiv \sum_{i=1}^{n} p_{\perp i}^2 \,.$$

We see from this that the weight function $\mathscr{F}_j$ depends on a single p_i only so to say through the *average* over the n perpendicular and the n longitudinal components of the momenta. The alternative form of $\mathscr{F}_j$ is

$$\mathscr{F}_j = \frac{1}{2\pi^2}\int \mathrm{d}\boldsymbol{n}\int_0^\pi \mathrm{d}\omega \sin^2\frac{\omega}{2}\,\mathscr{D}^{(j)}_{0,0}(\boldsymbol{n},\omega)\exp\left[-2a^2\Theta^2\right](1-\cos\omega)\,, \tag{7.13}$$

where

$$\Theta^2 = \sum_{i=1}^{n}(\boldsymbol{p}_i\times\boldsymbol{n})^2\,,$$

$$= \text{sum of the projection squared of } \boldsymbol{p}_i \text{ on a plane perpendicular to the axis of rotation } \boldsymbol{n}.$$

We shall not use this form for computation, but it is useful for qualitative discussion.

8. – The classical limit of the phase-space integral.

T. ERICSON ([12]) has been able to derive many results of statistical theory with angular momentum conservation by treating the $\boldsymbol{l}_i$-vectors of each single particle as classical vectors, *i.e.* by neglecting the fact that $\boldsymbol{r}$, $\boldsymbol{p}$ and $\boldsymbol{l}$ do not commute.

What happens in our case when we neglect these commutators? The rotation of a plane wave is then written as

$$\left\{\begin{aligned}\exp\left[\omega(\boldsymbol{n},\,\boldsymbol{r}\times\nabla)\right]\exp\left[i(\boldsymbol{p},\boldsymbol{r})\right] &= \exp\left[i\omega(\boldsymbol{n},\boldsymbol{r}\times\boldsymbol{p})+i(\boldsymbol{p},\boldsymbol{r})\right],\\ &= \exp\left[i(\boldsymbol{r},\,\boldsymbol{p}+\omega(\boldsymbol{p}\times\boldsymbol{n})\right],\end{aligned}\right. \tag{8.1}$$

so that now $\boldsymbol{K}=\omega(\boldsymbol{p}\times\boldsymbol{n})$.

$$\mathscr{F}_j^{(\text{Classical})} = \frac{1}{2\pi^2}\int \mathrm{d}\boldsymbol{n}\int_0^\pi \mathrm{d}\omega\,\mathscr{D}^{(j)}_{0,0}(\boldsymbol{n},\omega)\exp\left[-a^2\Theta^2\omega^2\right], \tag{8.2}$$

with $\mathscr{D}^{(j)}_{0,0}(\boldsymbol{n},\omega)$ as given in (5.7).

When is this a good approximation? In all such cases where

$$\exp\left[-a^2\Theta^2\omega^2\right] \approx \exp\left[-2a^2\Theta^2(1-\cos\omega)\right] \tag{8.3}$$

([12]) T. ERICSON: *Nuovo Cimento*, **21**, 605 (1961).

as is easily seen by comparing (8.2) with (7.13); this means when $a^2\Theta^2$ is so big that moderate values of ω make the factor $\exp[-a^2\Theta^2\omega^2]$ already vanishingly small. The condition is then

$$a^2 \sum_{i=1}^{n} (\boldsymbol{p}_i \times \boldsymbol{n})^2 \gg 1 .$$

Because $\boldsymbol{n}$ is an integration variable (over the unit sphere) this is only sure if the p_i's are big enough, and with fairly spread out directions. The last point is true on the average, for n not too small, because configurations of $\boldsymbol{p}_i$ which cluster together occur very seldom and contribute therefore a negligible amount to the phase-space integral. The physical requirement for the classical picture to hold is then

a) $\langle p^2 \rangle \gg \dfrac{1}{na^2}$;

b) n rather large to assure the probable spreading of directions.

If we can neglect the particles' masses as compared to their energies the first condition can be stated as a condition on the total energy which has to be larger than

$$E_{\min} = n\sqrt{\langle p^2 \rangle} \gg \sqrt{n}\frac{1}{a} = \sqrt{6n}\frac{1}{R} . \tag{8.4}$$

We shall see in Section 9 the exact limits of validity of the classical approximation by comparing the exact end formula with the classical one. Eq. (8.4), however, shows already that in most practical cases condition *a*) will be fulfilled. For *e.g.* 6 particles and $R \approx 1.4 \cdot 10^{-13}$ cm one has $E_{\min} \approx 1$ GeV.

9. – Explicit form of the phase-space integrand.

We shall presently carry out the integrations in formula (7.12) for $\mathcal{F}_n$. The integrals over α and γ are simple and of the form

$$\int_0^{2\pi} \mathrm{d}\alpha \int_0^{2\pi} \mathrm{d}\gamma \exp[A \cos(\alpha + \gamma)] = 4\pi^2 I_0(A) , \tag{9.1}$$

where $I_0(A) = J_0(iA)$, the Bessel function of pure imaginary argument. After

this we are left with one more integral

$$(9.2)\quad \mathscr{F}_j = \frac{1}{2}\int_0^\pi \mathrm{d}\beta \sin\beta P_j(\cos\beta) \exp[-2a^2Q^2] \exp[2a^2Z^2\cos\beta] I_0[a^2T^2(1-\cos\beta)] .$$

Remembering that $Q^2 = T^2 + Z^2$ the integrand can be written as a product of three factors

$$F_1(\cos\beta) = P_j(\cos\beta)\sin\beta ,$$

$$F_2(\cos\beta) = \exp[-(2a^2Z^2 + a^2T^2)(1-\cos\beta)] ,$$

$$F_3(\cos\beta) = \exp[-a^2T^2(1+\cos\beta)] I_0(a^2T^2(1+\cos\beta)) .$$

We shall first transform the integral to get rid of the oscillating $P_j(\cos\theta)$. The factor $F_3(\cos\beta)$ can be expressed as a Laplace transform using the formula

$$(9.3)\qquad \exp[-bp] I_0(bp) = \frac{1}{\pi}\int_0^{2b} \exp[-pt](2bt - t^2)^{-\frac{1}{2}} \mathrm{d}t .$$

Putting for a moment

$$2a^2Z^2 + a^2T^2 = a^2(Q^2 + Z^2) \equiv A ,$$

$$a^2T^2 = a^2(Q^2 - Z^2) \equiv B ,$$

we have

$$(9.4)\quad \mathscr{F}_j = \frac{1}{2\pi}\int_0^{2B} \frac{\mathrm{d}t}{(2Bt - t^2)^{\frac{1}{2}}} \int_0^\pi \mathrm{d}\beta \sin\beta P_j(\cos\beta) \exp[-A(1-\cos\beta) - t(1+\cos\beta)]$$

$$(9.5)\qquad = \sqrt{\frac{1}{2\pi}} \exp[-A]\int_0^{2B} \frac{\mathrm{d}t}{(2Bt - t^2)^{\frac{1}{2}}} \exp[-t] \frac{1}{(A-t)^{\frac{1}{2}}} I_{j+\frac{1}{2}}(A-t)$$

$$(9.6)\qquad = 4\pi\sqrt{2\pi} \exp[-t_0](A-t_0)^{-\frac{1}{2}} \exp[-(A-t_0)] I_{j+\frac{1}{2}}(A-t_0) \exp[-B] I_0(B) ,$$

where the last line is derived from the foregoing by using the mean value theorem, t_0 being a value between 0 and $2B$. For most practical purposes A is a large number, because the particles' momenta are larger than $\mu = 1/R$, except perhaps for very high multiplicities; it is of the order of $n(R^2\langle p_j^2\rangle/6)$.

Because $I_{j+\frac{1}{2}}(x)$ is a fast growing function of x (see further down for their general behaviour), the important contributions to the integral come from

small values of t; for $j+\frac{1}{2}<2A$ the width (*i.e.* where $\exp[-t](A-t)^{-\frac{1}{2}}\cdot I_{j+\frac{1}{2}}(A-t)=\frac{1}{2}A^{-\frac{1}{2}}I_{j+\frac{1}{2}}(A)$) it $t\approx\frac{1}{2}\log 2$, which is quite negligible compared to A. In most cases it will therefore be a good approximation to take simply $A-t_0\approx A$ and $\exp[-t_0]\approx 2^{-\frac{1}{2}}$. For extreme cases one will have to resort to a numerical evaluation.

Taking for the moment the approximate formula one gets

$$\mathscr{F}_j=\frac{1}{2\sqrt{\pi}}\exp[-a^2T^2]I_0(a^2T^2)\exp[-a^2(2Z^2+T^2)]\cdot \cdot I_{j-\frac{1}{2}}(a^2(2Z^2+T^2))\frac{1}{a(2Z^2+T^2)^{\frac{1}{2}}}. \tag{9.7}$$

Before discussing how to calculate the phase-space integral with this function in the integrand we shall discuss the general behaviour of $\mathscr{F}_j$.

The functions $\exp[-x]I_\nu(x)$ are smooth, real functions of x and ν. For very small or very large values of x they can be easily approximated by the first term of a power-series expansion, or of an asymptotic series respectively. We have as a matter of definition

$$I_\nu(x)=\sum_{s=0}^{\infty}\frac{(\frac{1}{2}x)^{\nu+2s}}{s!\,(\nu+s)!}=i^{-\nu}J_\nu(ix)\,, \tag{9.8}$$

therefore for $x\ll 1$

$$\exp[-x]I_\nu(x)\approx\frac{(\frac{1}{2}x)^\nu}{\nu!}\left(1-x+\frac{(\frac{1}{2}x)^2}{\nu+1}+\ldots\right). \tag{9.9}$$

For $x\gg 1$ *and* $x\gg\nu$

$$\exp[-x]I_\nu(x)\approx\frac{1}{\sqrt{2\pi x}}\left(1-\frac{4\nu^2-1}{8x}+\ldots\right). \tag{9.10}$$

For moderate or large ν the following form is more accurate (Debye asymptotic form)

$$\exp[-x]I_\nu(x)\approx\sqrt{\frac{\operatorname{tgh}\gamma}{2\pi\nu}}\exp[-x+\nu(\operatorname{cotgh}\gamma-\gamma)]\cdot \cdot\left[1+\frac{1}{24\nu}\operatorname{tgh}\gamma(3-5\operatorname{tgh}^2\gamma)+\ldots\right], \tag{9.11}$$

with

$$\sinh\gamma\equiv\frac{\nu}{x}\qquad i.e.\qquad \operatorname{tgh}\gamma=\frac{\nu}{\sqrt{\nu^2+x^2}}\,.$$

For moderate ν and $\nu<\frac{1}{2}x$ formula (9.11) is approximately (up to terms $0(\nu^3/x^3)$)

$$\exp[-x]I_\nu(x)\approx\frac{1}{\sqrt{2\pi x}}\exp\left[-\frac{\nu^2}{2x}\right]\left(1-\frac{1}{4}\frac{\nu^2}{x^2}\right). \tag{9.12}$$

In Fig. 2 and 3 are shown the functions for $\nu=0,\ \frac{1}{2},\ \frac{3}{2}$ and further for $\nu=1, 3, \ldots, 11$. As may be seen from (9.8) only $\exp[-x]I_0(x)$ does not vanish

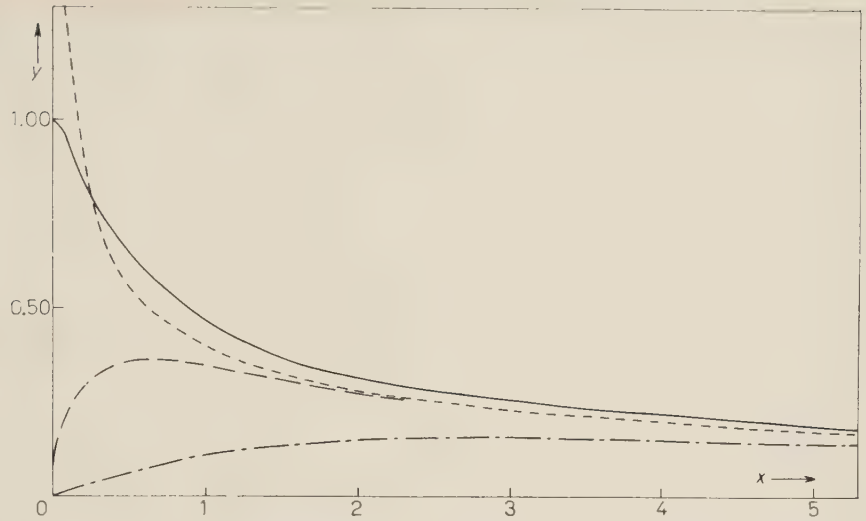

Fig. 2. – Graphs of the functions: $y = 1/\sqrt{2\pi x}$: - - - -, $y = \exp[-x]I_{\frac{1}{2}}(x)$: – –, $y = \exp[-x]I_0(x)$: ———, $y = \exp[-x]I_{\frac{3}{2}}(x)$: –·–·–.

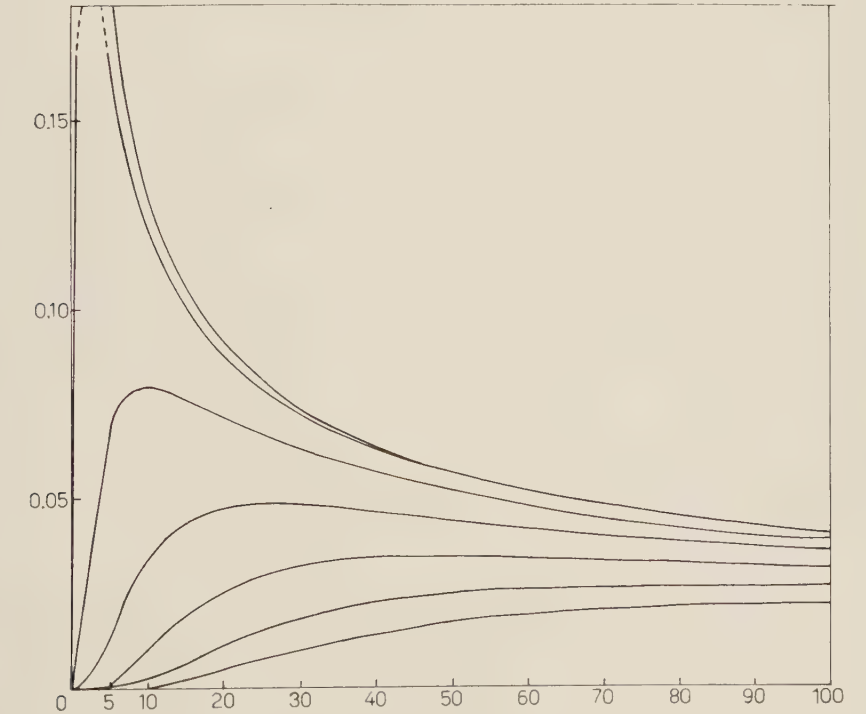

Fig. 3. – Graphs of the functions $\exp[-x]I_n(x)$ for $n = 0, 1, 3, 5, 7, 9, 11$ (counting from top to bottom).

for $x=0$ $(I_0(0)=1)$. All the other functions start from 0, and remain practically 0 up to $x\approx\nu$. From there they rise to a maximum around $x\approx\nu^2$. and beyond this point can be fairly well approximated by $\exp[-x]I_\nu(x)\approx$ $\approx 1/\sqrt{2\pi x}$.

To understand the formula one can think therefore of $\exp[-x]I_\nu(x)$ as a cut-off function: for *given* x it is zero (very roughly speaking) for $\nu > x^2$, for $\nu < x^2$ it is equal to $1/\sqrt{2\pi x}$; cf. *e.g.* Fig. 4.

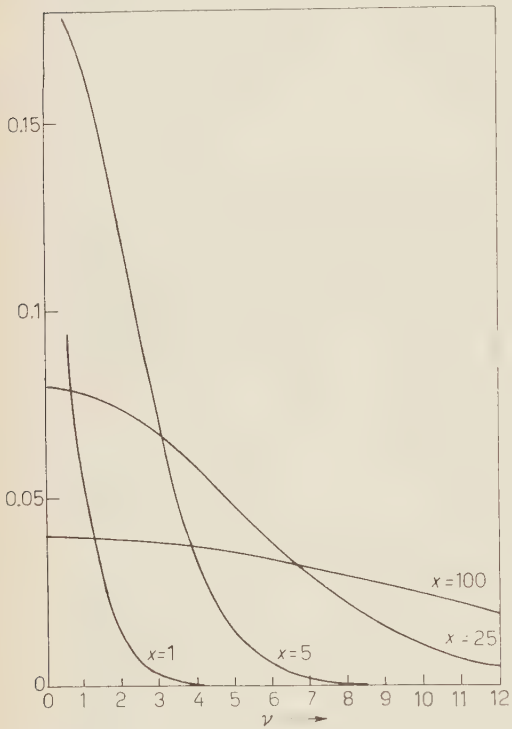

Fig. 4. – The functions $\exp[-x]I_\nu(x)$ plotted *vs.* the order ν, for different values of the variable x. The cut-off character is quite apparent.

The functions $I_{l+\frac{1}{2}}(x)$ have been tabulated ([13]). They can always be expressed as

$$I_{l+\frac{1}{2}}(x) = \sqrt{\frac{2}{\pi x}}\left| A_n\left(\frac{1}{x}\right)\cosh(x) + A_{n-1}\left(\frac{1}{x}\right)\sinh x\right| .$$

with $A_n(t)$ a n-th order polynomial in t, *e.g.* ([13])

$$I_{\frac{1}{2}}(x) \quad \sqrt{\frac{2}{\pi x}}\sinh x ,$$

$$I_{\frac{3}{2}}(x) \quad \sqrt{\frac{2}{\pi x}}\left|\cosh x - \frac{1}{x}\sinh x\right| .$$

The approximation we have made in deriving formula (9.7) $a^2Q^2 \gg \frac{1}{2}\log 2 = 0.346$ coincides more or less with the first of the two assumptions made by the classical approximation. From the discussion on p. 978 we know that it should be all right in practice.

How does formula (9.7) compare then to the classical approximation? Taking the asymptotic formulae (9.10) and (9.12) we find for

$$(9.13) \qquad \mathscr{F}_j \approx (2\pi)^{-\frac{3}{2}}2^{-\frac{1}{2}}(aT)^{-1}[a^2(2Z^2+T^2)]^{-1}\exp\left|-\frac{(j+\frac{1}{2})^2}{2a^2(2Z^2+T^2)}\right| ,$$

([13]) C. W. Jones: *A short table of the Bessel functions* $I_{n+\frac{1}{2}}(x)$, $(2/\pi)K_{n+\frac{1}{2}}(x)$, (Cambridge, 1952).

up to terms of order $(j/aQ)^2$ and comparing this with the formula (4.4) of ERICSON (remember $6a^2 = R^2$) [12]

$$\mathscr{F}_j^{(\text{Class cal})} = (2\pi)^{-\frac{3}{2}} \frac{1}{(\frac{2}{9}R^2Q^2)^{\frac{3}{2}}} \exp\left[-\frac{j^2}{\frac{4}{9}R^2Q^2}\right], \tag{9.14}$$

one sees that both are equal if $Z^2 = 1/3Q^2 = 2/3T^2$ (neglecting the difference between j^2 and $j(j+1)+\frac{1}{4}$, which is to be expected from a classical approximation and the factor $1/\sqrt{2}$ which comes from taking $t_0 = \frac{1}{2}\log 2$). So $\mathscr{F}^{\text{Class cal}}$ is strictly valid only for isotropic distribution of momenta; however, for angular momenta j small compared to RQ the difference is not important.

10. – Angular momentum zero.

This special case is of practical importance in annihilation of anti-nucleons at rest (together with the case $j = 1$). Going back to formulae (9.5) and (9.7) we find

$$\mathscr{F}_0 = 2^{-\frac{1}{2}}\pi^{-1} \exp[-a^2T^2] I_0(a^2T^2) \exp[-a^2(2Z^2+T^2)] \frac{\sinh[a^2(2Z^2+T^2)]}{a^2(2Z^2+T^2)}. \tag{10.1}$$

One knows that for very small momenta $|\boldsymbol{p}_i|$ (*i.e.* many particles sharing a small total energy (*), all end particles are necessarily in s-states, and the total angular momentum must be zero; this follows also at once from the exact formula (9.2), because there for

$$aT \to 0\,, \qquad aZ \to 0\,,$$

we have $\mathscr{F}_0 = 1$, (*i.e.* a constant independent of T and Z, and n) up to terms of order $a^2(Z^2+T^2)$. This leads to

$$W(E, 0, 0) = C_n \left(\frac{1}{2}\sqrt{\frac{2\pi}{3}}\right)^n \left(\frac{4\pi}{3}R^3\right)^n \int \mathrm{d}\boldsymbol{p}_1 \ldots \int \mathrm{d}\boldsymbol{p}_n \cdot \tag{10.2}$$

$$\cdot \delta\Big(E - \sum_i \sqrt{p_i^2 + m_i^2}\Big)\, \delta\Big(\sum_i \boldsymbol{p}_i\Big)\,,$$

i.e. essentially the expression one gets without introducing angular-momentum conservation; this is not surprising since all available states are necessarily

(*) A mathematically equivalent statement is: for very small a, *i.e.* very short radius of the interaction volume.

s-states, and hence no additional constraint is imposed on the phase-space by J-conservation.

Conversely, the expressions (10.2) or (1.1) are only strictly valid for s-states, although they may still be a good approximation when the outgoing particles can have *e.g.* p and d waves. The above hypothesis ($aQ \gg 0$) is however very unrealistic in all cases of practical importance

For annihilation we have $\langle n \rangle \approx 4.7$ and $\langle \sqrt{p^2+\mu^2} \rangle \approx 0.4$ GeV. We find $a^2Q^2 \approx \frac{1}{6}R^2 \cdot n\big((E/n)^2 - \mu^2\big) \approx 5.51$ for the case $n = 6$, *e.g.*, which allows to use the formula (9.7). This may be further checked: numerical integration of (9.5) yields in the above mentioned case 12.93 as compared with 12.37 from (9.7). For $n < 6$ the approximation is still better.

As no direction is privileged, the classical approximation may therefore be used, which gives

$$\mathscr{F}_0 \approx \frac{1}{[(4\pi/9)\,R^2Q^2]^{\frac{1}{2}}} .$$

One sees how this will affect the multiplicity: the higher n, the lower Q, and the higher $\mathscr{F}_0$. Angular momentum conservation will therefore *increase* the multiplicity of pions in annihilation at rest. Also for $j = 1$ the above conclusion will be almost true.

Part II

THE VALUE OF THE PHASE-SPACE INTEGRAL WITH ANGULAR MOMENTUM CONSERVATION

11. – Problem.

In the previous part we derived the following expression for the phase-space integral

$$\varrho_n(E, j) = \int \mathrm{d}\boldsymbol{p}_1 \ldots \int \mathrm{d}\boldsymbol{p}_n \delta\Big(E - \sum_{i=1}^{n} \sqrt{p_i^2 + m_i^2}\Big)\,\delta\Big(\sum_{i=1}^{n} \boldsymbol{p}_i\Big)\mathscr{F}_j \,, \tag{11.1}$$

with

$$\mathscr{F}_j = 2^{-\frac{1}{2}} \exp\left[-\tfrac{1}{6}R^2T^2\right] I_0\left(\tfrac{1}{6}R^2T^2\right)\left[\tfrac{1}{6}R^2(2Z^2 + T^2)\right]^{-\frac{1}{2}} \cdot$$

$$\cdot \exp\left[-\tfrac{1}{6}R^2(2Z^2 + T^2)\right] I_{j+\frac{1}{2}}\left[\tfrac{1}{6}R^2(2Z^2 + T^2)\right] ,$$

$$Z^2 = \sum_{i=1}^{n} p_{z_i}^2 \,,$$

$$T^2 = \sum_{i=1}^{n} \boldsymbol{p}^2 \,, \cdot$$

One has now to devise ways and means to compute this expression in practice. The simpler problem with $\mathscr{F}_j = 1$ has been studied in the past ([14-17]), and it has appeared that there the big difficulty comes from the square-roots $\sqrt{p_i^2 + m_i^2}$, which make a closed-form expression of the integral very difficult.

Two approximations based on the hypotheses

$$A) \quad \sqrt{p_i^2 + m_i^2} \approx p_i\,, \qquad \text{(ultrarelativistic)};$$

$$B) \quad \sqrt{p_i^2 + m_i^2} \approx m_i + \frac{p_i^2}{2m_i}\,, \qquad \text{(unrelativistic)};$$

have been proposed, which yield both fairly simple formulae, but whose practical importance is small, because neither A) nor B) is true in practice.

A Monte-Carlo method, which is free from the bias of A) or B) has been used to treat many problems, in statistical theory without angular momentum conservation ([15]). All the above mentioned methods make use of the fact that the integration over all directions of $\boldsymbol{p}_i$ can be done in closed form, because the integrand is isotropic.

Because $\mathscr{F}_j$ introduces the direction of the z-axis, the p_z and $p_\perp$ have now to be treated separately; one introduces cylindrical co-ordinates, p_z, p

$$\varrho_n(E, j) = \prod_{i=1}^{n} \left[\int_0^\infty p_{\perp i}\, \mathrm{d}p_{\perp i} \int_{-\infty}^{+\infty} \mathrm{d}p_{zi} \int_0^{2\pi} \mathrm{d}\varphi_i \right] \mathscr{F}_j \cdot \tag{11.2}$$

$$\cdot\, \delta\Big(E - \sum_{i=1}^{n} \sqrt{p_{\perp i}^2 + p_{zi}^2 + m_i^2}\Big)\, \delta\Big(\sum_{i=1}^{n} \boldsymbol{p}_{\perp i}\Big)\, \delta\Big(\sum_{i=1}^{n} p_{zi}\Big)\,.$$

The angles φ_i appear only in $\delta(\sum_i \boldsymbol{p}_{\perp i})$. The angular integration is therefore, using the Fourier transform of the two-dimensional δ-function

$$\frac{1}{(2\pi)^2} \int_{\text{plane}} \mathrm{d}\boldsymbol{\lambda} \prod_{i=1}^{n} \int_0^{2\pi} \exp\left[-i(\boldsymbol{\lambda}, \boldsymbol{p}_{\perp i})\right] \mathrm{d}\varphi_i : \tag{11.3}$$

now

$$\int_0^{2\pi} \mathrm{d}\varphi \exp\left[-i(\boldsymbol{\lambda}, \boldsymbol{p}_\perp)\right] = \int_0^{2\pi} \mathrm{d}\varphi \exp\left[-i\lambda p_\perp \cos\varphi\right] = 2\pi J_0(\lambda p_\perp)\,,$$

([14]) R. H. Milburn: *Rev. Mod. Phys.*, **27**, 1 (1955).

([15]) S. Z. Belenkii, V. Makzimenko, A. Nikisov and I. Rosental: *Fortsch. d. Phys.*, **6**, 524 (1958).

([16]) G. Fialho: *Phys. Rev.*, **105**, 328 (1957).

([17]) F. Cerulus and R. Hagedorn: *Suppl. Nuovo Cimento*, **9**, 646 (1958).

and the angular integration reduces to

$$(11.4) \qquad (2\pi)^{n-1}\int_0^\infty \lambda\,\mathrm{d}\lambda J_0(\lambda p_{\perp 1})\ldots J_0(\lambda p_{\perp n})\,.$$

This expression is a well-known result in random-walk theory: there

$$P^{(2)}(r;a_1,\ldots,a_n)=\int_0^\infty \lambda J_0(r\lambda)\prod_{i=1}^{n} J_0(a_i\lambda)\,\mathrm{d}\lambda\,,$$

is the probability that the n vectors in a plane with lengths $a_1 \ldots a_n$ will add up to a resultant r, when all directions are equally probable. We shall assume that this function is known (cf. Appendix).

Similarly, we can interpret the p_z integration as a random-walk in one dimension: consider the integral

$$(11.5) \qquad J\equiv\int_{-\infty}^{+\infty}\mathrm{d}z_1\ldots\int_{\infty}^{+\infty}\mathrm{d}z_n F(z_1^2,\ldots,z_n^2)\,\delta(z_1+z_2\ldots+z_n-Z)$$

where we can split the integration regions in a negative and a positive part

$$(11.6) \qquad J=\sum_{(\sigma)}\int_0^\infty \mathrm{d}z_1\ldots\int_0^\infty \mathrm{d}z_n F(z_1^2\ldots z_n^2)\,\delta(\sigma_1 z_1+\sigma_2 z_2+\ldots+\sigma_n z_n-Z)\,,$$

where $\sum_{(\sigma)}$ means a sum over all combinations of $\sigma_i=\pm 1$ and $F(z_1^2\ldots z_n^2)$ is an arbitrary even function of the $z_1,\ldots,z_n$. The function

$$(11.7) \qquad P^{(1)}(Z;z_1,\ldots,z_n)=(\tfrac{1}{2})^n\sum_{(\sigma)}\delta(\sigma_1 z_1+\ldots+\sigma_n z_n-Z)\,,$$

is the probability that a particle moving along a line in successive steps of magnitude z_1, z_2, ... but random sign will reach after n steps the position Z. This is the random-walk function in one dimension. Here we shall also assume this function to be known (and give formulae for it in the Appendix).

We are then faced with the integral (putting $p=a$, $p_z=z$)

$$(11.8) \qquad 2^n(2\pi)^{n+1}\varrho_n(E,j)=\prod_{i=1}^{n}\left[\int_0^\infty a_i\,\mathrm{d}a_i\int_0^\infty \mathrm{d}z_i\right]\delta\Big(E-\sum_i\sqrt{a_i^2+z_i^2+m_i^2}\Big)\cdot$$
$$\cdot P^{(2)}(0;a_1,\ldots,a_n)P^{(1)}(0;z_1,\ldots,z_n)\,.$$

To this it seems feasible to apply a Monte-Carlo method similar in principle to the one used for $\varrho_n^*(E)$, *i.e.* the phase-space integral without angular momentum conservation.

12. – A Monte-Carlo method.

Let us first transform the integration $\int_0^\infty \mathrm{d}a \int_0^\infty \mathrm{d}z$ to polar co-ordinates: a and z are considered as rectangular co-ordinates in a plane, whereas

$$p = \sqrt{a^2 + z^2},$$

$$\theta = \operatorname{arctg} \frac{a}{z},$$

are corresponding polar co-ordinates. So we have now

$$(12.1) \qquad \varrho_n(E, j) = 2^{-1}\pi^{n-1} \int_0^\infty \dots \int_0^\infty \mathrm{d}p_1 \dots \mathrm{d}p_n \int_0^{\pi/2} \dots \int_0^{\pi/2} \mathrm{d}\theta_1 \dots \mathrm{d}\theta_n \delta\Big(E - \sum_i \sqrt{p_i^2 - m_i^2}\Big) \cdot$$
$$\cdot p_1^2 \dots p_n^2 \sin\theta_1 \dots \sin\theta_n P^{(2)}(0;\, p_1 \sin\theta_1, \dots, p_n \sin\theta_n) \cdot$$
$$\cdot P^{(1)}(0;\, p_1 \cos\theta_1 \dots p_n \cos\theta_n)\, \mathscr{F}_j(Z^2;\, T^2) .$$

One can go over to kinetic energies, instead of momenta by putting $t_i = \sqrt{p_i^2 + m_i^2} - m_i$ and write consequently

$$\mathrm{d}p_1 \dots \mathrm{d}p_n\, p_1^2 \dots p_n^2\, P^{(2)}(0;\, p_1 \sin\theta_1, \dots)\, P^{(1)}(0;\, p_1 \cos\theta_1, \dots)\, \mathscr{F}_j(Z^2;\, T^2) ,$$

as function of the t_i and of the $\cos\theta_i$

$$\Phi(t_1, t_2, \dots, t_n;\, \cos\theta_1, \dots, \cos\theta_n)\, \mathrm{d}t_1 \dots \mathrm{d}t_n .$$

And, as proved in [17], $\varrho_n(E, j)$ can be written as

$$(12.2) \qquad \varrho_n(E, j) = 2^{-1}\pi^{n-1} \int_0^T \mathrm{d}T_1 \int_{T_j}^T \mathrm{d}T_2 \dots \int_{T_{n-2}}^T \mathrm{d}T_{n-1} \int_0^1 \mathrm{d}(\cos\theta_1) \dots \int_0^1 \mathrm{d}\cos\theta_n) \cdot$$
$$\cdot \Phi(T_1,\, T_2 - T_1, \dots, T - T_{n-1};\, \cos\theta_1, \dots, \cos\theta_n) .$$

This integral is computed by Monte-Carlo by drawing N times two samples A) and B).

A) $n-1$ random numbers, according to a uniform probability distribution from the segment $(0, T)$. These are labelled in ascending order of magnitude

$$T_1,\ T_2,\ \ldots,\ T_{n-1}\,.$$

B) n random numbers, according to a uniform probability distribution from the segment (0, 1). These are labelled (in the order in which they come)

$$\cos\theta_1,\ \ldots,\ \cos\theta_n\,.$$

For each sample one computes the expression

$$\Phi(T_1,\ \ldots,\ T-T_{n-1};\ \cos\theta_1,\ \ldots,\ \cos\theta_n)$$

adds up these numbers for all samples, takes the average value; this is proportional to $\varrho_n(E, j)$.

In the same way as in the method described in [17] one can compute here kinetic energy spectra; these can even now be split into transverse kinetic energy and longitudinal kinetic energy, giving in principle the answer of the statistical theory as to the distribution of transverse momenta in a high-energy collision.

13. – Estimates of the influence of angular momentum conservation.

As long as the method outlined in the previous chapter has not been put to work it will not be possible to have detailed predictions of the statistical theory. What we propose to do here is an approximation that should enable us to compare semi-quantitatively the results of the theory with and without angular momentum conservation.

Let us write the phase-space integral again, but taking out of the integration the mean value of the weight function $\mathscr{F}_j(p_1 \ldots p_n)$:

$$\varrho_n(E, j) \quad \mathscr{F}_j \int \mathrm{d}\boldsymbol{p}_1 \ldots \int \mathrm{d}\boldsymbol{p}_n\, \delta\Big(E - \sum_{i=1}^{n} \sqrt{p_i^2 + m_i^2}\Big)\, \delta\Big(\sum_i \boldsymbol{p}_i\Big) = \mathscr{F}_j\, \varrho_n^*(E)\,, \tag{13.1}$$

where $\varrho_n^*(E)$ is the phase-space integral as conventionally defined [17]. This mean value, which is precisely defined by formula (13.1), we are now going to replace by the function $\mathscr{F}_j(\langle p_1\rangle, \langle p_2\rangle \ldots)$ where we shall take

$$p_i\rangle \equiv \sqrt{\langle \varepsilon_i\rangle^2 - m_i^2}\,,$$

whith $\langle \varepsilon_i \rangle$ the average value of the energy computed from the conventional phase-space integral; *e.g.*

$$(13.2) \qquad \varrho_n^*(E)\langle \varepsilon_1 \rangle = \int \mathrm{d}\boldsymbol{p}_1 \ldots \int \mathrm{d}\boldsymbol{p}_n \sqrt{p_i^2 + m_i^2}\, \delta\Big(E - \sum_i \sqrt{p_i^2 + m_i^2}\Big)\, \delta\Big(\sum_i \boldsymbol{p}_i\Big) .$$

This is, of course, an approximation the error of which could only be ascertained by comparison with an exact calculation. We shall use it, as mentioned, as an exploratory tool.

For two cases which have been computed previously (6 GeV p-p collisions [18] and N-$\bar{N}$ annihilation at rest [19]) we shall compute $\langle \mathscr{F}_j \rangle$ and see how the new results compare with the old ones. A source of uncertainty is that the old calculation gives $\langle \varepsilon_i \rangle$ all right, but averaged over all angles, whereas to compute $\langle \mathscr{F}_j \rangle$ we should know separately $\langle Z^2 \rangle = \langle \sum_{i=1}^{n} p_{zi}^2 \rangle$ and $\langle T^2 \rangle = \langle \sum_{i=1}^{n} p_{\perp i}^2 \rangle$. We shall *assume* here near-isotropy as the most probable configuration on which to base our estimate of $\langle \mathscr{F}_j \rangle$, at least for not too high values of j. This assumption is good as long as the classical approximation to $\mathscr{F}_j$, is valid, *i.e.* $a^2 Q^2 \gg j^2$. With $\mathscr{F}_j = 1$ (*i.e.* no angular momentum conservation) one gets of course that $\langle Z^2 \rangle = \frac{1}{3}\langle Q^2 \rangle$, because then no direction is privileged. We take therefore

$$(13.3) \qquad 2Z^2 + T^2 = Z^2 + Q^2 = \tfrac{4}{3} Q^2 = \tfrac{4}{3}\Big[\sum_{j=1}^{2} \langle p_N \rangle^2 + \sum_{i=1}^{n} \langle p_\pi \rangle^2\Big] ,$$

for the p-p collisions, because we want to distinguish between nucleons and pions. In the annihilation only pions are taken into account in the final state.

The result of substituting then in the calculations for p-$\bar{\mathrm{p}}$ annihilation at rest the expression (13.1) instead of $\varrho^*(E)$ is that the average number of pions is increased:

$$\langle n_\pi \rangle \quad \Big(\text{with } J\text{-conservation and } \Omega = \frac{4\pi}{3}\lambda_\pi^3\Big) = 3.73 ,$$

as compared to

$$\langle n_\pi \rangle \quad \Big(\text{without } J\text{-conservation and } \Omega = \frac{4\pi}{3}\lambda_\pi^3\Big) = 3.40 .$$

Alternatively, one can try to adjust Ω so as to have the observed multiplicity

[18] R. Hagedorn: *Nuovo Cimento*, **15**, 246 (1960).
[19] F. Cerulus: *Nuovo Cimento*, **14**, 827 (1959).

of ≈ 4.7

$$\Omega = 10\,\frac{4\pi}{3}\,\lambda_\pi^3 \text{ yields } \langle n_\pi \rangle \approx 4.7 \text{ without } J\text{-conservation},$$

$$\Omega = \;5\,\frac{4\pi}{3}\,\lambda_\pi^3 \text{ yields } \langle n_\pi \rangle \approx 4.8 \text{ with } J\text{-conservation}.$$

All this is of course done *not* assuming any π-π isobar. For the p-p collisions at 6 GeV the results are displayed in Fig. 5, as a function of the total

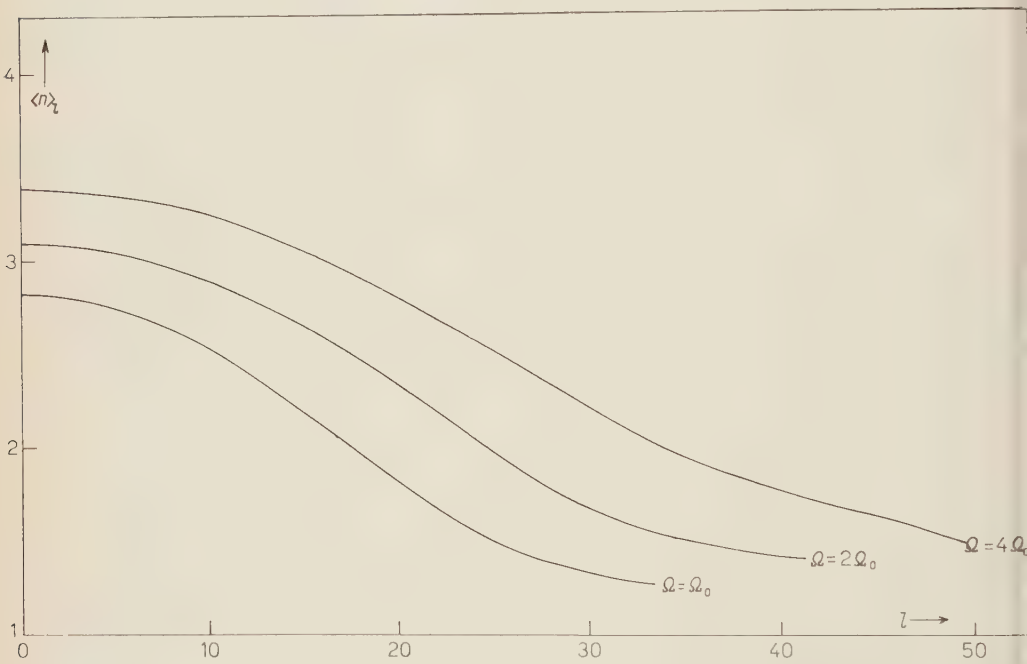

Fig. 5. – Average number of pions produced in a 6 GeV p-p collision, as a function of total angular momentum and of interaction volume $\Omega_0 = (4\pi/3)\lambda_\pi^3$.

angular momentum l. To get the average multiplicity one has to sum over all l. If one takes the hot-spot model seriously enough all phase relationships between initial and final states are destroyed, and the only thing that counts is the statistical weight w_l of the l-th partial wave in the plane wave incident on the sphere Ω

$$w_l = \int_{\Omega} \mathrm{d}\xi_1 \int_{\Omega} \mathrm{d}\xi_2 \langle i \,|\, \mathscr{P}_l \mathscr{P}_{m=0}\, \delta(\boldsymbol{x}_1 - \boldsymbol{\xi}_1)\, \delta(\boldsymbol{x}_2 - \boldsymbol{\xi}_2) \,|\, i \rangle\,, \tag{13.4}$$

where $|i\rangle = \exp[i(\boldsymbol{k}, \boldsymbol{r}_1 - \boldsymbol{r}_2)]$ is the wave function of the two colliding par-

ticles in their c.m.s.; (13.4) is a special case ($n = 2$) of formula (2.5). w_l is akin to the « penetration factor » in nuclear physics. We obtain

$$w_l = 2^{-\frac{3}{2}}\pi^{\frac{1}{2}}(2l+1)(ak)^{-1}\exp[-4a^2k^2]I_{l+\frac{1}{2}}(4a^2k^2)\,, \tag{13.5}$$

where again we have taken the Gaussian cut-off (7.4). For the 6 GeV p-p collision this is shown in Fig. 6. The linear rise for small l corresponds to the factor $(2l+1)$ in the classical picture of the geometrical partial cross-section $\sigma_{r,l} = (2l+1)\pi\lambda^2$, which is valid for $ak \ll 1$.

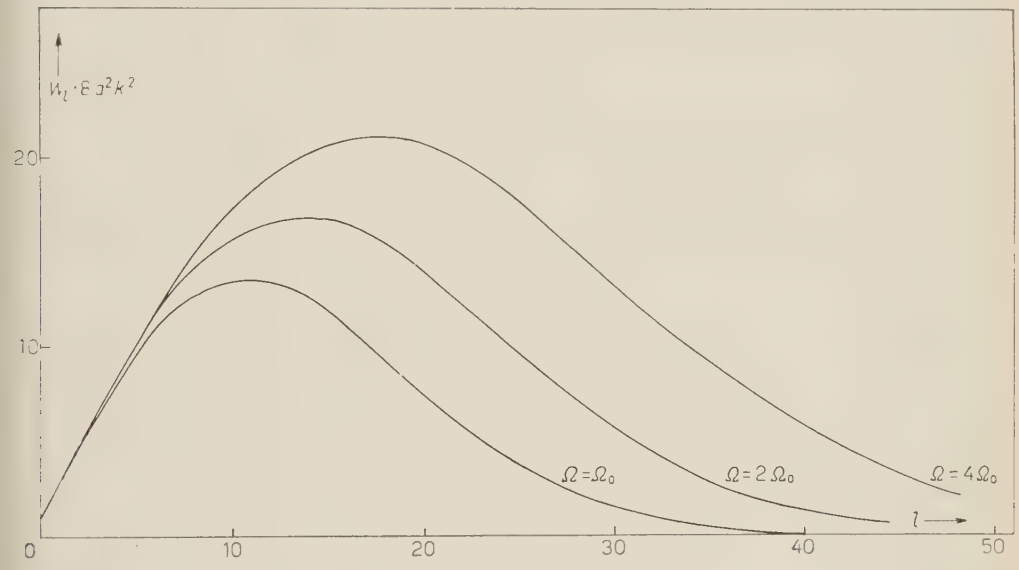

Fig. 6. – The penetration factors w_l of the partial waves for different interaction spheres; $\Omega_0 = (4\pi/3)\lambda_\pi^3$; k corresponds to 6 GeV p-p collision in the c.m.s.

The average pion number then, resulting from folding $\langle n_\pi \rangle$ for given l with the w_l, is found to be

$$\langle n_\pi \rangle = 2.25 \qquad \text{with } J\text{-conservation}\,,$$

against

$$\langle n_\pi \rangle = 2.50 \qquad \text{without } J\text{-conservation}\,.$$

One sees that here the correction is in the opposite direction as in annihilation. This is easily understood because in a high-energy collision the high-angular momenta contribute most, and for those the exponential factor in $\mathcal{F}_l$ (9.13) makes itself felt.

The numbers just mentioned are obtained using $\Omega = (4\pi/3)\lambda_\pi^3 = \Omega_0$ and the existence of a π-N isobar; cf. [18]. In order to obtain $\langle n_\pi \rangle = 2.5$ with J-conservation one should take $\Omega = 2.0\,\Omega_0$.

14. – Conclusions.

Examination of the formulae used in conventional statistical theory has led us to interpret them in such a way that the probability to produce n particles in a high-energy collision can be simply related to the probability of finding n particles together in a volume Ω. The transition matrix elements squared will behave that way if the process proceeds via an intermediate « hot spot » and the formation and decay of this « hot spot » are statistically independent. The assumptions one really makes are, however, weaker than this, because the matrix element should only reproduce this behaviour on the average. As one asks however for more and more information (spectra, angular correlations and distributions) from the statistical theory, the averaging is done over less and less parameters and the assumptions are stronger and stronger.

Asking for angular distributions in the conventional theory is probably making too strong an assumption on the matrix elements, which—save for S waves—is in contradiction with angular momentum conservation.

By considering in the averaging process over the unobserved parameters of the final states only states of given total angular momentum this contradiction can be avoided. One has still of course to make hypotheses on $|f|S|i|^2$, and these are most easily found by comparison with the hot-spot model.

The averaging over final states having specified values of J, E and $P = 0$ can be done using the projection operators on states with these quantum numbers. If one leaves out the P-conservation the Koba theory results.

The projection operators are given in integral form; the integrals converge and can be well approximated by fairly simple formulae in most cases of practical interest, where the available energy is several GeV and the radius of the interaction volume is $\approx \lambda_\pi$.

The theory has then given a modified form of the phase-space integral, which has to be computed to get detailed results.

As a further guide to methods of extracting information from the phase-space integral it will be useful to consider the so-called « classical » theory of T. Ericson; by a comparison with the present method it is seen that in many cases its results should be good approximations. Some qualitative features can, however, be extracted at once.

For high values of J, the phase-space integral will be depressed; also in this case there will be a marked correlation of the end particles, which will

tend to come out peaked backward-forward. For low values of J, as *e.g.* in N-$\bar{N}$ annihilation the phase-space integral is increased, no correlation is introduced by J-conservation.

Because the integrand of the phase-space integral depends only on the average momentum of all the particles (for a given multiplicity) the effect on the spectrum of a single particle will be fairly small. One could therefore expect that the spectra of particles (averaged over angles in the c.m.s.) from events with given multiplicity should not be much different from those obtained by the conventional theory.

The Monte Carlo method proposed should be able to obtain reliable spectra, both averaged over angles longitudinal and transverse. It is of course an interesting problem to find out how much backward-forward peaking J-conservation is able to give, or what magnitude of J one has to assume to be able to reproduce the experimentally observed peaking.

The assumptions of the hot-spot model are badly needed, finally, if one tries to estimate *e.g.* multiplicities from a high-energy collision where the initial state is a plane wave with definite phase relationship between the partial waves. Averaging over all angular momenta incoherently is only justified by the statistical independence of the two phases of the collision process. A consequence of this independence is that the angular distributions in this form of statistical theory are necessarily symmetric with respect to a plane perpendicular to the collision line; this feature is also clear from the phase-space integrand where only the squares of the longitudinal momenta appear.

Finally, the changes introduced by J-conservation in the multiplicity of N-$\bar{N}$ annihilation and of high-energy p-p collision (increasing the former, reducing the latter) make that one has now to take new values of the interaction volume Ω in order to get agreement with experiment; the long-standing discrepancy between the different values of Ω needed in each case is now reduced:

$$\Omega_{\text{annih}} = 2.5\,\Omega_{\text{collision}}$$

but has not disappeared completely.

* * *

It is a pleasure to thank L. Van Hove, director of the CERN Theoretical Division, both for hospitality at CERN and for illuminating discussions. The author owes much also to discussions with T. Ericson, A. Pais and R. Hagedorn. G. A. Erskine has kindly computed tables of Bessel functions of large imaginary argument.

Appendix

Random-flight functions.

The probability that n ν-dimensional vectors of given lengths $a_1, a_2, \ldots, a_n$ have a resultant whose length lies between r and $r+\mathrm{d}r$ is [20]

$$(A.1) \qquad P^{(\nu)}(r)\,\mathrm{d}r = 2\left\{\Gamma\left(\frac{\nu}{2}\right)\right\}^{n-1} r \int_0^\infty t\left(\frac{tr}{2}\right)^{\nu/2} J_{(\nu/2)-1}(rt) \ldots \prod_{m=1}^{n} \frac{J_{(\nu/2)-1}(a_m t)}{(\frac{1}{2}a_m t)^{(\nu/2)-1}}\,\mathrm{d}t\,.$$

In a first approximation these $P^{(\nu)}(r)$ are Gaussians. It has been proved [21] for $a_1 = a_2 \ldots = a_n$ or more generally for all a's of the same order of magnitude [22] that integral (A_1) can be approximated, up to terms of order $1/n^2$ by the following expressions.

$$(A.2) \qquad P^{(1)}(r)\,\mathrm{d}r = (2\pi)^{-1}A^{-1}\exp\left[-\frac{r^2}{2A^2}\right]\left[1-\frac{1}{24}\frac{B^4}{A^4}\left(3-6\frac{r^2}{A^2}+\frac{r^4}{A^4}\right)\right]\mathrm{d}r\,.$$

$$(A.3) \qquad P^{(2)}(r)\,\mathrm{d}r = 2rA^{-2}\exp\left[-\frac{r^2}{A^2}\right]\left[1-\frac{1}{4}\frac{B^4}{A^4}\left(2-4\frac{r^2}{A^2}+\frac{r^4}{A^4}\right)\right]\mathrm{d}r\,.$$

$$(A.4) \qquad P^{(3)}(r)\,\mathrm{d}r = 4\left(\frac{3}{2}\right)^{\frac{3}{2}}\pi^{-\frac{1}{2}}A^{-3}\exp\left[-\frac{3}{2}\frac{r^2}{A^2}\right]\left[1-\frac{1}{20}\frac{B^4}{A^4}\left(15-30\frac{r^2}{A^2}+9\frac{r^4}{A^4}\right)\right]\mathrm{d}r\,,$$

where, for $\nu = 1, 2, 3$, one has defined

$$A^2 = \sum_{i=1}^{n} a_i^2\,,$$

$$B^4 = \sum_{i=1}^{n} a_i^4\,.$$

The function $P^{(1)}(r)$ given in (A.2) is *sensu stricto* not the probability to reach a point r on a line after n steps, which is a discontinuous function, but rather the density of the points that can be reached in n steps.

[20] G. N. Watson: *Bessel Functions* (Cambridge, 1945).
[21] F. G. Tricomi: *Funzioni ipergeometriche confluenti* (Roma, 1954).
[22] F. Cerulus: to be published.

RIASSUNTO (*)

Si dimostra che la teoria statistica convenzionale (con conservazione dell'energia-impulso, ma senza conservazione del momento angolare) dà gli stessi risultati (molteplicità e spettri) che si possono ottenere da un modello che presuppone l'esistenza di un « hot-spot » intermedio nella collisione di due particelle di alta energia, se la formazione dell'« hot-spot » è statisticamente indipendente dal suo decadimento in numerose particelle. Questo modello è suggerito dalle formule usate nella teoria statistica, che in effetti pongono la probabilità di produrre n particelle proporzionale alla probabilità di trovare assieme n particelle in un volume Ω. La conservazione del momento angolare (assieme alla conservazione dell'energia e della quantità di moto) può essere soddisfatta prendendo in considerazione solo stati di n particelle con valori prescritti del J totale, dell'energia e della quantità di moto. Facendo uso del formalismo della matrice di densità e di una espressione esplicita degli operatori di proiezione su stati di dato momento angolare, si arriva ad una forma modificata dell'integrale dello spazio delle fasi, che è semplicemente collegata con la probabilità di produrre n particelle. Si mostra che la teoria con momento angolare, ma senza conservazione della quantità di moto, esposta da Koba, è un caso speciale facilmente derivabile dal presente formalismo. Si dimostra che la teoria « classica » della conservazione del momento angolare di T. Ericson è un caso limite che tuttavia ha una vasta applicabilità. Strettamente parlando la teoria convenzionale è valida solo se tutte le particelle finali sono nello stato s. Le formule sono state derivate per una forma sferica gaussiana di Ω. In linea di principio si possono ammettere forme contratte. Si propone un programma tipo Monte Carlo per valutare questo integrale dello spazio delle fasi. Il metodo permetterà di calcolare gli spettri degli impulsi longitudinali e trasversi delle particelle finali. Si calcolano gli effetti della conservazione di J sulla molteplicità. In confronto della teoria convenzionale la molteplicità è accresciuta del 10% nelle annichilazioni p-p e diminuito del 10% nelle collisioni p-p di 6 GeV.

(*) *Traduzione a cura della Redazione.*

A Possible Means to Obtain Evidence Concerning the Spin of the K′-Meson.

B. T. Feld (*) and D. B. Lichtenberg (**)

CERN - Geneva

(ricevuto il 6 Settembre 1961)

Summary. — It is shown that antiproton-proton annihilation at rest into a K′ and $\overline{\text{K}}'$ meson can provide information about the spin of the K′ if a number of assumptions are justified. These assumptions are: 1) the K′ has spin either zero or one; 2) the annihilation occurs in an S-state; 3) the K′ and $\overline{\text{K}}'$ decay as free particles; 4) the background of annihilation events which cannot be distinguished kinematically from K′$\overline{\text{K}}'$ production is small. The method consists in showing that if the K′ has spin one, it is extremely unlikely that the angular distributions will be isotropic with respect to all the angles specified by the production and decay of the K′ and $\overline{\text{K}}'$. The degree of anisotropy is not unique. However, it would require a triple coincidence for isotropy; *i.e.* three relationships would have to hold among the parameters specifying the interaction. If the K′ has spin zero, the angular distribution is of course isotropic. All of the assumptions are open to some question. Nevertheless, it may be possible to obtain some evidence about the spin of the K′ from the angular distributions, even if the assumptions are false.

1. – Introduction.

In anti-proton annihilations at rest, it may be possible to interpret a number of events according to the reaction

$$\overline{\text{p}} + \text{p} \to \text{K}' + \overline{\text{K}}' \,, \tag{1}$$

(*) John Simon Guggenheim fellow. Permanent address: Department of Physics, M.I.T., Cambridge, Mass.

(**) Supported by a grant from the National Science Foundation. Permanent address: Physics Department, Michigan State University, East Lansing, Mich.

where K′ is the meson (1) reported by ALSTON *et al.* (2) with mass 885 MeV, full width 16 MeV, and known decay mode

$$K' \to K + \pi . \tag{2}$$

It is proposed to use angular correlations in the decay of the K′ produced in reaction (1) as a possible means to determine the spin of the K′. In particular, it will be shown that it is useful to measure the angular distributions of the final products with respect to three different angles, which will be defined in the next section. The point of looking at three angles is the following: if the K′ has spin different from zero, the angular distribution of its decay products may still accidently be isotropic. However, by looking at the decay of both K′ mesons, angular correlation measurements may be made with respect to two additional angles which might still show anisotropy even in the case the angular distribution of a single K′ is isotropic. *A priori*, it is extremely unlikely that all three angular distributions will be isotropic if the spin of the K′ is different from zero.

Another analysis, making use of only one of the angles considered here, has independently been made by D'ESPAGNAT, PRENTKI and YAMAGUCHI (3). Still another proposal, based on the reaction $\bar{p} + p \to K' + \overline{K}$, has been made by SCHWARTZ (4).

Our detailed analysis depends on the validity of a number of assumptions which are outlined below. However, it may be possible to obtain some information even if one or more of the assumptions is incorrect.

1) We assume the K′ has spin either zero or one.
2) We assume, following the arguments of DAY, SNOW and SUCHER (5), that the annihilation at rest takes place from an *S*-state.
3) We assume that the K′ and $\overline{K}'$ decay as free particles.

In view of the small (16 MeV) width of the K′, this assumption is perhaps not too bad. Each K′ from the $\bar{p}p$ annihilation travels at about $\frac{1}{3}$ the speed of light, and has a mean decay length of $\sim 4 \cdot 10^{-13}$ cm, somewhat longer than

(1) We use the term « meson » for convenience. Alternatively, we may say « resonant state of K and π ». That the resonance really occurs in a single state has not been established, but we assume it to be true.

(2) M. ALSTON, L. W. ALVAREZ, PH. EBERHARD, M. L. GOOD, W. GRAZIANO, H. K. TICHO and S. G. WOJCICKI: *Phys. Rev. Lett.*, **6**, 300 (1961).

(3) B. D'ESPAGNAT, J. PRENTKI and Y. YAMAGUCHI: to be published. We wish to thank these authors for illuminating discussions about their work.

(4) M. SCHWARTZ: *Phys. Rev. Lett.*, **6**, 556 (1961).

(5) T. DAY, G. SNOW and J. SUCHER: *Phys. Rev. Lett.*, **3**, 61 (1959). The argument for $\bar{p}p$ interactions proceeding from an *S*-state is not as good as for Kp interaction, G. SNOW: private communication. See also B. P. DESAI: *Phys. Rev.*, **119**, 1385 (1960).

the range of interaction. In addition to neglecting dynamical final-state interactions, we neglect any effect of Bose statistics on the two final state pions.

4) We assume there is only a small background of $K\bar{K}2\pi$ events which cannot be distinguised kinematically from the desired events.

Whether this background will indeed be small is a matter that only experiment can decide. An estimate of background based on a simple model taking into account the effect of a $\pi\pi$ resonance, was made by D'ESPAGNAT, PRENTKI and YAMAGUCHI [3]. These authors found that there is a region in phase space in which the reaction

$$\bar{p} + p \to K + \bar{K} + \pi^* \to K + \bar{K} + 2\pi \tag{3}$$

cannot be distinguished kinematically from reaction (1). They show that it is possible to select events so as to eliminate this interference. Other sources of background of course remain.

Of course, we also assume that the usual strong interaction conservation laws are valid in the production of the $K'\bar{K}'$ pair and in their decay. Also we make one very reasonable dynamical approximation that the annihilation radius is small enough to exclude orbital angular momentum $L = 3$ for the outgoing $K'\bar{K}'$ pair. This approximation is made only for convenience; a more complete treatment is given in the Appendix.

In Section 2, we give a detailed analysis, treating the assumptions as true. In Section 3, we briefly discuss the validity of the assumptions and indicate how the analysis must be modified if they are incorrect.

2. – The angular distribution.

If the antiproton and proton annihilate in an S-state, the parity of the system is odd, and the $K'\bar{K}'$ pair must be emitted in a state of odd orbital angular momentum L. Suppose first that the K' has spin zero. Then the reaction cannot take place in the singlet state of the $\bar{p}p$ system (total angular momentum $J = 0$), since then L would be even (zero) and parity would not be conserved. The reaction can go in the triplet state, and of course, the angular distribution of the decay products must be isotropic.

Next, suppose that the K' has spin $s = 1$. Then the reaction can go either via the singlet or triplet states of $\bar{p}p$. Since the reaction amplitudes in these states are unknown, the angular distribution is not unique.

Let us consider the case $s = 1$ in greater detail. We distinguish 3 directions:

1) the line of flight of the $K'\overline{K}'$ pair,
2) the line of flight of the K and π in the rest system of the K′, and
3) the line of flight of the $\overline{K}$ and π in the rest system of the $\overline{K}'$.

First, consider that the reaction takes place from the singlet state of $\bar{p}p$. The total spin S of the $K'\overline{K}'$ system must be $S=1$ and must be combined with orbital angular momentum $L=1$ to give total angular momentum $J=0$. Since the K and π from the decay of the K′ each have spin 0, the quantum numbers (l, m) of their orbital angular momentum will be the same as the quantum numbers $(s=1, m_s)$ of the spin of the K′. (The same is of course true for the $\overline{K}'$ decay into $\overline{K}+\pi$.) Thus the angular part of the final state wave function will be an eigenfunction of three orbital angular momentum operators, each orbital angular momentum being equal to unity, and all three combining to form $J=0$. This eigenfunction can easily be constructed from products of three spherical harmonics.

The amplitude A_0 for the reaction (1) is then of the form

$$A_0 = a \sum_{\mu m} (11\mu,\ m-\mu \mid 1m)(11m,\ -m \mid 00)\, Y_1^{-m}(1)\, Y_1^{\mu}(2)\, Y_1^{m-\mu}(3)\,, \tag{4}$$

where $(j_1 j_2 m_1 m_2 \mid jm)$ are appropriate Clebsh-Gordan coefficients to make $J=0$, a is a complex number specifying the amplitude of the reduced matrix element for the reaction, and the Y_1^m's are spherical harmonics with arguments 1, 2, 3 specifying the angles $\theta_1\varphi_1$, $\theta_2\varphi_2$, $\theta_3\varphi_3$ of the three directions defined previously with respect to an arbitrary z axis.

In the triplet state, the expression for the transition amplitude may be simplified by making use of the invariance of the system under charge conjugation C [6]. The $\bar{p}p$ system is an eigenstate of C with eigenvalue $(-1)^{L+S}$. Then the $K'\overline{K}'$ must also be an eigenstate. If annihilation occurs in the ${}^3S_1$ state, $C=-1$. Since the $K'\overline{K}'$ system has L odd, this implies that S is even. Thus if the K′ and $\overline{K}'$ have spin 1, they can combine to form $S=0$ or 2, but not $S=1$. Likewise, if annihilation is from the ${}^1S_0$ state, the total spin of the $K'\overline{K}'$ must be $S=1$. (This is another reason for the reaction being forbidden in the ${}^1S_0$ state if the K′ has spin $s=0$.)

If $J=1$ (annihilation from triplet state), the orbital angular momentum L of the $K'\overline{K}'$ must be $L=1$ or $L=3$. Since the relative momentum of the $K'\overline{K}'$ pair is low, $L=3$ cannot occur with an appreciable amplitude for a reasonable interaction radius. An analysis including $L=3$ is relegated to the Appendix; we neglect this amplitude in the following.

The amplitudes A_1^M for the reaction in the triplet state proceeding from

[6] Note that both isobaric spin states of the nucleon-antinucleon system are permitted, so that the relative $K'^+K'^-$ and $K'^0\overline{K}'^0$ ratio is arbitrary.

an initial state $J=1$, with projection M may be written

$$A_1^M = b\sum_m (11m, -m|00)(010M|1M)\, Y_1^M(1)\, Y_1^m(2)\, Y_1^{-m}(3) + \\ + c\sum_{m\mu} (11m, \mu-m|2\mu)(21\mu, M-\mu|1M)\, Y_1^{M-\mu}(1)\, Y_1^m(2)\, Y_1^{\mu-M}(3)\,, \tag{5}$$

where b and c are complex numbers specifying the reduced matrix elements of the reaction corresponding to total spin $S=0$ and $S=2$, respectively. The transition probability $W(123)$ for the reaction $\bar{p}p \to K' + \bar{K}' \to (K+\pi) + (\bar{K}+\pi)$ will be proportional to

$$W(123) \propto |A_0|^2 + \sum_M |A_1^M|^2\,. \tag{6}$$

It is convenient to take direction 3 as the z axis and to integrate over the angles q_1 and q_2. The resulting transition probability is denoted by $W(\theta_1\theta_2)$ where θ_1 is the angle between the line of flight of the $\bar{K}'$ and the line of flight of its decay products in its own rest system; and θ_2 is the angle between the lines of flight of the decay products of the K' and $\bar{K}'$, each measured in the appropriate rest system. The quantity $W(\theta_1\theta_2)$ is given by

$$W(\theta_1\theta_2) \propto \tfrac{1}{2} + \tfrac{9}{20}Rx + \left(\tfrac{9}{20}Rx - \tfrac{1}{2}\right)\cos^2\theta_1 + \left(2R - \tfrac{1}{2} - \tfrac{41}{20}Rx - 2Ry\right)\cos^2\theta_2 + \\ + \left(\tfrac{1}{2} + \tfrac{3}{4}Rx + 6Ry\right)\cos^2\theta_1\cos^2\theta_2\,. \tag{7}$$

This expression depends on three real parameters R, x and y which are functions of the complex aplitudes a, b, and c as follows

$$R = \frac{|b|^2+|c|^2}{|a|^2}, \qquad x = \frac{|c|^2}{|b|^2+|c|^2}, \qquad y = 2\left(\frac{x-x^2}{5}\right)^{\frac{1}{2}}\cos\delta\,, \tag{8}$$

where δ is the relative phase between b and c. Note that these parameters have restricted ranges

$$0 \leqslant R \leqslant \infty\,, \quad 0 \leqslant x \leqslant 1\,, \quad -1 \leqslant \cos\delta \leqslant 1\,. \tag{9}$$

Integrating $W(\theta_1\theta_2)$ over θ_2, we get the distribution in the variable θ_1:

$$W(\theta_1) \equiv \int W(\theta_1\theta_2)\,\mathrm{d}(\cos\theta_2) \propto \left(\frac{1}{2} + R - \frac{7}{20}Rx - Ry\right)\sin^2\theta_1 + \\ + R\left(1 + \frac{7}{10}x + 2y\right)\cos^2\theta_1\,. \tag{10}$$

It can be readily seen that this expression can be isotropic for allowed values of the parameters. For this reason we also consider $W(\theta_1\theta_2)$ integrated over θ_1 to obtain the correlation function in θ_2. We get

$$(11) \quad W(\theta_2) \int W(\theta_1\theta_2)\,\mathrm{d}(\cos\theta_1) \propto \left(\frac{1}{2} + \frac{9}{10}Rx\right)\sin^2\theta_2 + 3R\left(1 - \frac{3}{5}x\right)\cos^2\theta_2 .$$

For both these angular distributions to be isotropic, a double coincidence must occur, *i.e.* two independent relations between R, x and δ must hold. Nevertheless, since isotropy can occur, it may be useful to consider $W(\theta_1\theta_2)$. This expression (eq. (7)) can be used by dividing the events into two groups depending on whether θ_2, say, is greater or less than 45°, and observing whether there is anisotropy in θ_1 for either group. For the above expression to be isotropic the coefficients of $\cos^2\theta_1$, $\cos^2\theta_2$ and $\cos^2\theta_1\cos^2\theta_2$ must separately vanish. This actually happens to be possible for allowed values of R, x and $\cos\delta$; the unique solution is,

$$(12) \qquad R = \frac{7}{6}, \qquad x = \frac{20}{21}, \qquad \cos\delta = -1 .$$

A priori, such a situation is extremely unlikely.

Alternatively to considering $W(\theta_1\theta_2)$, we can consider the angular distribution with respect to still another angle φ. This angle is defined as follows: the direction of the K′ and the direction of its decay products establish a plane. The production and decay of the $\overline{\mathrm{K}}'$ establish another plane. Then φ is the angle between these two planes. The angular distribution in this variable can be found by returning to eq. (5) for $W(123)$. Letting direction 1 be the z axis, and integrating over θ_2 and θ_3, we obtain an expression which depends on $\varphi_2 - \varphi_3$, which is just the angle φ defined above. The expression is given by

$$(13) \qquad W(\varphi) \propto 1 + 3R + \left(2R - 1 - 2Ry - \tfrac{8}{5}Rx\right)\cos 2\varphi .$$

Unfortunately, if $W(\theta_1\theta_2)$ is isotropic, so is $W(\varphi)$, *i.e.* they are not independent. Nevertheless, it may be useful to measure both $W(\theta_1\theta_2)$ and $W(\varphi)$ to give a check against experimental bias.

3. – Discussion.

In conclusion, we may say the following. If our assumptions are justified a completely isotropic distribution means that it is very likely the K′ has spin zero. If the K′ has spin one, there is some anisotropy in the variables θ_1, θ_2 or φ, unless the parameters specifying the interaction have the unique

values given in eq. (12). In addition, it is apparent that if the K′ has spin one, measurement of the degree of anisotropy provides enough information to determine the parameters R, x, and $\cos\delta$ which characterize the annihilation into $K'\bar{K}'$. If the amplitude for orbital angular momentum $L = 3$ cannot be neglected, the conclusions of the last two sentences must be modified. In this case (see Appendix) the three angular distributions are given in terms of five, rather than three parameters. It is apparent that for isotropy with respect to all three angles, three relationships would still have to be satisfied by these five parameters.

We now discuss validity of our assumptions. If the K′ has spin greater than one, or if the $\bar{p}p$ annihilation sometimes occurs in a P-state, the angular distributions are not given by the expressions obtained here. Nevertheless, it remains true that $W(\theta_1)$, $W(\theta_2)$ and $W(q)$ are independent in the sense that the isotropy of one does not imply the isotropy of the others. Therefore, it is still unlikely that $W(\theta_1)$, $W(\theta_2)$ and $W(q)$ will all be isotropic unless the K′ has spin zero. We also remark that D'ESPAGNAT [7] has made a proposal to check whether $\bar{p}p$ annihilation occurs from the S-state.

Evidence as to whether the K′ decays as a free particle can be obtained from experiment. If the decay is free, conservation of parity requires that equal number of π's must be emitted forward and backward with respect to the direction of the K′. Any forward-backward asymmetry indicates either that the decay is not free or that there are background events. The events in which the decay is not free will in general not only alter the observed angular distribution, but will alter the momentum spectrum as well. In other words, the width of the K′ will appear to be greater than 16 MeV if there are an appreciable number of non-free decays. For this reason, these events may be considered together with other background events.

Next consider a background of $K\bar{K}\pi\pi$ events. These events can be grouped into two classes: those arising from $\bar{p} + p \to K + \bar{K} + \pi^*$, and those arising from other causes. As mentioned previously, D'ESPAGNAT, PRENTKI and YAMAGUCHI [3] have shown that it is possible to eliminate events arising from the $\pi\pi$ resonance. The interested reader is referred to their paper for details [8].

Finally, consider a background of «other» $K\bar{K}\pi\pi$ events. These background events will have a different momentum spectrum from the $K'\bar{K}'$ events, so the fraction of background events can be determined. Unless this fraction is very small, it requires a rather elaborate analysis to obtain information

[7] B. D'ESPAGNAT: *Nuovo Cimento*, **20**, 1217 (1961).

[8] This selection of events is of two kinds. The first makes use of the properties of the wave function in charge space, the second in physical space. Clearly, the first type of selection of events can be combined with this analysis. The second will in general distort the angular distributions. However, it is possible to select so that $W(\theta_1)$ remains undistorted.

about the spin of the K′. We merely sketch one possible method of analysis.

Away from the region of phase space corresponding to $K'\overline{K}'$ production, there will be an angular distribution due entirely to background events. This will have the form, say, $\left|\sum_i \varepsilon_i P_i(\cos\theta)\right|^2$, where the ε_i are parameters. In the resonance region of phase space, the distribution will be $\left|\sum(\alpha_i + \varepsilon_i)P_i(\cos\theta)\right|^2$, where the α_i are known in terms of at most three unknown parameters if assumptions 1) and 2) are valid and if $L = 3$ is excluded. These parameters are R, x and δ if the K′ has spin 1; if the spin is zero, only α_0 is different from zero. Since the ε_i can be determined in the non-resonant region, some information can be obtained about the α_i if the ε_i are assumed to vary smoothly through the resonance. It may be necessary to repeat this process for the angles θ_2 and q, but in a favourable case one should be able to obtain enough information to decide between spin zero and one.

* * *

The authors would like to thank Professor J. Ballam for calling to their attention the possibility of observing the process considered here and raising the question of whether it might be useful for determination of the K′ spin. They are also grateful to Professor L. Van Hove for his hospitality and for a helpful discussion.

Appendix

If the amplitude for $\bar{p}p$ annihilation into $K'\overline{K}'$ with $L = 3$ is not negligibly small, the analysis is more complicated. Let the $J = 1$ amplitude be a_1^M. Then

$$a_1^M = A_1^M + B_1^M ,$$

where A_1^M is given by eq. (5) and B_1^M is the contribution from the $L = 3$ state. It is

$$B_1^M = d \sum_{m\mu} (11m, \mu - m \,|\, 2\mu)(32\mu, M - \mu \,|\, 1M)\, Y_3^{M-\mu}(1)\, Y_1^m(2)\, Y_1^{\mu-m}(3) ,$$

where d is an additional complex parameter.

The angular distribution $W(\theta_1)$ becomes

$$W(\theta_1) \propto \left(\tfrac{1}{2} + R - \tfrac{7}{20}Rx + \tfrac{3}{5}R' - Ry + z + \tfrac{1}{10}z'\right)\sin^2\theta_1 + \\ + \left(R + \tfrac{7}{10}Rx + \tfrac{9}{5}R' + 2Ry - 2z - \tfrac{1}{5}z'\right)\cos^2\theta_1 ,$$

where

$$R' = \frac{|d|^2}{|a|^2}, \quad z = 2\left(\frac{3RR'(1-x)}{10}\right)^{\frac{1}{2}} \cos\delta', \qquad z' = 2\left(\frac{3}{2}RR'x\right)^{\frac{1}{2}} \cos(\delta - \delta'),$$

and δ' is the phase difference between b and d. The angular correlation $W(\theta_2)$ is

$$W(\theta_2) \propto \left(\tfrac{1}{2} + \tfrac{9}{10}Rx + \tfrac{9}{10}R'\right) \sin^2\theta + \left(3R - \tfrac{9}{5}Rx + \tfrac{6}{5}R'\right) \cos^2\theta_2 .$$

Finally, $W(\varphi)$ becomes

$$W(\varphi) \propto 1 + 3R + 3R' - \left(1 - 2R + \tfrac{8}{5}Rx - \tfrac{3}{5}R' + 2Ry - 2z + \tfrac{2}{5}z'\right) \cos 2\varphi .$$

These angular distributions may all be isotropic for certain values of the parameters, but it would require a three-fold coincidence for this to occur, *i.e.* three relationships would have to be satisfied by the 5 parameters R, R', x, δ, δ' for isotropy.

Note added in proof.

After this paper was completed, we came upon two other proposals to determine the spin of the K′. See D. O. Caldwell: *Phys. Rev. Lett.*, **7**, 259 (1961), and M. Bég, P. De Celles and R. Maar: *Phys. Rev.*, **124**, 622 (1961). Additional references may be found in this latter work.

RIASSUNTO (*)

Si dimostra che l'annichilazione di un protone ed un antiprotone in quiete con produzione di un mesone K′ ed un $\bar{\text{K}}'$ può fornire informazioni sullo spin del $\bar{\text{K}}'$ se alcune ipotesi sono giustificate. Esse sono: 1) il K′ ha spin 0 o 1; 2) l'annichilazione ha luogo nello stato S; 3) il K′ e il K′ decadono come particelle libere; 4) il fondo di eventi di annichilazione che non possono essere cinematicamente distinti dalla produzione di $\text{K}'\bar{\text{K}}'$ è piccolo. Il metodo consiste nel mostrare che se il K′ ha spin 1, è estremamente inverosimile che le distribuzioni angolari siano isotropiche rispetto a tutti gli angoli determinati dalla produzione e dal decadimento del K′ e del $\bar{\text{K}}'$. Il grado di anisotropia non è unico. Comunque per l'isotropia si richiederebbe una tripla coincidenza, cioè tra i parametri che individuano l'interazione dovrebbero valere tre relazioni. Se il K′ ha spin 0, la distribuzione angolare naturalmente è isotropica. Tutte le ipotesi sono soggette a discussione. Ciononostante dalle distribuzioni angolari si potrebbe ottenere qualche indicazione sullo spin del K′, anche se le ipotesi sono false.

(*) *Traduzione a cura della Redazione.*

Correlation Theory of Stationary Electromagnetic Fields.

Part IV – Second Order Conservation Laws (*).

P. Roman

Department of Physics, Boston University - Boston, Mass. (**)

(ricevuto l'8 Settembre 1961)

Summary. — By imitating well-known techniques to obtain the energy-equation in Maxwell's theory, eight independent higher order conservation laws are found for the various second order correlation functions associated with stationary random electromagnetic fields. Two further conservation laws are deduced which involve the physically so significant energy coherence tensor and the flow coherence tensor.

1. – Introduction and notation.

Much effort has been expended in the last few years to formulate the behavior of random, statistical electromagnetic fields in terms of operationally defined measurable quantities, such as various correlation functions [1-4].

Among other results, rigorous laws for the propagation of the second order correlation functions related to stationary random fields have been formulated. Roman and Wolf [5] derived a set of basic first-order differential equations

(*) The research reported in this paper has been sponsored in part by the Electronic Research Directorate, Air Force Cambridge Research Laboratories, Office of Aerospace Research, under contract No. AF 19(604)-8022.

(**) Present address: Department of Theoretical Physics, The University, Manchester 13, England.

(1) E. Wolf: *Nuovo Cimento*, **12**, 884 (1954).

(2) E. Wolf: *Nuovo Cimento*, **13**, 1165 (1959).

(3) E. Wolf: *Contr. in Proc. Symposium on Astronom. Optics* (Amsterdam, 1956), p. 177.

(4) G. B. Parrent and P. Roman: *Nuovo Cimento*, **15**, 370 (1960).

(5) P. Roman and E. Wolf: *Nuovo Cimento*, **17**, 462 (1960).

which govern the space-time behavior of the aforementioned correlation tensors. In a subsequent paper ([6]) we generalized these results to the case when the field is coupled to random-stationary charge and current sources. In this case the coupled field equations became second-order partial differential equations.

In another paper ([7]) we pointed out that the basic first-order field equations (for the case of free fields) can be cast into a form which resembles an equation of continuity. More precisely, by suitably combining the basic field equations, several classes of conservation laws can be obtained. These laws refer directly to the various correlation tensors but, when going to the limiting case of coinciding space points and no time-shift, two of these laws go over into the time-averaged form of the conventional energy conservation and momentum conservation laws. But, of course, the laws obtained in ([7]) are much more general and experimentally accessible relations. We even found some laws which do not have a « classical » limit.

The aim of the present paper is to derive further conservation laws which are completely different in character and scope from those obtained in ([7]). They are actually conservation laws referring to bilinear contractions of the correlation tensors, and contain therefore fourth-order products of the electric and magnetic fields.

Before deriving these conservation laws we first recall the relevant basic results of ([5]) and ([7]).

The electromagnetic correlation tensors have been defined as follows:

$$
\left\{
\begin{aligned}
&\mathscr{E}_{jk}(\boldsymbol{x}_1, \boldsymbol{x}_2, \tau) = \langle E_j(\boldsymbol{x}_1, t+\tau)\, E_k^*(\boldsymbol{x}_2, t)\rangle\,, \\
&\mathscr{H}_{jk}(\boldsymbol{x}_1, \boldsymbol{x}_2, \tau) = \langle H_j(\boldsymbol{x}_1, t+\tau) H_k^*(\boldsymbol{x}_2, t)\rangle\,, \\
&\mathscr{G}_{jk}(\boldsymbol{x}_1, \boldsymbol{x}_2, \tau) = \langle E_j(\boldsymbol{x}_1, t+\tau) H_k^*(\boldsymbol{x}_2, t)\rangle\,, \\
&\tilde{\mathscr{G}}_{jk}(\boldsymbol{x}_1, \boldsymbol{x}_2, \tau) = \langle H_j(\boldsymbol{x}_1, t+\tau)\, E_k^*(\boldsymbol{x}_2, t)\rangle\,.
\end{aligned}
\right. \tag{1.1}
$$

Here H_j and H_k are the *analytic signals* associated with the corresponding field and $\langle \ldots \rangle$ denotes time averaging over t. The tensors (1.1) satisfy the symmetry relations

$$
\left\{
\begin{aligned}
&\mathscr{E}_{jk}^*(\boldsymbol{x}_1, \boldsymbol{x}_2, \tau) = \mathscr{E}_{kj}(\boldsymbol{x}_2, \boldsymbol{x}_1, -\tau)\,, \\
&\mathscr{H}_{jk}^*(\boldsymbol{x}_1, \boldsymbol{x}_2, \tau) = \mathscr{H}_{kj}(\boldsymbol{x}_2, \boldsymbol{x}_1, -\tau)\,, \\
&\tilde{\mathscr{G}}_{jk}^*(\boldsymbol{x}_1, \boldsymbol{x}_2, \tau) = \mathscr{G}_{kj}(\boldsymbol{x}_2, \boldsymbol{x}_1, -\tau)\,.
\end{aligned}
\right. \tag{1.2}
$$

Besides these basic quantities we shall also use the energy coherence tensor

([6]) P. ROMAN: *Nuovo Cimento*, **20**, 759 (1961). See also: Scientific Report no. 1, contract no. AF 19(604)-8022, March 1961.

([7]) P. ROMAN and E. WOLF: *Nuovo Cimento*, **17**, 477 (1960).

and the flow coherence tensor

$$\begin{cases} \mathscr{W}_{jk}(\boldsymbol{x}_1, \boldsymbol{x}_2, \tau) = \mathscr{E}_{jk}(\boldsymbol{x}_1, \boldsymbol{x}_2, \tau) + \mathscr{H}_{jk}(\boldsymbol{x}_1, \boldsymbol{x}_2, \tau) , \\ \mathscr{S}_{jk}(\boldsymbol{x}_1, \boldsymbol{x}_2, \tau) = \mathscr{G}_{jk}(\boldsymbol{x}_1, \boldsymbol{x}_2, \tau) - \tilde{\mathscr{G}}_{jk}(\boldsymbol{x}_1, \boldsymbol{x}_2, \tau) . \end{cases} \tag{1.3}$$

The basic field equations satisfied by the correlation tensors (1.1) are

$$\varepsilon_{jkl}\partial_k^1 \mathscr{E}_{lm} + \frac{1}{c}\frac{\partial}{\partial\tau}\tilde{\mathscr{G}}_{jm} = 0 , \tag{1.4a}$$

$$\varepsilon_{jkl}\partial_k^1 \tilde{\mathscr{G}}_{lm} - \frac{1}{c}\frac{\partial}{\partial\tau}\mathscr{E}_{jm} = 0 , \tag{1.4b}$$

$$\varepsilon_{jkl}\partial_k^1 \mathscr{H}_{lm} - \frac{1}{c}\frac{\partial}{\partial\tau}\mathscr{G}_{jm} = 0 , \tag{1.4c}$$

$$\varepsilon_{jkl}\partial_k^1 \mathscr{G}_{lm} + \frac{1}{c}\frac{\partial}{\partial\tau}\mathscr{H}_{lm} = 0 . \tag{1.4d}$$

As a consequence of these equations, the $\mathscr{W}$ and $\mathscr{S}$ tensors satisfy

$$\varepsilon_{jkl}\partial_k^1 \mathscr{W}_{lm} - \frac{1}{c}\frac{\partial}{\partial\tau}\mathscr{S}_{jm} = 0 , \tag{1.5a}$$

$$\varepsilon_{jkl}\partial_k^1 \mathscr{S}_{lm} + \frac{1}{c}\frac{\partial}{\partial\tau}\mathscr{W}_{jm} = 0 . \tag{1.5b}$$

In the following we shall imitate the tecnhiques by which one usually obtains the energy conservation law in the conventional Maxwell theory. In this manner we shall get a great number of laws. Considering the eq. (1.4), we can combine (*a*–*b*), (*a*–*c*), (*a*–*d*), (*b*–*c*), (*b*–*d*), (*c*–*d*) to get a couple of conservation laws in each case, but some of them are contained in the others. Equations (1.5*a*) amd (1.5*b*) give another couple of conservation laws.

2. – The first class of conservation laws.

Let us multiply eq. (1.4*a*) by $\tilde{\mathscr{G}}_{jm}$ and eq. (1.4*b*) by $-\mathscr{E}_{jm}$. Upon addition we then have

$$\varepsilon_{jkl}\tilde{\mathscr{G}}_{jm}\partial_k \mathscr{E}_{lm} - \varepsilon_{jkl}\mathscr{E}_{jm}\partial_k \tilde{\mathscr{G}}_{lm} = -\frac{1}{2c}\frac{\partial}{\partial\tau}(\mathscr{E}_{jm}\mathscr{E}_{jm} + \tilde{\mathscr{G}}_{jm}\tilde{\mathscr{G}}_{jm}) . \tag{2.1}$$

(For the sake of brevity, from now on we write simply ∂_k instead of the more precise notation ∂_k^1.)

The left hand side of eq. (2.1) can be cast into the form of a divergence. To this end, let us change, in the first term, the dummy indices according to $j \to l$, $l \to k$, $k \to j$; and in the second term according to $j \to k$, $k \to j$. We then obtain for the left hand side

$$\varepsilon_{ljk}\,\tilde{\mathcal{G}}_{lm}\partial_j\mathcal{E}_{km} - \varepsilon_{kjl}\mathcal{E}_{km}\partial_j\tilde{\mathcal{G}}_{lm} = \varepsilon_{jkl}\partial_j(\mathcal{E}_{km}\tilde{\mathcal{G}}_{lm})\,,$$

where use has been made of the antisymmetry of ε_{jkl}. Putting this back into (2.1), we arrive at our first conservation law

$$\partial_j(\varepsilon_{jkl}\mathcal{E}_{km}\,\tilde{\mathcal{G}}_{lm}) + \frac{\partial}{\partial\tau}\left[\frac{1}{2c}\,(\mathcal{E}^2 - \tilde{\mathcal{G}}^2)\right] = 0\,. \tag{2.2}$$

where, for the sake of brevity, we have written simply $\mathcal{E}^2$ for $\mathcal{E}_{jm}\mathcal{E}_{jm}$ and likewise $\tilde{\mathcal{G}}^2$ for $\mathcal{G}_{jm}\mathcal{G}_{jm}$. (We shall also use the same shorthand notation for complete contractions in what follows.)

Proceeding in a manner exactly analogous with eqs. (1.4*c*) and (1.4*d*), we obtain

$$\partial_j(\varepsilon_{jkl}\,\mathcal{G}_{km}\mathcal{H}_{lm}) + \frac{\partial}{\partial\tau}\left[\frac{1}{2c}\,(\mathcal{G}^2 + \mathcal{H}^2)\right] = 0\,. \tag{2.3}$$

We remark that, actually, this second conservation law can be formally obtained from (2.2) by performing the replacements

$$\mathcal{E} \rightleftarrows -\mathcal{H}\,, \qquad \mathcal{G} \rightleftarrows \tilde{\mathcal{G}}\,, \tag{2.4}$$

under which the basic set (1.4) is invariant, as has been pointed out in [5].

Next we multiply eq. (1.4*a*) by $\mathcal{H}_{jm}$ and (1.4*c*) by $-\mathcal{E}_{jm}$, obtaining on addition

$$\varepsilon_{jkl}\partial_j(\mathcal{E}_{km}\mathcal{H}_{lm}) = -\frac{1}{c}\left(\mathcal{H}_{jm}\frac{\partial}{\partial\tau}\,\tilde{\mathcal{G}}_{jm} + \mathcal{E}_{jm}\frac{\partial}{\partial\tau}\,\mathcal{G}_{jm}\right). \tag{2.5}$$

Now the left hand side is already a divergence, but we must reformulate the right hand side. In fact, in our shorthand notation,

$$\mathcal{E}\,\frac{\partial}{\partial\tau}\,\mathcal{G} \equiv \frac{\partial}{\partial\tau}\,(\mathcal{G}\mathcal{E}) - \mathcal{G}\,\frac{\partial}{\partial\tau}\,\mathcal{E}\,, \tag{2.6a}$$

$$\mathcal{H}\,\frac{\partial}{\partial\tau}\,\tilde{\mathcal{G}} \equiv \frac{\partial}{\partial\tau}\,(\tilde{\mathcal{G}}\mathcal{H}) - \tilde{\mathcal{G}}\,\frac{\partial}{\partial\tau}\,\mathcal{H}\,. \tag{2.6b}$$

Now we use (1.4*b*) to express the second term on the right in (2.6*a*), and (1.4*d*)

to express the second term on the right in (2.6*b*). Then the right hand side of eq. (2.5) can be written as

$$-\frac{1}{c}\frac{\partial}{\partial\tau}(\mathcal{G}\mathcal{E}+\tilde{\mathcal{G}}\mathcal{H})-\varepsilon_{jkl}(\mathcal{G}_{jm}\partial_k\tilde{\mathcal{G}}_{lm}-\tilde{\mathcal{G}}_{jm}\partial_k\mathcal{G}_{lm})\,.$$

In order to cast the second term into the form of a divergence, we have only to make suitable changes in the notation of the dummy indices and to utilize the antisymmetry of ε_{jkl}. Then, substituting back into (2.5), we eventually obtain the conservation law

$$\partial_j[\varepsilon_{jkl}(\mathcal{E}_{km}\mathcal{H}_{lm}+\tilde{\mathcal{G}}_{km}\mathcal{G}_{lm})]+\frac{\partial}{\partial\tau}\left[\frac{1}{c}(\mathcal{G}\mathcal{E}+\tilde{\mathcal{G}}\mathcal{H})\right]=0\,. \tag{2.7}$$

In order to get the next conservation law, we multiply (1.4*a*) by $\mathcal{G}_{jm}$ and (1.4*d*) by $\mathcal{E}_{jm}$. Then, applying algebraic manipulations similar to those discussed above and using (1.4*b*) and (1.4*c*) to eliminate disturbing terms, we obtain

$$\partial_j[\varepsilon_{jlk}(\mathcal{H}_{lm}\tilde{\mathcal{G}}_{km}+\mathcal{G}_{lm}\mathcal{E}_{km})]+\frac{\partial}{\partial\tau}\left[\frac{1}{c}(\mathcal{E}\mathcal{H}+\mathcal{G}\tilde{\mathcal{G}})\right]=0\,. \tag{2.8}$$

No further laws can be obtained along these lines: combination of (1.4*b*) and (1.4*c*) leads again to (2.8), whereas combination of (1.4*b*) and (1.4*d*) gives merely the sum of (2.2) and (2.3).

As has been pointed out in [7], the $\mathcal{W}$ and $\mathcal{S}$ fields have a more appealing physical interest than the basic $\mathcal{E}$, $\mathcal{H}$, $\mathcal{G}$, $\tilde{\mathcal{G}}$ fields. Hence, it will be desirable to deduce higher order conservation laws involving $\mathcal{W}$ and $\mathcal{S}$. Indeed, applying the same simple technique to (1.5*a*) and (1.5*b*) as has been used to obtain (2.2), we easily obtain the interesting conservation law

$$\partial_j[\varepsilon_{jkl}\mathcal{W}_{lm}\mathcal{S}_{km}]+\frac{\partial}{\partial\tau}\left[\frac{1}{2c}(\mathcal{S}^2+\mathcal{W}^2)\right]=0\,. \tag{2.9}$$

Since $\mathcal{W}$ and $\mathcal{S}$ are linear combinations of the basic fields, (2.9) could have been obtained, as a matter of fact, by suitably combining the basic conservation laws listed above.

3. – The second class of conservation laws.

Further, non-equivalent, conservation laws can be obtained if we use as multiplying factors not the fields themselves, but rather their complex conju-

gates. Thus, for example, multiplying (1.4*a*) by $\tilde{\mathcal{G}}^*_{jm}$ and (1.4*b*) by $-\mathcal{E}^*_{jm}$, we obtain after some simple manipulations, very similar to those described above, the new conservation law

$$\partial_j[\varepsilon_{jkl}(\tilde{\mathcal{G}}^*_{lm}\mathcal{E}_{km}+\mathcal{E}^*_{km}\tilde{\mathcal{G}}_{lm})]+\frac{\partial}{\partial\tau}\left[\frac{1}{c}(\tilde{\mathcal{G}}^*\mathcal{G}+\mathcal{E}^*\mathcal{E})\right]=0\,. \tag{3.1}$$

Similarly, from (1.4*c*) and (1.4*d*) we obtain

$$\partial_j[\varepsilon_{jkl}(\mathcal{G}^*_{km}\mathcal{H}_{lm}+\mathcal{G}_{km}\mathcal{H}^*_{lm})]+\frac{\partial}{\partial\tau}\left[\frac{1}{c}(\mathcal{G}^*\mathcal{G}-\mathcal{H}^*\mathcal{H})\right]=0\,. \tag{3.2}$$

Likewise, from (1.4*a*) and (1.4*c*) we get the somewhat more complicated law

$$\partial_j[\varepsilon_{jkl}(\mathcal{E}^*_{km}\mathcal{H}_{lm}+\mathcal{E}_{km}\mathcal{H}^*_{lm}+\tilde{\mathcal{G}}^*_{km}\mathcal{G}_{lm}+\tilde{\mathcal{G}}_{km}\mathcal{G}^*_{lm})]+ \tag{3.3}$$
$$+\frac{\partial}{\partial\tau}\left[\frac{1}{c}(\mathcal{G}^*\mathcal{E}+\mathcal{G}\mathcal{E}^*+\tilde{\mathcal{G}}^*\mathcal{H}+\tilde{\mathcal{G}}\mathcal{H}^*)\right]=0\,.$$

Also (1.4*a*) and (1.4*d*) yield a similar looking law

$$\partial_j[\varepsilon_{jlk}(\mathcal{G}_{lm}\mathcal{E}^*_{km}+\mathcal{E}_{lm}\mathcal{G}^*_{km}+\mathcal{H}_{lm}\mathcal{G}^*_{km}+\mathcal{H}^*_{lm}\tilde{\mathcal{G}}_{km})]+ \tag{3.4}$$
$$+\frac{\partial}{\partial\tau}\left[\frac{1}{c}(\mathcal{E}^*\mathcal{H}+\mathcal{E}\mathcal{H}^*+\mathcal{G}^*\tilde{\mathcal{G}}+\mathcal{G}\mathcal{G}^*)\right]=0\,.$$

The other possible pairs of equations do not give new conservation laws. But (1.5*a*) and (1.5*b*) can be processed to give

$$\partial_j[\varepsilon_{jkl}(\mathcal{W}^*_{lm}\mathcal{S}_{km}+\mathcal{W}_{lm}\mathcal{S}^*_{km})]+\frac{\partial}{\partial\tau}\left[\frac{1}{c}(\mathcal{S}\mathcal{S}^*+\mathcal{W}\mathcal{W}^*)\right]=0\,. \tag{3.5}$$

4. – Conclusion.

We have seen that by considering the field eqs. (1.4) and (1.5) as natural generalizations of the Maxwell equations, and that by applying customary techniques to them, we are led, in a systematic way, to the independent higher order conservation laws (2.2), (2.3), (2.7), (2.8) as well as (3.1), (3.2), (3.3) (3.4). We further obtained the particularly symmetric and presumably more important laws (2.9) and (3.5), which are actually suitable combinations of the previous ones.

The conservation laws relate space and time derivatives of operationally defined observables. Further investigations will have to clarify their deeper physical significance and the various ways in which they may be utilized in practice.

RIASSUNTO (*)

Imitando le ben note tecniche per ottenere l'equazione energetica nella teoria di Maxwell, si trovano otto leggi di conservazione indipendenti di ordine superiore per le varie funzioni di correlazione di secondo ordine associate con campi magnetici stazionari casuali. Si deducono due ulteriori leggi di conservazione, che coinvolgono il tensore di coerenza dell'energia, così significativo dal punto di vista fisico, ed il tensore di coerenza del flusso.

(*) *Traduzione a cura della Redazione.*

On the Diffusion of an Electric Field in a Collisionless Plasma (*).

F. Engelmann, M. Feix (**), E. Minardi and J. Oxenius

Groupe de Recherche de l'Association Euratom-C.E.A. - Fontenay-aux-Roses (Seine)

(ricevuto il 9 Settembre 1961)

Summary. — By means of the linearized Vlasov equation the propagation of an electric field in a one-dimensional collisionless plasma is studied using a temporally and spatialy localized perturbation as an experimentally realizable initial condition. The asymptotic behaviour for large times of the so excited electric field turns out to be independent of the special velocity distribution function which may give rise to Landau damping or not. On the other hand, around the perturbation centre a zone whose size increases as $t^{\frac{1}{2}}$ is established, in which the amplitude of the electric field, oscillating with plasma frequency, is spatially almost constant and decreases in time as $t^{-\frac{1}{2}}$, thus showing essential characteristics of a diffusion process.

Introduction.

In the present paper a plasma consisting of electrons moving in a fixed background of ions is considered. The plasma is assumed to be infinite and initially uniform; only electrostatic forces are taken into account. Our purpose is to study the Vlasov-Landau problem for a class of macroscopic initial conditions corresponding to certain well defined experiments (Section 1). In a linearized approximation different initial velocity distributions without and with cut-off at a maximum electron velocity are considered. First, a single k-component of the spatial Fourier expansion of the electric field is investigated

(*) A summary of this paper was communicated at the Conference on Plasma Physics and Controlled Nuclear Fusion Research, Salzburg, 4-9 September 1961 (Ref. CN-10/102).

(**) On leave of absence at General Atomic, San Diego, Cal.

(Section 2). Ordinary Landau damping is recovered for small k. In the case of a cut-off distribution it happens that undamped oscillations appear which are very sensitive to the way of cutting off. Because of the different group velocities of small and large k-components one finds that the front of the signal propagating from a localized perturbation gathers all small wave lengths (Section 3), which are, however, smoothed out when macroscopic conditions are considered. On the other hand, the asymptotic time behaviour of the electric field in the region around the initial perturbation follows the laws of ordinary diffusion superposed to a fast oscillation with plasma frequency. Then only small k yield a contribution in this zone and all results are independent of the particular velocity distribution, irrespectively whether it gives rise to Landau damping or not. The appearance in a collisionless theory of a diffusion effect due to collective interactions suggests that by a proper choice of the macroscopic framework the Vlasov equation may be susceptible of leading to important transport coefficients.

1. – The initial conditions in the Landau-Vlasov problem.

It may be doubtful whether the Vlasov equation, which implies the one-particle distribution function f_1 only, is well adapted to describe all details of the space and time behaviour of a plasma. As a consequence one should remain in the frame of macroscopic situations when using it. On the other hand, it has already been noted by some authors, *e.g.* [1-3], that in this context a proper choice of initial conditions plays a central rôle. It is therefore our aim to study by means of the Vlasov equation the response of a plasma to a well defined external macroscopic excitation.

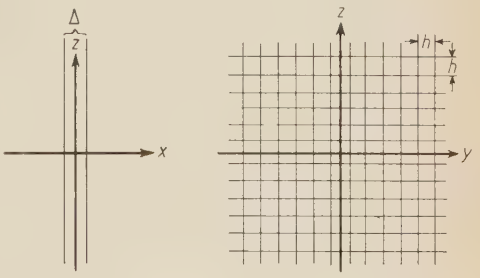

Fig. 1. – Experimental device for creating the plasma perturbation.

There are only two experimental possibilities of such a macroscopic excitation: first, by a beam of particles, where a difficult boundary problem arises, and secondly, by the application of an electric field. In this case we can think of the following possible experimental device: we consider in a plasma two infinite parallel plane grids with a distance Δ and a wire diameter Φ, h being the distance between two wires (see Fig. 1). Let

[1] L. D. Landau: *Žurn. Èksp. Teor. Fiz.*, **10**, 25 (1946).
[2] N. G. van Kampen: *Physica*, **21**, 949 (1955).
[3] N. G. van Kampen: *Physica*, **23**, 641 (1957).

$\Phi \ll h \ll \Delta$ so that the two grids, from an electrical point of view, form a plane condenser allowing, however, the electrons to pass through freely. Between the two grids we establish an electric field E^e during the time τ. The problem is thus one-dimensional. Now we consider the limit $\Delta \to 0$, $\tau \to 0$ and $E^e \to \infty$ such that $E^e \tau \Delta = K$. In a linearized theory, this signal plays a central rôle since any arbitrary signal $E^e(x, t)$ can be written

$$E^e(x, t) = \iint_{x_0\, t_0} E^e(x_0, t_0)\, \delta(x - x_0)\, \delta(t - t_0)\, \mathrm{d}x_0\, \mathrm{d}t_0 \,. \tag{1}$$

Let now be $F(v)$, supposed normalized ($\int F \mathrm{d}v = 1$) and even ($F(-v) = F(v)$), the electron velocity distribution function before the perturbation. The distribution function after the perturbation applied at $t = 0$ is then

$$f_1(x, v, 0) = F(v) + \delta f(x, v, 0)$$

with $\int \delta f \mathrm{d}v = 0$. From the above mentioned initial condition one calculates simply in a linear approximation

$$\delta f(x, v, 0) = \begin{cases} -\dfrac{eE^e\tau}{m} \dfrac{\mathrm{d}F}{\mathrm{d}v}\,, & \text{for } -\dfrac{\Delta}{2} < x < \dfrac{\Delta}{2}, \\ 0\,, & \text{elsewhere,} \end{cases}$$

($e =$ charge, $m =$ mass of electrons).

With this special form of δf one gets by means of the linearized Vlasov equation as the Fourier-Laplace transform of the electric field the simple expression

$$2\pi E(k, x) = -\frac{1 - H(k, s)}{H(k, s)}\,, \tag{2}$$

with

$$H(k, s) = 1 + i\,\frac{\omega_p^2}{k} \int \frac{(\mathrm{d}F/\mathrm{d}v)\, \mathrm{d}v}{s - ikv}\,,$$

($\omega_p =$ plasma frequency).

We have put $k = 1$ which does not restrict generality in any way.

2. – Treatment of a single Fourier component of the electric field.

The treatment of a single Fourier component as due to LANDAU [1] is based on an analytic continuation of $H(k, s)$ to the left half plane of s, implying the knowledge of $F(v)$ for a complex v, which is physically meaningless. Moreover

the number of poles and their contribution to $E(k, t)$ depends very sensitively on the behaviour of $F(r)$ for $|v| \to \infty$. In order to avoid these difficulties, other methods have been proposed, *e.g.* by VAN KAMPEN [3] and BUNEMAN [4].

To compute $E(k, t)$ we integrate eq. (2) with respect to s along the straight line $s = \varepsilon + i\omega$, where $\varepsilon > 0$. Supposing that there are no singularities in the right half plane, *i.e.* that no instabilities occur, we may consider the limit $\varepsilon \to 0$ and we find

$$(3a) \qquad (2\pi)^2 E(k, t) = \lim_{\varepsilon \to 0} \int_{-\infty - i\varepsilon}^{+\infty - \varepsilon i} \frac{1 - H(k, \omega)}{H(k, \omega)} \exp[i\omega t] \, \mathrm{d}\omega \,,$$

with

$$(3b) \qquad H(k, \omega) = 1 + \frac{\omega_p^2}{k} P \int \frac{(\mathrm{d}F/\mathrm{d}v) \, \mathrm{d}v}{\omega - kv} + i\pi \frac{\omega_p^2}{k^2} \left(\frac{\mathrm{d}F}{\mathrm{d}v} \right)_{v = \omega/k}$$

(P indicates the principal value of the integral). From this formula one can now easily derive some known results concerning $E(k, t)$.

2·1. *The Landau damping for a distribution without cut-off.* – With the hypothesis that there are no zeros of $H(k, \omega)$ on the real ω-axis eq. (3*a*) can be written

$$(4) \qquad (2\pi)^2 E(k, t) = \int_{-\infty}^{+\infty} \frac{1 - H(k, \omega)}{H(k, \omega)} \exp[i\omega t] \, \mathrm{d}\omega \,.$$

Noting that one can put

$$\frac{1 - H(\omega)}{H(\omega)} = L(\omega) + iM(\omega) \,,$$

where L and M are an even and an odd function of ω respectively and tha $E(k, t)$ as represented by the integral (4) vanishes for negative values of t, one obtains for $t > 0$

$$(2\pi)^2 E(k, t) = \int_{-\infty}^{+\infty} [L(\omega) + iM(\omega)] \exp[i\omega t] \, \mathrm{d}\omega =$$

$$= 2 \int_{-\infty}^{+\infty} L(\omega) \exp[i\omega t] \, \mathrm{d}\omega = 2i \int_{-\infty}^{+\infty} M(\omega) \exp[i\omega t] \, \mathrm{d}\omega \,.$$

(4) O. BUNEMAN: *Phys. Rev.*, **112**, 1504 (1958).

The last expression is particularly convenient and gives

$$2\pi E(k,t) = -i\frac{\omega_p^2}{k^2}\int_{-\infty}^{+\infty} \frac{(\mathrm{d}F/\mathrm{d}v)_{v=\omega/k}\exp[i\omega t]\,\mathrm{d}\omega}{\left[1+\frac{\omega_p^2}{k}P\int_{-\infty}^{+\infty}\frac{(\mathrm{d}F/\mathrm{d}v)\,\mathrm{d}v}{\omega-kv}\right]^2+\pi^2\frac{\omega_p^4}{k^4}\left(\frac{\mathrm{d}F}{\mathrm{d}v}\right)^2_{v=\omega/k}} . \tag{5}$$

Landau's well-known damping effect [1] is obtained from this equation in the limit of small k. In this limit one has a resonance at a frequency ω_k given by

$$1+\frac{\omega_p^2}{k}P\int_{-\infty}^{+\infty}\frac{(\mathrm{d}F/\mathrm{d}v)\,\mathrm{d}v}{\omega_k-kv}=0 , \tag{6}$$

which is just the dispersion relation given by LANDAU. Around the resonance the integral (5) has the form

$$\int\frac{B\exp[i\omega t]\,\mathrm{d}\omega}{A^2(\omega-\omega_k)^2+B^2} ,$$

and a variation $\exp[i\omega_k t]\exp[-\gamma_k t]$ is obtained with γ_k given by

$$\gamma_k=\frac{\pi}{2}\omega_k\frac{\omega_p^2}{k^2}\left|\frac{\mathrm{d}F}{\mathrm{d}v}\right|_{v=\omega_k/k}\left(1-\frac{\mathrm{d}\omega_k/\mathrm{d}k}{\omega_k/k}\right). \tag{7}$$

This result has also been derived by JACKSON [5].

2·2. *Distributions with cut-off.* – We suppose $F(v)=0$ for $|v|>a$. This case gives in general rise to undamped oscillations of the electric field, as has been pointed out by VAN KAMPEN [3]. The poles of the integrand in eq. (3*a*) are given by the zeros of $H(k,\omega)$. Let us consider the case $\omega/k>a$. In this domain the imaginary part of H vanishes and these poles are therefore determined by eq. (6) which is a relation $\omega=\omega(k)$. Only those k are in accordance with the condition $\omega>ka$ which are smaller than k_m, which is given by $\omega(k_m)=k_m a$ or

$$k_m^2=-\omega_p^2\int_{-a}^{+a}\frac{(\mathrm{d}F/\mathrm{d}v)\,\mathrm{d}v}{a-v} . \tag{8}$$

Two different cases can occur. If $(\mathrm{d}F/\mathrm{d}v)_{v=a}\neq 0$ (« abrupt » cut-off) the in-

[5] J. D. JACKSON: *Journ. Nucl. Energy*, Part C, **1**, 171 (1960).

tegral in eq. (8) diverges and one gets undamped waves for all wave lengths. For large k the dispersion relation is $\omega_k \approx ka$. However, if $(\mathrm{d}F/\mathrm{d}v)_{v=a} = 0$ (« soft » cut-off) we get undamped waves for wave numbers going from 0 to k_m where $0 < k_m \leqslant \infty$ depending on the particular behaviour of $\lim_{v \to a} \mathrm{d}F/\mathrm{d}v$.

One can see from the preceding results that by cutting off a distribution function at a maximum velocity a considerable ambiguity is introduced in the time evolution of the Fourier component $E(k, t)$. On the other hand, both the position and the shape of the cut-off has no physical significance provided that the cut-off velocity is sufficiently larger than the root mean square (r.m.s.) velocity, since in this region important fluctuations occur. We perceive, however, that an abrupt cut-off gives always rise to undamped oscillations.

In particular, for small k ordinary Landau damping (exponential decrease of wave amplitudes) is recovered; however, it is not only very weak but also its validity is limited because of the possible appearance of undamped wave modes with phase velocities greater than the maximum particle velocity a. For large k, one can show, starting from eq. (3), that the amplitudes of the eventually appearing undamped waves are very small for distributions cut off at a velocity much greater than the r.m.s. velocity; the other wave modes are so rapidly damped that even the concept of an exponentially damped wave is no more valid, as was pointed out by JACKSON [5]. Moreover, in the here adopted macroscopic framework for the Vlasov equation, the undamped modes correspond for large k to so fine a space and time structure that they yield no contribution when a really macroscopic—and not a δ-shaped excitation in the sense of eq. (1) is assumed. Then Fourier components $E(k, t)$ of the electric field corresponding to large k are not significant here.

In order to overcome the remaining ambiguity concerning small wave numbers we must proceed to an integration over k.

3. – The diffusion of the electric field.

The electric field $E(x, t)$ is obtained by performing the Fourier transformation of eq. (3). We begin with the special case of a rectangular distribution

$$F(v) = \begin{cases} \dfrac{1}{2a}, & \text{for } -a < v < a, \\ 0, & \text{elsewhere,} \end{cases}$$

for which all calculations can be rigorously carried out. Furthermore, this distribution is of particular interest because there is no Landau damping for any wave number. We shall see later that all essential results are independent of this special choice of the distribution function.

From eq. (3) one has then after a simple calculation

$$2\pi E(k,t) = -\frac{\omega_p^2}{\omega_k}\sin\omega_k t\,, \qquad \text{with } \omega_k^2 = \omega_p^2 + a^2k^2, \tag{9}$$

and by Fourier inversion

$$E(x,t) = \begin{cases} -\dfrac{\omega_p^2}{2a} J_0\left(\omega_p\sqrt{t^2-\dfrac{x^2}{a^2}}\right), & \text{for } |x|<at, \quad (10a) \\ 0\,, & \text{for } |x|>at, \quad (10b) \end{cases}$$

(J_0 is the Bessel function of order zero). We note from eq. (10b) that the propagation velocity of the perturbation front is the maximum velocity of the electrons. For $t \gg \omega_p^{-1}$ and $|x| \ll at$ one derives from eq. (10a) the asymptotic form

$$E^{as}(x,t) = -\frac{\omega_p}{\sqrt{2\pi\zeta t}}\cos\left(\omega_p t - \frac{x^2}{2\zeta t} - \frac{\pi}{4}\right), \tag{11}$$

with $\zeta = a^2/\omega_p$. $E(x,t)$ as a function of x for a given value of t is plotted in Fig. 2.

In the zone $|x| \ll at$ the temporally asymptotic behaviour of the electric field is essentially given by a fast oscillation with frequency ω_p and an amplitude decreasing proportionally to $t^{-\frac{1}{2}}$. The extension of the region where the electric field is nearly independent of x increases like $t^{\frac{1}{2}}$. At a distance of the order of magnitude of at a microstructure appears which becomes finer and finer with time, the distance between two adjacent zeros being of the order $a/(\omega_p^2 t)$. In consequence, the influence of the large wave numbers is concentrated just behind the wave front. We must therefore, if we want to remain within a macroscopic framework, limit our discussion to the region $|x| \ll at$ where the asymptotic form (11) is valid. The spatial structure expressed by the distance between two adjacent zeros here always exceeds the Debye length D (defined as the ratio r.m.s. velocity divided by ω_p). The temporal decrease of the amplitude of the oscillating electric field found in this zone is exclusively caused by wave mixing.

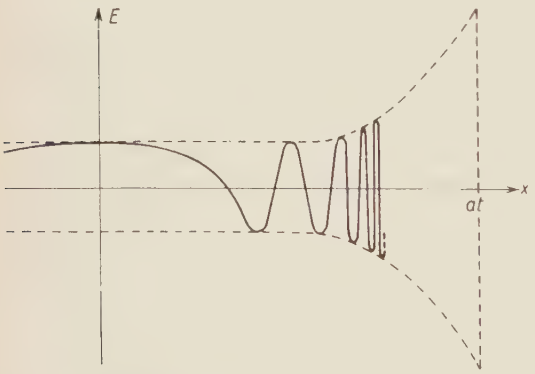

Fig. 2. Spatial dependence of the electric field $E(x,t)$ for given t in the case of a rectangular distribution function $F(v)$.

In order to separate the fast and the slow variation of the electric field with respect to time we calculate now the spatial moments of $E^{as}(x, t)$

$$M_n^{as}(t) = \int_{-\infty}^{+\infty} x^n E^{as}(x, t)\, dx .$$

One gets

$$M_n^{as}(t) = -\omega_p \sin\left(\omega_p t - n\frac{\pi}{4}\right)\cdot \mu_n(t) , \tag{12}$$

where the $\mu_n(t)$ are the moments of order n of the Gaussian distribution, *i.e.*

$$\mu_n(t) = \int_{-\infty}^{+\infty} x^n G(x, t)\, dx ,$$

with

$$G(x, t) = \frac{1}{(2\pi\zeta t)^{\frac{1}{2}}} \exp\left(-\frac{x^2}{2\zeta t}\right) .$$

The slow variation is now contained in the factors $\mu_n(t)$ and the fast one in a sinusoidal function oscillating with plasma frequency. The function G is known to describe the diffusion of initially δ-shaped perturbations like that, for example, of particles due to Brownian motion. The slow variation of $E(x, t)$ may thus be associated with a kind of diffusion of the electric field, caused by collective interactions. In particular, the electric field in the region where its amplitude is nearly constant in space shows precisely a diffusion-like behaviour. Indeed, as before-mentioned, this region extends like $\sqrt{\zeta t}$ whereas the amplitude of the field decreases like $1/\sqrt{2\pi\zeta t}$.

In the zone $\sqrt{\zeta t} < |x| \ll at$ a spatial structure of the electric field occurs which is connected with the propagation of the excited macroscopic wave modes, *i.e.* with $k \ll D$ [1]. However, the diffusion aspects persists for the spatial mean values.

As already mentioned, all these results remain valid for any distribution function $F(v)$. The only differences appear in the microstructured wave front. We shall discuss in the following the asymptotic behaviour of the electric field for large times in the general case. It has been seen in the preceding section that for this purpose only the Fourier components corresponding to small wave numbers are important. The integral in eq. (3*a*) is therefore determined by the poles given by eq. (6) which for $k \ll \omega_p/\sqrt{3\overline{r^2}}$ yields the well-known dispersion relation ($\overline{v^2}$ = mean square velocity)

$$\omega_k^2 = \omega_p^2 + 3\overline{v^2}k^2 .$$

By applying the residue theorem to the poles $\omega = \pm\omega_k$ one obtains

$$E(k, t) = -\frac{\omega_k}{2\pi}\sin\omega_k t\,. \tag{13}$$

We calculate now

$$E(x, t) = -\frac{1}{2\pi}\int_{-\hbar}^{+\hbar}\omega_k \sin\omega_k t\,\exp\left[-ikx\right]\mathrm{d}x\,,$$

with an $\hbar \ll \omega_p/\sqrt{3\overline{v^2}}$. Since the essential dependence on k of the integrand comes from the sinusoidal function, ω_k can be replaced by ω_p outside this function. Hence, using the dispersion relation in the linearized approximation $\omega_k = \omega_p + (3\overline{v^2}k^2/2\omega_p)$, one derives

$$E(x, t) = -\frac{\omega_p}{2\pi}\left\{\frac{\sin\omega_p t}{2}\left[\int_{-\hbar}^{+\hbar}\cos\left(\tfrac{1}{2}\zeta t k^2 + kx\right)\mathrm{d}k + \int_{-\hbar}^{+\hbar}\cos\left(\tfrac{1}{2}\zeta t k^2 - kx\right)\mathrm{d}k\right] + \right.$$

$$\left. + \frac{\cos\omega_p t}{2}\left[\int_{-\hbar}^{+\hbar}\sin\left(\tfrac{1}{2}\zeta t k^2 + kx\right)\mathrm{d}k + \int_{-\hbar}^{+\hbar}\sin\left(\tfrac{1}{2}\zeta t k^2 - kx\right)\mathrm{d}k\right]\right\},$$

where now $\zeta = 3\overline{v^2}/\omega_p$. The further mathematical problem concerns the evaluation of integrals of the type

$$I = \int_{-\hbar}^{+\hbar}\exp\left[i\left(\tfrac{1}{2}\zeta t k^2 \mp kx\right)\right]\mathrm{d}k\,.$$

With the new variable $\xi = \sqrt{\zeta t}\,\left(k \mp (x/\zeta t)\right)$ one has

$$I = \exp\left(\frac{-ix^2}{2\zeta t}\right)\cdot\frac{1}{\sqrt{\zeta t}}\int_{-\hbar\zeta t \mp (x/\sqrt{\zeta t})}^{\hbar\zeta t \mp (x/\sqrt{\zeta t})}\exp\left(\frac{i}{2}\xi^2\right)\mathrm{d}\xi\,.$$

In the asymptotic limit $t \gg \omega_p^{-1}$ and for the region $|x| \ll t\sqrt{3\overline{v^2}}$ one can integrate between the limits $\mp\infty$ and the value of the integral in the preceding expression is $\sqrt{\pi}(1 - i)$. The asymptotic form of the electric field is then

$$E^s(x, t) = -\frac{\omega_p}{\sqrt{2\pi\zeta t}}\cos\left(\omega_p t - \frac{x^2}{2\zeta t} - \frac{\pi}{4}\right). \tag{11'}$$

This expression is just equal to the asymptotic form (11) of the electric field found in the case of a rectangular distribution function. Thus the asymptotic behaviour of the electric field is shown to be independent of the distribution function and all results obtained above for the rectangular distribution are valid in general, irrespectively whether the distribution function gives rise to Landau damping or not. On the contrary, Landau damping will affect the region just behind the wave front, eventually damping out contributions of large wave numbers, *i.e.* the microstructure. We note that in the particular case of distribution functions with abrupt cut-off, we need the supplementary condition $k \ll \omega_p/a$ for the derivation of the used dispersion relation. The validity of our results is then restricted to $t \gg (a^2/3\overline{v^2})\omega_p^{-1}$ and $|x| \ll (3\overline{v^2}/a)t$. This means that the region of validity is the same as before when the cut-off velocity a is of the order of $\sqrt{3\overline{v^2}}$. Such a value of a cuts the distribution function certainly in its fluctuating tail.

Finally, we should like to indicate a property of the temporally integrated electric field. By calculating

$$\int_0^\infty E(x, t)\,\mathrm{d}t = \int_0^\infty \mathrm{d}t \int_{-\infty}^{+\infty} \mathrm{d}k\, E(k, t) \exp\left[-ikx\right],$$

where $E(k, t)$ is given by eq. (3) one obtains

$$\int_0^\infty E(x, t)\,\mathrm{d}t = -\frac{1}{2L} \exp\left[-\frac{|x|}{L}\right], \tag{14}$$

with

$$\frac{1}{L^2} = -\omega_p^2 \int \frac{(\mathrm{d}F/\mathrm{d}v)\,\mathrm{d}v}{v}, \tag{15}$$

provided that $L^2 > 0$.

For a Maxwellian distribution one has $L = D$. A temporally integrating measure of the electric field exhibits then a kind of shielding of the initial perturbation characterized by the Debye length. For a general distribution function eq. (15) can also be written

$$\frac{1}{L^2} = -\omega_p^2 \int \frac{F(v) - F(0)}{v^2}\,\mathrm{d}v\,. \tag{16}$$

If we limit ourselves to the class of symmetric distribution functions with at most one minimum we may compare the preceding expression with the electrostatic stability criterion of PENROSE ([6]). Then one sees that those dis-

tributions which lead to $L^2 > 0$ are just the stable ones. The limit of stability corresponds to $L \to \infty$, *i.e.* to the vanishing of the « shielding » effect.

Moreover, spatial integration of eq. (14) shows that

$$\int_{-\infty}^{+\infty} \mathrm{d}x \int_{0}^{\infty} \mathrm{d}t \, [E(x, t) + E^{e}(x, t)] = 0 \, ,$$

where $E^{e}(x, t)$ represents the initially δ-shaped perturbing electric field. This relation is likewise valid for an arbitrary perturbation $E^{e}(x, t)$, provided that the linear approximation holds.

(6) O. PENROSE: *Phys. of Fluids*, **3**, 256 (1960).

RIASSUNTO

Mediante l'equazione linearizzata di Vlasov si studia la propagazione di un campo elettrico in un plasma unidimensionale e senza collisioni assumendo come condizione iniziale sperimentalmente realizzabile una perturbazione spazialmente e temporalmente localizzata. Il comportamento temporale asintotico del campo elettrico così eccitato risulta indipendente dalla forma particolare della funzione di distribuzione delle velocità, che può dare origine o no ad uno smorzamento di Landau. D'altra parte attorno al centro della perturbazione si stabilisce una zona la cui estensione aumenta proporzionalmente a $t^{\frac{1}{2}}$ nella quale l'ampiezza del campo elettrico, oscillante con la frequenza del plasma, si mantiene quasi costante nello spazio e diminuisce col tempo come $t^{-\frac{1}{2}}$ mostrando così gli aspetti essenziali di un fenomeno di diffusione.

IL NUOVO CIMENTO Vol. XXII, N. 5 1° Dicembre 1961

A Relativistic Scattering Model Satisfying Unitarity, Crossing Symmetry and Analyticity.

N. N. Khuri (*)

CERN - Geneva

(ricevuto il 14 Settembre 1961)

Summary. — A model is constructed which can generate a class of scattering amplitudes that have the same analytic properties as conventional perturbation theory, are crossing symmetric, and satisfy the unitarity condition in the elastic region in all three channels. The model consists of a non-linear off-shell integral equation whose solution gives a different amplitude for each different first order term or « generalized potential » that one starts with. The main new condition on these « potentials » is that they cannot have elastic cuts in any channel. The relation of this model to the problem of the uniqueness of the Chew-Mandelstam program is discussed.

1. – Introduction.

Recently, in an effort to by-pass the difficulties of conventional field theory, attempts have been made to construct scattering amplitudes from the unitarity conditions, the condition of crossing symmetry, and the analytic properties of the usual Feynman diagrams. Such a program was first initiated by Chew and Mandelstam [1] and has been applied by several authors [2] to problems of strong interactions.

(*) Permanent address: Physics Department, American University of Beirut, Beirut, Lebanon.

(1) G. F. Chew and S. Mandelstam: *Phys. Rev.*, **119**, 467 (1960).

(2) For a complete list of references see G. F. Chew: *Double dispersion relations and unitarity as the basis for a dynamical theory of strong interactions*, published in the book *Dispersion Relations* edited by G. R. Screaton (Edinburgh, 1961).

This general approach is based on the assumption that for moderate energies the nearest singularities dominate the behaviour of the amplitude. This means that in the unitarity conditions one takes only the contributions from one- and two-particle terms. Indeed, in their treatment of the pion-pion problem, CHEW and MANDELSTAM only make use of the two-particle elastic unitarity relation and neglect all inelastic contributions.

The other starting point of the Chew-Mandelstam program, namely that of analyticity, is usually expressed by the Mandelstam representation. However, the validity of the Mandelstam representation is not necessary for the Chew-Mandelstam approach. The only requirement, in view of the assumption concerning the nearby singularities, is that any extra singularities not exhibited by the Mandelstam representation should not lie near the low energy region and could be neglected with the inelastic singularities.

It would be interesting to investigate the uniqueness of amplitudes determined by the three starting points of CHEW and MANDELSTAM: elastic unitarity, crossing symmetry, and the analytic properties of perturbation theory. If these conditions do not uniquely determine a scattering amplitude, one would like to see explicitly the nature of the non-uniqueness in the hope of finding out what other physical information is needed to determine a scattering amplitude.

In this paper we shall obtain a model for the scattering of two neutral bosons of equal mass. This model can generate an infinite set of scattering amplitudes which:

i) are relativistically invariant,
ii) satisfy unitarity in the elastic region,
iii) are crossing symmetric,
iv) have the same analytic properties as the conventional Feynman graphs.

Our model consist of an off-shell non-linear integral equation for the scattering matrix element, which can generate by iteration a different scattering amplitude for each different first order term, *i.e.*, « potential », that one starts with.

Even though one obtains an infinite number of amplitudes, it is still true that the four conditions listed above are very restrictive, and they impose strong conditions on the « potentials » one can start with. It turns out that none of these potentials can have a cut in the elastic region (in our model below $16\,m^2$). One might argue that in view of the assumption about the nearest singularities, all these « potentials » are equivalent since they somehow represent inelastic effects. However, one can easily show that these potentials contribute to the Mandelstam spectral functions in the region of the elastic strip. Thus by taking very different potentials one can get very different

contributions to the Mandelstam weight functions in the strip. Even with the assumption about nearest singularities this non-uniqueness is real and has to be dealt with in any calculation.

In Section 2 we start with a Bethe-Salpeter type equation and then construct an equivalent non-linear off-shell equation whose structure is similar to that of unitarity. This non-linear equation is obtained by first constructing the total Green's function of the Bethe-Salpeter differential equation from a complete set of off-shell solutions of a certain off-shell generalization of the Bethe-Salpeter differential equation. The off-shell generalization needed turns out to be quite different from the obvious one and gives a novel off-shell two-particle propagator. The relation between this non-linear equation and unitarity is discussed.

In Section 3 a crossing symmetric amplitude is defined by a symmetrized generalization of the non-linear equation of Section 2. The form of the equation and the nature of the symmetrization process are such that unitarity in the elastic region is still valid if our generalized « potentials » have no elastic cuts.

2. – A non-linear Bethe-Salpeter equation.

We start by considering a relativistically invariant differential equation for two interacting, spinless and neutral particles of mass m. We write

$$(1) \qquad (\Box_1 - m^2)(\Box_2 - m^2)\Psi(x_1, x_2) = -\frac{i}{2} V(x_1, x_2) .$$

Here $V(x_1, x_2)$ is a relativistically invariant function of the difference of the two four vectors, $(x_1 - x_2)^2$, which will be defined in more detail below.

We consider solutions of (1) that satisfy the following integral equation

$$(2) \qquad \Psi_{p_1 p_2}(x_1, x_2) = \Phi_{p_1 p_2}(x_1, x_2) - \frac{i}{2}\int\!\!\int \mathrm{d}^4x_1' \, \mathrm{d}^4x_2' \Delta_c(x_1 - x_1') \Delta_c(x_2 - x_2') V(x_1', x_2') \Psi(x_1', x_2') ,$$

where Δ_c is the usual causal Green's function [3]

$$(3) \qquad \Delta_c(x) = -\frac{1}{(2\pi)^4}\int \mathrm{d}^4k \, \frac{\exp[ik\cdot x]}{k^2 - m^2 + i\varepsilon} ,$$

[3] Our causal function is related to the usual Feynman function by $\Delta_c = (i/2)\Delta_F$.

and

$$\Phi_{p_1p_2}(x_1, x_2) = \frac{1}{(2\pi)^4} \exp[-ip_1\cdot x_1] \exp[-ip_2\cdot x_2], \qquad p_1^2 = p_2^2 = m^2. \tag{4}$$

To define a scattering matrix element we get

$$T(p_1' p_2' | p_1 p_2) = (\Phi_{p_1' p_2'}, V\Psi_{p_1p_2}). \tag{5}$$

Here we also take $p_1'^2 = p_2'^2 = m^2$. We use the notation

$$T(p_1' p_2' | p_1 p_2) = T(s, t)\,\delta^4(p_1' + p_2' - p_1 - p_2), \tag{6}$$

with

$$s = (p_1 + p_2)^2; \quad t = (p_1 - p_1')^2; \quad u = (p_1 - p_2')^2. \tag{7}$$

From (5) and (2) it is very easy to obtain a linear integral equation of the Bethe-Salpeter type for T. One gets

$$T(p_1' p_2' | p_1 p_2) = U(p_1' p_2' | p_1 p_2) - \frac{i}{2}\int \mathrm{d}^4k_1\,\mathrm{d}^4k_2 \frac{U(p_1' p_2' | k_1 k_2)\,T(k_1 k_2 | p_1 p_2)}{(k_1^2 - m^2 + i\varepsilon)(k_2^2 - m^2 + i\varepsilon)}, \tag{8}$$

where

$$\begin{cases} U(p_1' p_2' | p_1 p_2) = U(t)\,\delta^4(p_1' + p_2' - p_1 - p_2), \\ U(t) = \dfrac{1}{(2\pi)^4}\displaystyle\int \exp[-i(p_1 - p_1')\cdot x]\,V(x)\,\mathrm{d}^4x. \end{cases} \tag{9}$$

The eq. (9) is not completely defined until we specify how we are going to define the off-shell $U(p_1' p_2' | k_1 k_2)$. In order to satisfy condition iv) and end up with a T with essentially the same analytic properties as in the usual perturbation theory, we restrict ourselves to « potentials » which are of the form

$$V(x_1, x_2) = \frac{(2\pi)^4}{\pi}\int_{4m^2}^{\infty} \sigma(\mu^2)\,\Delta_c(\mu^2 | x_1 - x_2)\,\mathrm{d}\mu^2, \tag{10}$$

where σ is real. Using (3) and (9) we get

$$\begin{cases} U(q_1 q_2 | k_1 k_2) = U\big((q_1 - k_1)^2\big)\,\delta^4(q_1 + q_2 - k_1 - k_2), \\ U\big([q_1 - k_1]^2\big) = -\dfrac{1}{\pi}\displaystyle\int_{4m^2}^{\infty} \frac{\sigma(\mu^2)}{(q_1 - k_1)^2 - \mu^2 + i\varepsilon}\,\mathrm{d}\mu^2. \end{cases} \tag{11}$$

In this last equation any or all of the vectors q_1, q_2, k_1, k_2 could be off the mass shell. In (10) and (11) we have neglected to put pole terms just to simplify the writing. They can be included without changing the essence of the arguments that follow in this section.

The iteration of (8) now leads to a series of ladder type diagrams of the form shown in Fig. 1 where the straight internal lines correspond to the usual Feynman propagators $(k^2 - m^2 + i\varepsilon)^{-1}$ and the curly lines correspond to $(k^2 - \mu^2 + i\varepsilon)^{-1}\sigma(\mu^2)$. The only difference between our diagrams and the usual Feynman diagrams is the final integration over the weight functions σ.

Fig. 1. – Diagrams generated by eq. (8).

The amplitude T defined by (8) satisfies the elastic unitarity condition for $4m^2 < s < 16m^2$ as it is the usual Bethe-Salpeter amplitude.

$$\text{(12)} \qquad \operatorname{Im} T(p_1' p_2' \mid p_1 p_2) - $$

$$= \frac{(2\pi)^2}{4} \int \mathrm{d}^4 q_1 \, \mathrm{d}^4 q_2 \, T(p_1' p_2' \mid q_1 q_2) \, T^*(p_1 p_2 \mid q_1 q_2) \, \delta(q_1^2 - m^2) \, \delta(q_2^2 - m^2) \, \theta(q_1) \, \theta(q_2) \, .$$

Here $\operatorname{Im} T$ is taken at fixed t. If (11) has a pole term at $(q_1 - k_1)^2 = m^2$ then (12) is only valid for $4m^2 < s < 9m^2$, otherwise if U is represented as in (11) then (12) is valid at least for $4m^2 < s < 16m^2$.

To define a crossing symmetric scattering amplitude one can easily crossing symmetrize (8) and obtain a linear equation that will define a new T which is crossing symmetric. However, this new amplitude will not, in general, satisfy unitarity any more. To avoid this difficulty and still be able to construct a unitary crossing symmetric amplitude, we choose to work with a non-linear equation which is equivalent to (8) but whose structure is more similar to that of unitarity. We can obtain such an equation by first constructing the total Green's function of eq. (1) from a complete set of off-shell solutions of (1).

We consider the following off-shell generalization of (1),

$$\text{(13)} \qquad (\Box_1 - m^2)(\Box_2 - m^2) \Psi_{k_1 k_2}(x_1, x_2) - (m^2 - k_1^2)(m^2 - k_2^2) \Psi_{k_1 k_2}(x_1, x_2) =$$

$$= -\frac{i}{2} V(x_1, x_2) \Psi_{k_1 k_2}(x_1, x_2) \, .$$

When $k_1^2 = k_2^2 = m^2$, this equation obviously reduces to (1). The choice of this off-shell generalization instead of the obvious one, *i.e.*

$$(\Box_1 - k_1^2)(\Box_2 - k_2^2) \Psi_{k_1 k_2} + \frac{i}{2} V \Psi_{k_1 k_1} = 0 \, ,$$

is necessary if one wants to construct the total Green's function of (1) from the off-shell Ψ's in a way analogous to ordinary potential scattering.

As in (2), we take solutions of (13) which satisfy the following integral equation

$$(14)\qquad \Psi_{k_1k_2}(x_1, x_2) = \Phi_{k_1k_2}(x_1, x_2) - \frac{i}{2}\int\!\!\int \mathrm{d}^4x_1'\,\mathrm{d}^4x_2' K(k_1^2k_2^2|x_1-x_1', x_2-x_2')\,V(x_1', x_2')\Psi_{k_1k_2}(x_1', x_2'),$$

where the off-shell propagator K is given by

$$(15)\qquad K(k_1^2k_2^2|x_1-x_1', x_2-x_2') = \frac{1}{(2\pi)^8}\int \mathrm{d}^4q_1\,\mathrm{d}^4q_2\,\frac{\exp[iq_1\cdot(x_1-x_1')]\exp[iq_2\cdot(x_2-x_2')]}{[(q_1^2-m^2+i\varepsilon_1)(q_2^2-m^2+i\varepsilon_1)-(k_1^2-m^2+i\varepsilon_2)(k_2^2-m^2+i\varepsilon_2)]}.$$

The choice of sign of the $i\varepsilon_2$ in the second term in the denominator will be explained later on. Nevertheless, it is still obvious that

$$K(m^2m^2|x_1-x_1'; x_2-x_2') = \Delta_c(x_1-x_1')\,\Delta_c(x_2-x_2').$$

Thus eq. (14) reduces to (2) when $k_1^2 = k_2^2 = m^2$ and $\varepsilon_2 \to 0$. The function $\Phi_{k_1k_2}$ in (114) is just a product of two plane waves as in (4) and for any k_1 and k_2 is a solution of the homogeneous off-shell equation

$$(16)\qquad [(\Box_1-m^2)(\Box_2-m^2)-(m^2-k_1^2)(m^2-k_2^2)]\Phi_{k_1k_2}(x_1, x_2) = 0.$$

In order to express the Green's function of (1) in terms of an expansion of products of eigenfunctions the usual procedure has to be slightly modified since the differential operator we are dealing with, $D \equiv (\Box_1-m^2)(\Box_2-m^2)+(i/2)V$, is not hermitian. We rewrite (13) in an abstract form

$$(13')\qquad D\Psi_\alpha = \alpha\Psi_\alpha,$$

where $\alpha = (m^2-k_1^2)(m^2-k_2^2)$. The operator D^* has the following set of eigenstates

$$(17)\qquad D^*\tilde{\Psi}_\beta = \beta\tilde{\Psi}_\beta.$$

Here we choose solutions of (17) that satisfy the following integral equation

$$(18)\qquad \tilde{\Psi}_{k_1k_2}(x_1, x_2) = \Phi_{k_1k_2}(x_1, x_2) + \frac{i}{2}\int\!\!\int K(k_1^2k_2^2|x_1-x_1', x_2-x_2')\,V^*(x_1', x_2')\tilde{\Psi}_{k_1k_2}(x_1', x_2')\,\mathrm{d}^4x_1'\,\mathrm{d}^4x_2'.$$

Now it is an elementary matter to show that $\tilde{\Psi}_\beta$ and Ψ_α are orthogonal when $\alpha \neq \beta$, *i.e.* $\int \tilde{\Psi}^*_\beta \Psi_\alpha \, \mathrm{d}^4x_1 \, \mathrm{d}^4x_2 = 0$, and $\tilde{\Psi}$ and Ψ form a bi-orthogonal set of functions [4]. One should notice from (18) that $\tilde{\Psi}$ is not Ψ^*. The total Green's functions for (13) can now be written as

$$(19) \qquad G_{k_1k_2}(x_1x_2 \,|\, y_1y_2) =$$

$$= \int \mathrm{d}^4k_1' \, \mathrm{d}^4k_2' \frac{\Psi_{k_1'k_2'}(x_1, x_2) \, \tilde{\Psi}^*_{k_1'k_2'}(y_1, y_2)}{[(k_1'^2 - m^2 + i\varepsilon_1)(k_2'^2 - m^2 + i\varepsilon_1) - (k_1^2 - m^2 - i\varepsilon_2)(k_2^2 - m^2 - i\varepsilon_2)]} .$$

The total Green's function for (1) is obtained from (19) by setting $k_1^2 = k_2^2 = m^2$ and letting $\varepsilon_2 \to 0$. The Green's function defined in (19) is a solution of the following equation

$$(20) \qquad \left[(\Box_1 - m^2)(\Box_2 - m^2) + \frac{i}{2} V\right] G_{k_1k_2} - (m^2 - k_1^2)(m^2 - k_2^2) G_{k_1k_2} =$$

$$= \delta^4(x_1 - y_1) \, \delta^4(x_2 - y_2) .$$

Here one uses the completeness of the off-shell Ψ's which can be written as

$$(21) \qquad \iint \mathrm{d}^4k_1' \, \mathrm{d}^4k_2' \Psi_{k_1'k_2'}(x_1, x_2) \tilde{\Psi}^*_{k_1'k_2'}(y_1, y_2) = \delta^4(x_1 - y_1) \, \delta^4(x_2 - y_2) .$$

With the help of (19) one can formally write down the solution of (14)

$$(22) \qquad \Psi_{k_1k_2}(x_1, x_2) -$$

$$= \Phi_{k_1k_2}(x_1, x_2) - \frac{i}{2} \iint \mathrm{d}^4y_1 \, \mathrm{d}^4y_2 G_{k_1k_2}(x_1x_2 \,|\, y_1y_2) \, V(y_1, y_2) \, \Phi_{k_1k_2}(y_1, y_2) .$$

Similarly, one can construct the Green's function $\tilde{G}$ for (17) which will be given by the same formula as (19) with Ψ and $\tilde{\Psi}$ interchanged. One obtains for the solutions of (18) the following

$$(23) \qquad \tilde{\Psi}_{k_1k_2}(x_1, x_2) =$$

$$= \Phi_{k_1k_2}(x_1, x_2) + \frac{i}{2} \iint \mathrm{d}^4y_1 \, \mathrm{d}^4y_2 \tilde{G}_{k_1k_2}(x_1, x_2 \,|\, y_1, y_2) \, V^*(y_1, y_2) \, \Phi_{k_1k_2}(y_1, y_2) .$$

One can now define the following two off-shell matrix elements

$$(24) \qquad \begin{cases} T(q_1q_2 \,|\, k_1k_2) = (\Phi_{q_1q_2}, V\Psi_{k_1k_2}) , \\ \tilde{T}(q_1q_2 \,|\, k_1k_2) = (\tilde{\Psi}_{k_1k_2}, V\Phi_{q_1q_2}) . \end{cases}$$

[4] For a more detailed discussion of the Green's function of a non-hermitian operator see P. M. Morse and H. Feshbach: *Methods of Theoretical Physics* (New York, 1953), pp. 884-886.

From (14) and (18) and the definitions (24) we find that T and $\tilde{T}$ satisfy the following two linear integral equations, which are off-shell generalizations of (8).

$$(25)\qquad T(q_1q_2|k_1k_2) = -U(q_1q_2|k_1k_2) - \frac{i}{2}\iint \mathrm{d}^4k_1'\,\mathrm{d}^4k_2'\,K(k_1'^2k_2'^2,\ \varepsilon_1\ k_1^2k_2^2,\ \varepsilon_2)\,U(q_1q_2\ k_1'k_2')\,T(k_1'k_2'|k_1k_2)\,.$$

$$(26)\qquad \tilde{T}(q_1q_2|k_1k_2) = -U(k_1k_2|q_1q_2) - \frac{i}{2}\iint \mathrm{d}^4k_1'\,\mathrm{d}^4k_2'\,K^*(k_1'^2k_2'^2,\ \varepsilon_2\ k_1^2k_2^2,\ \varepsilon_1)\,U(k_1'k_2'\ q_1q_2)\,\tilde{T}(k_1'k_2'\ k_1k_2)\,.$$

The propagator $K(k_1'^2k_2'^2,\ \varepsilon_1/k_1^2k_2^2,\ \varepsilon_2)$ is just the Fourier transform of that given in (15) and is given by

$$(27)\qquad K(k_1'^2k_2'^2,\ \varepsilon_1|k_1^2k_2^2,\ \varepsilon_2) = [(k_1'^2 - m^2 + i\varepsilon_1)(k_2'^2 - m^2 + i\varepsilon_1) - (k_1^2 - m^2 - i\varepsilon_2)(k_2^2 - m^2 - i\varepsilon_2)]^{-1}\,.$$

Clearly, $K(k_1'^2k_2'^2,\ \varepsilon_1|m^2m^2)$ reduces to the product of two Feynman propagators as $\varepsilon_2 \to 0$. The relabelling of ε_1 and ε_2 in the kernel of eq. (26) is just for later convenience and has no significance at the present stage.

The non-linear equations we are seeking follow immediately from the definitions (24) if one substitutes in them the expressions (22) and (23) for Ψ and $\bar{\Psi}$ making use of (19). One obtains

$$(28)\qquad T(q_1'q_2'|q_1q_2) = -U(q_1'q_2'|q_1q_2) - \frac{i}{2}\iint \mathrm{d}^4k_1\,\mathrm{d}^4k_2\,T(q_1'q_2'|k_1k_2)\,\tilde{T}(q_1q_2\ k_1k_2)\,K(k_1^2k_2^2,\ \varepsilon_1\ q_1^2q_2^2,\ \varepsilon_2)\,,$$

and

$$(29)\qquad \tilde{T}(q_1'q_2'|q_1q_2) = U(q_1q_2|q_1'q_2') - \frac{i}{2}\iint \mathrm{d}^4k_1\,\mathrm{d}^4k_2\,\tilde{T}(q_1'q_2'|k_1k_2)\,T(q_1q_2\ k_1k_2)\,K^*(k_1^2k_2^2,\ \varepsilon_2|q_1^2q_2^2,\ \varepsilon_1)\,.$$

The system of equations given above is completely equivalent to (25) and (26), and when the q's are all on the mass shell (28) and (29) are equivalent to the Bethe-Salpeter equation, (8), that we started with. Superficially, however, it seems that an iteration of (28) and (29), even in the case when all the q's are on the mass shell, will involve the use of the off-shell propagators K, while the iteration of (8) will have nothing but the usual Feynman propagators. For what follows it will be instructive for us to check explicitly at this stage

that the two iterations are equivalent in lowest orders. That they are equivalent in first and second order is obvious, and the first non-trivial case will be third order. The third order term in the iteration of (28) and (29) is

$$
\begin{aligned}
(30)\qquad & T^{(3)}(q_1'q_2'|q_1q_2) = \\
& -\frac{1}{4}\int U(q_1'q_2'|k_1'k_2')\,K(k_1'^2k_2'^2,\,\varepsilon_1|k_1^2k_1^2,\,\varepsilon_2)\,U(k_1'k_2'|k_1k_2)\,K(k_1^2k_2^2,\,\varepsilon_1|q_1^2q_2^2,\,\varepsilon_2)\cdot \\
& \qquad\cdot U(k_1k_2|q_1q_2)\,\mathrm{d}^4k_1\,\mathrm{d}^4k_2\;\mathrm{d}^4k_1'\,\mathrm{d}^4k_2' - \\
& -\frac{1}{4}\int U(q_1'q_2'|k_1k_2)\,K(k_1^2k_2^2,\,\varepsilon_1|q_1^2q_2^2,\,\varepsilon_2)\,U(k_1'k_2'|q_1q_2)\,K^*(k_1'^2k_2'^2,\,\varepsilon_2|k_1^2k_2^2,\,\varepsilon_1)\cdot \\
& \qquad\cdot U(k_1k_2|k_1'k_2')\,\mathrm{d}^4k_1\,\mathrm{d}^4k_2\,\mathrm{d}^4k_1'\,\mathrm{d}^4k_2'\,.
\end{aligned}
$$

In order to simplify this expression we need the following properties of the propagator K

$$
(31)\qquad K^*(k_1^2k_2^2,\,\varepsilon_1|k_1'^2k_2'^2,\,\varepsilon_2) = -K(k_1'^2k_2'^2,\,\varepsilon_2|k_1^2k_2^2,\,\varepsilon_1)\,,
$$

$$
\begin{aligned}
(32)\qquad & K(k_1'^2k_2'^2,\,\varepsilon_1|k_1^2k_2^2,\,\varepsilon_2)\,[K(k_1^2k_2^2,\,\varepsilon_1|q_1^2q_2^2,\,\varepsilon_2) - K(k_1'^2k_2'^2,\,\varepsilon_1|q_1^2q_2^2,\,\varepsilon_2)] = \\
& \qquad = K(k_1^2k_2^2,\,\varepsilon_1|q_1^2q_2^2,\,\varepsilon_2)\,K(k_1'^2k_2'^2,\,\varepsilon_1|q_1^2q_2^2,\,\varepsilon_2)\,.
\end{aligned}
$$

These equations follow immediately from the definition, (27), of K. We now interchange the integration variables k and k' in the second term of (30) and then use (31) and (32) to get

$$
\begin{aligned}
(33)\qquad & T^{(3)}(q_1'q_2'|q_1q_2) = \\
& -\frac{1}{4}\int U(q_1'q_2'|k_1'k_2')\,K(k_1'^2k_2'^2,\,\varepsilon_1|q_1^2q_2^2,\,\varepsilon_2)\,U(k_1'k_2'|k_1k_2)\,K(k_1^2k_2^2,\,\varepsilon_1|q_1^2q_2^2,\,\varepsilon_2)\cdot \\
& \qquad\cdot U(k_1k_2|q_1q_2)\,\mathrm{d}^4k_1\,\mathrm{d}^4k_2\,\mathrm{d}^4k_1'\mathrm{d}^4k_2'\,.
\end{aligned}
$$

This is exactly the same form as the iteration of the linear eq. (25) and when $q_1^2 = q_2^2 = m^2$ and $\varepsilon_2 \to 0$ the two propagators K in (33) reduce to products of ordinary Feynman propagators as in the iteration of (8). A similar reduction takes place in higher orders. At this stage it becomes clear why we chose the signs of the $i\varepsilon_2$ in (15) as we did, namely we wanted to guarantee that this reduction will take place. In doing this we were guided very much by the case of non-relativistic potential scattering where a similar non-linear off-shell equation exists which is equivalent to the linear Lippman-Schwinger equation. Essentially, the same kind of reduction takes place in potential scattering as that between (30) and (33).

In potential scattering the potentials are always real and the non-linear equation analogous to (28) and (29) gives immediately the unitarity condition.

In the present case the connection between unitarity and (28) and (29) is not immediately apparent. We shall turn to a discussion of this point.

When all four external momenta are on the mass shell (28) can be rewritten as

$$(28') \quad T(p_1'p_2'|p_1p_2) = U(p_1'p_2'|p_1p_2) - \\ -\frac{i}{2}\int \mathrm{d}^4k_1\mathrm{d}^4k_2\, T(p_1'p_2'|k_1k_2)\,\tilde{T}(p_1p_2|k_1k_2)(k_1^2 - m^2 + i\varepsilon)^{-1}(k_2^2 - m^2 + i\varepsilon)^{-1}.$$

Here we have relabelled ε_1 as ε. A similar equation holds for $\tilde{T}(p_1'p_2' \; p_1p_2)$. Now if we use the fact that $T(p_1'p_2'|p_1p_2) = T(p_1p_2 \; p_1'p_2')$ when all the p's are on the mass shell we obtain

$$(34) \quad T(p_1'p_2'|p_1p_2) - \tilde{T}(p_1'p_2'|p_1p_2) = -\frac{i}{2}\int \mathrm{d}^4k_1\,\mathrm{d}^4k_2\, T(p_1'p_2'|k_1k_2)\cdot$$

$$\cdot[(k_1^2 - m^2 + i\varepsilon)^{-1}(k_2^2 - m^2 + i\varepsilon)^{-1} - (k_1^2 - m^2 - i\varepsilon)^{-1}(k_2^2 - m^2 - i\varepsilon)^{-1}]\tilde{T}(p_1p_2|k_1k_2).$$

This last equation is not yet the usual unitarity condition but as we shall see below it is equivalent to it for $4m^2 < s < 16m^2$. Unitarity is concerned with the difference between $T^{(+)} = T$ and $T^{(-)}$, where $T^{(-)}$ is obtained by changing all the $+i\varepsilon$ in $T^{(+)}$ to $-i\varepsilon$. However, $\tilde{T}$, as we have defined it, is obtained from $T^{(+)}$ by changing $+i\varepsilon$ to $-i\varepsilon$ only in Feynman propagators corresponding to the straight internal lines in Fig. 1 and *not* changing the sign of the $i\varepsilon$ in the « potential » propagators corresponding to the curved lines of Fig. 1. Clearly then, for physical scattering and for « potentials » given by (11), $\tilde{T}$ is essentially the same as $T^{(-)}$ as long as $4m^2 < s < 16m^2$. Any singularities coming from cutting across a potential line will lie beyond $s = 16m^2$. One can now use the arguments of CUTKOSKY [5] and write, from (34) for $4m^2 < s < 16m^2$

$$(35) \quad T^{(+)} - T^{(-)} = -\frac{i}{2}\int \mathrm{d}^4k_1\,\mathrm{d}^4k_2\, T^{(+)}(p_1'p_2'|k_1k_2)\cdot$$

$$\cdot[(2\pi i)^2\,\delta(k_1^2 - m^2)\,\delta(k_2^2 - m^2)\,\theta(k_1^0)\,\theta(k_2^0)]\,T^{(-)}(p_1p_2|k_1k_2).$$

This last equation is just the unitarity condition.

3. – The crossing symmetric equation.

In this section we shall symmetrize the set of eq. (28) and (29) and obtain two equations which define a new amplitude that is both unitary and crossing

[5] R. E. CUTKOSKY: *Journ. Math. Phys.*, **1**, 429 (1960).

symmetric and still has the same analytic properties as the usual perturbation theory.

The symmetrization is easier if we take all our external momenta as ingoing momenta and consider

$$M(q_1 q_2 | q_3 q_4) \equiv M(q_i \cdot q_j)\, \delta^4(q_1 + q_2 + q_3 + q_4)\,. \tag{36}$$

In analogy to (28) we shall define M by the following non-linear equation

$$M(q_1 q_2 | q_3 q_4) = U(q_1 q_2 | q_3 q_4) + U(q_1 q_3 | q_2 q_4) + U(q_1 q_2 | q_4 q_3) - \\ - \frac{i}{2} \int \left\{ \frac{1}{8} \sum_{\text{perm}} M(q_1' q_2' | k_1 k_2)\, \widetilde{M}(-q_3', -q_4' | k_1 k_2) \right\} K(k_1^2 k_2^2, \varepsilon_1\ q_3^2 q_4^2, \varepsilon_2)\, \mathrm{d}^4 k_1\, \mathrm{d}^4 k_2\,, \tag{37}$$

where q_1', q_2', q_3', q_4' is a permutation of q_1, q_2, q_3, q_4 and we sum over all permutations of the external momenta. Here U is given by a slightly different notation than in the previous section. We take

$$U(q_1 q_2 | q_3 q_4) = U([q_1 + q_3]^2)\, \delta^4(q_1 + q_2 + q_3 + q_4)\,,$$

and $U((q_1 + q_3)^2)$ has the same form as in (11) except for the fact that, as we shall find out below, unitarity forces us in this case to have $\sigma(\mu^2) = 0$ for $\mu^2 < 16 m^2$. Similarly, $\widetilde{M}$ is defined by

$$\widetilde{M}(q_1 q_2 | q_3 q_4) = U(q_3 q_4 | q_1 q_2) + U(q_2 q_4 | q_1 q_3) + U(q_4 q_3 | q_1 q_2) - \\ - \frac{i}{2} \int \left\{ \frac{1}{8} \sum_{\text{perm}} \widetilde{M}(q_1' q_2' | k_1 k_2)\, M(-q_3', -q_4' | k_1 k_2) \right\} K^*(k_1^2 k_2^2, \varepsilon_2\ q_1^2 q_2^2, \varepsilon_1)\, \mathrm{d}^4 k_1\, \mathrm{d}^4 k_2\,. \tag{38}$$

It is clear that M as defined in (37) is not completely crossing symmetric since the q_3^2 and q_4^2 appearing in the propagator K are not permuted and summed over with the permutations. However, when M is on the mass shell and $q_i^2 = m^2$, then M defined by (37) is manifestly crossing symmetric. We have in that case for $p_i^2 = m^2$

$$M(p_1 p_2 | p_3 p_4) = U(p_1 p_2 | p_3 p_4) + U(p_1 p_3 | p_2 p_4) + U(p_1 p_2 | p_4 p_3) - \\ - \frac{i}{2} \int \left\{ \frac{1}{8} \sum_{\text{perm}} M(p_1' p_2' | k_1 k_2)\, \widetilde{M}(-p_3', -p_4' | k_1 k_2) \right\} \cdot \\ \cdot (k_1^2 - m^2 + i\varepsilon)^{-1} (k_2^2 - m^2 + i\varepsilon)^{-1}\, \mathrm{d}^4 k_1\, \mathrm{d}^4 k_2\,. \tag{39}$$

The fact that the K's are kept outside the sum over the permutations allows us in the iteration of (37) and (38) to carry through the same reduction of the K propagators as was done in the previous section in eqs. (30)–(33). The algebra is still the same and the products of K and K^* propagators will

appear in the same form in the iteration of (37) and (38) as in the iteration of (28) and (29). One can again check the reduction in lowest orders explicitly. Thus the iteration of (37) will reduce to terms that are composed of products of U's and ordinary Feynman propagators when all four external momenta are on the mass shell. Some of the crossing symmetric sets of diagrams generated by (37) are shown in Fig. 2, where the straight lines correspond to ordinary Feynman propagators $(k^2-m^2+i\varepsilon)^{-1}$ and the circles represent the potentials. Each circle corresponds to a propagator of the form $(q^2-\mu^2+i\varepsilon)^{-1}\sigma(\mu^2)$ joining two pairs of the four lines coming to the circle in one of three different ways. Except for the final integrations over the σ's our iteration leads to ordinary Feynman graphs, and the analytic properties of our amplitude M will be the same as the analytic properties of ordinary Feynman diagrams. The graphs that we obtain are such that in at least one of the three s, t, u channels a graph has at least one two-particle intermediate state. If one cuts the graph perpendicular to the internal lines representing this intermediate state one obtains two graphs that still belong to the set generated by (37). In this section we are using the notation

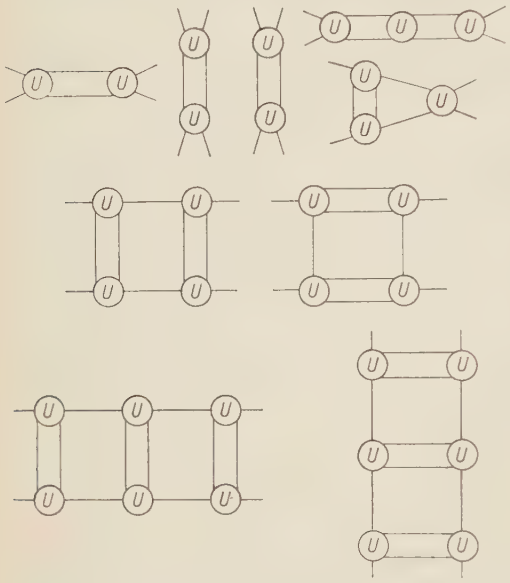

Fig. 2. – Diagrams generated by eq. (37).

$$s=(p_1+p_2)^2\,;\qquad t=(p_1+p_3)^2\,;\qquad u=(p_1+p_4)^2\,.$$

We are left now with the task of demonstrating that the symmetrization effected in this section does not violate unitarity in the elastic region. It is immediately apparent from (39) that the potentials U cannot have a cut below $16m^2$ if we want to satisfy unitarity in the physical s-channel for $4m^2<s<16m^2$. For since our first order term consists of a sum of $[U(t)+U(u)+U(s)]$ (after we take out the over-all δ-function), we would then have a contribution to $\mathrm{Im}\,M$ in first order in U which would be impossible to reconcile with unitarity. Hence we must restrict ourselves to U's that can be represented as

$$U(t)=-\frac{1}{\pi}\int_{16m^2}^{\infty}\frac{\sigma(\mu^2)}{t-\mu^2+i\varepsilon}\,\mathrm{d}\mu^2\,. \tag{11'}$$

A limiting case of these potentials would occur when the onset of the cut moves out to infinity; *i.e.*, $U(s)+U(t)+U(u)=\lambda$ where λ is just a constant. This would lead to g^4 type theory and the circles in the diagrams of Fig. 2 will collapse to points. Another way to avoid having first order contributions to Im M in the elastic region is to take U's that consist of pole terms with the position of the poles lying below $4m^2$. We shall not discuss these cases here for they are uninteresting for the pion-pion problem and also lead to a more complicated situation in higher orders.

By restricting ourselves to U's of the form given by (11′) we not only avoid difficulties with the first order contribution but are also able to avoid further difficulties in higher orders. The argument now runs as in the previous section and one obtains, in analogy to (34), from (37) and (38)

$$(40)\qquad M(p_1p_2|p_3p_4)-\widetilde{M}(p_1p_2|p_3p_4)=$$

$$=-\frac{i}{2}\int\left\{\frac{1}{8}\sum_{\text{perm}}M(p_1'p_2'|k_1k_2)\,\widetilde{M}(-p_3',-p_4'|k_1k_2)\right\}[(k_1^2-m^2+i\varepsilon)^{-1}(k_2^2-m^2+i\varepsilon)^{-1}-$$

$$-(k_1^2-m^2-i\varepsilon)^{-1}(k_2^2-m^2-i\varepsilon)^{-1}]\,\mathrm{d}^4k_1\,\mathrm{d}^4k_2\,,\qquad 4m^2<(p_1+p_2)^2<16m^2,$$

where all $p_i^2=m^2$; p_1', p_2', p_3', p_4' is a permutation of p_1, p_2, p_3, p_4; and the p's are in the physical region of the s-channel. The term in the straight bracket is the obviously zero when both k_1^2 and k_2^2 are off the mass shell. Now one again remarks that the only difference between $\widetilde{M}$ and $M^{(-)}$ is the sign of the $i\varepsilon$ in the potential propagators. Clearly, because of (11′) and the theorem of Cutkosky, the difference $M^{(+)}-\widetilde{M}$ and $M^{(+)}-M^{(-)}$ are the same form $4m^2<s<16m^2$. In other words, in finding contributions to singularities in the elastic region one, because of (11′), does not have to cut the potential lines. If we now again use the Cutkosky theorem [5] and replace the straight bracket term in (40) by a product of δ-functions we get the unitarity condition

$$(41)\qquad M^{(+)}(p_1p_2|p_3p_4)-M^{(-)}(p_1p_2|p_3p_4)=$$

$$=-\frac{i}{2}\int M^{(+)}(p_1p_2|k_1k_2)[(2\pi i)^2\delta(k_1^2-m^2)\,\delta(k_2^2-m^2)\theta(k_1^0)\theta(k_2^0)]\cdot$$

$$\cdot\,M^{(-)}(p_3p_4|k_1k_2)\,\mathrm{d}^4k_1\,\mathrm{d}^4k_2\,,\qquad 4m^2<s<16m^2.$$

All the permutations in (40) which lead to δ-functions of the form $\delta(p_1+p_3+k_1+k_2)$ and $\delta(p_1+p_4+k_1+k_2)$ drop out when k_1^2 and k_2^2 are on the mass shell since we are considering physical scattering in the s-channel and both $t=(p_1+p_3)^2$ and $u=(p_1+p_4)^2$ are negative. Only eight of the 4! permutations contribute equally and the factor $\frac{1}{8}$ gives us (41).

Similarly, by considering p_1, p_2, p_3, p_4 in the physical region of the t- and u-channels, respectively, one obtains equations analogous to (40) and (41) giving unitarity in the t-channel and the u-channel for $4m^2 < t < 16m^2$ and $4m^2 < u < 16m^2$, respectively.

The symmetrization exhibited in (37) and (38) does, of course, introduce diagrams which have intermediate states of four, six, eight or more particles. This is a necessary by-product of making the two-particle amplitudes crossing symmetric, and it does not affect the unitarity condition below $16m^2$ in any channel. It is clear, however, that our amplitude M violates unitarity for s, t, or u greater than $16m^2$, even if $\sigma(\mu^2)$ is zero beyond $16m^2$. One should also add here that in the present case one has to be much more careful in applying the Cutkosky theorem and going from (40) to (41) than in the similar argument of the previous section. To check that in going from (40) to (41) we made no errors, we make the following remark. The class of Feynman diagrams generated by (37) has the property that whenever one diagram is cut perpendicular to any two-particle intermediate state, one obtains two lower order diagrams which are also in the class generated by (37). Similarly, it is evident from the structure of (37) that if any two diagrams generated by (37) are fused together by joining a pair of external lines from each, the resulting higher order diagram will also belong to the class generated by (37). These properties would be enough to guarantee unitarity below $16m^2$ if the number (or multiplicity) of our diagrams is the same as in the usual perturbation theory. We have checked the multiplicity of our diagrams in lowest orders and they give the correct results consistent with unitarity and perturbation theory. That the multiplicity is consistent with elastic unitarity is clear since eq. (40) is similar enough to unitarity to guarantee at least that.

One final remark we can make here is that in writing down (37) and (38) one need to restrict himself to first order terms of the form $V(t) + V(s) + V(u)$. One can presumably start with any crossing symmetric function, $f(s, t, u)$, which satisfies the Mandelstam representation with a spectral function that vanishes whenever at least one of the variables is less than $16m^2$. This ensures that f has no elastic cuts. The off-shell « potential » f could then be obtained from the on-shell f by analytic continuation via the Mandelstam representation for f.

4. – Conclusions.

In their present form eq. (37) and (38) are not, to say the least, very useful for any direct calculation. In addition to their off-shell character they also generate diagrams which have the conventional divergences of ordinary per-

turbation theory. In principle, one can renormalize them by subtracting from (39) a similar equation for M evaluated at $s_0 = t_0 = u_0 = 4m^2/3$. In the case where $U(s)+U(t)+U(u) = \lambda$, *i.e.*, the φ^4 case, the potential will disappear in this subtraction and our new « coupling constant » will be $M(s_0, t_0, u_0)$ just as in the Chew-Mandelstam treatment of the pion-pion problem.

Nevertheless, the eq. (37) and (38) answer the question posed in the introduction concerning the uniqueness of a scattering amplitude determined from the four conditions listed in Section **1**. As we mentioned earlier, even though $\sigma(\mu^2) = 0$ for $\mu^2 < 16m^2$ still our « potentials » will contribute to the Mandelstam spectral functions in second order in U in the elastic strip. In other words for large enough s there is a contribution to $\varrho(s, t)$ in the region $4m^2 < t < 16m^2$, and similarly for large enough t there is a contribution to $\varrho(s, t)$ in the region $4m^2 < s < 16m^2$. It is clear that we can choose very different σ's that will generate quite different amplitudes. Thus, at least in the language of the present model, one must somehow determine σ by adding some extra conditions to the four listed in the introduction. Furthermore, we add here that if the Mandelstam representation is correct in perturbation theory (at least for the nearest singularities) then any set of equations derived from elastic unitarity and the Mandelstam representation such as those recently given by TER-MARTIROSYAN [6] and ZIMMERMANN [7] and the original equations of Chew and Mandelstam [1] do not have a unique solution. Any solution of (37) will be a solution of any of these equations.

In this connection, one can distinguish three different situations. The first would be that, as implied in the original approach to the pion-pion problem, the weight function $\sigma(\mu^2)$ is essentially zero even much beyond $\mu^2 = 16m^2$ and its exact form is not needed. In this case one has essentially the g^4 theory. However, in solving the Chew-Mandelstam equations one must make sure in this case that one picks the solution that corresponds to $\sigma(\mu^2) \sim 0$. The second situation would be that one would try to put more restrictions on $\sigma(\mu^2)$ by considering other physical conditions such as the idea of the saturation of the unitarity condition. The third situation would result if the short range effects are important. In that case one would have to put in more information and clearly one would not be able to construct the σ's from any « bootstrap » operation. In fact, we would be fortunate if just the σ's and the four conditions listed in the introduction are enough to describe the physical situation without the necessity of going into the details of four-particle intermediate states.

[6] K. A. TER-MARTIROSYAN: *Sov. Phys. JETP*, **12**, 575 (1961); see also *Nucl. Phys.*, **25**, 353 (1961).

[7] W. ZIMMERMANN: *Nuovo Cimento*, **21**, 36 (1961).

* * *

The author is grateful to CERN for its kind hospitality and support. This work was started at the Physics Department of the American University of Beirut, and he wishes to acknowledge a travel grant from the Research Committee of the Faculty of Arts and Sciences at the university. It is a pleasure to thank Dr. J. D. Bjorken for several helpful discussions.

RIASSUNTO (*)

Si costruisce un modello che può generare una classe di ampiezze di scattering che presentano le stesse proprietà analitiche che hanno nella convenzionale teoria della perturbazione, hanno simmetria incrociata e soddisfano la condizione di unitarietà nella regione elastica in tutt'e tre i canali. Il modello consiste in una equazione integrale non lineare off-shell, la cui soluzione dà un'ampiezza diversa per ciascuno dei diversi termini di primo ordine o « potenziali generalizzati » con cui si comincia. La principale condizione nuova per questi « potenziali » è che essi non possono avere tagli elastici in nessun canale. Si discute la relazione di questo modello con l'unicità del programma di Chew-Mandelstam.

(*) *Traduzione a cura della Redazione.*

IL NUOVO CIMENTO Vol. XXII, N. 5 1° Dicembre 1961

Convergence of the Perturbation Expansion in Some Models of the Field Theory.

I. Bialynicki-Birula (*)

University of Rochester - Rochester, N. Y.

W. M. Frank

U. S. Naval Ordnance Laboratory - Silver Spring, Md.

(ricevuto il 16 Settembre 1961)

Summary. — It is shown that in a class of models of the quantum field theory the perturbation expansion of the resolvent operator, $(H - z)^{-1}$, converges for all complex z. The class of models consists of all theories with Yukawa coupling in which the vacuum polarization has been neglected. The method used is that of comparison with the exactly solvable neutral scalar model.

The purpose of the present note is to discuss the convergence of the field-theoretic models in which vacuum polarization is absent and fermions interact with a meson field by means of a linear coupling. So little is known about the convergence of the perturbation expansion in a realistic field theory that the investigation of even such simple models may turn out to be of interest. We restrict ourselves to the investigation of the non-renormalized perturbation series and a cut-off function will be used extensively to make the perturbation expansion meaningful. We show that the perturbation series converges by comparing it with the exactly solvable neutral scalar theory (1). Our results apply in particular to the Chew-Low-Wick theory.

(*) Present address Warsaw University, Warsaw, Poland.

(1) One of us (W.M.F.) has developed another method of proving the convergence of models without vacuum polarization. A presentation of this method will be given elsewhere.

The proof of convergence will be carried over for a system described by the Hamiltonian

$$H = H_0 + H_{\mathrm{I}} = \int E(\boldsymbol{p}) \sum_r a_r^+(\boldsymbol{p}) a_r(\boldsymbol{p}) \, \mathrm{d}\boldsymbol{p} + \int \omega(\boldsymbol{k}) C^+(\boldsymbol{k}) C(\boldsymbol{k}) \, \mathrm{d}\boldsymbol{k} + \tag{1}$$

$$+ \frac{g}{(2\pi)^{\frac{3}{2}}} \int \frac{\mathrm{d}\boldsymbol{p} \, \mathrm{d}\boldsymbol{k} f(k)}{\sqrt{2E(\boldsymbol{p}) E(\boldsymbol{p}-\boldsymbol{k}) \omega(\boldsymbol{k})}} \left[\sum_{r,s} a_r^+(\boldsymbol{p}) \Gamma^{rs}(\boldsymbol{p}, \boldsymbol{k}) a_s(\boldsymbol{p}-\boldsymbol{k}) C(\boldsymbol{k}) - \text{h.c.} \right],$$

where

$$E(\boldsymbol{p}) = \sqrt{m^2 + \boldsymbol{p}^2} \qquad \text{and} \qquad \omega(\boldsymbol{k}) = \sqrt{\mu^2 + \boldsymbol{k}^2} \, .$$

The matrix $\Gamma^{rs}(\boldsymbol{p}, \boldsymbol{p})$ depends on the type of coupling. The generalization to the case of charged bosons is straightforward.

Let us consider the standard expression for the S operator,

$$S = T \exp \left[-i \int_{-\infty}^{\infty} H_{\mathrm{I}}(t) \, \mathrm{d}t \right] . \tag{2}$$

The matrix elements of S between the eigenstates $|E\rangle$, $|E'\rangle$ of the free Hamiltonian H_0 can be written in the form [2]

$$\langle E' | S | E \rangle = \langle E' | E \rangle - 2\pi i \, \delta(E - E') \langle E' | R_E | E \rangle \, , \tag{3}$$

where

$$R_E = H_{\mathrm{I}} - H_{\mathrm{I}} \frac{1}{H_0 - E - i\varepsilon} H_{\mathrm{I}} + H_{\mathrm{I}} \frac{1}{H_0 - E - i\varepsilon} H_{\mathrm{I}} \frac{1}{H_0 - E - i\varepsilon} H_{\mathrm{I}} - \ldots \, . \tag{4}$$

Because of the presence of energy shifts this simple formalism does not give correct answers to scattering problems. We are however concerned only with the *convergence* of the S matrix [3]. We will prove now the convergence of the series

$$\langle E'' | R_E | E' \rangle = \langle E'' | H_{\mathrm{I}} | E' \rangle - \langle E'' | H_{\mathrm{I}} \frac{1}{H_0 - E - i\varepsilon} H_{\mathrm{I}} | E' \rangle + \ldots \, , \tag{5}$$

[2] S. S. Schweber: *An Introduction to Relativistic Quantum Field Theory* (1961), p. 335.

[3] The convergence of the field-theoretic version of the scattering formalism will be discussed in another paper.

in the simplest non-trivial case; namely for the fermion propagator. The convergence of the power series (5) for more complicated matrix elements can be proved with the use of the same technique.

The n-th order term in (5) is the sum of the contributions from all diagrams. We can write it in the form

$$(6)\qquad \langle \boldsymbol{p}'' \,|\, R_E^{(n)} \,|\, \boldsymbol{p}' \rangle = \delta(\boldsymbol{p}' - \boldsymbol{p}'') \sum_{\text{all diagrams}} \frac{g^{2n}}{(2\pi)^{3n}} \int \frac{\mathrm{d}\boldsymbol{k}_1}{2\omega_1} \cdots \frac{\mathrm{d}\boldsymbol{k}_n}{2\omega_n} f(k_1) \ldots f(k_n) \cdot$$

$$\cdot \frac{m}{E(\boldsymbol{p}_n)} \cdots \frac{m}{E(\boldsymbol{p}_1)} \frac{\Gamma(\boldsymbol{p}_n, \boldsymbol{k}_n)}{E(\boldsymbol{p}_n) - \sum^{(n)} \omega_i - E - i\varepsilon} \cdots \frac{\Gamma(\boldsymbol{p}_1, \boldsymbol{k}_1)}{E(\boldsymbol{p}_1) - \sum^{(1)} \omega_i - E - i\varepsilon} .$$

Assuming E real and less than m we can easily find an upper bound for the expression (6),

$$(7)\qquad \left| \langle \boldsymbol{p}'' \,|\, R_E^{(n)} \,|\, \boldsymbol{p}' \rangle \right| \leqslant \delta(\boldsymbol{p}' - \boldsymbol{p}'') \sum_{\text{all diagrams}} \frac{g^{2n}}{(2\pi)^{3n}} \int \frac{\mathrm{d}\boldsymbol{k}_1 \bar{f}(k_1)}{2\omega_1 \left(m + \sum^{(1)} \omega_i - E \right)} \cdots$$

$$\cdots \frac{\mathrm{d}\boldsymbol{k}_n \bar{f}(k_n)}{2\omega_n \left(m + \sum^{(n)} \omega_i - E \right)} ,$$

where $\bar{f}(k)$ is so chosen that $\bar{f}(k) > 2 f(k) \,|\, \Gamma^{rs}(\boldsymbol{p}, \boldsymbol{k}) \,|\, m / E(\boldsymbol{p})$. The right-hand side of (7) is exactly the same as obtained by the perturbation expansion of the neutral scalar theory with fixed fermions. We know however that the perturbation expansion converges in that case since we know the exact solution [4], so that for negative values of energy E the perturbation series (5) converges. To prove the convergence of (5) for complex values of E, say z, we notice that

$$(8)\qquad \left| \frac{1}{E_i + \sum \omega_i - z} \right| \leqslant \left(1 + \left| \frac{E - z}{\operatorname{Im} z} \right| \right) \left| \frac{1}{E_i + \sum \omega_i - E} \right| ,$$

so that

$$(9)\qquad \left| \langle E'' \,|\, R_z^{(n)} \,|\, E' \rangle \right| \leqslant \left(1 + \left| \frac{E - z}{\operatorname{Im} z} \right| \right)^n \left| \langle E'' \,|\, R_E^{(n)} \,|\, E' \rangle \right| .$$

The perturbation expansion of R_z converges therefore for sufficiently small values of g provided $(E - z)/\operatorname{Im} z$ is finite. Our method does not allow us to prove convergence for real z greater than m. This was to be expected since in general there are singularities in this region.

[4] S. S. Schweber: loc. cit., p. 347.

* * *

The authors would like to acknowledge the hospitality of the Brandeis University Summer School on whose premises this work was discussed.

RIASSUNTO (*)

Si dimostra che in una classe di modelli della teoria quantistica dei campi lo sviluppo della perturbazione dell'operatore risolvente, $(H-2)^{-1}$, converge per tutti gli z complessi. La classe di modelli consiste di tutte le teorie con accoppiamento di Yukawa in cui la polarizzazione del vuoto è stata trascurata. Il metodo usato è quello di confronto con il modello scalare neutro esattamente risolubile.

(*) *Traduzione a cura della Redazione.*

IL NUOVO CIMENTO Vol. XXII, N. 5 1° Dicembre 1961

A New Limit to the Electric Dipole Moment of the Muon.

G. Charpak (*), F. J. M. Farley, R. L. Garwin (**), T. Muller (**), J. C. Sens and A. Zichichi

CERN - Geneva

(ricevuto il 18 Settembre 1961)

Summary. — By storing polarized positive muons in a magnetic field for as many as 1200 revolutions, a new upper limit to the electric dipole moment has been determined. The value is

$$\text{EDM} \leqslant (3 \pm 6) \cdot 10^{-5} \cdot \frac{eh}{mc} \qquad \text{or} \qquad \text{EDM} \leqslant e \cdot (0.6 \pm 1.1) \cdot 10^{-17} \text{ cm} ,$$

consistent with time-reversal invariance.

1. – Introduction.

In 1960 we reported an upper limit to the electric dipole moment (EDM) of the muon (1). We have now lowered this limit by a factor ~ 5, using the same experimental principle but with greatlyi mproved technique. The existence of an EDM to the extent permitted by othere xperimental evidence would imply a correction to the experiments on the magnetic moment of the free electron, or free muon, which is far outside the quoted limits of error.

In recent years, investigations have been carried out concerning the existence of an EDM for the electron, the positron, the proton, the neutron and the muon. The results, up to May 1959, have been tabulated by Nelson

(*) On leave from Centre National de la Recherche Scientifique, Paris.

(**) IBM Watson Laboratory, Columbia University, New York, N. Y.

(***) On leave from Centre National de la Recherche Scientifique, and Institut de Recherches Nucléaires, Strasbourg.

(1) G. Charpak, L. M. Lederman, J. C. Sens and A. Zichichi: *Nuovo Cimento*, **17**, 288 (1960).

et al. [2] and show upper limits of the order $e \cdot 10^{-13}$ cm for the first three particles and of the order $e \cdot 10^{-20}$ cm for the neutron, while our more recent value for the muon was $e \cdot (5.0 \pm 5.0) \cdot 10^{-17}$ cm. Theoretically, the existence of an EDM for a stable elementary particle violates simultaneously parity and time-reversal invariance [3], but it has been pointed out by ZEL'DOVITCH [4] that time-reversal invariance does not absolutely forbid an EDM if the particle is unstable.

2. – Principle of the experiment.

When muons of velocity $\boldsymbol{v} = \beta c$ turn in an orbit perpendicular to a magnetic field $\boldsymbol{B}$ (assumed vertical for clarity), the spin turns slightly faster than the momentum vector because of the anomalous part a of the gyromagnetic ratio $g \equiv 2(1+a)$. In fact, the angular velocity (in the laboratory), of the spin relative to the momentum is

$$\omega_a = a\omega_c$$

parallel to $\boldsymbol{B}$, where ω_c is the cyclotron frequency for zero-energy muons eB/m_0c. This precession is in the plane of the orbit. By making muons turn up to 1200 times in the magnetic field and studying the change in spin direction, we have used this effect to measure the anomalous part of the magnetic moment [5].

If, in addition, the muon has an electric dipole moment parallel to the spin of magnitude $D = feh/mc$, where f is a numerical factor to be determined, there will be an additional precession of the spin out of the orbit plane. This arises because in its rest frame the muon experiences an electric field $\boldsymbol{E}' = \gamma' \boldsymbol{\beta} \cdot \boldsymbol{B}$, and this, acting on the EDM, makes the spin precess about the axis $\boldsymbol{E}'$. In the laboratory the result is a precession about the instantaneous axis $\boldsymbol{v} \times \boldsymbol{B}$ (radial to the orbit) with angular velocity [1,2,6].

$$\omega_e = 2f\beta\omega_c \,.$$

[2] D. F. NELSON, A. A. SCHUPP, R. W. PIDD and H. R. CRANE: *Phys. Rev. Lett.*, **2**, 492 (1959); see also R. L. GARWIN and L. M. LEDERMAN: *Nuovo Cimento*, **11**, 776 (1959).

[3] L. LANDAU: *Nucl. Phys.*, **3**, 127 (1957).

[4] I. B. ZEL'DOVITCH: *Sov. Phys. JETP*, **12**, 1030 (1961) *Žurn. Eksp. Teor. Fiz.*, **39**, 1483 (1960). This suggestion appears to be incorrect. (J. S. BELL, S. M. BERMAN and T. D. LEE: private communications.)

[5] G. CHARPAK, F. J. M. FARLEY, R. L. GARWIN, T. MULLER, J. C. SENS, V. L. TELEGDI and A. ZICHICHI: *Phys. Rev. Lett.*, **6**, 1505 (1961).

[6] V. BARGMAN, L. MICHEL and V. L. TELEGDI: *Phys. Rev., Lett.*, **2**, 435 (1959).

We are interested in the orientation of the spin relative to the momentum and, therefore, choose a frame of reference the origin of which is fixed in the laboratory but rotates with the momentum vector. In this frame the spin precesses around the resultant of two stationary orthogonal angular velocities ω_a parallel to $\boldsymbol{B}$ (vertical), and ω_r radial to the orbit (horizontal) (see Fig. 1).

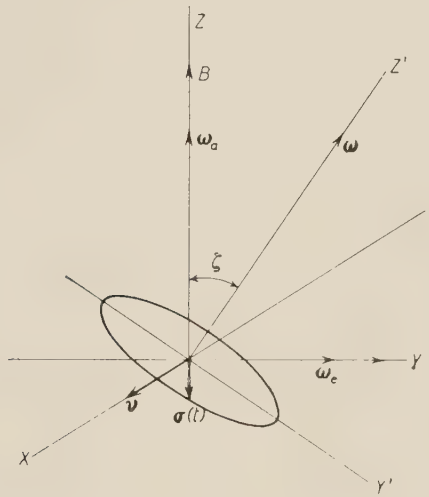

Fig. 1. – Precession of the spin relative to the momentum resulting from the combined effects of an anomaly in the magnetic moment and the presence of an electric dipole moment. $\omega_a \equiv$precession frequency due to « $g-2$ », the magnetic moment anomaly. $\omega_r \equiv$precession frequency due to the torque exerted by the electric field $E' = \gamma\beta \times B$ on the electric dipole moment. $\omega \equiv$resultant frequency. $\operatorname{tg}\zeta = \omega_r/\omega_a$. This reference frame rotates with the particle cyclotron frequency ω_c/γ, *i.e.*, the $X \equiv X'$ axis coincides with the direction of motion v for all t. The spin precesses at a uniform rate ω in the plane of the ellipse. $B \equiv$laboratory magnetic field.

The resultant angular velocity ω is inclined to the vertical at angle ζ given by $\operatorname{tg}\zeta = \omega_r/\omega_a = 2f\beta/a$ with the result that the spin rotates in a plane inclined to the horizontal, and there is a sinusoidally varying vertical component of polarization

$$P_v = P_0 \cdot \frac{2f\beta}{(a^2 + 4f^2\beta^2)^{\frac{1}{2}}} \cdot \sin \omega t \,, \tag{1}$$

where P_0 is the initial longitudinal polarization.

This vertical oscillation has the same frequency and the same phase (*) as the oscillation of the horizontal transverse component which has already been

(*) If the initial spin direction is not parallel to the momentum this is not strictly true: see Appendix for the general case.

studied experimentally (5). To detect the EDM, we then measure the vertical component of spin and look for an oscillation of which the frequency and phase are already known.

It is important to note (2) that if the EDM exists the observed frequency ω is not strictly equal to ω_a as assumed in the measurements of the magnetic anomaly of muon (5) and electron (7). In fact, for the muon, our old value (1) of f, $(2.7 \pm 2.8)\cdot 10^{-4}$, gives $\omega_r/\omega_a = 0.29 \pm 0.31$ introducing an uncertainty of 0 to -20% into the determination of the anomalous moment. For the electron the situation is even worse: independent evidence on the EDM (8) gives only $f \geqslant 3\cdot 10^{-3}$ which makes the magnetic anomaly possibly smaller by a factor of the order of ~ 2, although a result is quoted to $\pm 0.2\%$.

We can now follow one of two lines of argument:

i) to maintain that theoretically the EDM is extremely small and therefore the experimental value of the magnetic anomaly is correct; or,

ii) to note that the measured magnetic moment agrees with theory (and in the case of the electron with independent measurements on the bound electron), and use this fact to put limits on the EDM (2).

Neither of these arguments is wholly satisfactory; unless there is independent evidence as to the EDM, one cannot logically claim any accuracy for the measurement of the magnetic anomaly for either the electron or the muon (*). It is hard to justify the use of the same experimental data to establish values both for the magnetic anomaly and for the EDM (2,7). In the case of the muon we prefer to measure the EDM separately to sufficient accuracy to validate the experiment on the anomalous moment.

3. – Apparatus.

The apparatus used for storing muons in a magnetic field for a known time t, and for finally measuring their polarization, is the same as that already described (5), and is to be the subject of a more comprehensive report.

In brief, longitudinally polarized muons formed by forward decay of pions in flight inside the cyclotron are injected into a 6-metre long magnet ($B = 16$ kG) and stored for times ranging from 2 to 6.5 μs before they reach the other end and are ejected. The time t spent in the magnet is measured by means of

(7) A. A. Schupp, R. W. Pidd and H. R. Crane: *Phys. Rev.*, **121**, 1 (1961).
(8) G. Feinberg: *Phys. Rev.*, **112**, 1637 (1958).
(*) In principle the magnetic anomaly could be smaller, and the EDM could be such as to increase the frequency to the theoretical value.

counters at injection and ejection, and used to select one of 50 channels in a « pulse-height analyser ».

The muons emerging from the magnet fall on the polarization analyser (Fig. 2) where they are stopped in a field-free region (< 0.05 G) in a methylene iodide target, E. The electronics stores events associated with backward decay electrons (coincidence 6 6′ with appropriate gating) in channels 1-50 of the memory as a function of the storage time t of the parent muon in the magnet; similarly, events associated with forward-decay electrons in telescope 7 7′ are classified according to storage time in memory channels 51-100.

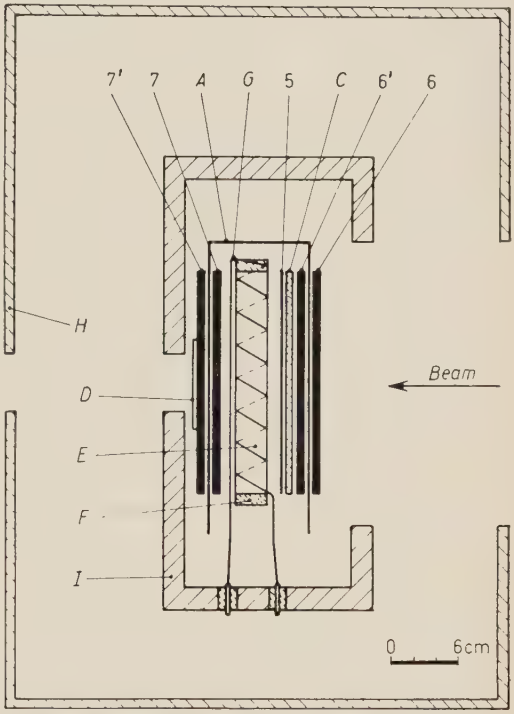

Fig. 2. The polarization analyser (seen from above): A) mumetal shield; C) 6 mm lucite sheet; D) mirror; E) 3 cm thick CH_2I_2 target; F) lucite container; G) flipping coil; H) 1 cm Armco Iron shielding box; I) 2 cm Armco Iron shielding box.

In the experiment on the anomalous moment the apparatus was made sensitive to the *horizontal* transverse component of polarization by means of a pulsed *vertical* magnetic field, which flipped the spin in successive runs through $\pm 90°$ in the horizontal plane in the 1.0 μs following the arrival of the muon. But now the pulsed magnetic field is made *horizontal*, in the plane of the target, so that it is the *vertical* component of the spin that is flipped into the forward or backward direction, while the horizontal component is either not flipped at all (transverse spin) or flipped into the vertical plane where it generates no asymmetry (longitudinal spin).

From the counts c_{n+} and c_{n-} in the n-th channel for $\pm 90°$ flipping, one can compute independently for each channel an asymmetry proportional to the vertical component of spin,

$$A_n = (c_{n+} - c_{n-})/(c_{n+} + c_{n-}) = \frac{2\beta f \cdot A \sin \omega t}{(a^2 + 4f^2\beta^2)^{\frac{1}{2}}},$$

where A is the maximum asymmetry observable with this beam and counter geometry. The value of ω and A are known from the magnetic moment ex-

periment in which a was measured. The amplitude of the observed oscillation is therefore a measure of f.

Consider now the systematic errors that can arise due to an initial vertical component of spin, and to various small rotations of the analyser. They will be serious only if they generate an apparent EDM oscillation which could either cancel or add to the true effect. An initial vertical component of spin will not precess in the magnet and therefore gives a constant asymmetry independent of t. The result should therefore be fitted to an equation of the form $A_n = a_0 + a_1 \sin \omega t$.

A rotation of the analyser about a vertical axis will change the phase of the sine wave, but small errors will not affect the value of a_1 which best fits the data. A tilt backwards or forwards will introduce a small term in $\cos \omega t$ which will again not affect the value of a_1. A rotation of the flipping field through angle θ out of the horizontal is, however, serious. This will introduce a term $A \sin\theta \cdot \sin \omega t$, but it is not difficult to align the coil so that $\theta < 0.01$ radian, and we were careful to wind the coil so that there was no net circulation of current in the horizontal plane which would give a vertical component of field: this error is also negligible.

4. – Results and discussion.

Fig. 3 shows (*) the asymmetries observed per 4 time channels (1 channel; $= 0{,}1$ μs), each point being the mean asymmetry for the forward and backward telescopes, $A = \frac{1}{2}(A_f - A_b)$.

A least squares fit for a_0 and a_1 gave the results shown in the following Table which also includes the goodness of fit for a straight line ($a_1 = 0$, a_0 adjusted).

	Forward telescope	Backward telescope	Forward and backward telescopes combined
$a_0 \cdot 10^4$	-96	$+79$	-81
$a_1 \cdot 10^4$	$-(24 \pm 177)$	$+(93 \pm 161)$	$-(63 \pm 120)$
χ^2	54.5	59.4	52.9
χ^2 for $a_1 = 0$	54.5	59.8	53.1

(The probability of finding $\chi^2 \geqslant 54$ is $\sim 30\,\%$).

(*) Some minor improvements were made to the storage magnet for this run. These include some readjustment of the shimming, and the addition of a magnetic channel to concentrate more of the ejected muons onto the polarization analyser. These modifications account for the change [with respect to ref. (5)] in the storage-time spectrum which may be noticed in Fig. 3.

It is clear that the straight line ($a_1 = 0$) fits the results almost as well as the optimum sinusoid so there is no evidence for an EDM. Using the com-

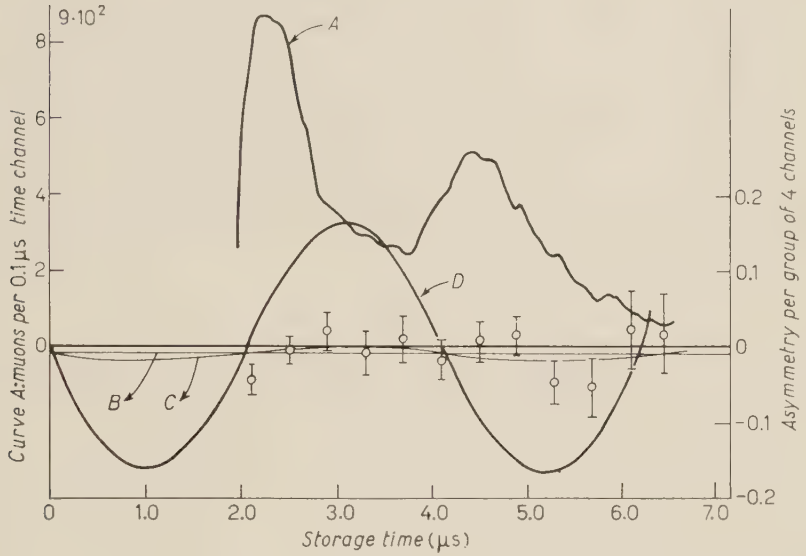

Fig. 3. – Curve A: storage time distribution of muons that stop in the polarization analyser and give rise to decay electrons. Curve B (right-hand scale): the straight line is a best fit to the observed points assuming the EDM to be zero. Curve C (right-hand scale): best fit to the data, allowing for a finite EDM; the frequency of the sine-wave is taken equal to the « $g - 2$ » frequency, as measured in ref. [5]. The points are averages of « forward » and « backward » decaying muons. Curve D (right-hand scale): for comparison, the best fit to the measured variation of muon decay asymmetry with storage time, caused by the magnetic moment anomaly, is reproduced from ref. [5].

bined result of the amplitude a of the optimum sinusoid with $\beta = 0.65$, $A = 0.17$, as measured previously [5] we find

$$f = (3 \pm 6) \cdot 10^{-5}$$

corresponding to

$$\text{EDM of muon} = e \cdot (0.6 \pm 1.1) \cdot 10^{-17} \text{ cm} .$$

To one standard deviation we can now assert that $f < 10^{-4}$, which means that $\omega - \omega_a$ to within 0.5 %. Our $\pm$ 1.9 % result [5] on the magnetic anomaly of the muon is therefore justified, and the ground is prepared for another measurement at improved accuracy.

APPENDIX

Consider a frame X, Y, Z moving with the particle such that the X-axis points at all times t in the direction of its momentum. The main magnetic field B is along the Z-axis, as is the corresponding spin angular velocity vector ω_a. The EDM causes the spin to precess about the direction $\hat{\boldsymbol{B}} \times \hat{\boldsymbol{V}}$ (*i.e.*, the Y axis) as well, with angular velocity ω_e. The resultant angular velocity ω is then a vector in the Z-Y plane, making an angle ζ with the Z-axis. We consider a particle whose spin at the instant of entry into the magnetic field makes an angle φ, in the X-Y plane, with its momentum, *i.e.*, its transverse spin component lies in the horizontal plane. The components in the XYZ frame are thus initially

$$\text{(A.1)} \qquad \sigma_X = \sigma \cos\varphi\,, \qquad \sigma_Y = \sigma \sin\varphi\,, \qquad \sigma_Z = 0 \qquad (t=0)\,.$$

Now by rotating XYZ into $X'Y'Z'$ (see Fig. 1) through angle ζ, the equation of motion $\mathrm{d}\boldsymbol{\sigma}/\mathrm{d}t = \boldsymbol{\omega}\times\boldsymbol{\sigma}$ takes on a simple form ($\boldsymbol{\omega} = \omega\hat{\boldsymbol{z}}'$), while initially one has, in the primed frame,

$$\text{(A.2)} \qquad \sigma_{X'} = \sigma\cos\varphi\,, \quad \sigma_{Y'} = \sigma\sin\varphi\cos\zeta\,, \quad \sigma_{Z'} = \sigma\sin\varphi\,\sin\zeta \quad (t=0)\,.$$

With (A.2) and the constraint

$$\sigma_{X'}^2 + \sigma_{Y'}^2 = \sigma_{X'}^2(t=0) + \sigma_{Y'}^2(t=0)\,,$$

the solutions in the primed frame are easily found. By rotating now through angle $-\zeta$, the solutions in the XYZ-frame become

$$\sigma_X = \sigma\sin\varphi\cos\zeta\sin\omega t + \sigma\cos\varphi\cos\omega t\,,$$

$$\sigma_Y = \sigma\sin\varphi\sin^2\zeta + \sigma\sin\varphi\cos^2\zeta\cos\omega t - \sigma\cos\varphi\cos\zeta\sin\omega t\,,$$

$$\sigma_Z = \sigma\sin\zeta[\cos\varphi\sin\omega t + \sin\varphi\cos\zeta(1-\cos\omega t)]\,.$$

The last of these equations reduces to (1) in the text in the absence of an initial transverse component of spin.

RIASSUNTO

Estendendo fino a 1200 rivoluzioni la cattura in campo magnetico di muoni positivi, longitudinalmente polarizzati, è stato possibile fissare un nuovo limite al valore del loro momento di dipolo elettrico (EDM). Il risultato è

$$\mathrm{EDM} \leqslant (3\pm 6)\cdot 10^{-5}\cdot\frac{e\hbar}{mc} \qquad \text{ovverossia} \qquad \mathrm{EDM} \leqslant e\cdot(0.6\pm 1.1)\cdot 10^{-17}\ \mathrm{cm}\,,$$

consistente con l'ipotesi della invarianza rispetto all'inversione del tempo.

Bemerkungen zur Unitäräquivalenz von Lorentzinvarianten Feldern.

H. Reeh und S. Schlieder

Max-Planck-Institut für Physik und Astrophysik - München

(ricevuto il 29 Settembre 1961)

Summary. — At the beginning (Sect. **2**) we consider such field theories, which are characterized by operators defined on spacelike surfaces. In this connection Haag's theorem is discussed. Then the properties of the field operator algebra are investigated (Sect. **3**). It follows that the algebra $\mathfrak{B}$, defined in Sect. **3**·5, is already cyclic. Furthermore, the algebra $\hat{\mathfrak{B}}$, essentially arrived at by adjoining to $\mathfrak{B}$ the projection operator onto the vacuum state, is irreducible.

1. – Voraussetzungen und Inhaltsangabe.

Man kann sich die Frage: Wann stimmen zwei Feldtheorien überein, in zweierlei Hinsicht stellen. Die eine besteht darin, daß nach der Gleichheit der sich ergebenden S-Matrizen gefragt ist. Man nimmt dann außer den allgemeinen Bedingungen, die hier unter (1), (2), ..., (6) aufgeführt sind, zusätzlich an, daß eine Asymptotenbedingung etwa im Sinne von L.S.Z. [1] zu erfüllen ist. So kann man, wie es z.B. Borchers [2] tat, Kriterien angeben, wann zwei Felder die gleich S-Matrix interpolieren. Eine andere Frage ist die nach der Gleichheit oder Unitäräquivalenz der interpolierenden Felder selbst, zu der hier einige Bemerkungen gemacht werden sollen.

Wir betrachten skalare Felder, die mit sich selbst in Wechselwirkung stehen können und welche die folgenden Voraussetzungen erfüllen [3]:

(1) H. Lehmann: K. Symanzik and W. Zimmermann: *Nuovo Cimento*, **1**, 205 (1955).

(2) H. J. Borchers: *Nuovo Cimento*, **15**, 784 (1960).

(3) A. S. Wightman: *Problèms Mathématiques de la Théorie Quantique des Champs* (Paris, 1958).

(1) *Lorentzinvarianz.* Das erste Stück der inhomogenen Lorentzgruppe wird so unitär dargestellt, daß

$$\mathcal{U}(a, \Lambda)\, A(x)\, \mathcal{U}^{-1}(a, \Lambda) = A(\Lambda x + a) \qquad \text{gilt.}$$

(Λ homogene Lorentztransformation, a Translation.)

(2) Es gibt genau ein Vakuum Ω.
Ω ist der einzige invariante Zustand unter den Transformationen der Lorentzgruppe.

(3) Spektrumsbedingung.
Jede Zustandsfunktion im Impulsraum hat ihren Träger im Vorwärtslichtkegel.

(4) Die Vakuumerwartungswerte der Feldoperatoren sind temperierte Distributionen.

(5) Definite Metrik im Zustandsraum.

(6) Lokalität

$$[A(x), A(y)] = 0 \qquad \text{für } x - y \text{ raumartig.}$$

Im Abschnitt 2, der als eine Vorstufe zum Abschnitt 3 verstanden werden sollte, sind weitere Voraussetzungen gemacht. Es wird angenommen, daß es sinnvoll sei, Feldoperatoren einer raumartigen Fläche, z.B. der Ebene $t = 0$ zuzuordnen. Dann sollen bereits die Matrixelemente von Operatoren der Gestalt $\int A(\mathfrak{x}) f(\mathfrak{x})\, \mathrm{d}^3\mathfrak{x}$, $\int A(\mathfrak{x}) g(\mathfrak{x})\, \mathrm{d}^3\mathfrak{x}$ mit geeigneten Testfunktionen f, g, ... gewöhnliche Funktionen von t sein. Solche Theorien sollen im folgenden flächenhaft heißen. Es kann sogar sein, daß die von solchen Operatoren erzeugte Algebra irreduzibel ist; im folgenden nennen wir sie dann flächenirreduzibel.

Abschnitt 2 bringt einen Beweis des Haagschen Theorems (4), der im wesentlichen eine Verbindung der Ergebnisse von Hall und Wightman (5) und Überlegungen von Federbush und Johnson bzw. Schroer und Jost (6) darstellt. Die Absicht ist, die ausschlaggebende Eigenschaft der Flächenirreduzibilität hervortreten zu lassen. Der Unterabschnitt 2·4 zeigt, daß die Beweiskraft der Methode über freie Theorien hinausgeht und leitet gleichzeitig zu dem folgenden Abschnitt 3 über.

(4) R. Haag: *Dan. Vid. Selsk. Mat.-Fys. Medd.*, **29**, no. 12 (1955); O. W. Greenberg: *Phys. Rev.*, **115**, 706 (1959).

(5) D. Hall und A. S. Wightmann *Dan. Vid. Selsk. Mat.-Fys., Medd.*, **31**, no. 5 (1957).

(6) *a*) P. G. Federbush und K. A. Johnson *Phys. Rev.*, **120**, 1926 (1960); *b*) B. Schroer und R. Jost: unveröffentlicht.

Im Abschnitt 3 wird die Flächenhaftigkeit der Feldtheorien aufgegeben. Die Träger der Testfunktionen sind vierdimensionale Teile des Minkowskiraumes. Sobald die Wightmanfunktionen innerhalb ihres reellen Regularitätsbereiches betrachtet werden, lassen wir die Testfunktionen oft stillschweigend weg. Der Unterabschnitt 3·1 enthält den Hinweis darauf, wie wenig man von den Wightmanfunktionen wissen muß, um nach dem Charakterisierungssatz (7) die Feldtheorie bis auf Isomorphie festzulegen. In 3·2 zeigt sich, daß man nur eine gewisse Teilmenge von Zuständen des Zustandsraumes braucht, um durch ihre Matrixelemente einen Operator festzulegen. In 3·5 werden Eigenschaften gewisser Operatoralgebren bewiesen, die in engem Zusammenhang mit dem Haagschen Zeitschichtaxiom (8) stehen. Während die Grundlage für die analytische Seite des Beweises das « Edge of the Wedge »-Theorem (9) bildet, sind die algebraischen Grundlagen im vorangehenden Abschnitt 3·4 zusammengefaßt.

Wenn eine Operatoralgebra keinen echten abgeschlossenen invarianten Teilraum besitzt (oder äquivalent dazu, wenn jeder mit ihr vertauschbare beschränkte Operator ein skalarer Operator ist), so soll sie hier irreduzibel heißen. Wir haben vermieden, diese Eigenschaft vollständig zu nennen, um sie nicht mit topologischen Begriffen zu vermengen.

2. – Flächenhafte Theorien. Haagsches Theorem.

2·1 *Vorbemerkung.* – Das Haagsche Theorem geht von zwei Feldtheorien aus, von denen die eine die freie Feldgleichung $(\Box + m^2) A_1(x) = 0$ erfüllt. Die zweite $A_2(x)$ soll der ersten auf einer raumartigen Fläche, z.B. auf der Ebene $t = 0$ unitäräquivalent oder ihr dort sogar gleich sein. Wie in den folgenden Abschnitten dargelegt wird, kann man mit weiteren Annahmen dann beweisen, daß auch das zweite Feld die freie Gleichung erfüllt; weiterhin läßt sich die Unitäräquivalenz der beiden Felder zeigen.

Die Unitäräquivalenz der beiden Theorien auf einer raumartigen Fläche setzt voraus, daß man einer solchen Fläche in sinnvoller Weise Feldoperatoren zuordnen kann, genauer, daß z.B. für die Fläche $t = 0$ Operatoren der Gestalt

$$\int f(\mathrm{r}, 0)\, A_1(\mathrm{r}, 0)\mathrm{d}^3\mathrm{r}\,, \qquad \int g(\mathrm{r}, 0)\, \dot{A}_1(\mathrm{r})\,\mathrm{d}^3\mathrm{r}\,, \quad \ldots\,,$$

(7) *z.B.*: A. S. Wightman: *Phys. Rev.*, **101**, 860 (1956); oder auch M. A. Neumark: *Normierte Algebren* § 17, *VEB Deutscher Verlag der Wissenschaften* (Berlin, 1959).

(8) R. Haag: Konferenz in Lille (1957).

(9) *z.B.*: F. J. Dyson: *Phys. Rev.*, **110**, 579 (1958); H. Epstein: *Journ. Math. Phys.* 1 n. 6, 524 (1960).

sinnvoll sind, wobei f, g, ... einem geeigneten Raum von Testfunktionen angehören. Im Abschnitt 2 soll diese über die Voraussetzungen (1), (2) ... (6) hinausgehende Annahme gemacht werden.

Im Unterabschnitt 2'2 wird sogar angenommen, daß man aus diesen Operatoren eine irreduzible Algebra erzeugen kann, eine Auffassung, die z.B. dem kanonischen Quantisierungsverfahren zugrunde liegt.

2'2. *Eines der Felder ist flächenirreduzibel.* – Betrachtet sei z.B. die Ebene $t=0$. Das System der Operatoren für das Feld A_1

$$1, \quad \int A_1(\mathfrak{x}) f(\mathfrak{x})\,\mathrm{d}^3\mathfrak{x}, \quad \int \dot{A}_1 g(\mathfrak{x})\,\mathrm{d}^3\mathfrak{x}, \quad \int \ddot{A}_1 h(\mathfrak{x})\,\mathrm{d}^3\mathfrak{x}, \ldots, \quad \int A_1^{(m)} s(\mathfrak{x})\,\mathrm{d}^3\mathfrak{x}\,,$$

(das Argument $t=0$ ist weggelassen) mit geeigneten komplexwertigen Testfunktionen f, g, ... s erzeuge eine irreduzible Algebra $\tilde{\mathfrak{A}}_1$. D.h., jeder beschränkte Operator C, welcher mit allen Ausdrücken der Gestalt

$$A_1(f_{\mathfrak{x}})A_1(g_{\mathfrak{x}}) \ldots \dot{A}_1(h_{\mathfrak{x}}) \ldots A_1^{(m)}(s_{\mathfrak{x}})\,, \tag{7}$$

mit $A_1(f_{\mathfrak{x}}) = \int A_1(\mathfrak{x}) f(\mathfrak{x})\,\mathrm{d}^3\mathfrak{x}$ usw., vertauscht, ist ein Vielfaches der Einheit. Abgekürzt geschrieben:

Aus

$$[C, \tilde{\mathfrak{A}}_1] = 0 \quad \text{folgt} \quad C = \lambda I\,. \tag{8}$$

Dabei steht in (7) ein Produkt von endlich vielen Integralen; die Elemente von $\tilde{\mathfrak{A}}_1$ sind endliche Summen von Ausdrücken der Gestalt (7).

Ein zweites Feld $A_2(x)$ sei auf der Fläche $t=0$ zusammen mit seinen Ableitungen bis zur m-ten Ordnung dem ersten Feld und dessen Ableitungen durch eine isometrische Transformation verknüpft:

$$\left|\begin{array}{ll} A_2(f_{\mathfrak{x}}) & \gamma\, A_1(f_{\mathfrak{x}})\,\gamma^{-1}\,, \\ \dot{A}_2(g_{\mathfrak{x}}) & \gamma\, \dot{A}_1(g_{\mathfrak{x}})\,\gamma^{-1}\,, \\ \vdots & \\ A_2^{(m)}(s_{\mathfrak{x}}) & \gamma\, A_1^{(m)}(s_{\mathfrak{x}})\,\gamma^{-1}\,. \end{array}\right. \tag{9}$$

Die unitären Darstellungen der Lorentzgruppe $\mathscr{U}_1(\mathfrak{a}, A)$ für das erste Feld, $\mathscr{U}(\mathfrak{a}, A)$ für das zweite Feld induzieren für die Operatoren auf der Fläche Darstellungen der Euklidischen Gruppe $\mathscr{U}_1(\mathfrak{a}, \vartheta)$, $\mathscr{U}_2(\mathfrak{a}, \vartheta)$:

$$\mathscr{U}_1(\mathfrak{a}, \vartheta)\, A_1(f_{\mathfrak{x}})\, \mathscr{U}_1^{-1}(\mathfrak{a}, \vartheta) = \int A_1(\vartheta\mathfrak{x} + a) f(\mathfrak{x})\,\mathrm{d}^3\mathfrak{x} = A_1(f_{\mathfrak{x}}^{(\mathfrak{a}, \vartheta)})\,, \tag{10}$$

$$\mathscr{U}_2(\mathfrak{a}, \vartheta) A_2(f_{\mathfrak{x}})\, \mathscr{U}_2^{-1}(\mathfrak{a}, \vartheta) = A_2(f_{\mathfrak{x}}^{(\mathfrak{a}, \vartheta)})\,. \tag{11}$$

Aus (9), (10) und (11) folgt

$$\mathscr{U}_1^{-1}(\mathfrak{a}, \vartheta)\mathscr{V}^{-1}\mathscr{U}_2(\mathfrak{a}, \vartheta)\mathscr{V}\mathfrak{A}_1 = \mathfrak{A}_2\mathscr{U}_1^{-1}(\mathfrak{a}, \vartheta)\mathscr{V}^{-1}\mathscr{U}_2(\mathfrak{a}, \vartheta)\mathscr{V} .$$

Nach Voraussetzung (8) ergibt sich

$$\mathscr{U}_2(\mathfrak{a}, \vartheta) = \exp[i\alpha(\mathfrak{a}, \vartheta)]\mathscr{V}\mathscr{U}_1(\mathfrak{a}, \vartheta)\mathscr{V}^{-1}$$

wobei α eine reelle Funktion von $\mathfrak{a}$, ϑ ist. Unter Voraussetzung der Stetigkeit der Darstellung läßt sich zeigen: $\alpha \equiv 0$ ([10]), so daß man

$$\mathscr{U}_2(\mathfrak{a}, \vartheta) = \mathscr{V}\mathscr{U}_1(\mathfrak{a}, \vartheta)\mathscr{V}^{-1} \quad \text{erhält.} \tag{12}$$

Aus (12) ergibt sich

$$\mathscr{U}_2(\mathfrak{a}, \vartheta)\mathscr{V}\Omega_1 = \mathscr{V}\mathscr{U}_1(\mathfrak{a}, \vartheta)\Omega_1 = \mathscr{V}\Omega_1 .$$

Wenn man nicht nur, wie in (2) gefordert, annimmt, daß Ω_2 der einzige invariante Zustand unter den Transformationen der Lorentzgruppe, sondern daß er auch der einzige invariante Zustand unter den Transformationen der Euklidischen Gruppe ist ([11]), so folgt,

$$\mathscr{V}\Omega_1 = \Omega_2 . \tag{13}$$

Dabei ist eine unwesentliche Konstante vom Betrag 1 auf der rechten Seite von (13) weggelassen.

Zusammengefaßt: Bei einer Isometrie zu einer bestimmten Zeit im Sinne von (9), bei Irreduzibilität der Flächenalgebra $\mathfrak{A}_1$ des ersten Feldes und wenn Ω_2 der einzige invariante Zustand unter den Transformationen der Euklidischen Gruppe für das zweite Feld ist, führt die Äquivalenztransformation Ω_1 in Ω_2 über.

Wie man erkennt, sind dann die Vakuumerwartungswerte für Argumente zu gleichen Zeiten gleich:

$$\langle\Omega_1, A_1(\mathfrak{x}_1, t)A_1(\mathfrak{x}_2, t) \dots A_1(\mathfrak{x}_n, t)\Omega_1\rangle = \langle\Omega_2, A_2(\mathfrak{x}_1, t) \dots A_2(\mathfrak{x}_n, t)\Omega_2\rangle \quad (n \text{ beliebig}).$$

Hieraus folgt nach HALL und WIGHTMAN, daß die ersten 4 Vakuumerwartungswerte

$$\langle\Omega_1, A_1(x_1) \dots A_1(x_n)\Omega_1\rangle = \langle\Omega_2, A_2(x_1) \dots A_2(x_n)\Omega_2\rangle \quad (n = 1, 2, 3, 4) \tag{14}$$

übereinstimmen.

([10]) *z.B.*: G. MACKEY: *Ann. Math.*, **55**, 101 (1951).
([11]) E. P. WIGNER: *Ann. Math.*, **40**, 149 (1939).

(14) läßt sich natürlich auch beweisen, wenn man auf die Flächenirreduzibilität der Algebra des ersten Feldes verzichtet und statt dessen deren Folge (13) unmittelbar fordert.

2·3 *Haagsches Theorem.* – Zu einem Sonderfall von (14) gelangt man, wenn $A_1(x)$ gleich einem freien Feld $A_0(x)$ ist. Es soll gelten

$$(15) \qquad (\Box + m^2) A_0(x) = 0 , \qquad [A_0(x), A_0(y)]_- = -i\,\Delta(x-y) .$$

Aus (15) und der Forderung, daß ein Vakuum vorhanden sein soll, ergibt sich eine Standarddarstellung für die freien Feldoperatoren. Die Transformation (9) wird hier für das Feld und die erste Ableitung vorausgesetzt; es wird angenommen, daß die von $A_0(f_\mathrm{r})$, $\dot{A}_0(g_\mathrm{r})$ erzeugte Algebra im Zustandsraum irreduzibel sei. Bezeichnet man $A_2(x)$ mit $A(x)$ und die Vakua entsprechend, so gilt

$$(16) \qquad \langle \Omega_0, A_0(x_1) \dots A_0(x_n)\Omega_0\rangle = \langle \Omega\, A(x_1) \dots A(x_n)\Omega\rangle \qquad (n = 1, 2, 3, 4)$$

(wobei die Distributionen für $n = 1, 3$ verschwinden).
Aus (16) kann man nun beweisen, daß auch $A(x)$ die freie Feldgleichung erfüllt.

Seien etwa $f, g, \dots$ Testfunktionen aus dem Raum $\mathfrak{D}$ (unendlich oft differenzierbar, mit kompaktem Träger), so gilt mit $k_x = \Box_x + m^2$

$$\iint f(x) f(y) \langle \Omega, k_x A(x)\, k_y A(y)\, \Omega\rangle \,\mathrm{d}x\,\mathrm{d}y = \\ = \iint f(x) f(y) \langle \Omega_0, k_x A_0(x)\, k_y A_0(y)\, \Omega_0\rangle \,\mathrm{d}x\,\mathrm{d}y = 0 .$$

Hieraus folgt wegen (5) (Definitheit der Metrik)

$$(17) \qquad \int f(x)\, k_x A(x)\, \Omega = 0 .$$

Aus (6) (Lokalität) und aus (17) ergibt sich dann auch für eine ganze reelle Umgebung z.B. eines Jostpunktes ([12]), der durch

$$\eta = \sum_{i=1}^{n} \lambda_i \xi_i , \qquad \lambda_i \geqslant 0 , \qquad \sum_{i=1}^{n} \lambda_i = 1 ,$$

und

$$\xi_1 = y_1 - y_2 , \quad \dots , \quad \xi_l = y_l - x , \quad \xi_{l+1} = x - y_{l+1} , \quad \dots , \quad \xi_n = y_{n-1} - y_n ,$$

([12]) A. S. Wightman: *Phys. Rev.*, **101**, 860 (1956); R. Jost: *Helv. Phys. Acta*, **30**, 409 (1957).

η raumartig, gekennzeichnet ist,

$$\langle \Omega A(y_1) \dots A(y_l) k_x A(x) A(y_{l+1}) \dots A(y_n) \Omega \rangle = 0$$

für l, $n \geqslant l$ beliebig.

Diese Funktionalgleichung muß auch im ganzen Regularitätsbereich gelten und daher sogar auf dem reellen Rande, sofern in $k_x = \Box_x + m^2$, $m^2 \neq 0$ ist. Denn in der Gleichung

$$m^2 \langle \Omega_1 A(y_1) \dots A(y_l) A(x) A(y_{l+1}) \dots A(y_n) \Omega \rangle =$$
$$= \langle \Omega, A(y_1) \dots A(y_l) k_x A(x) A(y_{l+1}) \dots A(y_n) \Omega \rangle$$

(hier sind die Argumente im allgemeinen komplexwertig) existieren für die linke Seite nach Voraussetzung überall die Randwerte für reelle Argumente als Distributionen nach WIGHTMAN, mithin auch für die rechte Seite und sind daher rechts und links gleich.

Die Operatoralgebra $\mathfrak{A}$, die von Operatoren $A(f) = \int A(x) f(x) \, \mathrm{d}x$, $A(g)$, ... erzeugt wird, liefert auf das Vakuum Ω angewendet, einen Raum $\mathfrak{P}$, der zu einem Hilbertraum $\mathfrak{H}$ so vervollständigt werden kann, daß $\mathfrak{P}$ in $\mathfrak{H}$ dicht liegt. Dieser soll den ganzen Zustandsraum ausmachen. Man kann nun so vorgehen: $k_x A(x) = j(x)$ ist zunächst in $\mathfrak{P}$ definiert und es gilt für φ, $\chi \in \mathfrak{P}$: $\langle \chi, j(x) \varphi \rangle = 0$; da $\mathfrak{P}$ dicht in $\mathfrak{H}$ liegt, gilt

$$\langle \psi, j(x) \varphi \rangle = 0 \; ; \qquad \varphi \in \mathfrak{P} \; ; \quad \psi \in \mathfrak{H} \, ,$$

$j(x)$ wird durch Abschließung auf ganz $\mathfrak{H}$ fortgesetzt; es gilt natürlich $j(x) = 0$ auf $\mathfrak{H}$.

Damit ist gezeigt: Sind $A(x)$ bzw. $\dot{A}(x)$ äquivalent im Sinne einer Isometrie zu $A_0(x)$ bzw. $\dot{A}_0(x)$ auf einer Fläche $t = \text{const.}$, ist $A_0(x)$ irreduzibel und Ω der einzige invariante Zustand unter den Transformationen der Euklidischen Gruppe für das Feld $A(x)$, so gilt

$$(\Box + m^2) A(x) = 0 \, .$$

Wie SCHROER und JOST ([6b]) gezeigt haben, kann man weiter beweisen, daß $A(x)$ derselben Vertauschungsrelation genügt wie $A_0(x)$. Damit ist gezeigt, daß $A(x)$ und $A_0(x)$ äquivalent sind.

2·4. *Das erste Feld erfüllt die Gleichung* $(\Box + m^2) A_1(x) = A_1^n(x)$. – Es ist fragwürdig, ob eine Feldtheorie gleichzeitig eine solche inhomogene Differentialgleichung und die Voraussetzungen (1), (2) ... (6) erfüllen kann. Wir wollen als heuristische Betrachtung für den Fall der Existenz einer solchen Theorie

Bedingungen derart angeben, daß auch das zweite Feld $A_2(x)$ die gleiche Differentialgleichung erfüllt.

Für den Fall, daß ein freies Feld vorliegt, hat WIGHTMAN gezeigt ([13]), wie man den Operator $A_0^n(x)$ sinnvoll definieren kann, nämlich durch das Wickprodukt. Es soll entsprechend angenommen werden, daß das Symbol $A_1^n(x)$ durch eine Operatorgleichung der folgenden Gestalt definiert ist:

$$A_1^n(x) = \lim_{x_1, x_2, \ldots x_k \to x} [A_1(x_1) A_1(x_2) \ldots A_1(x_k) + c(x_1, x_2, \ldots, x_k) + \\ + \sum c_{jk}(x_j, x_k) A_1(x_1) \ldots A_1(x_{j-1}) A_1(x_{j+1}) \ldots A_1(x_{k-1}) A_1(x_{k+1}) \ldots A_1(x_n) + \ldots .$$

Dabei sind die c, c_{jk}, ... geeignet zu wählende Distributionen, welche den angegebenen Grenzprozeß ermöglichen und den Matrixelementen von $A_1^n(x)$ die gleichen Regularitätseigenschaften verschaffen sollen, wie sie $(\Box - m^2) A_1(x)$ nach Voraussetzung besitzt.

Für das zweite Feld $A_2(x)$ kann man nach der gleichen Methode wie in 2·3 eine (17) entsprechende Gleichung ableiten:

$$\int \mathrm{d}x f(x) \{k_x A_2(x) - \lambda A_2^n(x)\} \Omega \rangle = 0 , \tag{18}$$

Dabei muß aber die Gleichheit der ersten $2n$ Wightmanfunktionen vorausgesetzt werden. Um die Gleichheit der ersten $2n$ Wightmanfunktionen zu sichern, kann man im Fall $(\Box + m^2) A_1(x) = \lambda A_1^2(x)$ an den Voraussetzungen von 2·2 festhalten, da durch sie die Übereinstimmung der ersten 4 Wightmanfunktionen gewährleistet ist.

Aus (18) folgt dann nach den Überlegungen des vorigen Abschnittes, daß auch $(\Box + m^2) A_2(x) = \lambda A_2^n(x)$ gilt.

3. – Der allgemeine Fall.

3·1. *Vorbermerkung.* – Im allgemeinen kann man nicht damit rechnen, daß man Feldoperatoren in sinnvoller Weise einer raumartigen Fläche zuordnen kann. Der Begriff der Äquivalenz oder Gleichheit der Feldoperatoren zweier Feldtheorien zu einem bestimmten Zeitpunkt verliert so zunächst den Charakter einer präzisen Aussage. Damit ist auch die Grundlage für die Voraussetzungen der im zweiten Abschnitt abgeleiteten Sätze verloren gegangen.

Man hat zunächst die Feldoperatoren

$$A(f) = \int A(x) f(x) \, \mathrm{d}x , \qquad A(g) , \ldots$$

([13]) Siehe ([3]).

mit $f, g \ldots$ in $\mathfrak{D}$ (beliebig oft differenzierbar, kompakter Träger) oder auch mit f, $g \ldots$ in $\mathfrak{S}$ (beliebig oft differenzierbar, von starkem Abfall im Unendlichen) vorliegen. Man kann das Feld zu einer Zeit t wohl annähernd durch einen Unterring $\mathfrak{D}_{t.t+\Delta t}$ oder $\mathfrak{S}_{t.t+\Delta t}$ von Testfunktionen, deren Träger in der Schicht $t \leqslant t' \leqslant t+\Delta t$ enthalten ist, charakterisieren. Aber es ist nicht zu erwarten, daß sich der Grenzprozeß $\Delta \to 0$ durchführen läßt. So wird man sich an Stelle des Feldes zu einem Zeitpunkt mit der Operatoralgebra auf einer dünnen Schicht (Haagsche Schicht ([14])) begnügen müssen; diese ist durch ein beliebig kleines, aber festes Δt gekennzeichnet.

Im folgenden wollen wir nicht mehrere Felder miteinander in Beziehung setzen, sondern, was auf dasselbe hinausläuft, prüfen, welche Bedingungen ein Feld festlegen. Wir weiten die Fragestellung etwas aus, indem wir auch andere Operatoren als die Feldoperatoren in Betracht ziehen. Es soll auch nicht nur von dem Feldoperator-Ring einer Schicht zwischen t und $t+\Delta t$ auf den ganzen Operator-Ring geschlossen werde. Da es für die Beweismethode gleichgültig ist, können wir auch einen Ring über irgendeinem vierdimensionalen Teile des Minkowski-Raumes betrachten, behalten aber den vom physikalischen Standpunkt aus interessanten Fall der Haagschen Schicht im Auge.

3·2. *Festlegung des Feldes durch seine Eigenschaften im Kleinen.* – Eine skalare reelle Feldtheorie, die den Voraussetzungen (1), (2) und (4) genügt, ist bekanntlich durch die Vakuumerwartungswerte

$$(19) \qquad \langle \Omega, A(f_1)A(f_2) \ldots A(f_n)\Omega \rangle = \int \mathrm{d}x_1 \ldots \mathrm{d}x_n f_1(x_1) \ldots f_n(x_n) W^{(n)}(x_1 \ldots x_n) ,$$

gegeben für alle $f_\nu \in \mathfrak{S}$ und für alle $n < \infty$) bis auf Unitäräquivalenz eindeutig bestimmt ([15]). Der Zustandsraum wird erzeugt durch eine zyklische Darstellung der Algebra des Feldoperators bezüglich des Vakuumzustandes. Unter den weiteren Voraussetzungen (3) und (5) sind die Wightmanfunktionen (besser Distributionen)

$$W^{(n)}(x_1, \ldots, x_n) = F^{(n-1)}(\xi_1, \xi_2, \ldots, \xi_{n-1}) , \qquad \xi_\nu = x_\nu - x_{\nu+1} .$$

Randwerte der analytischen Funktionen

$$F^{n-1}(\zeta_1, \zeta_2, \ldots, \zeta_{n-1}) , \qquad \zeta_\nu = \xi_\nu + i\eta_\nu , \qquad \eta_\nu \to 0 , \qquad \eta_\nu \in VK .$$

(VK ist der Vorwärtslichtkegel). Die Jostpunkte sind reelle Regularitätspunkte.

([14]) Siehe ([8]).
([15]) E. Scheibe: preprint (1961).

Sei G eine Teilmenge, die ein Gebiete G^0 (offene zusammenhängende (*) Menge $\neq \Phi$, Φ leere Menge) des Minkowski-Raumes enthält. Man kann in G^0 für beliebiges n $x_1, x_2 \ldots x_n$ so finden, daß die zugehörigen $\xi_1, \xi_2, \ldots, \xi_{n-1}$ einen Jostpunkt und eine reelle Umgebung dieses Jostpunktes bilden (s. Anhang 1).

Da die Wightmanfunktionen durch ihre Werte in einer reellen Umgebung eines Jostpunktes festgelegt sind, folgt:

Kennt man die Wightmanfunktionen für Testfunktionen mit Trägern in G, so ist die Feldtheorie bis auf Unitäräquivalenz festgelegt.

Für den Beweis ist der Umstand von Bedeutung, daß die Konstruktion des Hilbertraumes $\mathfrak{H}$ durch Vervollständigung des Raumes $\tilde{\mathfrak{P}}$ vorgenommen wird. Dieser wird mit Hilfe der Kenntnis der Wightmanfunktionen von beliebig großen, aber endlichen n gewonnen.

3·3 *Bestimmung eines Operators durch eine Teilmenge von Zuständen.* – In diesem Abschnitt erscheint es zweckmäßig, von einer etwas größeren Algebra $\mathfrak{A}$ auszugehen.

$\mathfrak{A}$ werde durch die Operatoren

$$a_0, \int a_1(x_1)\, A(x_1)\, \mathrm{d}x_1, \ldots, \int \ldots \int a_\nu(x_1, \ldots, x_\nu)\, A(x_1) \ldots A(x_\nu)\, \mathrm{d}x_1 \ldots \mathrm{d}x_\nu ,$$

$\nu \neq 0$, $a_\nu \in \mathfrak{S}^{(\nu)}$ (Raum der stark abfallenden Testfunktionen in ν Variablen, ν endlich) erzeugt. Der Raum $\mathfrak{P}$ werde durch Anwendung von $\mathfrak{A}$ auf Ω erhalten. Da $\tilde{\mathfrak{P}}$ ($\tilde{\mathfrak{P}}$ ist in 2·3 definiert) dicht in $\mathfrak{P}$ ist, führt die Vervollständigung von $\tilde{\mathfrak{P}}$ und $\mathfrak{P}$ zu dem gleichen Hilbertraum $\mathfrak{H}$ (**).

Sei C ein in ganz $\mathfrak{P}$ definierter linearer Operator. Z.B. sei C in $\mathfrak{P}$ beschränkt oder es sei $C \in \mathfrak{A}$. Dann gilt der Satz:

Die Matrixelemente von C mit Elementen aus $\mathfrak{P}$ sind bekannt, wenn die speziellen Matrixelemente

$$\langle \Omega, A(f_1) \ldots A(f_l)\, C(f_{l+1}) \ldots A(f_n)\Omega \rangle \tag{20}$$

mit $f_\nu \in \mathfrak{S}_G$ für alle l, $n - l$ bekannt sind. $\mathfrak{S}_G$ ist der Unterring der stark abfallenden Testfunktionen in einer Variablen, die ihren Träger in einer Menge G des Minkowski-Raumes haben. G enthalte wie in 3·2 ein offenes Gebiet G^0. Wenn C auf $\mathfrak{P}$ beschränkt ist, folgt hieraus die Kenntnis aller Matrixelemente mit Elementen aus $\mathfrak{H}$.

(*) Gemeint in der Topologie des R_4.

(**) Vom mathematischen Standpunkt aus kann man hier und bei gewissen anderen Sätzen nur die Isomorphie und nicht die Gleichheit der Räume behaupten. Vom physikalischen Standpunkt aus betrachtet, fällt der Unterschied zwischen Isomorphie und Gleicheit hier nicht sehr ins Gewicht, da für die vorzunehmende physikalische Interpretation zwei isomorphe Räume das gleiche leisten.

Der Beweis gelingt mit Hilfe des Edge of the Wedge-Theorems ([16]) und eines Hilfssatzes.

Hilfssatz: Sei C in ganz $\mathfrak{P}$ definiert, existiere also

$$\langle \Omega, A(f_1) \dots A(f_l)\, C\, A(f_{l+1}) \dots A(f_n)\Omega \rangle ,$$

dann ist

$$\langle \Omega, A(y_1) \dots A(y_l)\, C\, A(y_{l+1}) \dots A(y_n)\Omega \rangle$$

Randwert — der im allgemeinen im distributiven Sinn existiert — einer analytischen Funktion

$$(21)\quad F_{ln}(y_1 - y_2 + i\eta_1, \dots, y_{l-1} - y_l + i\eta_{l-1}, y_l + i\eta_l, -y_{l+1} + i\eta_{l+1}, \dots, y_{n-1} - y_n + i\eta_n$$

$$\eta_\nu \in V K, \quad \eta_\nu \to 0$$

(Beweis siehe Anhang II).

Nunmehr kann man den Beweis von Satz 1 führen: Wegen der Linearität des Operators C genügt es zu beweisen: Wenn die speziellen Matrixelemente (20) verschwinden, sind alle Matrixelemente 0.

Mit (20) verschwinden auch die Distributionen

$$F_{ln}(y_1 - y_2, \dots, y_{l-1} - y_l, \dots, y_l, -y_{l+1}, y_{l+1} - y_{l+2}, \dots, y_{n-1} - y_n) =$$

$$= F_{ln}(\xi_1, \dots, \xi_{l-1}, \xi_l, \xi_{l+1}, \dots, \xi_n)$$

für alle $y_\nu \in G^0$. Durch Translation läßt sich stets erreichen, daß G^0 übergeht in ein $\tilde{G}^0$, das eine volle reelle Umgebung des Nullpunktes enthält. O.B.d.A. können wir daher voraussetzen, daß G^0 eine Umgebung des Nullpunktes enthält. Die F_{ln} sind Randwerte von analytischen Funktionen. Die Voraussetzungen des Edge of the Wedge-Theorems sind erfüllt, so daß man auf $F_{ln} = 0$ im Regularitätsgebiet und mithin auch auf dem Rande schließen kann.

Für Operatoren eines Operatorfeldes der Gestalt

$$C(x) = c_0 + \int c_1(x_1 - x)\, A(x_1)\, \mathrm{d}x_1 + \iint c_2(x_1 - x, x_2 - x)\, A(x_1) A(x_2)\, \mathrm{d}x_1\, \mathrm{d}x_2 +$$

$$+ \dots + \int \dots \int c_n(x_1 - x, \dots, x_n - x)\, A(x_1) \dots A(x_n)\, \mathrm{d}x_1 \dots \mathrm{d}x_n ,$$

wobei die $c_\nu \in \mathfrak{S}^{(\nu)}$ sind, gilt offenbar ebenfalls Satz 1. G ist jetzt um x verschoben. Zu diesen Operatoren gehören die von Haag betrachteten fastlokalen Operatoren ([16]).

([16]) R. Haag: *Phys. Rev.*, **112**, 669 (1958).

3·4 *Abschließung der Algebra.* – Es sollen in diesem Abschnitt die vorkommenden Algebren als topologische Räume aufgefaßt werden [17]; wir denken sie uns z.B. mit der starken Operatortopologie versehen. Im folgenden soll gezeigt werden, daß man zum Hilbertraum $\mathfrak{H}$ auch durch die Abschließung einer etwas abgeänderten Algebra gelangen kann. Die Kenntnis dieses Sachverhaltes erweist sich für den folgenden Abschnitt als nützlich.

In den vorangehenden Abschnitten wurde $\mathfrak{H}$ auf folgende Weise erzeugt: Auf den Vakuumzustand Ω wurden die Elemente der Feldoperatoralgebra $\mathfrak{A}$ angewandt; auf diese Weise ergab sich ein Raum $\mathfrak{P}$. Dieser wurde zu dem Hilbertraum $\mathfrak{H}$ vervollständigt; $\mathfrak{P}$ lag dann dicht in $\mathfrak{H}$. Wir wollen auch im folgenden davon ausgehen, daß $\mathfrak{H}$ bezüglich Ω strikt zyklisch in $\mathfrak{P}$ ist (strikt zyklisch bezüglich Ω in $\mathfrak{P}$ heißt, daß $\mathfrak{A}\Omega = \mathfrak{P}$ ist, nicht nur, daß $\mathfrak{A}\Omega$ dicht in $\mathfrak{P}$ ist).

Es erscheint an dieser Stelle günstig, zur Algebra $\mathfrak{A}$ den Operator P_Ω (Projektionsoperator in $\mathfrak{P}$ auf den Vakuumzustand Ω) zu adjungieren (*). Die von $\mathfrak{A}$ und P_Ω erzeugte Algebra $\mathfrak{A}_1$ ist wie $\mathfrak{A}$ involutiv und zyklisch. Es soll im folgenden eine Unteralgebra $\hat{\mathfrak{A}}$ von $\mathfrak{A}_1$ betrachtet werden, die folgendermaßen gekennzeichnet ist: $\hat{\mathfrak{A}}$ ist die Algebra der linearen beschränkten Operatoren in $\mathfrak{P}$, die von den Elementen $A_k P_\Omega$, $P_\Omega A_j$, P_Ω erzeugt wird, mit $A_k \in \mathfrak{A}$, $A_j \in \mathfrak{A}$. $\hat{\mathfrak{A}}$ ist ebenfalls involutiv und zyklisch.

Über $\hat{\mathfrak{A}}$ lassen sich die folgenden weiteren Aussagen machen:

1) $\mathfrak{A}$ ist strikt irreduzibel auf $\mathfrak{P}$. Beweis: Seien y und z zwei beliebige elemente aus $\mathfrak{P}$, y sei von Null verschieden. Dann gibt es nach Voraussetzung in $\mathfrak{A}$ Operatoren A_y, und A_z, so daß

$$A_y \Omega = y\,, \qquad A_z \Omega = z\,.$$

Wegen $(y, y) = (\Omega, A_y^* A_y \Omega) = (\Omega, P_\Omega A_y^* y) \neq 0$ gibt es einen Operator A_{zy} in $\hat{\mathfrak{A}}$ derart, daß $A_{zy} y = z$ ist. Hierzu setze man $A_{zy} = \gamma \cdot A_z P_\Omega \cdot P_\Omega A_y^*$ mit einer geeigneten komplexen Zahl γ.

2) Nunmehr wird $\hat{\mathfrak{A}}$ als involutive Algebra auf $\mathfrak{H}$ aufgefaßt; das ist möglich, da beschränkte lineare Operatoren eindeutig auf die Abschließung des

[17] *z.B.*: J. DIXMIER: *Les Algèbres d'Opérateurs etc.*, Kap. I (Paris, 1957).

(*) Die Adjunktion von P_Ω zur Feldoperatoralgebra kann zunächst als beweistechnisches Hilfsmittel zum Beweis der Behauptung 1) im Abschnitt 3·5 angesehen werden. Darüber hinaus gelangt man durch die Adjunktion von P_Ω von zyklischen zu irreduziblen Darstellungen. Bei diesem Übergang können allerdings gewisse Züge der ursprünglichen Algebra verlorengehen; hierauf machte uns Herr BORCHERS aufmerksam.

Definitionsbereiches fortgesetzt werden können. Es folgt:

$$\overline{\hat{\mathfrak{A}}}\Omega = \mathfrak{H}$$

wobei $\overline{\hat{\mathfrak{A}}}$ die Abschließung bezüglich $\mathfrak{L}(\mathfrak{H})$ ($\mathfrak{L}(\mathfrak{H})$ sind alle beschränkten linearen Operatoren auf $\mathfrak{H}$) in der starken Operatortopologie bedeutet. D.h. $\overline{\hat{\mathfrak{A}}}$ ist strikt zyklisch auf $\mathfrak{H}$ bezüglich Ω. Beweis: Sei x ein beliebiges Element aus $\mathfrak{H}$ und $\mathfrak{V}(x)$ ein Fundamentalsystem von Umgebungen von x. $\mathcal{V}_i$, $\mathcal{V}_k$ seien Elemente von $\mathfrak{V}(x)$ derart, daß für $i<k$, $\mathcal{V}_i \supset \mathcal{V}_k$ gilt. Da $\mathfrak{P}$ dicht in $\mathfrak{H}$ liegt, gibt es zu jedem $\mathcal{V}_i$ einen Operator $T_i = A_i P_\Omega$ in $\hat{\mathfrak{A}}$, so daß $T_i\Omega$ in $\mathcal{V}_i$ liegt. Es gibt daher eine aus $T_1\Omega$, $T_2\Omega, \ldots, T_i\Omega, \ldots$ ausgewählte Teilfolge $\ldots, T_l\Omega, \ldots$, welche gegen x konvergiert: $\lim_{l\to\infty} T_l\Omega = x$. Die Folge der Operatoren $T_l = A_l P_\Omega$ konvergiert also im Sinne starker Operatorkonvergenz gegen einen Operator $A_x P_\Omega$ mit $A_x P_\Omega \Omega = x$. $A_x P_\Omega$ gehört zu $\overline{\hat{\mathfrak{A}}}$. Damit ist gezeigt, daß $\overline{\hat{\mathfrak{A}}}$ strikt zyklisch in $\mathfrak{H}$ bezüglich Ω ist.

3) $\overline{\hat{\mathfrak{A}}}$ ist strikt irreduzibel auf $\mathfrak{H}$. Da $\hat{\mathfrak{A}}$ strikt zyklisch bezüglich Ω auf $\mathfrak{H}$ ist, kann man diese Behauptung genau so wie die Behauptung 1) beweisen.

4) $\hat{\mathfrak{A}}$ als involutive Algebra von linearen Operatoren auf $\mathfrak{H}$ ist irreduzibel. Beweis: Bezeichnet man die Doppelkommutatoralgebra von $\hat{\mathfrak{A}}$ mit $\hat{\mathfrak{A}}''$ ($\hat{\mathfrak{A}}''$ ist die Algebra aller linearen beschränkten Operatoren, die mit $\hat{\mathfrak{A}}'$ kommutieren, wobei $\hat{\mathfrak{A}}'$ die Algebra aller linearen beschränkten Operatoren ist, welche mit $\hat{\mathfrak{A}}$ kommutieren), so gilt $\overline{\hat{\mathfrak{A}}} \subset \hat{\mathfrak{A}}''$. Wegen $\hat{\mathfrak{A}}' = \hat{\mathfrak{A}}'''$ gilt $\hat{\mathfrak{A}}' \subset \overline{\hat{\mathfrak{A}}}'$. $\hat{\mathfrak{A}}$ ist also ebenfalls irreduzibel auf $\mathfrak{H}$.

Im nächsten Abschnitt soll nun folgendermaßen vorgegangen werden: Wir betrachten eine Unteralgebra $\hat{\mathfrak{B}}$ von $\hat{\mathfrak{A}}$ und wollen zeigen: $\hat{\mathfrak{B}}' = \hat{\mathfrak{A}}'$. Dann ist auch $\hat{\mathfrak{B}}$ irreduzibel.

3·5 *Feldoperatoralgebren über einer Teilmenge des Minkowskiraumes.* – Der Inhalt dieses Abschnittes sollte im Zusammenhang mit dem Haagschen Zeitschichtaxiom ([8]) und einer Arbeit von Borchers ([18]) gesehen werden, die von der Irreduzibiltät der Feldoperatoralgebra über einer zeitartigen Röhre handelt.

Wir gehen aus von der Feldoperatoralgebra $\mathfrak{A}$, welche durch

$$a_0, \ldots, \int a_1(x_1)\, A(x_1)\, \mathrm{d}x_1, \ldots, \int a_\nu(x_1, \ldots, x_\nu)\, A(x_1) \ldots A(x_\nu)\, \mathrm{d}x_1 \ldots \mathrm{d}x_\nu ,$$

($a_\nu \in \mathfrak{S}^{(\nu)}$, $\nu < \infty$) erzeugt wird. Nach Voraussetzung ist sie zyklisch bezüglich Ω in $\mathfrak{H}$. Es sei G eine Teilmenge des Minkowskiraumes, die eine nicht leere offene Menge G^0 enthält. Es gelten dann die folgenden beiden Behauptungen:

([18]) H. J. Börchers: *Nuovo Cimento*, **19**, 787 (1961).

1) Die Algebra $\mathfrak{B}$, definiert durch

$$a_0, \ldots, \int b_1(x) A(x_1)\,\mathrm{d}x_1, \ldots, \int b_\nu(x_1, \ldots, x_\nu)\, A(x_1) \ldots A(x_\nu)\,\mathrm{d}x_1 \ldots \mathrm{d}x_\nu ,$$

($b_\nu \in \mathfrak{S}_G^{(\nu)}$, d.h. Testfunktionen mit Trägern in G, siehe Abschnitt 3·2 und 3·3), ist zyklisch bezüglich Ω in $\mathfrak{H}$.

2) Die Algebra $\hat{\mathfrak{B}}$, die aus $\mathfrak{B}$ entsprechend wie $\hat{\mathfrak{A}}$ aus $\mathfrak{A}$ gebildet wird (cf. 3·4), ist irreduzibel in $\mathfrak{H}$.

Zunächst wird die Behauptung 2) bewiesen:
$\hat{\mathfrak{B}}$ wird durch die Operatoren P_Ω,

$$\int b_1(x_1) A(x_1)\,\mathrm{d}x_1 \cdot P_\Omega, \ \ldots ,$$

$$\int b_\nu(x_1, \ldots, x_\nu) A(x_1) \ldots A(x_\nu)\,\mathrm{d}x_1 \ldots \mathrm{d}x_\nu \cdot P_\Omega, \qquad P_\Omega \cdot \int b_1(x_1) A(x_1)\,\mathrm{d}x_1, \ \ldots ,$$

$$P_\Omega \cdot \int b_\nu(x_1, \ldots, x_\nu)\, A(x_1) \ldots A(x_\nu)\,\mathrm{d}x_1 \ldots \mathrm{d}x_\nu ,$$

erzeugt (mit $b_\nu \in \mathfrak{S}_G^{(\nu)}$).

Es gilt zu beweisen

$$\hat{\mathfrak{A}}' = \hat{\mathfrak{B}}' . \tag{22}$$

Sicherlich ist $\hat{\mathfrak{B}}' \supset \hat{\mathfrak{A}}'$. Im folgenden soll das umgekehrte

$$\hat{\mathfrak{A}}' \supset \hat{\mathfrak{B}}' \tag{23}$$

gezeigt werden.

Sei C ein beschränkter linearer Operator; wir nehmen an: $[C, \hat{\mathfrak{B}}]_- = 0$, C vertauscht insbesondere mit P_Ω und mit den Elementen der Gestalt

$$\int b_\nu(x_1, \ldots, x_\nu) A(x_1) \ldots A(x_\nu)\,\mathrm{d}x_1 \ldots \mathrm{d}x_\nu \cdot P_\Omega .$$

Man hat also

$$0 = \Big\langle \Omega, A(g_1) \ldots A(g_l) \int \ldots \int \mathrm{d}x_1 \ldots \mathrm{d}x_\nu b_\nu(x_1, \ldots, x_\nu) \cdot \cdot [C, A(x_1) \ldots A(x_\nu) P_\Omega] A(g_{l+1}) \ldots A(g_n)\,\Omega \Big\rangle ,$$

für alle $g_1 \ldots g_n \in \mathfrak{S}_G$, $b_\nu \in \mathfrak{S}_G^{(\nu)}$, l und $n < \infty$.

Es gilt daher im distributiven Sinne für $x_1, ..., x_\nu$; $y_1, .., y_n$ in G^0:

$$0 = \langle \Omega, A(y_1) \dots A(y_l)\, CA(x_1) \dots A(x_\nu) P_\Omega A(y_{l+1}) \dots A(y_n)\Omega \rangle -$$

$$- \langle \Omega, A(y_1) \dots A(y_l) A(x_1) \dots A(x_\nu) P_\Omega\, CA(y_{l+1}) \dots A(y_n)\Omega \rangle .$$

Da $P_\Omega C = P_\Omega C P_\Omega$, folgt

$$0 = \langle \Omega, A(y_1) \dots A(y_l)\, CA(x_1) \dots A(x_\nu)\Omega \rangle \langle \Omega, A(y_{l+1}) \dots A(y_n)\Omega \rangle -$$

$$- \langle \Omega, A(y_1) \dots A(y_l) A(x_1) \dots A(x_\nu)\Omega \rangle \langle \Omega, C\Omega \rangle \langle \Omega, A(y_{l+1}) \dots A(y_n)\Omega \rangle .$$

Nach dem früher bewiesenen Hilfssatz kann man hierfür schreiben

$$0 = F_1(y_1 - y_2, .., y_{l-1} - y_l, y_l, -x_1, x_1 - x_2, ..., x_{\nu-1} - x_\nu, y_{l+1} - y_{l+2}, ., y_{n-1} - y_n) -$$

$$- F_2(y_1 - y_2, ..., y_{l-1} - y_l, y_l - x_1, x_1 - x_2, ..., x_{\nu-1} - x_\nu, y_{l+1} - y_{l+2}, ..., y_{n-1} - y_n) .$$

für $x_1, ..., x_\nu$; $y_1 ..., y_n \in G^0$.

Wir können uns das Koordinatensystem stets so gewählt denken, daß der Ursprung in G^0 liegt. F_1 und F_2 werden nun als Funktionen $\tilde{F}_1$ und $\tilde{F}_2$ ins Komplexe fortgesetzt. Wenn sämtliche Imaginärteile der Argumente, für F_1 also u.a. die Imaginärteile von y_l, $-x_1$, für F_2 u.a. derjenige von $y_l - x_1$, im Vorwärtslichtkegel (VK) liegen, so sind die Funktionen regulär. Läßt man die Imaginärteile von F_1 aus VK heraus gegen Null streben, so geht $\tilde{F}_1 \to F_1$, aber auch $\tilde{F}_2 \to F_2$, da dann ebenfalls die Imaginärteile der Variablen von F_2 aus VK gegen Null streben.

$\tilde{F}_1 - \tilde{F}_2$ ist also im Regularitätsgebiet von F_1 eine analytische Funktion mit den Eigenschaften, daß sie bei entsprechendem Grenzübergang gegen $F_1 - F_2$ strebt; sofern dabei die reellen Argumente in G^0 liegen, ist $F_1 - F_2 = 0$. Nach dem « Edge of the Wedge »-Theorem ist daher $\tilde{F}_1 - \tilde{F}_2 = 0$ und damit $F_1 - F_2 = 0$ für beliebige reelle Argumente. Daher gilt

$$0 = \left\langle \Omega, A(f_1) \dots A(f_l) \int \dots \int a_\nu(x_1, \dots, x_\nu)[C, A(x_1) \dots A(x_\nu) P_\Omega] A(f_{l+1}) \dots A(f_n)\Omega \right\rangle ,$$

$a_\nu(x_1, ..., x_\nu) \in \mathfrak{S}^{(\nu)}$; $f_1, ..., f_n \in \mathfrak{S}$.

Da der Beweis nicht davon abhängt, welchen Index ν man wählt, folgt, daß C mit allen Elementen der Gestalt $A_k P_\Omega$ die Gleichung

$$\langle \varphi, [C, A_k P_\Omega]\chi \rangle = 0$$

erfüllt; φ und χ sind Elemente des in $\mathfrak{H}$ dichten Teilraumes $\tilde{\mathfrak{P}}$. Also gilt über-

haupt

$$[C, A_k P_\Omega] = 0 .$$

Nach Voraussetzung vertauscht C auch mit den Elementen des Typs $P_\Omega B_x$:

$$\left[C, P_\Omega \int \ldots \int \mathrm{d}x_1 \ldots \mathrm{d}x_\nu b_\nu(x_1, \ldots, x_\nu) A(x_1) \ldots A(x_\nu)\right]_- = 0 .$$

Hieraus ergibt sich nach dem entsprechend geführten Beweis

$$[C, P_\Omega A_l] = 0 .$$

Damit ist gezeigt daß aus $[C, \hat{\mathfrak{B}}]_- = 0$ folgt $[C, \hat{\mathfrak{A}}]_- = 0$. Es ist also $\hat{\mathfrak{A}}' = \hat{\mathfrak{B}}'$. Da $\hat{\mathfrak{A}}$ irreduzibel ist, gilt dasselbe für $\hat{\mathfrak{B}}$. Die Behauptung 2) ist bewiesen.

Beweis der Behauptung 1): Da $\hat{\mathfrak{B}}$ irreduzibel auf $\mathfrak{H}$ ist, so ist es auch zyklisch auf $\mathfrak{H}$ bezüglich jedes Vektors, insbesondere bezüglich Ω. Sei $\hat{B}_x$ ein Element aus $\hat{\mathfrak{B}}$ und $\hat{B}_x \Omega = x$. Wie man sieht, gibt es dann auch ein Element B_x aus $\mathfrak{B}$, so daß $B_x \Omega = x$ ist. Also ist $\mathfrak{B}$ zyklisch bezüglich Ω in $\mathfrak{H}$.

Vergleichen wir das Ergebnis noch mit dem Zeitschichtaxiom. In seiner ursprünglichen Fassung hat es Haag folgendermaßen ausgesprochen: Ist die Feldoperatoralgebra irreduzibel, so soll bereits die Feldoperatoralgebra $\mathfrak{B}$ über einer Zeitschicht irreduzibel sein. Hier wurde aus den Voraussetzungen (1) bis (5) (die Voraussetzung über die Lokalität wurde nicht benutzt) bewiesen: Ist die Feldoperatoralgebra $\mathfrak{A}$ zyklisch, so ist bereits die Feldoperatoralgebra $\mathfrak{B}$ über einer beliebigen Menge G des Minkowskiraumes, welche eine offene Menge G^0 enthält, also insbesondere über einer Zeitschicht, zyklisch. Von den Algebren $\hat{\mathfrak{A}}$ und $\hat{\mathfrak{B}}$, die man aus $\mathfrak{A}$ bzw. $\mathfrak{B}$ im wesentlichen durch Hinzunahme von P_Ω (Projektionsoperator auf Ω) erhält, wurde gezeigt: $\hat{\mathfrak{A}}$ ist irreduzibel und sogar $\hat{\mathfrak{B}}$ ist irreduzibel.

Wie man sich für lokale Felder leicht überlegt, ist $\mathfrak{B}$ für ein kompaktes G der angegebenen Art nicht irreduzibel. Für eine Schicht (parallel zu $t = 0$) hat Haag durch ein Beispiel gezeigt (*), daß die zugehörige Algebra $\mathfrak{B}$ im allgemeinen noch nicht irreduzibel ist, wenn die Voraussetzungen (1) bis (6) erfüllt sind.

* * *

Herrn Prof. HEISENBERG danken wir für sein Interesse, Herrn Prof. HAAG für wichtige Hinweise. Herr E. SCHEIBE und Herr H. J. BORCHERS haben durch Verbesserungsvorschläge bzw. kritische Bemerkungen zur vorliegenden Fassung der Abschnitte 3·1 bzw. 3·5 beigetragen, wofür wir ihnen besonderen Dank schulden.

(*) Private Mitteilung.

Anhang I

Aufweisen eines Jostpunktes und seiner Umgebung.

G enthalte die offene Menge G^0 des Minkowski-Raumes. Dann kann man eine Gerade g in einer Ebene $t = \text{const.}$ gelegen, so finden, daß der Durchschnitt von G^0 mit g eine in der Topologie von g nicht leere offene Menge ist, *d.h.* eine Vereinigung von offenen Intervallen auf g. Sei y_1 die laufende Koordinate auf der Geraden g. Es genügt eines der offenen Intervalle z.B. $a < y_1 < b$ zum Beweis. Hierzu verteile man die Punkte $x_1, x_2, \ldots, x_n$ so auf der Geraden g, daß

$$x_1 = a + \frac{1}{n+1}(b-a), \qquad x_2 = a + \frac{2}{n+1}(b-a), \ \ldots, \ x_n = a + \frac{n}{n+1}(b-a),$$

ist. Durch Wahl eines genügend kleinen ε kann man erreichen, daß zu jedem n-Tupel $z_1, z_2, \ldots, z_n$, die in einer ε-Umgebung von $x_1, x_2, \ldots$ bzw. x_n liegen (die in der Topologie des R_1 gemeinte Umgebung ε kann und soll natürlich ganz in G^0 liegen)

$$\sum_{\alpha=0}^{3} (x_k^\alpha - z_k^\alpha)^2 < \varepsilon^2, \qquad k = 1, 2, \ldots, n,$$

ein Jostpunkt $z_1 - z_2$, $z_2 - z_3$, ..., $z_{n-1} - z_n$ gehört. Damit hat man eine reelle Umgebung zu $x_1 - x_2$, $x_2 - x_3$, ..., $x_{n-1} - x_n$ erhalten, die aus Jostpunkten besteht.

Anhang II

Beweis des Hilfssatzes.

Nach Voraussetzung existiert für alle Testfunktionen $f_\nu \in \mathfrak{S}$

$$(a) \qquad \langle \Omega, A(f_1) \ldots A(f_l)\, CA(f_{l+1}) \ldots A(f_n)\Omega \rangle ,$$

und ist stetig und linear in den f_ν. Denn wenn $f_\nu \to 0$, verschwindet auch (a). Daher stellt (a) eine temperierte Distribution dar, symbolisiert durch

$$(b) \qquad \langle \Omega, A(y_1) \ldots A(y_l)\, CA(y_{l+1}) \ldots A(y_n)\Omega \rangle .$$

Wegen der Spektrumsbedingungen hängt (b) in der durch (21) angegebenen Weise von den Koordinaten ab, und es ist die Fouriertransformierte $\widetilde{F}_{ln}(p_1, \ldots, p_l, p_{l+1}, \ldots, p_n)$ nur dann von Null verschieden, wenn alle p_α im VK liegen. Da $\widetilde{F}_{ln}$ mit F_{ln} auch temperierte Distribution ist, folgen die verlangten analytischen Eigenschaften genau wie bei den Wightmanfunktionen.

RIASSUNTO (*)

Al principio (Sez. 2) consideriamo quelle teorie di campo che sono caratterizzate da operatori definiti in superfici spazio-simili. In relazione a questo si discute il teorema di Haag. Poi si analizzano le proprietà dell'algebra degli operatori di campo (Sez. 3). Segue che l'algebra $\mathfrak{B}$, definita nella Sez. 3·5, è già ciclica. Inoltre l'algebra $\hat{\mathfrak{B}}$, a cui essenzialmente si perviene aggiungendo a $\mathfrak{B}$ l'operatore di proiezione nello stato vuoto, è irriducibile.

(*) *Traduzione a cura della Redazione.*

IL NUOVO CIMENTO Vol. XXII, N. 5 1° Dicembre 1961

Λ^0's from K^- Capture in Emulsion.

R. Cester, G. Ciocchetti, A. Debenedetti, A. Marzari Chiesa, G. Rinaudo

Istituto Nazionale di Fisica Nucleare - Sezione di Torino

C. Deney (*), K. Gottstein and W. Püschel

Max-Planck-Institut für Physik und Astrophysik - München

(ricevuto l'11 Ottobre 1961)

Summary. — The energy distribution of Λ^0 coming from K capture stars has been obtained measuring Λ^0 found by area scanning in two emulsion stacks. This distribution, compared to a theoretical one obtained with an optical model calculation, gives indication that the percentage of multi-nucleon captures in nuclear emulsions of the order of 30%. To the same conclusion we are led by the detailed study of 103 capture stars correlated to Λ^0 decay. From the study of the missing energy in K^- capture stars we deduce that the probability for a π^0 of being absorbed in nuclear matter is very low. There is evidence that the probability for the emission of a Λ^0 is not strongly dependent on the atomic weight of the nucleus in which the K^- was absorbed. The upper limit for the cryptofragment formation is 15%. A search for the formation of Y_1^{*-} in the reaction $K^- + 2n \to Y_1^{*-} + n$ of a K^- at rest in the emulsion nuclei gives no conclusive result due to the low statistics.

1. – Introduction.

Several investigations on K -meson absorptions in nuclear emulsion have been carried out in which the emission of neutral hyperons has been studied. Both direct and indirect methods have been used (1).

(*) Now at Louisiana State University, Baton Rouge.

(1) See, *e.g.*, D. H. Davis, M. Csejthey-Barth, J. Sacton, B. D. Jones, B. Sanjevaiah and J. Zakrzewski: *Nuovo Cimento*, **22**, 275 (1961). This paper gives also references to earlier work.

We have applied a direct method consisting in first collecting a sample of Λ^0-hyperons and then searching along their line of flight for their origins in K^- absorptions. The latter were then analysed with a view to studying the Λ^0 production modes.

2. – Experimental procedure.

A systematic scan for Λ^0-decays was made on two large stacks of G-5 emulsions exposed at two different times to a beam of 450 MeV/c K^- stopping in emulsion. In what follows we shall refer to the two stacks as T-stack and M-stack.

Experimental details are reported in Table I.

TABLE I.

	No. plates	No. of beam protons	Estimated number of K^- incident on the stack (*)	Scanned area (cm^2)	Λ^0/cm^2	Total number of Λ^0
M	120 (5 in. $\times$ 8 in. $\times$ 600 μm)	$4 \cdot 10^{14}$	10000	689	0.22	154
T	101 (6 in. $\times$ 9 in. $\times$ 600 μm)	$3.25 \cdot 10^{14}$	8000	376	0.52	194

(*) UCRL-8269.

15 plates of the T-stack were also scanned for K^- capture stars, in order to measure the space distribution of K^- interactions at rest and their total number. The total number of K^- stars present in the stack was estimated to be 1750, in reasonable agreement with the figure of Table I, when allowance is made for interactions in fligt.

The volume scanned for Λ^0 was located in the region of maximum K stop density.

In the Λ^0 search, all two-pronged stars were recorded, provided that no indication of the occurrence of a nuclear interaction (electron, blob) was visible at the vertex. The two prongs of the event were then followed until they came to rest, and their range was carefully measured; when they interacted or left the stack, their velocity was derived from ionization measurements. In the T-stack, those events (about 10% of the measured Λ^0's) in which the light

track had approximately the beam direction were not analysed, because of both the difficulty of following back, and the high background of one-prong interactions of the π^- beam tracks.

154 (M-stack) and 194 (T-stack) events were found to be compatible with Λ^0 decays from the calculated Q-value. The Q-value distribution is given in Fig. 1.

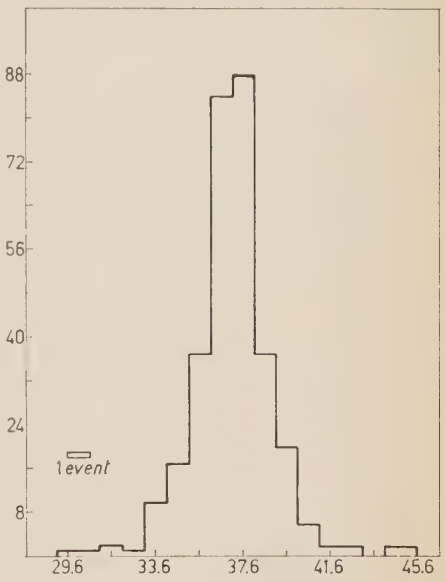

Fig. 1. – Q-value distribution.

The line of flight of 327 Λ^0 was then computed. For each Λ^0, the length $l_T = \tau(p_\Lambda/m_\Lambda)\ln 2$ (with $\tau = 2.505 \cdot 10^{-10}$ s) was also computed. l_T is defined as the path length in which a Λ^0 of momentum p_Λ has probability $\frac{1}{2}$ of decaying. In order to correlate the Λ^0 decay to its origin, a scan for K^- stops was made along the Λ^0 line of flight, for a length l_T.

The uncertainty in the determination of the Λ^0 direction, due to measurement errors, was taken to be $\Delta\alpha = 2°$ in the emulsion plane and $\Delta i = 3°$ in dip. These figures were increased to $\Delta\alpha = 4°$ and $\Delta i = 5°$ for events in which the proton range was shorter than 500 μm, and/or the dip angle of either particle was larger than 45°. The distribution of Λ^0 origins, as functions of $\Delta\alpha$ and Δi, for both the M and T-stacks, are given in Fig. 2.

The distribution in $\Delta\alpha$ and Δi for the T-stack indicate that the estimate of the error is reasonable, and that the number of Λ^0 origins outside the scanned cone is very small. The same is true for the $\Delta\alpha$ distribution in the M-stack. There is however an indication that in the M-stack the error in dip was larger than that estimated. This could explain the larger percentage found in the M-stack of Λ^0 uncorrelated with a K^- (*).

All K^- capture stars in the allowed cone were then carefully analysed, the energy of evaporation tracks was deduced from range measurements (tracks shorter than 110 μm were taken as α-particles, the others were assumed to be protons). Fast prongs were followed till they came to an end or left the stack.

(*) The same procedure was also tried using a length $l_T = \tau(p_\Lambda/m_\Lambda)\ln 5$. This is the path length for which the decay probability is $\frac{4}{5}$. It turned out, however, that a cone of length l_{T5} contained too high a background of uncorrelated K events in our stacks.

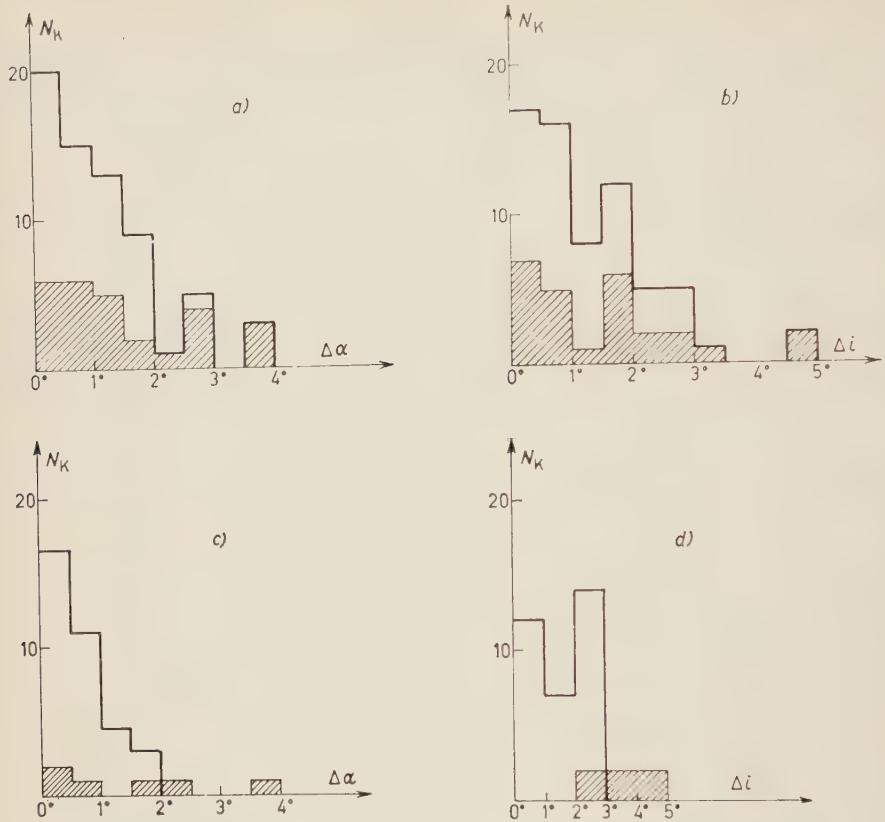

Fig. 2. – Distribution of K^- stars inside the Λ^0 « cone of flight » as a function of $\Delta\alpha(a, c)$ and $\Delta i(b, d)$ for the T-stack (a, b) and the M-stack (c, d). In the shaded area are events for which the cone of flight had opening angles $\Delta\alpha \leqslant 4°$ and $\Delta i \leqslant 5°$. (Events with only 1 K^- found in the cone).

3. – Scanning efficiency.

One of the purposes of the present work is to give the energy spectrum of the Λ^0 particles produced when K 's are captured at rest by emulsion nuclei ([2,3]). However, the results could get obscured by detection biases. It is well known that the scanning efficiency for two-prong stars in emulsion is in most cases rather low ([2]). In the T-stack, a determination of the scanning

([2]) C. J. Mason: *Thesis*, UCRL 9297.

([3]) J. Bogdanowicz, A. Filipkowsky, A. Krzywicki, E. Marquit, E. Skrzypczak, A. Wroblewski and J. Zakrzewskj: Institute of Nuclear Research - Polish Academy of Sciences. Report No. 107/VI (1959).

losses was carried out by re-scanning a fractional area. This gave an overal efficiency of about $(40 \pm 10)\%$.

As will be seen in Section 3, an efficiency of 46 % is obtained by comparing the total number of Λ^0's found in the scanned volume with that from a Monte-carlo calculation. In the M-stack, the efficiency was possibly still lower, as might be indicated by the data of Table I. However, the scan of the M-stack covered a larger area including regions of lower Λ^0 density. Moreover the general background was also higher in the M-stack than in the T-stack.

The possible sources of loss were carefully investigated with the aim of studying their dependence on the Λ^0 energy. Losses are due to:

1) surface-glass effect;

2) steepness of at least one of the tracks;

3) small difference in ionization between the tracks;

4) Λ^0 opening angle small or large;

5) short proton range;

6) low ionization of the tracks.

For 1), the loss was estimated to be about 12 % from the distribution of events as a function of the depth in emulsion. For 2) the loss was estimated by comparing the experimental distribution, as a function of the dip angle for both proton and pion, with the expected uniform distribution. This loss amounts to about 30 % for the T-stack, and 40 % for the M-stack.

Losses due to 1) and 2), however large, will not affect the shape of the Λ^0 energy spectrum. On the other hand, the percentage of events for which one of the conditions 3) to 6) holds true is a function of the Λ^0 energy; therefore losses due to these causes will tend to distort the energy distribution.

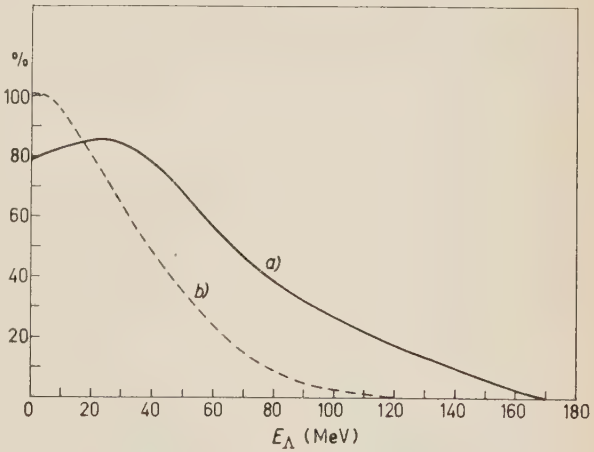

Fig. 3. – Efficiency curves as a function of Λ^0 energy: *a*) T-stack; *b*) M-stack.

In order to correct for this effect, we have built efficiency curves both for the M and T stack (see Appendix I) which are given in Fig. 3. The curves have been computed by comparing the experimental distributions with those expected if the decay particles are assumed to be emitted isotropically in the

Λ^0 center of mass. This hypothesis is supported by the center of mass distribution as a function of the Λ^0-π angle, which shows no evidence for a backward-forward asymmetry within the experimental uncertainties (4).

4. – Montecarlo calculation and Λ^0 energy distribution.

In order to estimate the total number and the characteristics of the Λ^0 decaying in the scanned volume, a Monte Carlo calculation was carried out. The input data are:

1) The experimental space distribution of stopping K's: $\varrho(x, y, z) = -\varrho(x)\,\varrho(y)\,\varrho(z)$ (the one dimensional distributions were found to be roughly independent). $\varrho(x, y, z)$ was measured in the T-stack and therefore the Monte Carlo results are directly comparable only to the data obtained in that stack.

2) The distribution of the Λ^0 production angle, taken to be isotropic in the laboratory system.

3) The Λ^0 decay law ($\tau = 2.505 \cdot 10^{-10}$ s).

4) The calculated energy distribution of Λ^0 emitted from emulsion nuclei when a K^- is captured at rest (Appendix II).

The output results of the Monte Carlo calculation are the following (some of the Monte Carlo outputs should not critically depend on the K distribution. In these case the M-stack and T-stack results were added for the comparison with the Monte Carlo output):

1) The total number of Λ^0 decaying in the scanned volume. In the T-stack, for a total number of 4 750 K's stopping in the stack, and with a probability 0.517 (5) that a K^- captured in emulsion gives a Λ^0 decaying by its charged mode, the expected number of Λ^0 in the scanned region is 120. The corresponding overall scanning loss is $(54 \pm 7)\%$ (*).

(4) *Proc. Rochester Conference 1960*, p. 441.

(5) K^- COLLABORATION: *Nuovo Cimento*, (I) **13**, 690 (1959); (II) **14**, 315 (1959).

(*) The possible formations of cryptofragments which would partly justify the discrepancy between experimental and Montecarlo results, has not been taken into account. In fact, from a rescan we know that our scanning efficiency for Λ^0 is $(40 \pm 10)\%$ which agrees, within the errors, with the expected efficiency of $(46 \pm 7)\%$, so that the assumption of a large fraction of cryptofragments is not justified. In order to set an upper limit to cryptofragment production we estimated by rescanning the lower limit for K stars detection efficiency which turned out to be 85%. This would mean that the fraction of cryptofragments is $\leqslant 15\%$ of all K^- captures.

2) The range distribution of the analysed Λ^0. This is given in Fig. 4 together with the experimental result. There is an indication that, scanning along the Λ^0 lines of flight, there was a loss of K^- origins within a distance of 4 mm from the Λ^0 decay point. This could be due to the fact that a small error in the co-ordinates of a K near the Λ^0 decay would lead to large errors in α and i; therefore in the selection of correlated events there could be a bias against short Λ^0 ranges.

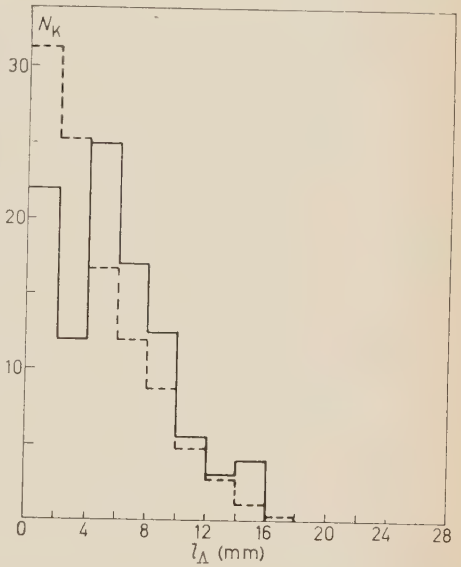

Fig. 4. – Distribution of flight lengths of Λ^0 with only one associated K (M-stack and T-stack). The dashed histogram gives the Monte Carlo output distribution.

3) The percentage of Λ^0 decaying within a length corresponding to a decay probability of $\frac{1}{2}$, inside the scanned volume. This was found to be 66%. This value must be corrected to take into account scattered Λ^0 (about 5.5% if the Λ^0 cross-section is assumed to be geometrical) and Λ^0 coming from Σ interactions (about 7.7% from the results of the K^- Collaboration ([5])).

As a result we should expect 100 Λ^0 to be correlated, while the experimental number is 82 (T-stack). This discrepancy is due to the low efficiency in detecting K_ϱ events (as can be seen comparing the value (0.08 ± 0.02) of the ratio K_ϱ/K_Λ (where K_Λ indicates capture stars with no charged strange particles emitted) to the value 0.2, found for the same ratio by the K^- collaboration group ([5])) and to the loss of K^- origins at a short distance from the Λ^0 vertex (see above).

4) The Λ^0 energy distribution, corrected for the finite volume scanned.

This Λ^0 energy distribution was multiplied by the efficiency curve plotted in Fig. 3-*a*, so that it could be directly compared with the experimental one. An analogous procedure was followed for the M-stack. The combined results are given in Fig. 5. In this a theoretical distribution is also reported, in which the percentage of multinucleon reactions has been taken to be zero. This one also had been previously corrected for finite volume and efficiency losses.

It appears from the comparison that the percentage of multinucleon reactions is not greater than 30%. However a precise estimate cannot be ob-

tained since the corrected energy distribution is rather insensitive to the percentage of multi-nucleon processes.

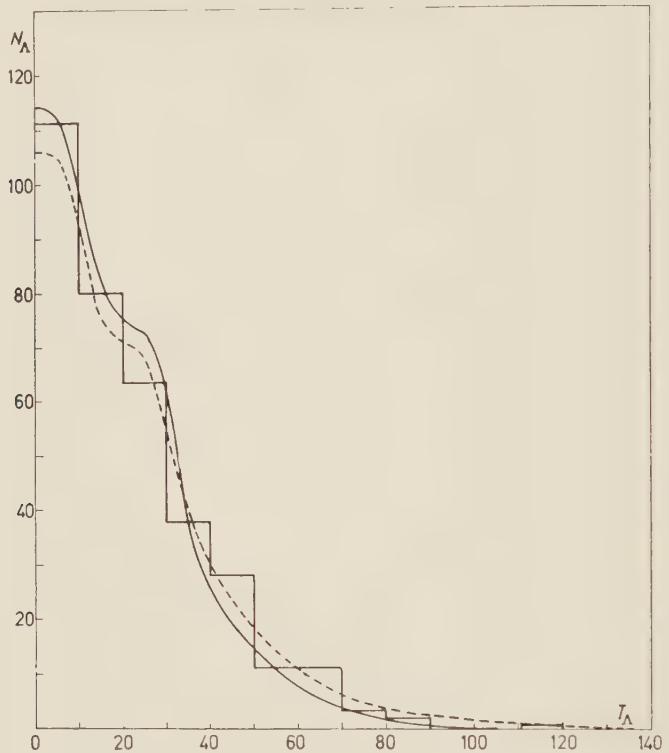

Fig. 5. – Energy distributions of Λ^0 (T+M stack). The curves give the calculated distributions if we take the $2\mathcal{N}$ reactions to be 0 (full line) or 30% (dashed line), modified to take into account finite volume and scanning efficiency effects.

5. – Correlation between Λ^0 and K^-.

The purpose of following back the Λ^0 along their line of flight to their K-capture origin is a detailed study of the features of such capture stars. The results of the scanning are reported in Table II.

TABLE II.

No. of K's in the cone of ½ probability	0	1	2	3	4	5	Total no. of K's
No. of events:							
T-stack	91	66	13	1	2	0	103
M-stack	108	37	4	3	1	1	63

The degree of correlation between the Λ^0 decays and the K^- stars found in the Λ^0 cone of flight (see Section **1**) will first be discussed. We have computed the total number of background K's expected to be present in the volume scanned for Λ^0 origins, and the spurious Λ^0 range distribution derived from that. This calculations could only be carried out for the T-stack, where the distribution of the K^- stars was known. The total number of background K's is 34, to be compared with the 103 K^- actually found. Fig. 6 gives the Λ^0 range distribution, together with the distribution expected if the background K's were consistently mistaken for Λ^0 origins; from the comparison of the two histograms, we estimate the maximum contamination of background K's among the events with only one K^- to be $\sim\frac{1}{4}$. An independent check of this result is provided by the number of K^- stars, found in the Λ^0 cones of flight, from which a charged strange particle was emitted (Σ and double stars). The number of such stars is found to be $(3\div4)\,\%$ of the total number of K^- captures. This value, compared to the 16% found by the K^- collaboration ([5]), leads us again to an estimate of $(20\div25)\,\%$ for the maximum number of background K's.

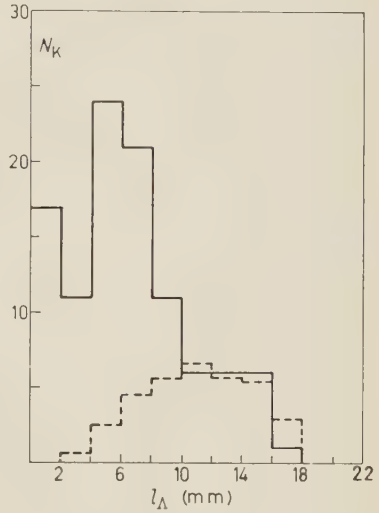

Fig. 6. – Distribution of all K's origins as a function of Λ^0 range (T-stack). The dashed histogram gives the calculated distribution of the background K^-.

Finally, we checked how well the Λ^0 range distribution fits an exponential decay law. For this purpose, we plotted in Fig. 7 the number of Λ^0 decays *vs.* the ratio l_Λ/l_T (where l_Λ is the Λ^0 range, and l_T has been defined in Section **9**).

The distribution corresponding to an exponential decay law is also shown. A comparison of the histogram and the curve shows a deviation of the experimental range distribution from the exponential decay law; this is obviously due

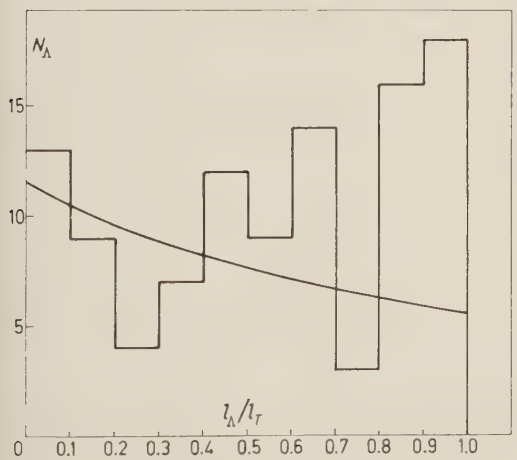

Fig. 7. – Distribution of Λ^0 as a function of l_Λ/l_T. The curve gives the exponential decay law distribution.

to the presence of background K's, whose distribution will be strongly peaked at large values of l_Λ/l_τ. If we normalize the two distributions given in Fig. 6 to the first half of the spectrum ($l_\Lambda/l_\tau < 0.5$), where the expected contribution of background K's is practically zero, we estimate the total contamination of background K's to Λ^0 origins to be about 25%, in good agreement with what was previously obtained.

We feel confident that in at least 75% of the cases in which only 1 K^- was found in the decay cone, the Λ^0 really originated in that K^- absorption.

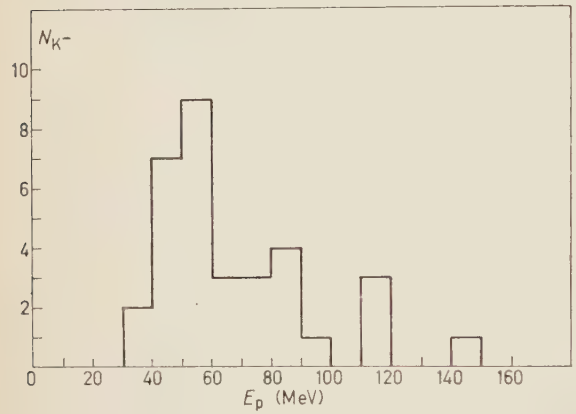

Fig. 8. - Energy distribution of charged π's emitted from Λ^0 origins.

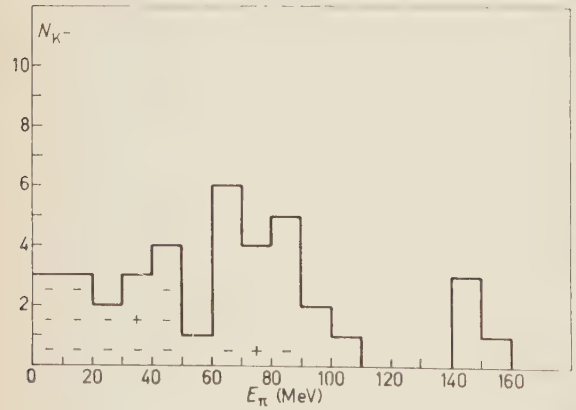

Fig. 9. – Energy distribution of fast protons (E_p 30 MeV) emitted from Λ^0 origins.

6. – Analysis of correlated K^- stars.

A detailed analysis of the Λ^0 origins was made only where there was no ambiguity in the choice of the K-star (only one K-capture in the cone of flight). The following considerations are therefore based on rather limited statistics. The characteristics of the stars are given in the Table III and Fig. 8, 9. (21 ± 5)% of the K^- stars emit a short prong (lenght between 5 μm and 41 μm). This is to be compared with the data of GROTE (6) *et al.*, who find that 22% of all K^- absorptions in emulsion are associated with a prong of that length. This indicates that the probability for the emission of a Λ^0 does not depend strongly on the atomic weight of the nucleus in which the K^- was absorbed.

(6) C. GROTE, I. HAUSER, U. KUNDT, U. KRECKER, K. LANIUS, K. LEWIN and H. W. MEIER: *Nuovo Cimento*, **14**, 532 (1959).

TABLE III. – (T+M)

No. of evaporation prongs	0	1	2	3	4	5	6
Events with a $\pi^{\pm}$	14	14	6	4	0	0	0
Events with a fast proton	10	7	2	7	0	1	2
Events with evaporation tracks only	8	10	6	5	3	4	0

In 38 out of 103 such stars, a charged π-meson was emitted. The efficiency for π detection was estimated to be nearly 1. All the pions were followed till they interacted, came to rest or left the stack. In 16 cases, the pion came to rest in emulsion, so that its charge could be determined. The ratio π^+/π^- is 2/14.

As already mentioned, the energy of the pions was estimated when possible from the range, otherwise from ionization measurements. 12 out of 38 π's have an energy greater than 86 MeV, which is the largest value expected for the energy of a π emitted together with a Σ in a one-nucleon reaction. The figure $12/38 = 0.31$ represents the minimum value of the ratio ($\pi^{\pm}$ with direct Λ^0)/($\pi^{\pm}$ with Λ^0 emitted) and can be compared with the corresponding ratio deduced from the results of the deuterium experiment. If we take the $\Sigma \to \Lambda^0$ conversion factor to be 0.5, the expected ratio would be 0.28.

The number of two-nucleon interactions can be indirectly estimated by subtracting from the total number of stars the number of events in which a pion is emitted. From the number of stars emitting charged pions, and from the results of the deuterium bubble chamber group ([7]), the number of π^0 has been estimated to be 29 ± 5. A value of 10% was assumed for the absorption of charged pions. The contribution of two-nucleon interactions without pion production turns out to be about 30%.

In Fig. 9 the energy of the fast proton ($E \geqslant 30$ MeV) emitted in the K-stars is given. The interpretation of the histogram is very involved, as many processes in nuclear matter contribute protons of energy greater than 30 MeV: π-absorption, Σ and Λ scattering, two-nucleon interactions. However, in the region $E_p \geqslant 80$ MeV, the main contribution should arise from two-nucleon processes, and, moreover, almost all the protons from two-nucleon interactions should have energy in this region. From the 9 protons in this energy region, and taking into account the possibility of fast neutrons being emitted, we obtain an estimate of about 20% two-nucleon interactions. Both these estimates of the contribution of two-nucleon reactions should be, however, taken as lower limits since the sample of Λ^0 we are studying is affected by an energy-

([7]) O. DAHL, N. HORWITZ, D. MILLER, J. MURRAY and M. WATSON: *Proc. Rochester Conference* (1960), p. 415.

dependent loss of Λ^0's and therefore biased against two-nucleon reactions (*).

The percentage of K^- absorptions in which a proton of energy > 60 MeV is emitted (15/103) agrees within statistics with that ($(12.7 \pm 0.7)\%$) given by DAVIS *et al.* (1), for K absorptions for which the emission of only stable particles (with or without pions) was assumed. DAVIS *et al.* conclude that a substantial proportion of fast protons is emitted as a result of stimulated decays of Λ^0 bound within cryptofragments. Our data show that these protons are emitted in the presence of Λ^0's.

We have tried to analyse the neutral component emitted from the K^- capture stars, studying the missing energy, in the reaction $K^- + n \to \Lambda^0 + \pi$, defined as $\Delta E = (M_K + M_n - E_B) - (M_\Lambda + T_\Lambda + M_\pi + T_\pi) - (T_{eV\ pr} + E_{GeV\ pr}) - E_A$ where E_B is the binding energy of the interacting nucleon, T_Λ, T_π, the kinetic energy of the Λ, π emitted in the reaction. $T_{eV\ pr}$ and $E_{GeV\ pr}$ the kinetic and binding energies of the charged evaporation prongs, and E_A the excitation energy of the nucleus.

In the events in which a charged π is emitted, the missing energy is associated with neutral stable prongs. The average value per event is 38.7 MeV; the corresponding value for emitted protons, deduced from the same events, is 16.9 MeV. The difference can be explained with the ratio $N/P = 2$ of nucleons emitted from nuclei ([8,9]).

In the events in which no charged π is emitted the missing energy will be shared by produced π^0, evaporated neutrons and fast neutrons emitted. In these events the analysis of the missing energy allows us to estimate the number of π^0 escaping from the nucleus, given the neutron evaporation just deduced, and the number and energy of fast neutrons. This is estimated from the number of fast protons, taking the ratio N/P to be 2 for energies less than 80 MeV and 1 for energies larger than 80 MeV. This last value is obtained (regarding these events as two-nucleon reactions) from I-spin considerations and from Eisenberg's results ([9]) on the (fast Σ^-)/(fast Σ^+) ratio. From their charged counterpart we then deduce the total energy of fast neutrons. If we take the total energy associated to a π^0 to be $E_{\pi^0} = m_{\pi^0} + T_\pi = 205$ MeV (where $m_{\pi^0} = 135$ MeV, and $T_\pi = 70$ MeV is the average $\pi^\pm$ kinetic energy), we deduce that 30 π^0 have been emitted from the nucleus. This value, compared to the number $N_{\pi^0} = 29 \pm 5$ of π^0 at production, indicates that the absorption of π^0 in nuclear matter is low, in contradiction with the conclusions of the K^- collaboration ([5]) work which suggests an absorption rate of 80%.

(*) We are grateful to Dr. Y. EINSENBEG for pointing out this fact.

([8]) N. METROPOLIS, R. BIVINS, M. STORM, A. TURKEVICH, J. M. MILLER and G. FRIEDLANDER: *Phys. Rev.*, **110**, 185, 204 (1958). The ratio P used is deduced from the results for absorption of π^- in ^{100}Ru.

([9]) Y. EISENBERG, M. FRIEDMANN, G. ALEXANDER and D. KESSLER: *Nuovo Cimento*, 22, 1 (1961).

7. – Search for the $\pi\Lambda$ resonance.

ALSTON *et al.* [10] have reported the production in hydrogen of the isobar Y_1^* which decays according to the mode:

$$Y_1^{*\pm} \to \Lambda^0 + \pi^\pm . \tag{1}$$

We have searched for the occurrence of Y_1^* production by two-nucleon absorption of K^- in the heavy nuclei of the emulsion. For this purpose we have applied the method of EISENBERG *et al.* [11] who investigated the production of Y_0^* by K^- absorption in emulsion.

The method consists in the calculation of the invariant mass

$$M = [(W_\pi + W_\Sigma)^2 - (P_\pi + P_\Sigma)^2]^{\frac{1}{2}} ,$$

where W is the total energy and P the vector momentum. The distribution of M should be narrower than that of $(W_\pi + W_\Sigma)$ if Σ and π are indeed due to the decay of Y_0^*.

We have applied Eisenberg's method to those of our events in which a Σ^0 and a charged pion were emitted. Fig. 10 shows the distribution of the invariant mass M, Fig. 11 for comparison that of $W = W_\Lambda + W_\pi$ « Clean » events

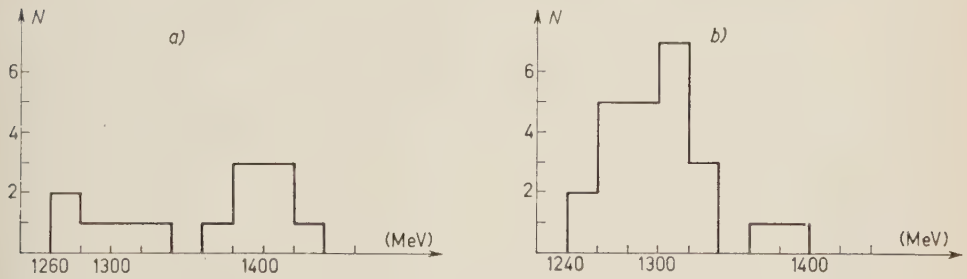

Fig. 10. – $M = (W^2 - P^2)^{\frac{1}{2}}$: *a*) « clean events »; *b*) « dirty » events.

are those in which no visible tracks emerge from the stopping point of the K^- apart from that of the pion. The « dirty » events contain also evaporation tracks.

[10] M. H. ALSTON, L. W. ALVAREZ, P. EBERHARD, M. L. GOOD, W. GRAZIANO, H. K. TICHO and S. G. WOJCICKI: *Phys. Rev. Lett.*, **5**, 520 (1960).

[11] Y. EISENBERG, G. YEKUTIELI, P. ABRAHAMSON and D. KESSLER: *Nuovo Cimento*, **21**, 563 (1961).

The « dirty » events show no evidence for a peak near 1400 MeV. Among the « clean » events, however, there is some indication for such a peak near 1400 MeV. This may be due to either one of two cases:

a) Direct production of Λ^0 in the reaction $K^- + n \to \Lambda^0 + \pi^-$. The expected value of W for this case would be 1434 MeV for a bound nucleon.

b) Y_1^{*-} production with subsequent decay according to (1).

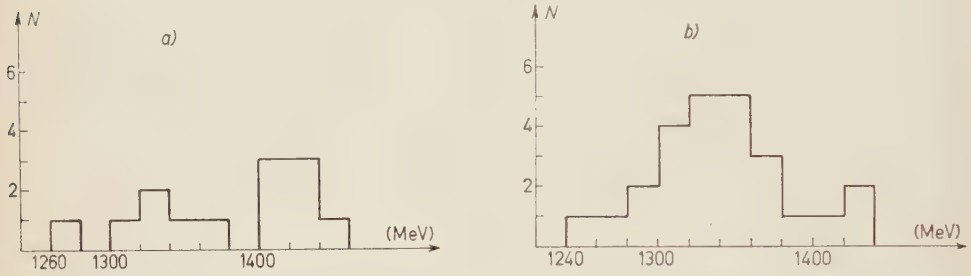

Fig. 11. – $W = W_\pi + W_\Lambda$: *a*) « clean events »; *b*) « dirty » events.

It should not be due to direct Σ^0 production and subsequent Σ^0 decay because in this case the maximum kinetic energy of the pion is 92 MeV and of the Λ^0 about 27 MeV which corresponds to a maximum value of W of only 1374 MeV.

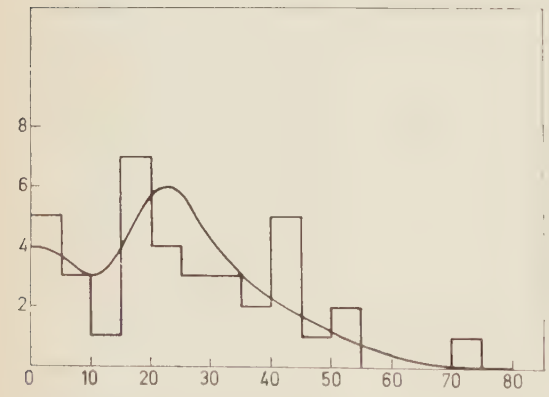

Fig. 12. – Energy distribution for Λ^0 emitted with a charged π. The curve shows the expected energy distribution if no Y_1^{*-} is found.

The indirect production of Λ^0 by a directly produced Σ is also unlikely to result in a value of W as high as 1400 MeV.

We have also plotted the energy distribution of the Λ^0 for all events together (Fig. 12). There is an indication of a broad peak around 20 MeV which may be interpreted as due to normal Λ^0 production, Fig. 12. There is no convincing evidence for a Y_1^{*-} effect.

8. – Conclusions.

The energy distribution of Λ^0 coming from K-capture stars has been obtained measuring Λ^0 found by area scanning in two emulsion stacks. This distribution, compared to a theoretical one obtained with an optical model

calculation gives indication that the percentage of multi-nucleon captures in nuclear emulsions is of the order of 30%. To the same conclusion we are led by the detailed study of 103 capture stars correlated to a Λ^0 decay, both from the percentage of stars emitting charged pions, and from the number of stars with a proton of energy larger than 80 MeV.

From the study of the missing energy in K^- capture stars we deduce that the probability for a π^0 of being absorbed in nuclear matter is very low.

There is evidence that the probability of emission of a Λ^0 is not strongly dependent on the atomic weight of the nucleus in which the K^- was absorbed.

Our results are compatible with the hypothesis that no cryptofragments are formed in K^- captures at rest in the emulsion nuclei. The upper limit to the occurrence of such events is 15%.

A search for the formation of Y_1^{*-} in the reaction $K^- + 2n \rightarrow Y_1^{*-} + n$ of a K^- in the emulsion nuclei gives no conclusive result due to the low statistics.

* * *

The authors wish to thank Dr. A. WERBROUCK for carrying out the Monte Carlo calculation and Mr. G. LÜTJENS for programming and supervising the kinematical calculations on the G2 electronic computer. We are grateful to Professors CASTAGNOLI, GARELLI, VIGONE and Dr. TIETGE for many stimulating discussions. Miss N. MARGEM took part in the early development of this work.

Thanks are due to the Munich and Torino scanning teams for their valuable work, in particular to Fr. BAUMBACH and Frl. HABENSCHADEN. Two of us (R.C. and C.D.) are grateful to the Max-Planck-Institut für Physik und Astrophysik for financial support and hospitality during the early part of this work. C.D. thanks for financial support also the Deutsche Akademische Austauschdienst.

APPENDIX I

For the calculation of an efficiency curve as a function of Λ^0 energy one would need to compare, for each energy interval, an expected number of events having certain characteristics (angle, ionization, etc.) with the number actually observed. This procedure requires a great subdivision of the events, and therefore a statistics much larger than what we have. The calculation we carried out, although not rigorous, gives an efficiency distribution such that losses for high energy are certainly over estimated. This allows us to set an upper limit to the frequency of high energy Λ^0, and therefore to the occurrence of multi-nucleon reactions.

We first computed the probability of detecting the following two types of events:

a) events in which there is a small difference in ionization between the tracks ($\Delta\beta \geqslant \beta_p - \beta_\pi$ small). In these cases the proton is emitted forward in the c.m.s. For Λ^0 in the observed energy interval, these events will appear to the scanner as small angle scatterings (Λ^0 opening angle large) and will easily be missed.

b) Events in which the Λ^0 opening in the laboratory system is small. These events are likely to have a high energy pion (emitted forward in the c.m.s.), and/or a short proton track. ($\Lambda_p \leqslant 200$ μm) and are therefore difficult to detected.

The procedure for computing the detection efficiency for events of type *a*) is the following.

The expected number of events with E_Λ less than 40 MeV was computed for each interval of $\Delta\beta$, assuming isotropy in the decay, in the c.m.s. The number of events was calculated assuming the true energy spectrum to be the experimental one up to $E_\Lambda = 40$ MeV. This implies the a priori assumption that the energy spectrum below 40 MeV is not distorted by energy dependent losses. As Fig. 3 shows this turns out to be not too far from the truth.

The ratio of the computed numbers of events to the experimental numbers, normalized to

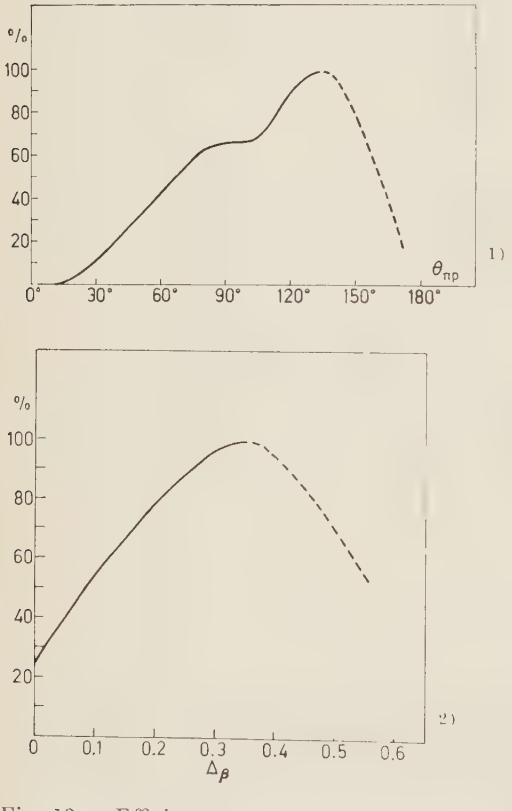

Fig. 13. – Efficiency curves as a function: 1) of Λ^0 opening angle; 2) of the difference in ionization between the two decay prongs; 3) of the decay proton energy.

the point of maximum efficiency, are plotted in Fig. 13-2). An analogous procedure applied to events of type *b*) leads to Fig. 13-1).

In order to take into account the energy-dependence we then calculated

the distribution of $\Delta\beta$ and $\theta_{\pi p}$ in every energy interval up to $E_\Lambda \sim 150$ MeV, and derived for each interval an efficiency factor from Fig. 13-1 (13-2).

This was done in the following way.

For Λ^0 energies below 20 MeV, it can easily be checked that events which lie on the left-hand side of the maximum efficiency point in curve 13-1, lie on the right-hand side of the maximum efficiency point in curve 13-2. For constructing the total efficiency curve below 20 MeV, we then use only the efficiency factor derived from the left-hand part of either curve 13-1 or 13-2.

For Λ^0 energies higher than 20 MeV, both $\Delta\beta$ and $\theta_{\pi p}$ can lie on the left-hand side of the curves. Since in these cases the detection efficiency is further decreased, we tried to take this into account by assuming that the total efficiency factor in these cases is given by the product of the two individual inefficiencies.

However, a third effect also appears at higher Λ^0 energies: due to the lower ionization of both π and p tracks, the total efficiency for given $\Delta\beta$ and $\theta_{\pi p}$ will be reduced as compared to smaller Λ^0 energies. From the analysis of our data, it appears that only one event in which both tracks had $\beta > 0.4$ was found. We tried to estimate the loss due to this effect by computing the probability of detecting an event with a high energy proton. However the efficiency curve could only be drawn for proton energy up to 50 MeV, (as we consistently used Λ^0 with energy $E_\Lambda \sim 40$ MeV), and had to be extrapolated for higher values of the proton energy (Fig. 13-3).

From the product of the efficiency factors for $\Delta\beta$, $\theta_{\pi p}$ and E_p in each energy interval the efficiency curve of Fig. 3 was obtained. Since however the E_p distribution is not independent of the two others, the efficiency for high energy Λ^0 is likely to be underestimated.

Appendix II

The energy distribution of Λ^0 emitted from emulsion nuclei when K^- are captured at rest can be considered as the superposition of distributions corresponding to the following six Λ^0 producing channels:

1) *a*) $K^- + n = \Lambda^0 + \pi$;

b) $= \Sigma + \pi$, Σ converted into Λ^0 in nuclear matter;

c) $= \Sigma^0 + \pi$, $\Sigma^0 = \gamma + \Lambda^0$ (decay).

2) *a*) $K^- + 2n = \Lambda^0 + n + (\pi)$;

b) $= \Sigma + n + (\pi)$, Σ converted into Λ^0 in nuclear matter;

c) $= \Sigma^0 + n + (\pi)$, $\Sigma^0 = \gamma + \Lambda^0$ (decay).

Making use of an optical model ([12]) we computed the distribution of Λ^0 and Σ directly produced in K capture. From the Σ distribution we obtained

([12]) R. Capps: *Phys. Rev.*, **107**, 239 (1957).

TABLE IV ([5-12]).

$V_\Lambda = -15$ MeV	$V_\pi = -35$ MeV
$V_\Sigma = -15$ MeV	$V_B + E_A$ (*) { 20 MeV for 1 nucleon; 40 MeV for 2 nucleons

(*) E_A = excitation energy.

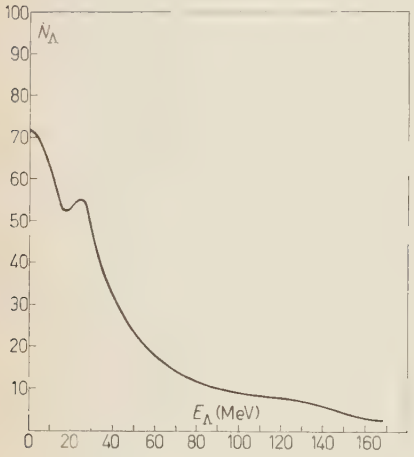

Fig. 14. – Monte Carlo input energy ditributions (2$\mathcal{N}$ reactions 30%).

the spectra of Λ^0 originated from process *b*) and *c*) (angular distributions were taken to be isotropic in the center of mass). For the momentum distribution of nucleons in nuclear matter we take

$$N(p)\,\mathrm{d}p = N_0 p^2 \exp[-p^2/\alpha^2]\,\mathrm{d}p\,,$$

$$\alpha = 160 \text{ MeV/c}:$$

The nuclear parameters used in the optical model calculation are reported in Table IV.

The spectra obtained from *a*), *b*) and *c*) were than weighted according to the results of the deuterium bubble chamber group ([6]) for one-nucleon interactions and taking for the Σ to Λ conversion ratio the value $(\Sigma \to \Lambda)/\text{all}\ \Sigma = 0.5$ ([5]).

The contribution of 2$\mathcal{N}$ reactions was tentatively assumed to be 30%. The result is given in Fig. 14.

RIASSUNTO

Si è ottenuta la distribuzione di Λ^0 prodotte in stelle di K^- catturati a morte in emulsione. Il paragone della distribuzione sperimentale di energia, con quella teorica calcolata con il modello ottico, indica che la percentuale di catture a più nucleoni nell'emulsione nucleare è circa del 30%. Alla stessa conclusione si giunge attraverso lo studio dettagliato di 103 stelle di cattura di K^- correlate a decadimenti di Λ^0. Le probabilità che un π^0 sia assorbito nella materia nucleare, ottenuta calcolando la « missing energy » nelle stelle di cattura dei K^- risulta molto piccola. Vi è indicazione che la probabilità di emissione di una Λ^0 non dipende molto dal peso atomico del nucleo in cui il K^- è catturato. Il limite superiore per la formazione di criptoframmenti risulta 15%. La scarsa statistica non permette di ottenere un risultato conclusivo sulla formazione dell'isobaro Y_1^{*-} nel processo $K^- + 2\mathcal{N} \to Y_1^{*-} + \mathcal{N}$ nei nuclei dell'emulsione.

LETTERE ALLA REDAZIONE

(La responsabilità scientifica degli scritti inseriti in questa rubrica è completamente lasciata dalla Direzione del periodico ai singoli autori)

Analysis of 1347 τ^- Decays (*).

M. Ferro-Luzzi (**), D. H. Miller, J. J. Murray,
A. H. Rosenfeld and R. D. Tripp

Lawrence Radiation Laboratory, University of California - Berkeley, Cal.

(ricevuto il 21 Agosto 1961)

Results are presented concerning the τ decay mode of a homogeneous sample of 1347 K^- decaying in flight in the 15 inch Lawrence Radiation Laboratory Hydrogen bubble chamber.

If weak interactions are invariant under time reversal, the spectra for the c.m. kinetic energies of the pions emitted in τ decay will be identical for both charged states of the K-meson. A comparison of our data with the total available statistics on τ^+ decay indicates good agreement between the two. For this reason, the data for τ^+ and τ^- have been combined, and the best fits to straight lines for the relevant spectra are given. Using the equations of Khuri and Treiman [1] to relate the combined data to the difference between the $I=2$ and $I=0$ S-wave $\pi\pi$ scattering lengths, we find $a_2 - a_0 = (0.9 \pm .1)(\hbar/m_\pi c)$.

The events studied are the decays of K^- mesons that varied in laboratory momentum P_K between 300 and 850 MeV/c [2]. Over this momentum range no appreciable scanning biases were observed. For reliable measurements, however, decay events were accepted only if they occurred within a preselected fiducial volume.

The measured track variables for 1440 « candidates » were fitted by our computer program, KICK, to conserve 4-momentum. The χ^2 distribution differs from that expected in two respects:

(*a*) There is a flat tail of 93 events ($\approx 6\%$). Most of these events are probably not τ decays at all, but events such as $K_{\pi 2}$ with a Dalitz pair. The remainder represent poor fits due to unnoticed plural scatterings or mismeasurements.

(*b*) Apart from this background, the χ^2 distribution has the expected *shape* but is still too wide by a scale factor of about 1.8, implying that our input errors (computed to allow for Coulomb scattering and estimated measurement accuracy) are too small by about $\sqrt{1.8}$, because of such factors as optical distortion and

(*) Work done under the auspices of the U. S. Atomic Energy Commission.

(**) National Academy of Sciences Fellow.

(1) N. N. Khuri and S. B. Treiman: *Phys. Rev.*, **119**, 1115 (1960).

(2) P. Schlein, P. Bastien, O. Dahl, J. J. Murray, M. Watson and R. G. Ammar: paper presented at the *Intern. Conf. on Instrumentation for High Energy Physics* (Berkeley, 1960).

turbulence. We used 1347 events whose values of $\chi^2/1.8$ corresponded to better than the 1% probability level for a 4-constraint fit. The calculated errors δT_π in the fitted c.m. kinetic energies are an increasing function of P_K. Typical values of δT_π (increased by $\sqrt{1.8}$) vary from ± 3 MeV for the lower momentum K-decays, up to ± 6 MeV for the higher ones.

Fig. 1 is a Dalitz plot of the 1347 events.

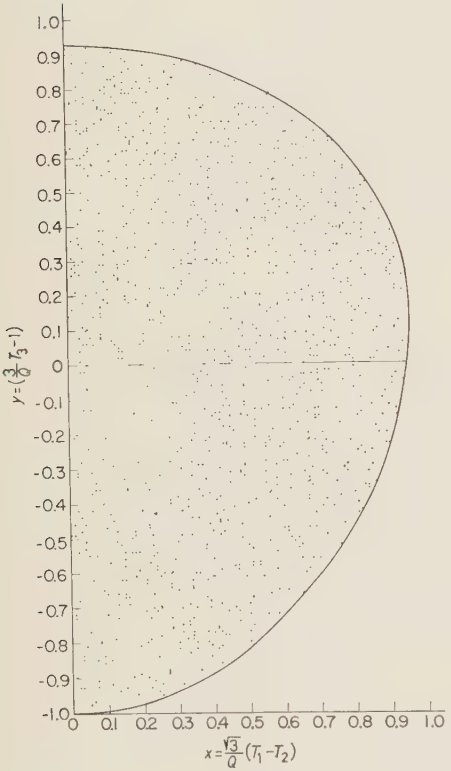

Fig. 1. – Dalitz plot of the distribution of pion energies for 1347 τ^- decays. The coordinates are those of Dalitz [ref. [10]]: T_1, T_2, and T_3 are respectively the c.m. kinetic energies of the two π^-, and of the π^+; and Q = 75.11 MeV.

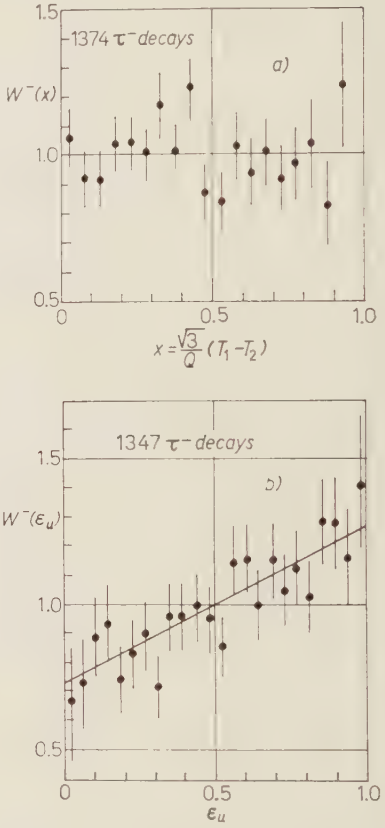

Fig. 2. – Energy dependence of the matrix element for 1347 τ^- decays on: (*a*) the like pion energy [through the coordinate $x=(\sqrt{3}/Q)(T_1-T_2)$]. (*b*) the unlike pion energy ($\varepsilon_u = T_3/T_{\max}$).

We first examine the x-dependence of the density of these events,

$$W^-(x) = \frac{1}{N\varrho(x)}\frac{\Delta N}{\Delta x}, \tag{1}$$

where N is 1347, $\varrho(x)$ is the Lorentz-invariant phase space, and $\Delta N/\Delta x$ is the vertical projection of the events in the interval Δx. If the matrix element for τ decay is called $M(x, y)$, then the spectrum $W(x)$ represents $|M|^2$ averaged over the allowed values of y. The symmetry of the two like pions forces $W(x)$ to be of the form $1 + bx^2 + \ldots$. Fig. 2*a* gives the data for $W(x)$. Within statistics, we

see no evidence for a quadratic dependence, *i.e.*,

$$W^-(x) = 1 \,, \tag{2}$$

gives a χ^2 probability of $\approx 60\%$. Therefore $|M(x, y)|^2$ depends only on y (*i.e.*, on the energy of the unlike pion).

To examine the y-dependence of $|M(x, y)|^2$, we form the analogue to eq. (1), $W^-(y)$. Parametrizing it to the form $1+ay+by^2+\ldots$, we find

$$W^-(y) = 1 + (0.28 \pm .045)\, y \,, \tag{3}$$

with no evidence for quadratic terms.

The results of eq. (2) and (3) can be summarized by the statement that $|M(x, y)|^2$ is well described by the plane

$$|M(x, y)|^2 = 1 + (0.28 \pm .045)\, y \,. \tag{4}$$

Although the variables x and y seem appropriate, it has become conventional in the case of positive τ decays (with which we must compare our data) to use different variables, namely ε_u (ε_l), given by the c.m. kinetic energy of the unlike (like) pion divided by the maximum allowed kinetic energy, 48.3 MeV. Here ε_u and y differ only by a scale factor of 2 $[(-1 \leqslant y \leqslant 1), (0 \leqslant \varepsilon_u \leqslant 1)]$, but ε_l is quite different from x. Fig. 2*b* shows our data for $W^-(\varepsilon_u)$ and the best straight line fit [eq. (3)] in this variable,

$$W^-(\varepsilon_u) = 1 + (0.56 \pm .09)(\varepsilon_u - \tfrac{1}{2}) \,. \tag{5}$$

To the extent that $|M|^2$ is just the plane as in eq. (3), it is easily shown [3] that our distribution in ε_l must have $-\frac{1}{2}$ the slope of eq. (4). We find

$$W^-(\varepsilon_l) = 1 - (0.26 \pm .09)(\varepsilon_l - \tfrac{1}{2}) \,. \tag{6}$$

Eq. (6) is written mainly for comparison with τ^+ data, but also constitutes a check on the form [eq. (3)] of $|M|^2$.

Our results, eq. (5) and (6), may be compared with the equivalent fits to 899 published τ^+ decays [4],

$$W^+(\varepsilon_u) = 1 + (0.48 \pm .11)(\varepsilon_u - \tfrac{1}{2}) \,, \tag{7}$$

and

$$W^+(\varepsilon_l) = 1 - (0.25 \pm .12)(\varepsilon_l - \tfrac{1}{2}) \,. \tag{8}$$

[3] S. WEINBERG: *Phys. Rev. Lett.*, **4**, 87 (1960).

[4] S. MCKENNA, S. NATALI, M. O'CONNELL, J. TIETGE and N. C. VARSHNEYA: *Nuovo Cimento*, **10**, 763 (1958). Of the events presented, 419 were from M. BALDO-CEOLIN, A. BONETTI, W. D. B. GREENING, S. LIMENTANI, M. MERLIN and C. VANDERHAEGHE: *Nuovo Cimento*, **6**, 84 (1957). Actually they give the slightly different value of 0.51 for the slope of eq. (7), but in treating their data identically with ours we find 0.48.

We see that the slopes of $W^+(\varepsilon_u)$ and $W^+(\varepsilon_l)$ are again related by the factor $-\frac{1}{2}$, as required by eq. (3).

The previous data indicate that, within statistics, the spectra for τ^+ and τ^- decays are identical as predicted by time-reversal invariance [5]. Therefore, in Fig. 3 we present the combined τ^+-τ^- spectrum. A straight line fit gives

$$W^{\pm}(\varepsilon_u) = 1 + (0.53 \pm .07)(\varepsilon_u - \tfrac{1}{2}) \,. \tag{9}$$

KHURI and TREIMAN [1] have used dispersion theoretic methods in an attempt to relate the τ decay matrix element to the S-wave $\pi\pi$ scattering amplitudes. With approximations suitable to small scattering lengths, they find

$$\frac{1}{4}|M|^2 \approx 1 + \frac{5}{3\pi} \frac{2\varrho^2}{(1 + \frac{1}{2}\varrho^2)^{\frac{1}{2}}} (a_2 - a_0)(\varepsilon_u - \tfrac{1}{2}) \,, \tag{10}$$

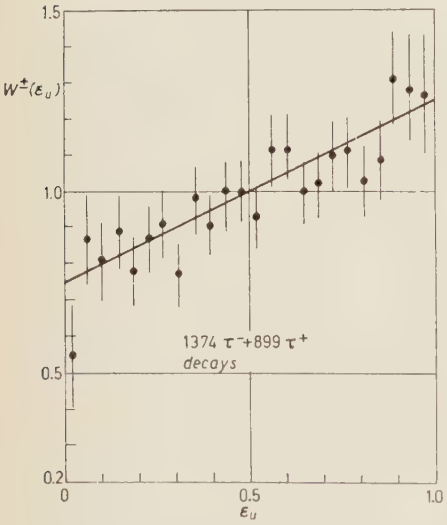

Fig. 3. – Energy dependence of the matrix element for 2246 combined τ^+ and τ^- decays on the unlike pion.

where ϱ^2 is a kinematical factor equal to 0.64, and $a_2 - a_0$ is the difference in the $I=2$ and $I=0$ S-wave $\pi\pi$ scattering lengths. Comparison with eq. (9) indicates

$$a_2 - a_0 = (0.9 \pm .1)(\hbar/m_\pi c) \,. \tag{11}$$

Apart from final state interactions, another — perhaps more reasonable — interpretation of the observed structure in τ decay is the possibility of introducing a small admixture of $I=1$ states of intermediate symmetry, thereby producing a dependence of the matrix element on y.

The fit to the combined data, eq. (9), may also be compared with the equivalent fit for τ'^+ decays. From the total available statistics of 119 τ'^+ decays summarized by BØGGILD *et al.* [6], we compute

$$W'^+(\varepsilon_u) = 1 - (1.0 \pm .4)(\varepsilon_u - \tfrac{1}{2}) \,. \tag{12}$$

WEINBERG [3] has pointed out that the $|\Delta I| = \frac{1}{2}$ rule requires that the coefficients of the linear terms in eq. (9) and (12) be in the ratio 1 to -2. This has already

[5] This is however not a sensitive test of time-reversal invariance: even if time-reversal invariance fails the spectra could still agree by accident or because: 1) the « primitive » (*i.e.* with the pion-pion interaction turned off) τ^+ and τ^- matrix elements may be so symmetric that the spectrum is dominated by final-state interactions, or 2) final-state interactions could be so weak as barely to affect the spectrum.

[6] J. K. BØGGILD, K. H. HANSEN, J. E. HOOPER, M. SCHAERF and P. K. ADITYA: *Nuovo Cimento*, **19**, 621 (1961)

been checked by BJORKLUND *et al.* [7] on the basis of 899 τ^+ and 72 τ'^+ events. We see that with slightly improved statistics $|\Delta I| = \frac{1}{2}$ is still well satisfied [8].

The decay of a τ in its center of mass can be completely specified by two independent kinematical quantities. In addition to the variables ε_a and ε_l, W has frequently been expressed in terms of two angles, which for τ^- decays we will call θ_{neutral} and θ_{--}. To discuss θ_{neutral} we assume that the K^- decays into a π^- and a neutral dipion. In the rest frame of the dipion, θ_{neutral} is the angle between its direction of motion and the relative momentum of the π^+

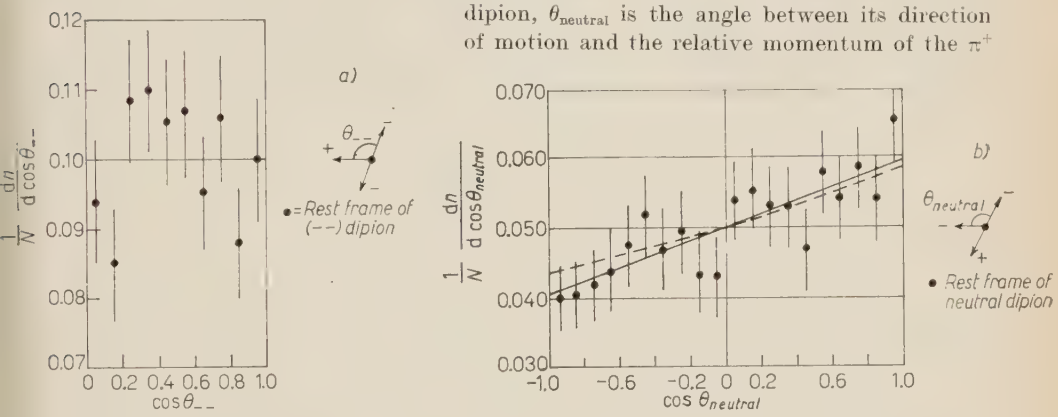

Fig. 4. – Angular dependence of the matrix element for 1347 τ^- decays: (*a*) angle with respect to the $\pi^-\pi^-$ rest frame. (*b*) angle with respect to the $\pi^+\pi^-$ rest frame. The dashed line is from ref. [9].

and π^- (see sketch beside Fig. 4). The square of the matrix element $W^-(\cos\theta_{\text{neutral}})$ is normalized by the definition

$$W^-(\cos\theta_{\text{neutral}}) = 1/N(\mathrm{d}n/\mathrm{d}\cos\theta_{\text{neutral}}).$$

Fig. 4 displays the $W^-(\cos\theta_{\text{neutral}})$ data and a straight line fitted thereto:

$$W^-(\cos\theta_{\text{neutral}}) \propto 1 \pm (0.2 \pm .04)\cos\theta_{\text{neutral}}. \tag{13}$$

Each τ^- decay yields two possible neutral dipions, but the two values of θ_{neutral} are correlated, so the errors have been calculated on the basis of 1347 events.

In the case of θ_{--}, there is a unique (— —) dipion, whose decay must be symmetric around $\cos\theta_{--} = 0$. The folded data give

$$W^-(\cos\theta_{--}) = 1 + (0.0 \pm .1)\cos^2\theta_{--}. \tag{14}$$

Insufficient data are published to calculate W^+ for these angles.

In contrast to KHURI and TREIMAN [1], THOMAS and HOLLADAY [9] have used the final state interaction formalism to estimate the effects of $\pi\pi$ scattering on the

[7] S. BJORKLUND, E. L. KOLLER and S. TAYLOR: *Phys. Rev. Lett.*, **4**, 424 (1960).
[8] This again is an insensitive test if the « primitive » matrix element is highly symmetric.
[9] B. S. THOMAS and W. C. HOLLADAY: *Phys. Rev.*, **115**, 1329 (1959).
[10] R. H. DALITZ: *Phil. Mag.*, **44**, 1068 (1953).

τ decay spectrum, assuming that only the $I=2$ S-wave scattering is important. Their curve for $W(\cos\theta)$, calculated for $a_2=1.0\hbar/m_\pi c$, is given in Fig. 1*b* as a dashed line. It fits well.

* * *

It is a pleasure to acknowledge the collaboration of all the others who are working on this K experiment: P. BASTIEN, J. P. BERGE, O. DAHL, J. KIRZ and M. WATSON. We thank Professor L. W. ALVAREZ and all his group for their interest and support, and Professor TREIMAN for theoretical advice.

Un metodo per la ricerca delle configurazioni di equilibrio nel modello a goccia.

S. Gallone

Istituto di Fisica dell'Università - Milano

(ricevuto il 17 Ottobre 1961)

Nei numerosi lavori svolti sull'argomento [1-5], la ricerca delle configurazioni di equilibrio viene generalmente impostata nel modo seguente: definiti i parametri α_i di deformazione del sistema, si calcola l'espressione dell'energia potenziale $U(\alpha_i)$ in funzione di questi parametri, e si impongono quindi le condizioni di stazionarietà

$$\frac{\partial U}{\partial \alpha_i} = 0 \,. \tag{1}$$

Un metodo diverso, analogo a quello che viene usato nella ricerca delle forme di equilibrio dei pianeti, consiste nell'esprimere direttamente la condizione di equilibrio della superficie del nucleo sotto l'azione delle forze di tensione superficiale e coulombiane [2,6].

Come è noto, questa condizione è:

$$OH + \varrho V = \text{Cost} \,. \tag{2}$$

in ogni punto della superficie; O essendo la tensione superficiale, H la curvatura media, V il potenziale coulombiano e ϱ la densità di carica elettrica.

Daremo ora un metodo approssimato di risoluzione della (2) valido per la ricerca di configurazioni di equilibrio che non si discostino troppo da un ellissoide di rotazione di semiasse maggiore a ed eccentricità e.

Nel sistema di coordinate sferoidali legate alle cartesiane delle relazioni

$$x = \sqrt{r^2 - e^2}\,\sin\theta\cdot\cos\varphi \,, \qquad y = \sqrt{r^2 - e^2}\,\sin\theta\,\sin\varphi \,, \qquad z = r\cos\theta \,, \tag{3}$$

(1) G. C. Wick: *Nuovo Cimento*, **16**, 229 (1939).
(2) N. Bohr e J. A. Wheeler: *Phys. Rev.*, **51**, 426 (1939).
(3) R. D. Present e J. K. Knipp: *Phys. Rev.*, **57**, 751, 1188 (1940).
(4) V. G. Nossof: A/Conf. 8/P/653, URSS (1955).
(5) U. L. Businaro e S. Gallone: *Nuovo Cimento*, **1**, 629 (1955).
(6) M. Silvestri: l'*Energia Elettrica*, Vol xxiii, fasc. iii (1946).

l'ellissoide di riferimento

$$\frac{x^2+y^2}{a^2-e^2}+\frac{z^2}{a^2}=1\,,$$

è definito da $r=a$.

Il profilo del nucleo individuato dai parametri di deformazione α_{ik} è descritto nel modo seguente:

$$r(\mu,\varphi)=a\left[1+\frac{a^2}{lm\nu}\sum_{ik}a_{ik}S_{ik}(\mu,\varphi)\right], \tag{4}$$

ove $\mu=\cos\theta$ e

$$l=\sqrt{\frac{a^2-e^2\mu^2}{a^2-e^2}}\,,\qquad m=\sqrt{a^2-e^2\mu^2}\,,\qquad \nu=\sqrt{a^2-e^2}\,. \tag{5}$$

Le funzioni sferiche $S_{ik}(\mu,\varphi)$ sono definite così a partire dai polinomi di Legendre $P_i(\mu)$:

$$S_{ik}(\mu,\varphi)=(-1)^{|k|}(1-\mu^2)^{|k|/2}\cdot\frac{\mathrm{d}^{|k|}P_i(\mu)}{\mathrm{d}\mu^{|k|}}\cdot\begin{cases}\cos k\varphi & k>0\,,\\ \dfrac{1}{\sqrt{2}} & k=0\,,\\ \sin k\varphi & k<0\,,\end{cases} \tag{6}$$

Per valutare il termine OH della (2) occorre poter esprimere la curvatura media H dell'ellissoide deformato a partire da quella H_0 dell'ellissoide di riferimento e dello spostamento

$$h=\frac{a^3}{m\nu}\sum_{ik}\alpha_{ik}S_{ik}\,.$$

Ora è possibile dimostrare in generale, per superfici qualsiasi, che se la superficie spostata è individuata spiccando sulla normale della superficie di riferimento un segmento di lunghezza h, si avrà, al primo ordine in h:

$$H=H_0-\nabla^2 h-C_0\,h\,. \tag{7}$$

Al secondo membro di questa equazione figurano la curvatura media H_0, il laplaciano ∇^2 ed il doppio della curvatura di Casorati C_0 della superficie di base (*).

(*) Per l'ellissoide di base si avrà, posto $y=e/a$:

$$H_0=\frac{1}{a}\cdot\frac{1}{\sqrt{1-y^2}}\cdot\frac{2-y^2-y^2\mu^2}{(1-y^2\mu^2)^{\frac{3}{2}}}\,,$$ — Curvatura media

$$C_0=\frac{1}{a^2}\cdot\frac{1}{1-y^2}\cdot\frac{(1-y^2\mu^2)^2+(1-y^2)^2}{(1-y^2\mu^2)^3}\,,$$ — Doppio della curvatura di Casorati

$$\nabla^2=\frac{1}{m}\cdot\frac{\partial}{\partial\mu}\left[\frac{1-\mu^2}{m}\cdot\frac{\partial}{\partial\mu}\right]+\frac{1}{\nu^2(1-\mu^2)}\cdot\frac{\partial^2}{\partial\varphi^2}\,,$$ — Laplaciano superficiale

Per il potenziale coulombiano V sulla superficie deformata, si ha, pure al primo ordine nello spostamento:

$$(8) \qquad V = V_0 + \frac{\partial V_0}{\partial r} \cdot \frac{a^3}{lmv} \sum_{ik} \alpha_{ik} S_{ik}(\mu, \varphi) + \varrho a^3 \sum_{ik} \alpha_{ik} \int\int \frac{S_{ik}(\mu', \varphi')}{R(\mu'\varphi', \mu\varphi)} \, \mathrm{d}\mu' \, \mathrm{d}\varphi' ,$$

dove $R(\mu'\varphi', \mu\varphi)$ indica la distanza tra due punti di coordinate $\mu'\varphi'$ e $\mu\varphi$ sull'ellissoide di base e V_0 il potenziale dell'ellissoide indeformato (*).

La (2) si potrà quindi scrivere, sempre trascurando le deformazioni di ordine superiore al primo:

$$(9) \qquad OH_0 - \frac{Oa^2}{v} [\nabla^2 + C_0] \frac{1}{m} \sum_{ik} \alpha_{ik} S_{ik}(\mu, \varphi) + \varrho V_0 + \varrho \frac{\partial V_0}{\partial r} \cdot \frac{a^3}{lmv} \sum_{ik} \alpha_{ik} S_{ik}(\mu, \varphi) +$$

$$+ \varrho^2 a^3 \sum_{ik} \alpha_{ik} \int\int \frac{S_{ik}(\mu', \varphi')}{R(\mu'\varphi', \mu\varphi)} \, \mathrm{d}\mu' \, \mathrm{d}\varphi' = \text{cost} .$$

In questa formula si porrà $a^3(1 - y^2) = R^3$ con R uguale al raggio del nucleo indeformato (sferico).

Moltiplicando ora i due membri della (9) per una generica $S_{rs}(\mu, \varphi)$ ed integrando su μ e φ si ottiene il sistema di infinite equazioni lineari nelle incognite α_{ik}:

$$(10) \qquad \sum_{ik} \alpha_{ik} A_{ik,rs} + a_{rs} = 0 .$$

Si è posto:

$$(11) \qquad \begin{cases} a(\mu) = OH_0 + \varrho V_0 - \text{cost} , \\ A_{ik}(\mu, \varphi) = -\frac{Oa^3}{v} [\nabla^2 + C_0] \frac{1}{m} S_{ik}(\mu, \varphi) + \varrho \frac{\partial V_0}{\partial r} \cdot \frac{a^3}{lmv} S_{ik}(\mu, \varphi) + \\ \qquad + \varrho^2 a^3 \int\int \frac{S_{ik}(\mu', \varphi')}{R(\mu'\varphi', \mu\varphi)} \, \mathrm{d}\mu' \, \mathrm{d}\varphi' , \end{cases}$$

e

$$(12) \qquad a_{rs} = \int\int a(\mu) S_{rs}(\mu, \varphi) \, \mathrm{d}\mu \, \mathrm{d}\varphi , \qquad A_{ik\,rs} = \int\int A_{ik}(\mu, \varphi) S_{rs}(\mu, \varphi) \, \mathrm{d}\mu \, \mathrm{d}\varphi ,$$

(*) Si ha:

$$V_0 = \frac{4\pi\varrho a^2}{3y} (1 - y^2) \left| Q_0\left(\frac{1}{y}\right) - Q_2\left(\frac{1}{y}\right) P_2(\mu) \right| , \qquad \text{Potenziale dell'ellissoide di base.}$$

L'ultimo termine della (8) si può scrivere:

$$\frac{4\pi\varrho a^2}{y} \sum_{ik} \frac{(i - |k|)!}{(i + |k|)!} \alpha_{ik} (-1)^{|k|} Q_i^{|k|}\left(\frac{1}{y}\right) P_i^{|k|}\left(\frac{1}{y}\right) S_{ik}(\mu, \varphi) ,$$

P e Q funzioni di Legendre di prima e seconda specie.

questi coefficienti godono delle proprietà seguenti:

$$(13)\qquad \begin{cases} a_{rs} \begin{cases} \neq 0 & \text{se } r \text{ è pari e } s = 0 \\ = 0 & \text{negli altri casi,} \end{cases} \\ A_{ik,rs} \begin{cases} \neq 0 & \text{se } i + r \text{ è pari e } k = s \\ = 0 & \text{negli altri casi.} \end{cases} \end{cases}$$

Le condizioni di conservazione del volume e del baricentro si esprimono semplicemente così:

$$\alpha_{00} \quad 0\,, \qquad \left.\begin{matrix} \alpha_{11} \\ \alpha_{10} \\ \alpha_{1-1} \end{matrix}\right\} = 0\,.$$

È interessante osservare che le (10) non coincidono con le equazioni di tipo (1), quali si possono ad esempio ricavare dal lavoro di G. C. Wick [1] imponendo le appropriate condizioni di conservazione del volume.

Si può tuttavia dimostrare che esse differiscono da queste ultime per termini del tipo:

$$(14)\qquad \alpha_{ik} \iint (OH_0 + \varrho V_0 - O\bar{H}_0 - \varrho \bar{V}_0) \frac{S_{ik} S_{rs}}{(1 - y^2\mu^2)^2} \, d\mu \, d\varphi\,,$$

con $\bar{H}_0$ e $\bar{V}_0$ valori medi della curvatura e del potenziale.

Ora, posto $r=0$ e $s=0$ nelle (10), si vede che l'espressione tra parentesi tonda sotto l'integrale (14) è del primo ordine nei parametri di deformazione. L'espressione (14) sarà quindi del secondo ordine e trascurabile rispetto agli altri termini.

Si può notare pure che, in virtù delle proprietà (13) dei coefficienti a_{rs} e $A_{ik,rs}$ le (10) danno luogo, per r pari e $s=0$, al sistema non omogeneo

$$(15)\qquad \sum_i \alpha_{i0} A_{i0,r0} + a_{r0} = 0\,,$$

che individua tutte le configurazioni di equilibrio assiali e simmetriche rispetto al baricentro.

In tutti gli altri casi sarà $a_{rs}=0$ e affinchè il sistema di equazioni omogenee corrispondente ammetta soluzioni non nulle, dovrà essere:

$$\| A_{ts,rs} \| = 0\,,$$

condizone che corrisponde all'apparire di forme non assiali e/o non simmetriche. Questa condizione indica pure l'inizio di instabilità dell'ellissoide di base per deformazioni del tipo suddetto, e può essere utilizzata per la ricerca di nuove forme di equilibrio.

Some Remarks on the Feynman–Gell-Mann Formulation of the Fermi Interaction (*).

L. C. Biedenharn

Duke University - Durham, N. C.

(ricevuto il 23 Ottoble 1961)

Feynman and Gell-Mann (1) gave a novel formulation of the theory of the Fermi interaction, which incorporated in a direct manner the form of the interaction ($V-A$) as well as the familiar parity non-conservation. Their formulation was equivalent to chiral invariance (2), but had the advantage of an intriguingly different theoretical viewpoint. The purpose of the present remarks is to explore briefly some of the consequences of the Feynman-Gell-Mann proposal, for the experimentally important case of β decay in the presence of an external Coulomb field ($\alpha Z/r$).

The theoretical viewpoint of these authors may be summarized as follows: Chirally projected solutions of the Dirac equation are two-component solutions (Φ) of the second order (iterated) Dirac equation. Conversely, solutions of the Dirac equation (ψ) may be constructed from every two-component solution of the second order equation. From the postulate that the two-component form will be regarded as fundamental for β decay, the presently accepted chirally invariant formulation follows.

Consider now the iterated Dirac equation:

$$[(i\partial_\mu - A_\mu)^2 + \sigma\cdot(B + iE)]\psi = m^2\psi\,. \tag{1}$$

Introducing radial coordinates and an external Coulomb field eq. (1) takes the form:

$$\left|\frac{1}{r^2}\frac{\partial}{\partial r}r^2\frac{\partial}{\partial r} - \frac{K^2-\alpha^2Z^2}{r^2} - \frac{2\alpha Z p_0}{r} + \frac{1}{r^2}(\varrho_3 K + i\alpha Z\varrho_1\sigma\cdot\hat{r}) + p_0^2 - m^2\right|\psi = 0\,,$$

where

$$K = \varrho_3(\sigma\cdot L + 1)\,. \tag{2}$$

(*) Supported in part by the Army Research Office (Durham) and the National Science Foundation.

(1) R. P. Feynman and M. Gell-Mann: *Phys. Rev.*, **109**, 193 (1958). Hereinafter referred to as F-G.

(2) E. C. G. Sudarshan and R. E. Marshak: *Phys. Rev.*, **109**, 1860 (L) (1958). The literature is summarized in S. Schweber: *Relativistic Quantum Field Theory* (Evanston, 1961).

One sees at once that *the iterated equation possesses two additional commuting operators over the Dirac equation.* The first of these, ϱ_1, as pointed out in ref. [1], commutes for arbitrary (E.M.) fields. The second is the operator

$$\Gamma \quad \sigma \cdot L \cdot 1 \cdot i\alpha Z \varrho_1 \sigma \cdot \hat{r} \ .$$

and is a particular consequence of the symmetry of the Coulomb field. The eigenvalues (γ) of the operator Γ are $\pm(\varkappa^2 - \alpha^2 Z^2)^{\frac{1}{2}}$. Both operators commute with Wigner time-reversal.

Following F-G we project out solutions with sharp ϱ_1. If we also introduce the notation $k^2 = p_0^2 - m^2$, $kr = \varrho$, $\eta = \alpha Z p_0/k$ and $\Gamma_1 = \sigma \cdot L + 1 + i\alpha Z \sigma \cdot \hat{r}$ we then find for the projected form of eq. (2):

$$\left[\frac{1}{\varrho^2} \frac{\partial}{\partial \varrho} \varrho^2 \frac{\partial}{\partial \varrho} - \frac{\Gamma_1^2 + \Gamma_1}{\varrho^2} - \frac{2k\eta}{\varrho} + 1 \right] \Phi = 0 \ . \tag{3}$$

Equation (3) *shows that the relativistic Dirac-Coulomb (radial) wave functions appropriate to the* F-G *two-component formulation are precise analogues to the non-relativistic Coulomb wave functions.* The sole change in the radial functions is to replace the angular momentum $l(\varkappa)$ by its (non-integer) relativistic analogon $l(\gamma)$, (defined by $\Gamma_1^2 + \Gamma_1 \to l(l+1)$). For the sake of brevity, we shall forego detailing the explicit normalized functions.

It is useful to note, however, that eq. (3) possesses as constants: the energy, the total angular momentum and its projection, as well as the eigenvalue of Γ_1. *It does not possess a sharp parity.* Yet if $\alpha Z = 0$ the solutions to eq. (3) would indeed possess a sharp parity. This is patently at variance with the well-known results for the two-component neutrino. The flaw, as is no doubt obvious, occurs in our assertion, with Feynman and Gell-Mann, that there exists a one-to-one correspondence between the solutions ψ and Φ. This is based on the (correct) assertions that: (a) to every ψ there belongs a Φ, and (b) to every Φ we may construct a ψ. The difficulty lies in the fact that for a one-to-one correspondence we must exclude null solutions. Precisely for the massless neutrino do we find projection into null solutions, and the mapping is, in fact, two-to-one.

Somewhat paradoxically we conclude, therefore, that the two-component formulation actually has the effect of re-introducing l (and thus parity) as a good quantum number (for $\alpha Z = 0$ and $m \neq 0$). Parity mixing occurs only for two cases: (a) $m = 0$ and (b) $\alpha Z \neq 0$. Even if the neutrino had non-zero mass, the F-G formulation would show parity mixing in the presence of external fields.

The use of the two-component radial Dirac-Coulomb functions is especially convenient for purposes of calculation, since these functions are very considerably simpler that the functions heretofore used. In addition, the specific effects of the nuclear Coulomb field are more clearly in evidence. (Actually, the use of the operator Γ (rather than Γ_1) allows these advantages to be carried over into the four-component solutions.) This work will be reported in detail elsewhere.

* * *

Helpful discussions with Professor E. Merzbacher, Dr. T. A. Griffy, and Dr. D. Saylor are gratefully acknowledged.

Some Remarks on Double Photoproduction.

D. Boccaletti

Istituto di Fisica dell'Università - Bologna
Istituto Nazionale di Fisica Nucleare - Sezione di Bologna

F. Selleri

CERN - Geneva

(ricevuto il 26 Ottobre 1961)

It has recently been pointed out by Drell [1] that photons are more effective than nucleons, when colliding on the same target, for the production of high-energy pions, due to the effect of the diagram in Fig. 1*a*. This fact makes possible the production of pion beams more intense than those obtained with proton-nucleus collisions.

It was also stated in reference [1] that the experimental data for double photo- production in the GeV region [2] provide a qualitative confirmation of such an effect.

Fig. 1.

Since one expects a total cross-section for the Drell effect (DE) reduced by roughly the fine structure constant $\alpha = 1/137$ from its geometric value ($\simeq 20$ mb), one sees that *a priori* the DE can be expected to be very important also at low energy ($\simeq (.5 \div 1)$ GeV), *e.g.* for the process

$$\gamma + p \to p + \pi^+ + \pi^- , \tag{1}$$

whose experimental cross-section is about 80 μb [2]. We have calculated the total cross-section for reaction (1) with the Drell diagram and found the behaviour reported in Fig. 2. The maximum value is at 1.2 GeV and is of about 10 μb. In all the $(0.5 \div 1)$ GeV region the calculated cross-section is of an order of magnitude smaller than the experimental one.

[1] S. D. Drell: *Phys. Rev. Lett.*, **5**, 278 (1960).

[2] B. M. Chasan, G. Cocconi, V. T. Cocconi, R. M. Schectman and D. H. White: *Phys. Rev.*, **119**, 811 (1960).

The smallness of the DE as compared with the photo-electric term in single photoproduction can be qualitatively attributed to the smallness of the pion-nucleon-(3.3) isobar coupling constant as compared with the π-N one.

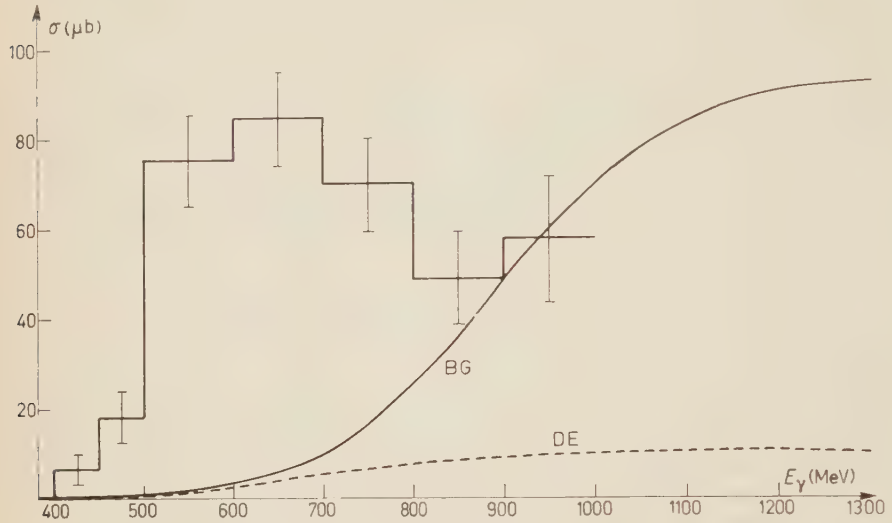

Fig. 2. – Total cross-section for $\gamma + p \to p - \pi^- + \pi$.

The experimental data for ref. ([1]) ([2]) show the qualitative behaviour which is expected from the DE (π^- c.m. angular distribution with a strong forward peak and formation of the 3.3 isobar). Since, however, this π^- forward peak includes roughly 50% of the interactions, we see that only a small part of it can be explained with the DE.

Another mechanism of interaction must thus be important, still giving 3.3 isobar formation and a π^- c.m. forward peak.

We do not think that this mechanism can be the electric dipole term considered by CUTKOSKY and ZACHARIASEN ([3]) because it can produce a forward peak in the π^- c.m. angular distribution neither directly (the π^- is expected in S-wave) nor through interference effects with the Drell diagram. This last statement rests on the fact that we have calculated the π^- c.m. angular distribution from DE and it is not sufficiently peaked to ressemble the experimental data, especially at the lower energies ($\lesssim$ 700 MeV). Useless to say, these criticisms do not touch the possibilities of producing intense pion beams with photons of much higher energies.

We thought it interesting to look at the typical effects of the pion-pion interaction as a primary mechanism contributing to reaction (1). The diagram is shown in Fig. 1*b* and has first been considered in detail by BOCCALETTI and GUALDI ([4]) (BG). For the sake of calculating it, one has to know *a priori* the matrix element of photoproduction of pions on pions. The knowledge of it has been reduced by GOURDIN and MARTIN ([5]) to the knowledge of the $T = J = 1$ $\pi\pi$ scattering amplitude and of

([3]) R. E. CUTKOSKY and F. ZACHARIASEN: *Phys. Rev.*, **103**, 1108 (1956).

([4]) D. BOCCALETTI and C. GUALDI: *Nuovo Cimento*, **18**, 895 (1960), see also D. BOCCALETTI, G. DE FRANCESCHI and C. GUALDI: *Nuovo Cimento*, **20**, 375 (1961).

([5]) M. GOURDIN and A. MARTIN: *Nuovo Cimento*, **16**, 78 (1960); see also M. GOURDIN and A. MARTIN: *Nuovo Cimento*, **17**, 224 (1960).

an arbitrary constant A. While, on the one hand, there begins to be rather convincing evidence (6) in favour of a $T=J=1$ $\pi\pi$ resonance at a total c.m. energy of 5 pion masses, on the other hand A has been determined by DE TOLLIS, FERRARI and MUNCZEK (7), by fitting the $d\sigma^-/d\sigma^+$ ratio in single photoproduction. The total cross-section for reaction (1) as obtained from the BG diagram using this information is shown in Fig. 2. A broad maximum is present at 1.3 GeV. The value of the theoretical cross-section at this energy is about 90 μb and, therefore, of the same size as the experimental one.

Of course the A-value we used could easily be changed by future more accurate determinations. Furthermore for both the theoretical curves shown in Fig. 2, one has to keep in mind that they constitute only a very rough estimate of the corresponding diagrams. The most drastic simplification is probably the neglect of the various form factors. Therefore, the calculated cross-sections constitute an upper bound to the corresponding physical effects. However, they should not be wrong by more than a factor of two.

We conclude than that above .9 GeV the BG diagram probably becomes of primary importance for reaction (1). Evidence for DE in the GeV region should instead be looked for in particularly favourable kinematical conditions (8).

We give in the following a few details about the performed calculations. The 4-vectors are defined in the following way: k (photon), $q_2(\pi^-)$, $q_3(\pi^+)$, p_1 and p_2 (initial and final protons). For the DE we neglect the diagrams in which π^- and p emerge from the same vertex because its contribution can be *a priori* estimated to be nine times smaller than that of the other one in which π^+ and p emerge together. Also the interference between these two diagrams is neglected. This is expected to be very small and in any case it is clear that it cannot change our conclusions about the smallness of the DE in the GeV region. The S-matrix element for DE will therefore be

$$S_{fi} = (2\pi)^{-\frac{3}{2}} \left(\frac{q_{10}}{2k_0 q_{20}}\right)^{\frac{1}{2}} \frac{e\varepsilon\cdot(q_2 - q_1)}{(q_2 - k)^2 + \mu^2} S_{\pi N}\,, \tag{2}$$

where q_1 is the 4-vector of the intermediate pion, the zero index indicates the energy component of a given vector, e is the electric charge.

$(e^2/4\pi = \alpha = 1/137)$ and ε is the polarization four-vector of the photon. $S_{\pi N}$ is a quantity which for $q_1^2 = -\mu^2$ reduces to the matrix element for πN scattering. Formula (2) is calculated in the « pole approximation » (9). The total cross-section can be easily calculated from (2) and turns out to be

$$\sigma_{\text{tot}} = \frac{\alpha}{2\pi W^2 k_B^3} \int_{m+\mu}^{W-\mu} \mathrm{d}u\, \sigma_{\pi N}(u)\, u^2 q^2 \left(\frac{1}{\beta}\log\frac{1+\beta}{1-\beta} - 2\right), \tag{3}$$

where $W^2 = -(k+p_1)^2$, $k_B = (W^2 - m^2)/2W$, $u^2 = -(q_3 + p_2)^2$, β is the c.m. velocity

(6) J. G. RUSHBROOKE and D. RADOJICIC: *Phys. Rev. Lett.*, **5**, 567 (1960); D. STONEHILL: *Phys. Rev. Lett.*, **6**, 624 (1961); A. R. ERWIN: *Phys. Rev. Lett.*, **6**, 628 (1961).

(7) B. DE TOLLIS, E. FERRARI and H. MUNCZEK: *Nuovo Cimento*, **18**, 198 (1960).

(8) An analysis of this kind has been done by F. HADJIOANNOU and has been reported by S. D. DRELL in *Rev. Mod. Phys.*, **33**, 458 (1961).

(9) E. FERRARI and F. SELLERI: *Nuovo Cimento*, **21**, 1028 (1961).

of the π^- and

$$q = \frac{1}{2u}\left(u^4 - 2u^2(m^2 + \mu^2) + (m^2 - \mu^2)^2\right)^{\frac{1}{2}}. \tag{4}$$

For the BG diagram we have

$$S_{fi} = (2\pi)^{-\frac{7}{2}} m (8k_0 p_{10} q_{20} q_{30} p_{20})^{-\frac{1}{2}} \frac{\bar{u}(p_2) G_r \gamma_5 u(p_1)}{(p_2 - p_1)^2 + \mu^2} \delta^4(P_f - P_i) M_{\gamma\pi}, \tag{5}$$

where G_r is the rationalized and renormalized $\pi N N$ coupling constant, and

$$M_{\gamma\pi} = \frac{1}{2i} \varepsilon_{\lambda\mu\nu\varrho} q_1^\lambda q_2^\mu q_3^\nu \varepsilon^\varrho F(\omega^2, r^2), \tag{6}$$

is the M matrix element for $\gamma\pi \to \pi\pi$ as defined in reference [5]. F is an invariant amplitude which in principle should depend also on $(p_2 - p_1)^2$. In the spirit of the pole approximation we neglect this dependence. The invariants ω^2 and r^2 are given by $\omega^2 = -(q_2 + q_3)^2$, $r^2 = (q_2 - k)^2$. For F we have used the approximate solution given in eq. (31) of reference [5]. The position and width of the $\pi\pi$ resonance which we have used are those of reference [10]. Finally, the arbitrary multiplicative constant which enters in this solution has been taken in agreement with the value found in reference [7]. We obtain in this way

$$\sigma_{\text{tot}} = \frac{G^2}{8\pi W^2 k_B^2} \int \frac{A^2}{(A^2 + \mu^2)^2} R(\omega^2)\, \sigma_{\gamma\pi}(\omega^2)\, \mathrm{d}A^2\, \mathrm{d}\omega^2, \tag{7}$$

where $G^2 = G_r^2/4\pi$, $A^2 = (p_2 - p_1)^2$, $R(\omega^2) = (\omega^2 - \mu^2)/2$ and the limits of integration are (B is for c.m.)

$$(A^2)_{\substack{\max \\ \min}} = -2m^2 + 2p_{20}^B p_{10}^B \pm 2p_2^B p_1^B, \tag{8}$$

on A^2, for fixed ω^2 and $\omega^2_{\min} = 4\mu^2$ and $\omega^2_{\max} = (W - m)^2$.

With the stated use of the published literature we can write

$$\sigma_{\gamma\pi}(\omega^2) = 0.06 \frac{\omega^2 - 1}{2} \left(\frac{\omega^2}{4} - 1\right)^{\frac{3}{2}} \exp\left[2\varrho(\omega^2)\right] |\varphi(\omega^2)|^2, \tag{9}$$

where

$$\exp\left[2\varrho(\omega^2)\right] = \frac{165.5 + 19.3\omega^2}{(8.95 + 0.25\omega^2)\left[(5.25 - 0.25\omega^2)^2 - 1 + 0.25\omega^2\right]}, \tag{10}$$

and

$$|\varphi(\omega^2)|^2 = \left(0.95 \frac{60.4 - \omega^2}{57.4 + 2\omega^2}\right)^2. \tag{11}$$

[10] J. Bowcock, N. W. Cottingham and D. Lurié: *Nuovo Cimento*, **16**, 918 (1960).

In the formulae (9) to (11) we have put $\mu = 1$. The numerical coefficient in (9) is however such as to give $\sigma_{\gamma\pi}$ in mb.

* * *

We wish to thank Prof. M. Cini, Prof. S. Fubini, Drs. M. Gourdin and A. Martin and Prof. A. Stanghellini for very useful discussions. We are indebted to Dr. S. D. Drell and Dr. F. Hadjionannonu for discussions which certainly helped in improving the clarity of this paper.

We are indebted also to Mr. W. Klein for his help in rapid numerical calculations. One of us (D.B.) wishes to thank Prof. L. Van Hove for kind hospitality in the theoretical group at CERN, where this work has been mostly carried out.

Energetic Electromagnetic Cascade Produced in a High Energy Nucleon-Nucleon Interaction.

P. L. Jain

Department of Physics, University of Buffalo - Buffalo, N. Y.

(ricevuto il 27 Giugno 1961; edizione riveduta ricevuta l'11 Novembre 1961)

In a stack [1] of 22 liter of Ilford G-5 emulsion, consisting of 200 pellicles, 60×30 cm, 600 thick exposed to cosmic radiation at an altitude of 116000 feet high we have observed an event of type $4+27p$. It is produced by a primary proton interacting with a single neutron on the periphery of a heavy nucleus, as suggested by the odd multiplicity of interaction. The incident proton of this event enters the stack with a zenith angle of 8.5° and a dip angle of about 2.0° with respect to the plane of the emulsion and travels about 7 cm in the emulsion before it makes an interaction with the emulsion nuclei. By following the central core of the shower particles, which could be followed for more than 33 cm inside the stack within a cone of half-opening angle of $1 \cdot 10^{-2}$ radian around the shower axis, two low energy interactions of type $6+17p$ and $10+18p$ at a distance of about 20 cm and 30 cm respectively, from the primary interaction were found. All the tracks in the outer cone were also followed until they produced a secondary interaction or left the stack.

The angular distribution of shower particles of the primary event in the laboratory system is shown in Fig. 1 in terms of $\lg \operatorname{tg} \theta_L$. The center of gravity of the event is denoted by an arrowhead which corresponds to center-of-momentum angle of emission $\bar{\theta} = 90°$. The energy of the primary event, as determined from the angular distribution of shower particles by making use of

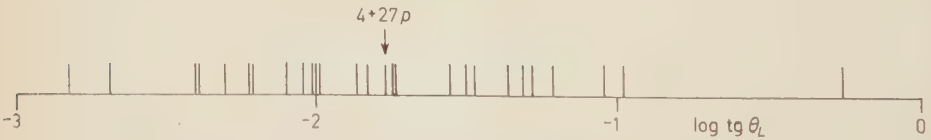

Fig. 1. The angular distribution of shower particles from the primary interaction $(4+27p)$ plotted over $\log_{10} \operatorname{tg} \theta_L$. The center is denoted by an arrowhead.

[1] P. L. Jain: *Phys. Rev.*, **122**, 1890 (1961)

Castagnoli's [2] formula (under-modified form [3]) is $3.3 \cdot 10^{12}$ eV.

The energies of the individual tracks in the primary event were found in almost all cases by scattering measurements. Low energy tracks in the outer cone were measured by the usual method of multiple scattering along the tracks, but for high-energy particles produced in the inner cone, the energy was estimated by relative scattering measurements. The experimental results for the energies and for the angles of all the tracks are shown in Table I. In a few cases when the track length available was not long enough or the energy was too high, or there was spurious scattering in the emulsion, only the lower limit of energy was given.

While scanning along the forward cone of the primary event, high-energy electromagnetic cascades were also observed. The analysis of the development of the electromagnetic cascades associated with a jet gives a measure of the total energy carried away by neutral pions, provided that any similar particles generated in secondary nuclear interactions are of low energy compared with those emitted from the primary. In the event under consideration, there was no high-energy secondary interaction and consequently no high-energy secondary cascade was found. Within a distance of about 1.5 cm from the origin of the primary jet, four high-energy electron pairs were found which were probably due to decay of π^0 mesons into $2\,\gamma$'s, each of which is further materialized into an electron-positron pair. Two of these electron pairs originate rather very energetic cascades in the stack. One of these two pairs, was found only at a distance of about 1.5 mm while the other was found at a distance of 1.2 cm from the primary interaction, but both pairs were very close to the axis of the primary particle. From the development of the cascades it was clear that these two were originated by two very high-energy γ-rays from the same π^0 meson and probably the other two cores of the cascades were originated by two other γ-rays which were at a larger distance from the first two cores and could be easily distinguished from the rest.

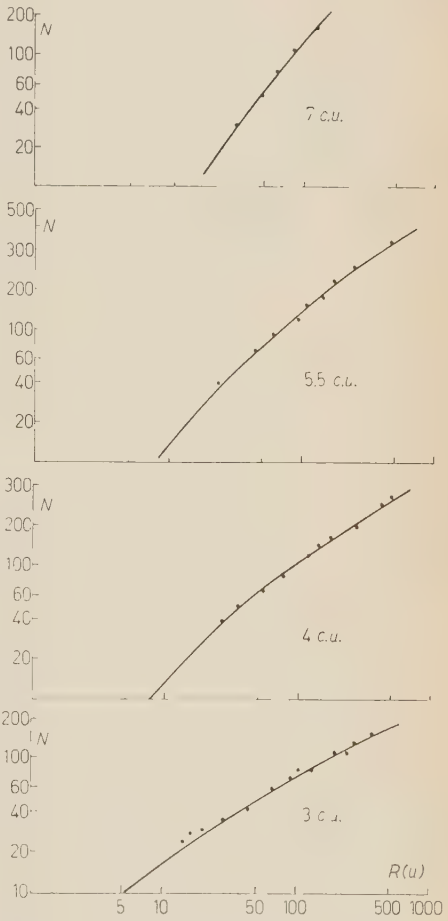

Fig. 2. – Lateral distribution of electrons at a distance of 3, 4, 5.5 and 7 c.u. from the origin of the pairs. $R(\mu)$ is the distance from cascade axis, dots represent the experimental results. Solid curve is drawn from the theoretical calculation of Nishimura [6].

[2] C. Castagnoli, G. Cortini, C. Franzinetti, A. Manfredini and D. Moreno: *Nuovo Cimento*, **10**, 1539 (1953).

[3] P. L. Jain, E. Lohrmann and M. W. Teucher: *Phys. Rev.*, **115**, 643 (1959).

TABLE I. - *Angles, energies and transverse momenta P_t of the primary event* 4+27p.

Track no.	θ	$P\beta$ (GeV/c)	P_t (GeV/c)	$P\beta$ determined from
1	6.0°	1.0 ± 0.5	0.105	scattering
2	3.0°	$4.0^{+6.2}_{-2.1}$	0.208	scattering
3	2.8°	2.2 ± 1.8	0.108	scattering
4	1.8°	> 2.5	> 0.078	scattering
5	2.0°	1.5 ± 0.75	0.105	scattering
6	2.5°	2.5 ± 1.2	0.110	scattering
7	29.0°	1.5 ± 0.9	0.726	scattering
8	$17 \cdot 10^{-3}$ rad	20^{+20}_{-10}	0.340	interaction 4+7p
9	$18 \cdot 10^{-3}$ rad	$> 7.0^{+8}_{-4}$	> 0.126	scattering
10	$14 \cdot 10^{-3}$ rad	11^{+1}_{-4}	0.154	scattering
11	$15 \cdot 10^{-3}$ rad	4.0 ± 2.0	0.060	scattering
12	$18 \cdot 10^{-3}$ rad	> 3.5	> 0.063	scattering
13	$28 \cdot 10^{-3}$ rad	5.0 ± 2.2	0.140	scattering
14	$10 \cdot 10^{-3}$ rad	25^{+20}_{-13}	0.250	scattering
15	$4 \cdot 10^{-3}$ rad	35^{+40}_{-17}	0.140	interaction 6+17p
16	$8 \cdot 10^{-3}$ rad	17.5^{+20}_{-13}	0,140	scattering
17	$1.5 \cdot 10^{-3}$ rad	120 ± 60	0.180	interaction 10+18p
18	$2 \cdot 10^{-3}$ rad	> 60	> 0.120	scattering
19	$4 \cdot 10^{-3}$ rad	30 ± 12	0.120	scattering
20	$5 \cdot 10^{-3}$ rad	> 35	> 0.175	scattering
21	$90 \cdot 10^{-3}$ rad	4.0 ± 1.8	0.360	scattering
22	$6 \cdot 10^{-3}$ rad	> 20	> 0.120	scattering
23	$60 \cdot 10^{-3}$ rad	5.0^{+6}_{-3}	0.300	scattering
24	$6 \cdot 10^{-3}$ rad	> 15	> 0.090	scattering
25	$9 \cdot 10^{-3}$ rad	> 14	> 0.126	scattering
26	$10 \cdot 10^{-3}$ rad	> 20	> 0.200	scattering
27	$10 \cdot 10^{-3}$ rad	15 ± 7.5	0.150	scattering

One can determine the energies of pairs and of the parent π^0 meson by several methods which are discussed in ref. (4). For the event 4+27p we measured and plotted the lateral distribution of the electrons at distances of 3, 4, 5.5 and 7 cascade units (1 c.u. = 2.9 cm in emulsion) from the origin of the pairs. A correction was applied to eliminate background tracks from the secondary nuclear interactions and neighboring cascades. The comparison between the theoretical distribution of $N(R)$ according to NISHIMURA and KAMATA (5) and our measurements is shown in Fig. 2 in which the integral number of electrons at $t=3$, 4, 5.5 and 7 cascades from the shower origin is plotted against the distance R from the cascade axis. The same method was applied to the other cascades developed by other mesons. We then tried to match the γ-rays by using the kinematical relations (6) between the opening angle and the energy of pair γ-rays. From these relations, we thus obtained the energy value of two π^0 mesons as $1.7 \cdot 10^{12}$ eV and $4 \cdot 10^{11}$ eV respectively. The energies of all other π^0 mesons were small as compared with these two values, as they did not originate comparably energetic cascades and their contribution at 4, 5.5 and 7 c.u. would be negligible. We may also mention that the energies of γ-rays were checked independently by measuring the decrease in ionization (known as Chudakov effect) (7,8) of the track of the pair near the point of conversion. This decrease in ionization is due to the destructive interference of the electromagnetic fields of two particles with equal charges but opposite in sign (like an electric dipole). At greater distances from the origin the electron and positron are well separated and behave as two independent monopoles. Ionization measurements are very reliable for photon energies greater than 100 GeV. In Fig. 3 is shown the ionization *vs.* the distance from the pair origin for the high-energy pair. The solid line is a theoretical curve (of energy ~ 850 GeV) for the case of equipartition of energy between an electron pair, as discussed by IWADARE (9). R is the ratio of the ionization produced by a pair (g_{pair}) to that of a

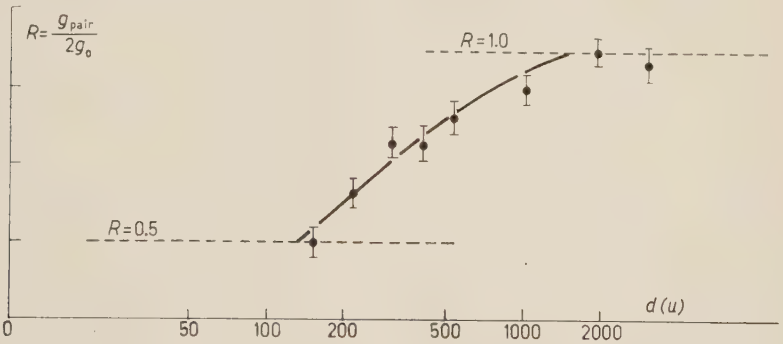

Fig. 3. – The ionization *vs.* the distance from the pair origin. The solid line is the theoretical curve for the equipartition of the energy.

(4) P. L. JAIN: in press in *Phys. Rev.*

(5) J. NISHIMURA and K. KAMATA: *Progr. Theor. Phys.*, **7**, 185 (1952); **5**, 889 (1950). Also Sept. 1958.

(6) Z. KOBA: *Proc. of the 1956 Sixth Annual Rochester Conference on High Energy Nuclear Physics*, vol. **4** (New York, 1956), p. 46.

(7) D. H. PERKINS: *Phil. Mag.*, **46**, 1146 (1955).

(8) A. E. ČUDAKOV: *Compt. Rend. Acad. Sci. U.R.S.S.*, **19**, 651 (1955).

(9) J. IWADARE: *Phil. Mag.*, **3**, 680 (1958).

singly-charged relativistic particle (g_0) in the region of the emulsion near the origin of the pair and is then given by $R = g_{\text{pair}}/2g_0$. The theoretical predictions and the experimental observations are quite in agreement. Ionization measurements also gave the same energies for all γ-rays as were found by the cascade measurements, within their experimental errors. It is very interesting to know that a single π^0 meson could take as high an energy as up to 50% of the total energy of the primary particle. These two π^0 mesons can carry away an appreciable fraction of the total energy going into meson production. Ordinarily one would expect that soft cascades contribute only about $\frac{1}{2}$ of the energy of the charged shower particles.

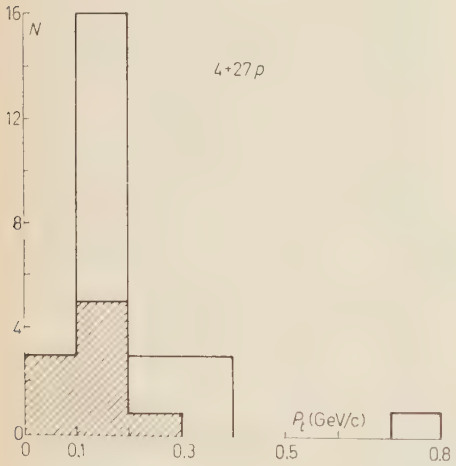

Fig. 4. – Distribution of transverse momentum for the primary event 4 + 27p. The shaded area represents measurements when only lower limits were obtained.

Fig. 5. – Transformation to c.m.s. of primary event 4 + 27p for $\gamma_L = 40$ and $E = 3.3$ GeV. The dashed line corresponds to a constant value of the transverse momentum $P_t = 1.5 m_\pi c$.

The values of P_t for all shower particles of this event are given in Table I. For 9 tracks out of 27 tracks, only a lower limit for P_t could be established. In Fig. 4 are shown the values of P_t for the primary event. The shaded area represents measurements when only lower limits were obtained. The peak value of the distribution is at about 0.2 GeV/c. No values of $P_t > 0.80$ were observed.

We considered the relativistic transformation from the laboratory system into the center-of-mass system for the primary event, assuming it as a nucleon-nucleon collision as discussed in ref. [4]. The correlation between the energy and the angle for the primary event is shown in Fig. 5. The distribution shows a sharp collimation of particles at small angles with the shower axis and is quite symmetrical. The dotted line corresponds to a constant value of the transverse momentum and it is also symmetrical with respect to the center. The energy of the primary event as calculated from the angular distribution has the value 3.3 TeV which corresponds to approximate values for $\gamma_c = 40$. The shape of the distribution indicates that the trans-

formation is not very sensitive ([4,10]) to the choice of γ_c at these high energies. All transformations were carried out under the assumption that all secondary charged particles are π-mesons.

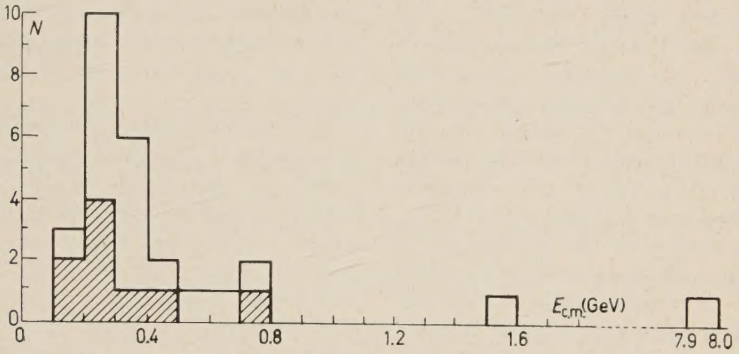

Fig. 6. – Energy distribution of the primary event 4 + 27p in c.m.s.

The energy distribution of the charged meson is given in c.m.s. in Fig. 6. The shaded area shows the measurements for only those events where only lower limits were obtained. The energy distribution of the meson in c.m.s. shows a peak towards low energies, and has a remarkably long tail at high energies extending up to 8.0 GeV. The average energy of the charged meson in c.m.s. is 0.67 GeV. This value is the lower limit because of the lower limits for several particles in the laboratory system. This result is not in agreement with Fermi's theory ([12]), which would predict a considerably higher value (several GeV). If the lower limit of the energy in c.m.s. is the true value of the average energy, then the experimental results to some extent are agreeable to Heisenberg's theory ([13]), but Landau's theory ([14]) can be adjusted to agree with our experimental value of average energy in either case, whether the lower limit of the average energy is the true energy or not. We may point out here that the average energies are very sensitive to the existence of a few particles in the high-energy tail of the distribution. Also if there are heavy mesons among the secondaries, there would be a small effect on the high-energy particles in the core, while the effect on the particles in the backward cone would be large. But on the assumption of approximate equipartition of energy, one can say that only those pions which show very low energy could be heavy mesons. On the whole the number of K-mesons in the backward cone cannot be more than one or two particles.

The total energy of the shower particles as determined by scattering measurements, shown in Table I, is about 483 GeV. This is not the true value as about 30% of the tracks have lower limits in their energy values. In order to determine the total energy of all the shower particles, we shall make use of the fact that the transverse momentum P_t of all the shower particles is

([10]) M. SCHEIN, D. HASKIN, E. LOHRMANN and M. TEUCHER: *Phys. Rev.*, **116**, 1238 (1959), (other references are given there).

([11]) L. F. HANSEN and W. B. FRETTER: *Phys. Rev.*, **118**, 812 (1960).

([12]) E. FERMI: *Progr. Theor. Phys.*, **5**, 570 (1950); *Phys. Rev.*, **81**, 683 (1951).

([13]) W. HEISENBERG: *Zeits. Phys.*, **126**, 569 (1949); **133**, 65 (1952).

([14]) S. BELEN'KIJ and L. LANDAU: *Suppl. Nuovo Cimento*, **3**, 15 (1956).

constant [6,10,11] and ~ 0.30 GeV/c. This gives us a value of 925 GeV for the total energy of the charged particles. If we add to this value the energies of two energetic electromagnetic cascades, then we get the total energy for the primary event as $925+2100=3025$ GeV. We have not added to this the energies of low energy soft cascades which were produced in the primary interaction. Thus, we see that the energy of the primary event as given from the angular distribution (*i.e.*, $3.3\cdot10^{12}$ eV) is approximately the « true » value.

If the energies of the primary event (*i.e.*, $3.3\cdot10^{12}$ eV) and of the very energetic electromagnetic cascade are the right values, then how can one explain that a single π^0 meson could take about 50% of the energy of the primary event where ordinarily one would expect that all the soft cascades would take only about $\frac{1}{2}$ of the energy of the charged shower particles? There have been some indications in the literature that a single π^0 meson could take up to $(30\div35)\%$ of the primary energy [1,18] but not up to 50% of the primary energy. We shall suggest a possible explanation for this as follows.

It is well known that in emulsions exposed at very high altitudes, the primary particle will consist almost exclusively of protons and heavier nuclei uncontaminated by secondary π-mesons. But at lower altitudes, say below 15 km, apart from protons and heavier nuclei, high-energy charged π-mesons which survive for much longer than their normal life span owing to their relativistic dilation of the time scale, will also be present among the primary particles. One can say that approximately the fraction of π-mesons of $E>10^4$ GeV is not more than about 0.1 at an altitude ~15 km. We may point out here that the fraction of high-energy events due to π-mesons, actually found in a stack, may be considerably larger than this value.

A nucleon-nucleon interaction may be considered relatively elastic, as only $\sim30\%$ of the energy of the primary particle appears in the form of secondary mesons, while the interactions due to primary pions with nucleons may be completely inelastic. For example they may frequently result in the sharing of all the energy of the incident π-meson among many secondaries. In that case a much larger fraction of the primary energy will contribute to the formation of the soft cascade. When a π-meson collides with a nucleon, it is possible that it may retain most of its energy and may undergo charge exchange. In that case, a large fraction of the primary energy may be transformed almost directly into a soft cascade. So, on this basis, we consider that the primary particle which produced the event 4+27p may be due to a charged π-meson instead of a proton, which was recorded in the stack during the ascending or the descending of the balloon flight. If so, then the high-energy electromagnetic cascade which takes about 50% of the primary energy, was produced by the primary π-meson which underwent charge exchange after its first interaction. This is further supported from the fact that no charged mesons of energy greater than 120 GeV were found in the primary interaction.

* * *

We appreciate very much the hospitality of the late Prof. M. SCHEIN of the University of Chicago where this work started.

[1] J. BARTKE, P. CIOK, J. GIERULA, R. HOŁYŃSKI, M. MIĘSOWICZ and T. SANIEWSKA: *Nuovo Cimento*, **15**, 18 (1960).

[18] J. GIERULA, M. MIĘSOWICZ and P. ZIELIŃSKI: *Nuovo Cimento*, **18**, 102 (1960).

[17] G. A. MILCHIN: *Žurn. Eksp. Teor. Fiz.*, **35**, 1185 (1958).

[18] G. B. ZHDANOV, E. A. ZAMCHALOVA, M. I. TRET'IAKOVA, and M. N. SHCHERBAKOVA: *Sov. Fis. JETP*, **7**, (34) 582 (1958).

LIBRI RICEVUTI E RECENSIONI

Libri ricevuti.

G. Thomson: *The Inspiration of Science*; Oxford University Press, London, 1961; pp. x-150; 18 s. net.

E. Merzbacher: *Quantum Mechanics*; John Wiley and Sons Inc. Pub., London, 1961; pp. xii-544; 96 s. net.

E. Dewitt: *Dispersion Relations and Elementary Particles*; John Wiley and Sons, 1961; pp. 672; 160 s. net.

M. J. P. Vigier: *Introduction à la Nouvelle Théorie des Particules*; Gauthier-Villars, Paris, 1961; pp. 108; 20 NF.

A. Visconti: *Théorie Quantique des Champs*. Tome I: *Formalisme Hamiltonien, Champs Libres*; Gauthier-Villars, Paris, 1961; pp. xix-299; 65 NF.

J. L. Destouches: *Leçons sur le Champ Fondamental*; Gauthier-Villars, Paris, 1961; pp. 158; 25 NF.

A. Dauvillier: *La Poussière Cosmique*: *Les milieux Interplantaire, Interstellaire et Intergalactique*; Masson et C.ie Editeurs, 1961; pp. 210; 25 NF.

R. M. Eisberg: *Fundamentals of Modern Physics*; John Wiley and Sons Inc. Pub., London, 1961; pp. xiii-729; 84 s. net.

Recensioni.

E. Bauer – *Elektronenbeugung*. Verlag Moderne Industrie, München, 1958; pp. 233, DM 32.

Si tratta di un volumetto introduttivo alla tecnica della diffrazione degli elettroni, e alle sue moderne applicazioni industriali.

I perfezionamenti raggiunti nella costruzione delle apparecchiature hanno assai sviluppato negli ultimi anni questo metodo per lo studio della struttura della materia, tanto da renderlo ormai in alcuni campi supperiore ai raggi X (per esempi nello studio delle superfici e delle polveri, dato che l'assai più forte interazione degli elettroni con la materia, fa sì che già sottilissimi strati diano figure di diffrazione, mentre non le danno con i raggi X).

Nel suo dichiarato scopo di guida introduttiva, il libro non ha pretese di compiutezza nè di particolare rigore scientifico, ma piuttosto vuole mettere il lettore in grado di comprendere la letteratura specifica, fornendogli le necessarie basi sia teoriche che sperimentali, e informarlo sulle possibilità di applicazione di questa tecnica nei vari campi dell'industria. Abbiamo così nella prima parte (« parte teorica ») un confronto fra le due tecniche, dei raggi X e degli elettroni, e una esposizione delle tre teorie usate per descrivere la diffrazione nei cristalli, in ordine di approssimazione successiva: la teoria geometrica di Bragg, quella cinematica o di Laue (che ottiene il raggio riflesso dalla sovrapposizione delle onde diffratte dai singoli atomi del reticolo) e quella dinamica, di Bethe

(che tiene conto anche delle interazioni delle varie onde riflesse, fra loro e con quella incidente). Senza soffermarsi troppo a ricavare le formule, per le quali rimanda ai testi specializzati, Bauer traccia piuttosto il cammino logico percorso, e con varie figure cerca di rendere il più possibile evidenti i risultati, così da facilitarne l'applicazione.

Piccoli riassunti e sommari parziali permettono al lettore di rendersi conto molto bene dei limiti e possibilità insiti in ognuna di queste approssimazioni.

Nella seconda parte (« parte sperimentale ») l'autore descrive piuttosto a fondo le varie parti componenti un diffrattometro (sorgente, portaoggetti, lenti, alimentazione, ecc.), fondando la sua illustrazione sulle apparecchiature prodotte dall'industria, sia diffrattometri veri e propri, sia microscopi elettronici, i quali si possono usare anche in diffrazione. Altri paragrafi riguardano le possibilità e i limiti, sia teorici che sperimentali, della tecnica; i metodi di preparazione dei campioni; l'interpretazione dei diagrammi; dopo di che il lettore dovrebbe essere in grado di usare praticamente questa tecnica.

La terza parte (« applicazioni ») risulta forse la più compressa: infatti non tenta di discutere i singoli usi, ma si limita ad indicarli schematicamente e a fornire la letteratura relativa; in sole 40 pagine vengono perciò rapidamente trattate le varie applicazioni nell'industria metallurgica, chimica, elettrica ed ottica. Una breve appendice richiama infine l'attenzione sull'uso degli elettroni lenti, e sulla utilizzazione dei microscopi elettronici come diffrattometri.

Più di cento figure accompagnano e chiarificano il testo, quasi seicento riferimenti bibliografici lo sostengono e giustificano, mentre un ricco indice analitico ne rende molto facile l'uso, oltre che per studio, anche per consultazione.

F. Dupré

L. D. Landau and E. M. Lifshitz – *Mechanics*. Pergamon Press, Oxford, 1960; pp. 175, prezzo 40 scellini.

Si tratta del primo volume del corso di fisica teorica dei due illustri autori russi, e secondo noi del più riuscito della serie e di notevole valore intrinseco. Il metodo un po' dogmatico sempre seguito da questi autori, che nuoce alla esposizione di argomenti ancora in evoluzione e che è forse la critica più seria che si possa muovere a tutta la loro opera, nel caso della meccanica è invece uno strumento adeguato per raggiungere chiarezza e concisione. Tutta la meccanica viene basata in questo libro sul principio di Hamilton di minima azione. Le leggi di conservazione seguono come teoremi, e l'integrazione dell'equazione del moto come applicazione analitica. La scelta dei pochi esempi fisici, trattati in dettaglio ed in latitudine è certo felice: collisioni fra particelle, piccole oscillazioni, moti rigidi.

Dato anche il basso costo, è auspicabile che questo volume faccia parte della biblioteca dei nostri studenti del secondo biennio.

G. Careri

Direttore responsabile: G. POLVANI Tipografia Compositori - Bologna

Questo Fascicolo è stato licenziato dai torchi il 13-XII-1961